25 November 2005

Science

Vol. 310 No. 5752
Pages 1229–1372 $10

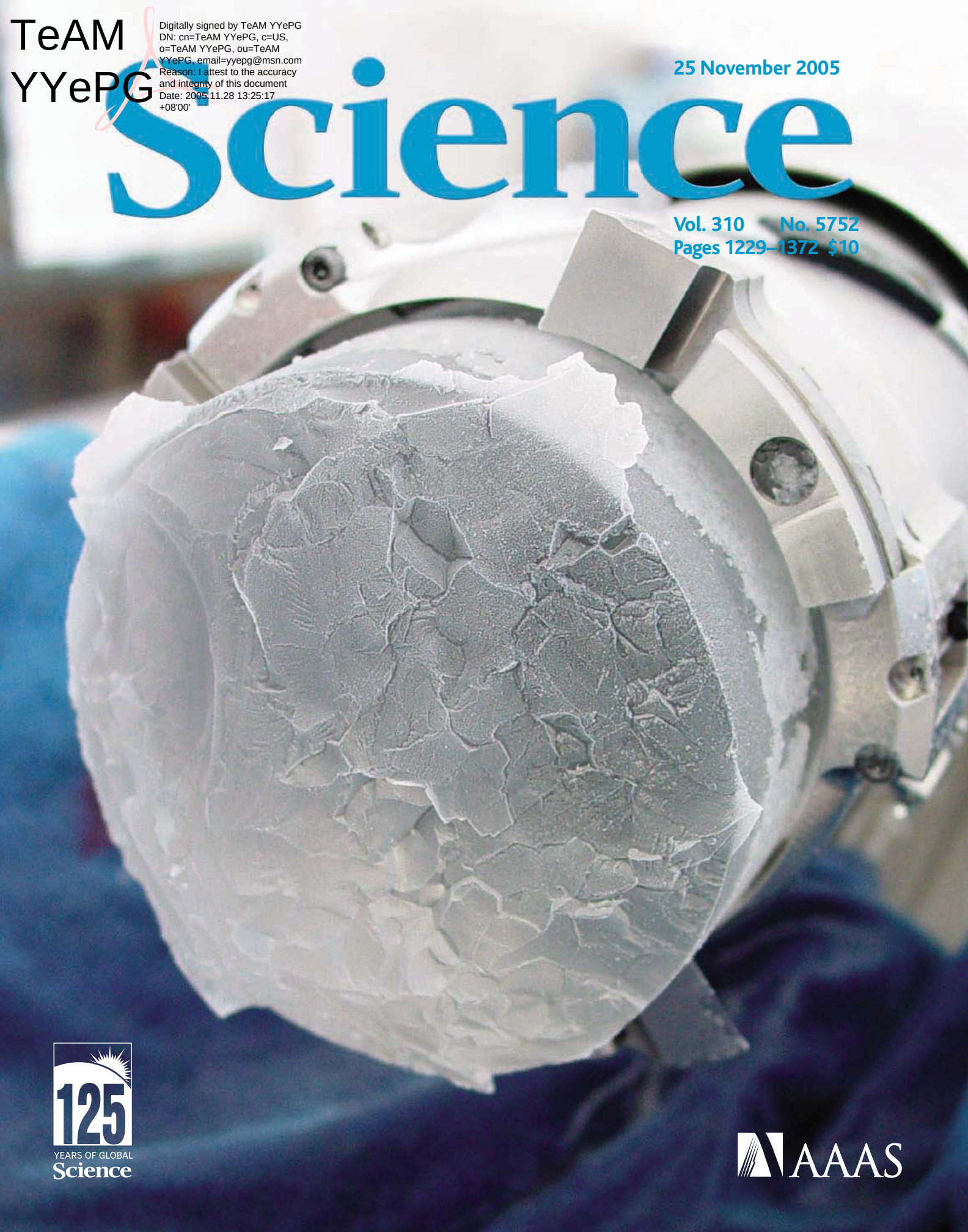

125 YEARS OF GLOBAL Science

AAAS

DuoSet® IC Assays | from R&D Systems

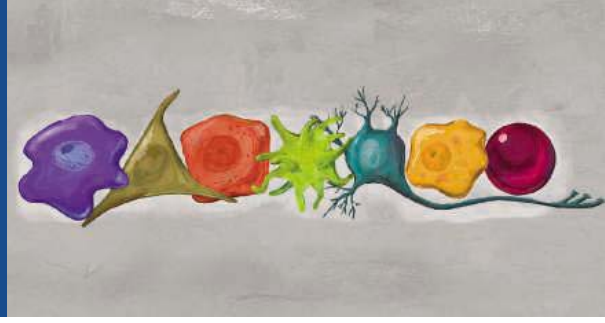

Quality | Selection | Performance | Results

Our DuoSet IC Assays include:

- Total and Phospho-Specific ELISAs
- Caspase Activity Assays
- Phosphatase Activity Assays
- Receptor Tyrosine Kinase Assays
- Transcription Factor Activity Assays
- Kinase Activity Assays

Advantages :

- High sensitivity
- High specificity
- Reproducibility
- Small sample size
- Thorough validation
- Extensive analyte selection

The Human Total β-Catenin Duoset IC ELISA specifically recognizes phosphorylated and non-phosphorylated β-catenin, and contains the basic components required for development of sandwich ELISAs to measure β-catenin in cell lysates.

Quantification of β-Catenin in Human Cell Lines

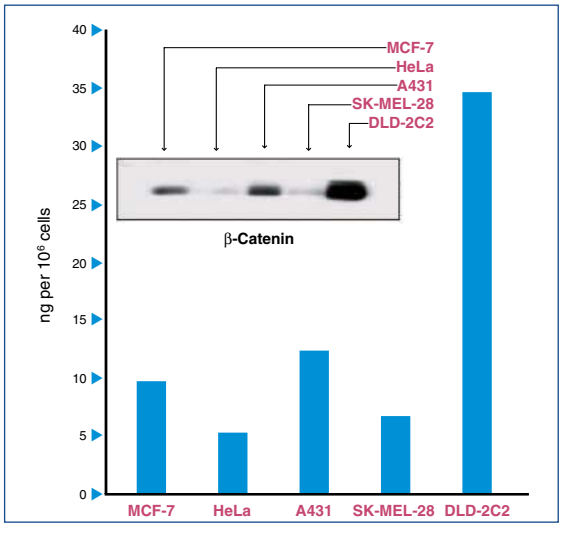

Lysates prepared from human MCF-7, HeLa, A431, SK-MEL-28, and DLD-2C2 cells were quantified with the Human Total β-Catenin DuoSet IC ELISA (R&D Systems Catalog # DYC1329). The same cell lysates were also immunoblotted (inset) with anti-β-catenin monoclonal antibody (R&D Systems Catalog # MAB1329). The DuoSet IC ELISA results correlate well with the total amounts of β-catenin detected by Western blot.

R&D Systems DuoSet® IC Assay Development Systems offer a fast, sensitive, and economical method to detect and quantify intracellular factors involved in apoptosis, signal transduction, and transcription. These products contain the basic components necessary for assay development and include detailed protocols to ensure your success.

www.RnDSystems.com | (800) 343-7475

U.S. & Canada
R&D Systems, Inc.
Tel: (800) 343-7475
info@RnDSystems.com

Europe
R&D Systems Europe Ltd.
Tel: 0800 37 34 15
info@RnDSystems.co.uk

Germany
R&D Systems GmbH
Tel: 0800 909 4455
infogmbh@RnDSystems.co.uk

France
R&D Systems Europe
Tel: 0800 90 72 49
info@RnDSystems.co.uk

R&D SYSTEMS

If it's in there, you'll find it.

StrataScript® QPCR cDNA Synthesis Kit generates cDNA from even the smallest amounts of RNA quickly and reliably.

Our StrataScript® Quantitative PCR (QPCR) cDNA Synthesis Kit* delivers maximum RNA sensitivity and dynamic range down to sub-picogram RNA levels. Achieve high efficiency reverse transcription and better R Squared values in our new buffer system and master mix format, which greatly reduces sample transfer errors known to hamper results. Each batch is QPCR-qualified to ensure you produce the most reliable two-step quantitative reverse-transcriptase PCR (QRT-PCR) data.

- **Maximum RNA sensitivity**
- **Excellent linearity**
- **Most reliable two-step QRT-PCR data**

Need More Information? Give Us A Call:

Stratagene USA and Canada
Order: (800) 424-5444 x3
Technical Services: (800) 894-1304 x2

Stratagene Europe
Order: 00800-7000-7000
Technical Services: 00800-7400-7400

Stratagene Japan K.K.
Order: 03-5159-2060
Technical Services: 03-5159-2070

www.stratagene.com

Ask Us About These Great Products:

StrataScript® QPCR cDNA Synthesis Kit	**50 rxn**	**600554**

*Purchase of this PCR-related product does not convey any rights under the foreign counterparts of the PCR patents owned by Roche Molecular Systems. A license to use the PCR process, where such process is covered by patents, accompanies the purchase of certain reagents from Stratagene when used in conjunction with an Authorized Thermal Cycler.

STRATAGENE®

HisTrap FF crude

Take an xpress run with HisTrap FF crude

The new ÄKTAxpress™ TWIN has chromatography knowledge built in. It automatically purifies eight samples delivering >95% pure tagged protein. ÄKTAxpress can extend from two to twelve modules, and has been designed to adapt to your future purification needs. By combining ÄKTAxpress with HisTrap™ FF Crude prepacked columns, you can now apply sonicated unclarified samples without the centrifugation/filtration steps. Getting more histidine-tagged protein with less effort just takes a little pure imagination.

Visit www.amershambiosciences.com/aktaxpress

ÄKTAxpress TWIN

imagination at work

GE14-05

Science

COVER Drill head with piece of an ice core retrieved on 30 November 2002 at Dome Concordia Station during the European Project for Ice Coring in Antarctica. This ice is from a depth of 2873 meters and is about 491,000 years old. The ice core contains a continuous record of greenhouse gases over the past 650,000 years. See page 1317. [Photo: Laurent Augustin, LGGE Grenoble]

Volume 310
25 November 2005
Number 5752

DEPARTMENTS

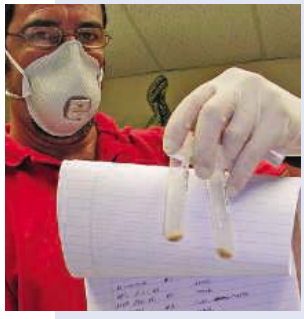

1267

NEWS OF THE WEEK

1280

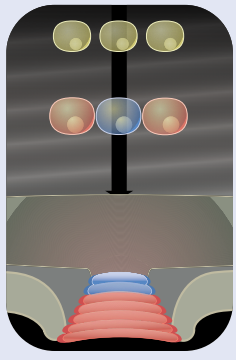

1288 & 1330

NEWS FOCUS

LETTERS

BOOKS *ET AL.*

POLICY FORUM

PERSPECTIVES

REVIEW

Contents continued

Integrated Solutions — RNAi

Potent, specific siRNA you can trust!

New siRNA Sets!

Spyro Mousses, Ph.D.

Head of Cancer Drug Development, Translational Genomics Research Institute (TGen), Maryland, USA. TGen headquarters are based in Phoenix, AZ.

Dr. Mousses and his colleagues at TGen use siRNA designed by QIAGEN to discover genetic weaknesses in cancer cell lines. In this example, 2000 siRNAs were used in a screen to compare relative survival of two cancer cell lines after gene knockdown.

"High-quality siRNA designed by QIAGEN has enabled TGen to significantly accelerate our global RNAi phenotype profiling and cancer drug target discovery. Having a reliable source for optimally designed siRNA that we can trust means we can spend less time on design and focus on our research. I am very happy with our results."

See how the Human Druggable Genome siRNA Set and the upcoming Human Whole Genome siRNA Set can enhance your research at www.qiagen.com/goto/HPsiRNA !

QIAGEN

Science Express www.sciencexpress.org

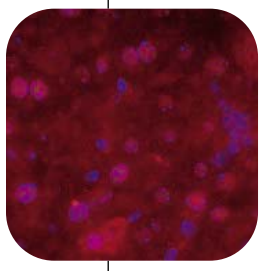

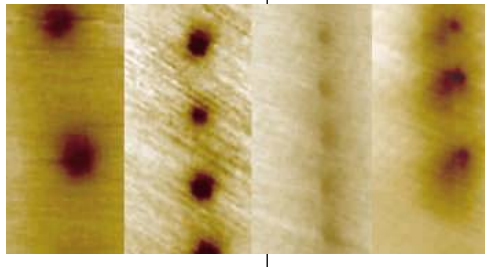

1304

Brevia

Research Article

Reports

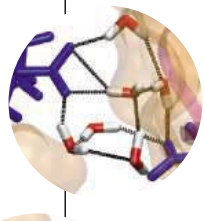

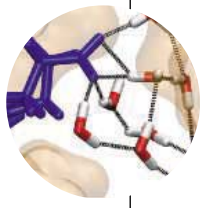

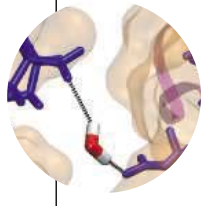

1311

Contents continued

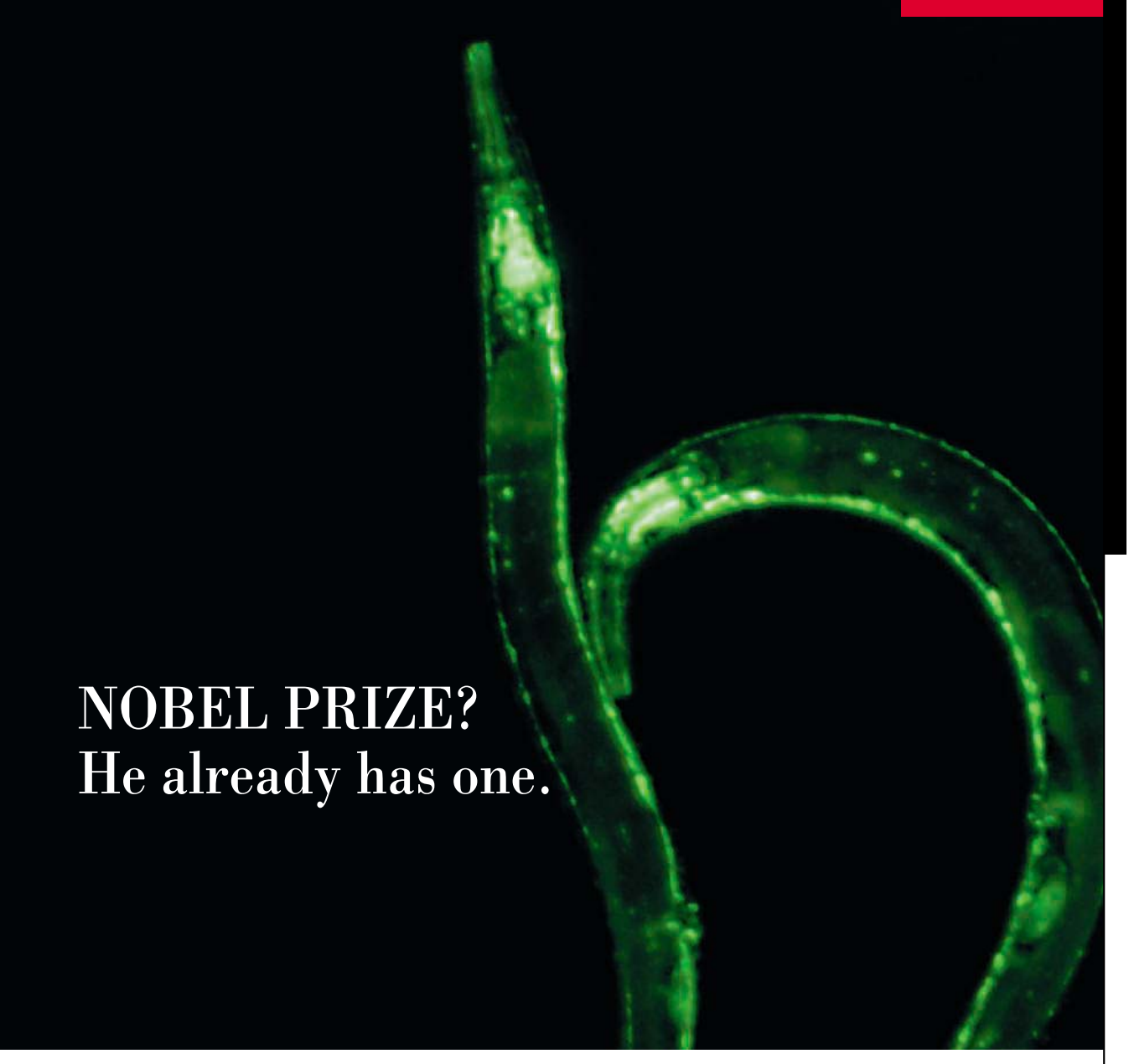

NOBEL PRIZE?
He already has one.

And what is your goal?

No matter how high you set your goals, the world's best motorized fluorescence stereomicroscope supports you. The Leica MZ16 FA automatically controls multi-fluorescence experiments, including filter change, zoom and focus, and offers top performance in every respect: 16:1 zoom, magnification up to 920x, resolution of 840 lp/mm up to 1500 lp/mm, finest visible structure width of 0.3 µm up to 0.6 µm. The largest range of modular accessories allows for expansion up to the software-controlled complete system for documentation and analysis.

@ www.stereomicroscopy.com

Leica
MICROSYSTEMS

Science

REPORTS CONTINUED

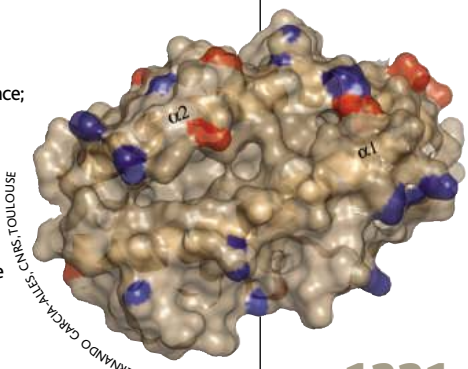

LUIS-FERNANDO GARCIA-ALLES, CNRS, TOULOUSE

1321

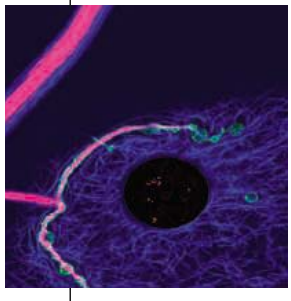

MICHAEL GORCZYCA/BUDNIK LABORATORY

1284 & 1344

AAAS
ADVANCING SCIENCE, SERVING SOCIETY

SCIENCE (ISSN 0036-8075) is published weekly on Friday, except the last week in December, by the American Association for the Advancement of Science, 1200 New York Avenue, NW, Washington, DC 20005. Periodicals Mail postage (publication No. 484460) paid at Washington, DC, and additional mailing offices. Domestic individual membership and subscription (51 issues): $135 ($74 allocated to subscription). Domestic institutional subscription (51 issues): $550; Foreign postage extra: Mexico, Caribbean (surface mail) $55; other countries (air assist delivery) $85. First class, airmail, student, and emeritus rates on request. Canadian rates with GST available upon request, GST #1254 88122. Publications Mail Agreement Number 1069624. **Printed in the U.S.A.**

Change of address: allow 4 weeks, giving old and new addresses and 8-digit account number. **Postmaster:** Send change of address to *Science*, P.O. Box 1811, Danbury, CT 06813–1811. **Single copy sales:** $10.00 per issue prepaid includes surface postage; bulk rates on request. **Authorization to photocopy** material for internal or personal use under circumstances not falling within the fair use provisions of the Copyright Act is granted by AAAS to libraries and other users registered with the Copyright Clearance Center (CCC) Transactional Reporting Service, provided that $15.00 per article is paid directly to CCC, 222 Rosewood Drive, Danvers, MA 01923. The identification code for *Science* is 0036-8075/83 $15.00. *Science* is indexed in the *Reader's Guide to Periodical Literature* and in several specialized indexes.

Contents continued

Now it's your turn to rock the world!

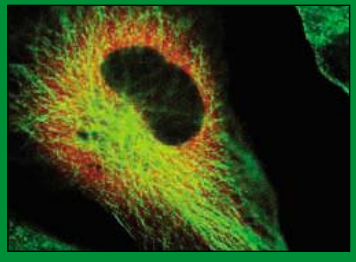

HaloTag™ Technology is ideal for both live- and fixed-cell imaging.

Every once in a while, a new technology comes along that sparks the imagination of innovative scientists. HaloTag™ is a revolutionary new technology that allows you to visualize cellular events and the protein processes that mediate those events. To find out how to apply HaloTag Technology to your experiments in cellular imaging, protein immobilization and protein interactions, visit www.promega.com/halotag

PROMEGA CORPORATION • www.promega.com

Promega

sciencenow www.sciencenow.org Daily News Coverage

Cats Be Damned
Mice lacking gene involved in cellular transport have nothing to fear.

The Zen of Skunk Cabbage
Mathematical model may explain how plant keeps its insides toasty.

Millions May Have Received Contaminated Polio Vaccine
Virus linked to cancer found in batches made by eastern European company.

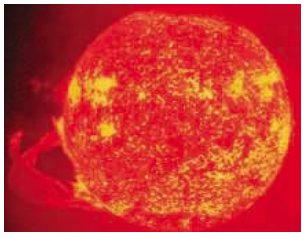

Energy research in the UK.

ScienceCareers.org www.sciencecareers.org Career Resources for Scientists

US: Soaring into Atmospheric Science *A. Fazekas*
Find out about the National Center for Atmospheric Research and its postdoc fellowship program.

UK: The Future of Energy Research *A. Agrawal*
Two of the UK's top research institutions are launching new initiatives in energy research.

Netherlands: The European Young Investigator Awards—Finding a Niche *E. Pain*
Edwin Cuppen is a group leader at the Netherlands Institute for Developmental Biology in Utrecht.

MiSciNet: Educated Woman—And Now for Something Completely Different *M. P. DeWhyse*
Micella takes her project on the road and does some of her research in Europe.

MiSciNet: AESEDA—Global Opportunities for Minority Earth Scientists *A. Sasso*
Penn State's Alliance for Earth Sciences, Engineering, and Development in Africa program engages minority students in the study of earth sciences.

science's sage ke www.sageke.org Science of Aging Knowledge Environment

Perspective: Mitochondrial Dynamics in Cell Life and Death *C. Scheckhuber*
Results discussed at a workshop on mitochondrial fusion and fission have relevance to apoptosis and aging.

News Focus: Shortchanged by Sir2 *M. Leslie*
Longevity protein cuts off yeast survival.

Longevity protein uprising.

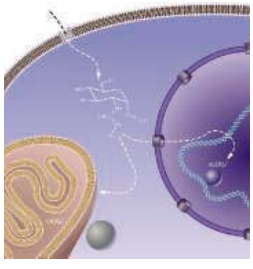

Differential localization of O-linked GlcNAc transferase.

science's stke www.stke.org Signal Transduction Knowledge Environment

Review: The Hexosamine Signaling Pathway—Deciphering the "O-GlcNAc-Code"
D. C. Love and J. A. Hanover
Addition and removal of O-linked *N*-acetylglucosamine from proteins may serve as a signaling mechanism and link protein activity to nutrient status.

Glossary
Find out what those acronyms and abbreviations mean in signaling research.

Separate individual or institutional subscriptions to these products may be required for full-text access.

Hard Nanowired

In transistor fabrication, regions with different types of semiconductor doping can be created through ion implantation and lithographic patterning. **Yang *et al.*** (p. 1304) now report on the gold-nanocluster–catalyzed synthesis of silicon nanowires that are both highly uniform in diameter with lengths exceeding 10 micrometers and whose pattern of doping can be altered anywhere along the nanowire. Regions of light or heavy n-type doping were created by changing the amount of phosphine introduced during growth and were imaged by scanning gate microscopy. Nanowires with different patterns of doping regions were used to create an address decoder, and at low temperatures, the different doping regions defined quantum dots that exhibited Coulomb oscillations.

Springing Back

Many materials can recover their shape after compressive stress, but they can pass a limit after which they either fail completely or fail to reexpand. **Cao *et al.*** (p. 1307) have fabricated freestanding films consisting of aligned carbon nanotubes that behave as open-cell flexible foams. The films can be reversibly squeezed to only 15% of their original thickness without structural failure, despite the significant zigzag bucking of the nanotubes. The nanotubes act as elastic compression springs; they are highly compressible along their axis but regain most of their free length after a compressive load is released.

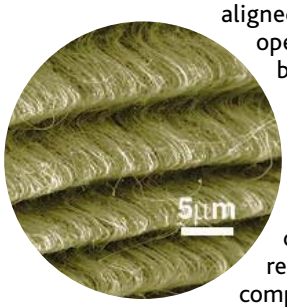

A Single Spiral Around Saturn

The braided structure of Saturn's delicate F ring, with its wispy interweaving strands, has long puzzled astronomers. From sequences of detailed images taken by the Cassini spacecraft, **Charnoz *et al.*** (p. 1300; see the Perspective by **Showalter**) show that the F ring is not so complex and takes the form of a loose single-arm spiral that wraps around the planet three times. After using simulations to explore the spiral's origin, the authors propose that the passage of one of Saturn's tiny moonlets close to the main F-ring band may have expelled material which, after many orbits, has been strung out into a spiral pattern.

Airing Out Older Glacial Cycles

Air trapped in glacial ice contains the only reliable direct record of atmospheric composition before scientific sampling began in the 18th century. Since 1997, the oldest ice available for analysis was that from the Vostok, Antarctica, ice core, which extends back to 420,000 years ago and covers four complete glacial cycles. A new ice core from the EPICA Dome C site in Antarctica now extends back to an age of 740,000 years or more. Two reports present data on the composition of the atmosphere between 400,000 and 650,000 years ago, an interval soon after glacial cycles switched from a dominantly 41,000-year period to the dominantly 100,000-year period that occurs today (see the Perspective by **Brook**). **Siegenthaler *et al.*** (p. 1313) present measurements of the atmospheric concentration of CO_2, the most important trace greenhouse gas, and show how its concentration varied during a much more narrow range than it did during the past 400,000 years. **Spahni *et al.*** (p. 1317; see the cover) present parallel measurements for two other important trace greenhouse gases, CH_4 and N_2O. As is the case for CO_2, CH_4 varied between much more narrow bounds during that time, although N_2O varied just as much as it did in the nearly half-million years since then. These data will be keys to understanding how the carbon cycle has operated since the middle of the Pleistocene epoch.

Hanging On to Introns

Evolution has increased the complexity of organisms, especially bacteria and single-celled eukaryotes that are contrasted with vertebrates, but it does not necessarily follow that the genes and genomes of organisms that arose early in evolution should be less complex than those of newer species. **Raible *et al.*** (p. 1325) analyzed the genome of the marine ragworm, *Platynereis dumerilii*, a possible "living fossil," and show that the structure of its genes is remarkably complex, and that its genome has an intron richness which resembles that of human genome. These two very different organisms have retained this genetic complexity, which has been lost in the other insects and nematodes whose genomes have been studied.

Promoting Lipid Processing for Presentation

A subpopulation of T cells recognizes antigens derived from lipids, rather than from proteins, and these lipid antigens are presented by members of the CD1 family of cell surface proteins. However, one CD1 family member, CD1e, does not seem to present lipids directly. **De la Salle *et al.*** (p. 1321) observed that a lipid antigen that depends on processing to stimulate T cells via another member of the CD1 family (CD1b) could not do so in the absence of CD1e. CD1e was required to assist in modifying a lipid precursor within the lysosome, which allowed intracellular association with CD1b and subsequent presentation to T cells. Thus, the role of this remaining CD1 family member appears to involve processing, rather than direct presentation of, antigenic lipids to T cells.

Cell Fate Specification in the Worm

Early in the development of the nematode worm *Caenorhabditis elegans*, the vulva is composed of six precursor cells that have the potential to develop into one of three vulval cell fates, termed 1°, 2°, and 3°. The 1° and 2° fates are patterned through the cross-talk between two signaling pathways, the EGFR-MAPK pathway and the LIN-12/Notch pathway. **Yoo and Greenwald**

CONTINUED ON PAGE 1243

CREDITS (TOP TO BOTTOM): SHOWALTER *ET AL.*; CAO *ET AL.*

From research to quality control – base your decisions on the best

For more than 15 years Biacore has been supplying the life science market with a growing range of advanced systems for protein interaction analysis. Unique, high-quality data generated from each instrument supports the many critical decisions that lead to increased productivity in academic and pharmaceutical environments.

Biacore® systems define proteins in terms of their concentration, their specificity of interaction with other molecules, the rates at which they interact, how tightly they bind to another molecule and the thermodynamics involved – all without the use of labels.

Data you can depend on – from the unrivalled global leader in protein interaction analysis.

Protein interaction analysis in:

- **Disease mechanisms**
- **Antibody characterization**
- **Proteomics**
- **Lead selection**
- **Immunogenicity**
- **Biotherapeutic development**

Define · Decide

BIACORE

www.biacore.com

(p. 1330, published online 20 October; see the Perspective by **Karp and Ambros**) now show that a specific microRNA (miRNA), identified by a computational prediction analysis, is involved in specifying the 2° vulval cell fate. The miRNA *mir-60* is a direct transcriptional target of LIN-12/Notch, and, in turn, an ortholog of the oncogene Vav is the target of *mir-60*. The regulatory circle is completed by the regulation of LIN-12 activity by Vav.

Greenhouse Europe

Assessing the likely affects of global climate change remains a high priority for all nations. **Schröter *et al*.** (p. 1333, published online 27 October) show how the pattern of Europe's vulnerability to global changes is likely to change in the 21st century caused by the decreased supply of ecosystem services such as plant growth, carbon sequestration, biodiversity, water, and soil fertility. They apply four climate models to Europe and combine them with socioeconomic scenarios to project the evolution of a range of ecosystem services for the coming century, ranging from carbon sequestration to freshwater provisioning and biodiversity. The loss of these services is likely to be accentuated particularly in the Mediterranean and in mountainous regions.

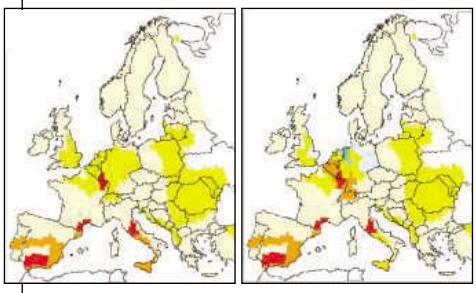

CREDIT: SCHRÖTER *ET AL.*

Action, Choice, and Reward

To attain specific goals, humans and animals choose actions based on current behavioral contexts and on past experiences. **Samejima *et al*.** (p. 1337) examined single unit activity within the basal ganglia in monkeys performing a simple motor decision task in which rewarded action and the relative reward value were independently manipulated. Cells were identified that showed activity associated with a preferred direction, amount of reward, or some combination of both. About one-third of neurons in the dorsal striatum coded for action value. A reinforcement learning algorithm, trained on the same sequence of trials presented to the animal, could predict trial-by-trial neural activity. The dorsal striatum may be the site of reinforcement learning of action values that are then used to select actions further downstream in the basal ganglia.

Getting to the Bottom of Drug Cravings

Behavioral sensitization, an animal model for drug craving, involves neural adaptations in the mesocorticolimbic regions of the brain, including the nucleus accumbens. Synaptic plasticity in the nucleus accumbens, especially long-term depression (LTD), plays an important role in behavioral sensitization. Using new synthetic peptide inhibitors, **Brebner *et al*.** (p. 1340) showed that LTD in nucleus accumbens is mediated by clathrin-dependent, regulated endocytosis of AMPA receptors. An AMPA-specific inhibitor delivered to neurons in the nucleus accumbens blocked behavioral sensitization. Thus, LTD in the nucleus accumbens is mediated by facilitated endocytosis of postsynaptic AMPA receptors and may be involved in the pathogenesis of drug craving.

Signaling from Wingless

Despite the extensive study of the Wingless (Wg) or Wnt signaling pathway in regulating development and cancer, a previously unrecognized mechanism has been uncovered for Wg signaling at developing synapses in the *Drosophila* nervous system. **Mathew *et al*.** (p. 1344; see the Perspective by **Arias**) found that the Wg receptor DFrizzled2 (DFz2) can be cleaved and translocated from the plasma membrane to the area of the cell just outside the nucleus. In response to Wg signals, the C terminal portion of the receptor then enters the nucleus, where it might act to regulate gene expression. Expression of a DFz2 mutant that could not be cleaved failed to rescue synapse formation in flies that expressed a mutant of DFz2 with defective signaling.

EndNote. Where millions of researchers, librarians and students begin.

Learn about new tools for your research and publishing—

Onfolio™
Organize RSS feeds and Web research

RefViz™
Visualize references

sciPROOF™
Proof your manuscript

EndNote, used by millions of researchers, students, professors, librarians and writers worldwide, is known for introducing innovative features such as the ability to search online bibliographic databases, organize references and images, and create instant bibliographies. With EndNote 9, you can work faster with increased performance, connect to more data sources worldwide, and share customized libraries with colleagues easily. EndNote is easy to use, easy to learn and is seamlessly compatible with Microsoft® Word for Windows® and Mac® OSX. There simply is no better way to manage your references and build instant bibliographies.

800-722-1227 • 760-438-5526
Fax: 760-438-5573
rs.info@thomson.com

Download your Free demo or buy online today.
www.endnote.com

NASA: Back to Eating Seed Corn

Since the U.S. National Aeronautics and Space Administration (NASA) and its problems last appeared on this page, new administrator Michael Griffin has had about 6 months to deal with his budget problems, one of the largest of which is funding the space shuttle program. Operating the shuttle for the next 5 years could cost $5 billion more than NASA had projected. Just to remind you, there was some hope in April that President Bush's Vision for Space Exploration (VSE, or Moon-to-Mars) would neither cripple basic science programs nor signal the end of a number of planned robotic space missions. Alas, there has been even more damage to both than *Science* expected. That would be enough bad news, but there's more to the story and it is an international problem, not just a domestic one .

Present concerns at NASA have gone beyond sorrow over the lost robotic missions. Instead, they now focus on the necessary preparations for the VSE mission itself. People are going to fly to the Moon, establish a base, and use the experience gained from getting and living there to send humans on the longest trip in history. Let's ponder the work that has to be done first.

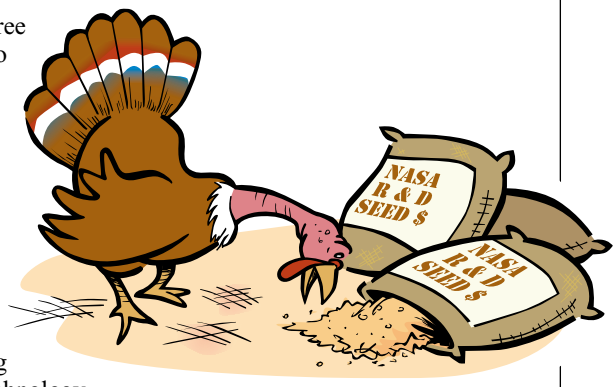

The International Space Station (ISS) has a limited crew (two or three instead of seven), and shuttle flights (of which NASA may only be able to afford eight) are arbitrarily scheduled to end at the end of this decade to meet the recommendations of the Columbia Accident Investigation Board. Some hope for a complete ISS soon after that, but doubts remain. Remember that ISS is an international project, billed to serve as a science laboratory for non-U.S. users. Russia helped build it and is using it. The European Space Agency and Japan have produced major components of the station, on the promise that they will get to work there. But important modules such as the Centrifuge Accommodation Module constructed by the Japanese will not be launched. The international space science community is dismayed at the bait-and-switch appearance of the situation.

Because the Moon mission comes first, research in support of the long Mars mission is being eliminated or "deferred." Basic science and technology programs, including physiology and life support, robotics, and information systems, have been "descoped": that's NASA-speak for dropped. Worse still, NASA's life science program has been relegated to a corner in an exploration office that is more concerned with rockets than with cutting-edge research.

How did all this come about? Charles Oman, the director of the Man Vehicle Laboratory at the Massachusetts Institute of Technology (MIT), was chair of NASA's Space Station Utilization Advisory Committee and was a member of its Biological and Physical Research Advisory Committee. When the president announced VSE, the latter group was assured by an associate administrator that basic research would be continued because it would be essential to the vision. Well, Oman's committee has been disbanded, and the associate administrator who gave the assurances has been reassigned. Oman adds that "all the NASA Advisory Council subcommittees that spoke to the value of basic research are gone."

What is likely to be the fate of science in this new vision for space exploration? Even if NASA finds the money and the will to do the research needed to protect the human travelers, the agency's history offers little reason for confidence. Larry Young, MIT bioengineer, longtime NASA adviser, and one-time payload specialist astronaut in training, has this to say about those prospects: "NASA always uses research as justification for its large manned missions, but once they are under way the engineering, political, and fiscal factors take over and the science constituency is often cast aside."

We can hope that VSE will come to represent the triumph of hope over experience. But will the basic and applied science be done beforehand that is necessary to keep the explorers safe and healthy, or will these professionals seem more like participants in another extreme sport? There are promises that some of these programs will be restarted after the Moon piece of VSE is done, but then the scientists will be someplace else, and NASA will need years to grow some more seed corn. Griffin should consider some fixes: First, restore NASA's Advisory Council to its full membership; second, ask it to conduct a thorough study of which life sciences efforts are essential to the new vision; and finally, rescue the life scientists and bring them back to the science office.

Donald Kennedy
Editor-in-Chief

10.1126/science.1122663

CREDIT: TIM SMITH

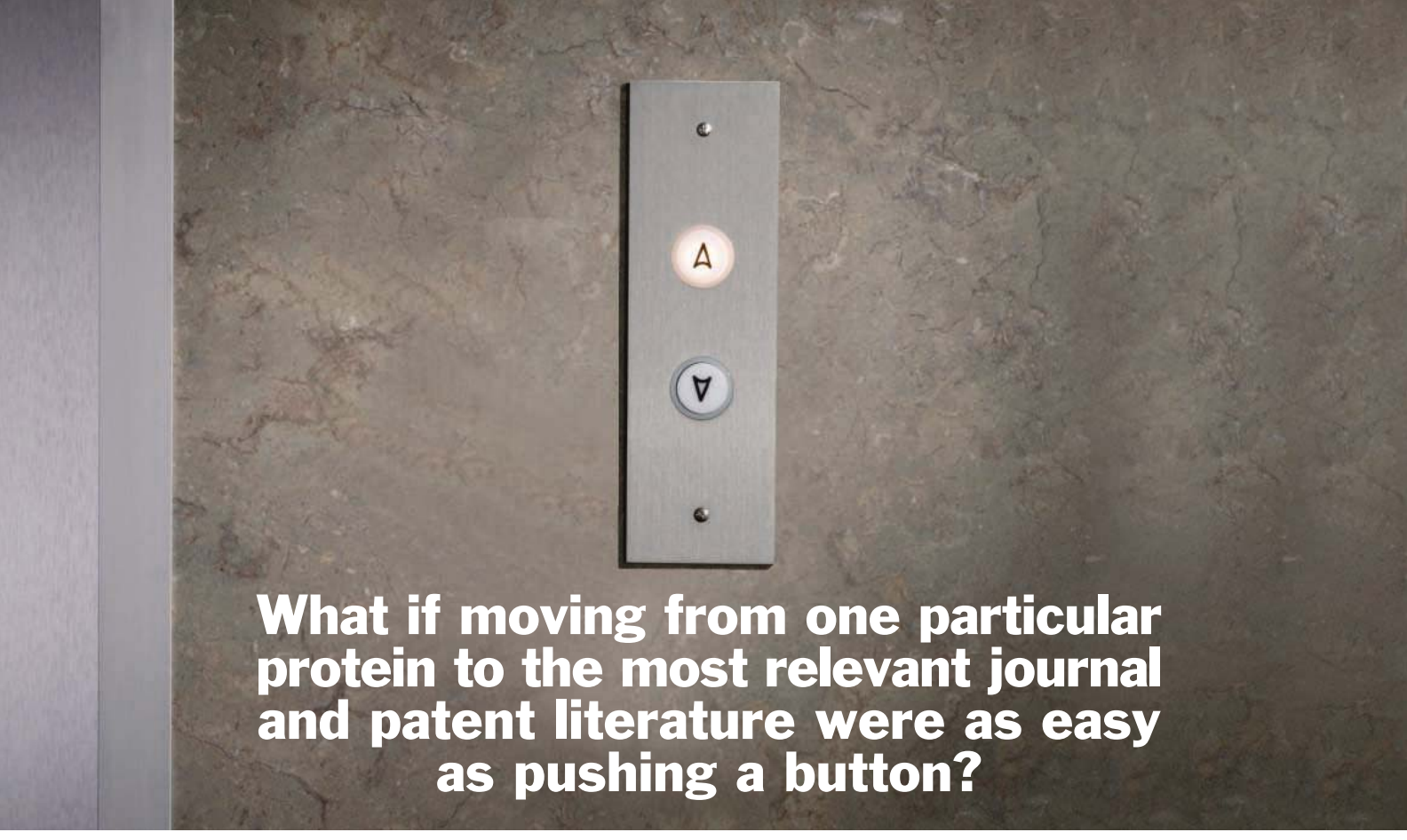

What if moving from one particular protein to the most relevant journal and patent literature were as easy as pushing a button?

It is.

Not only does SciFinder provide access to more proteins and nucleic acids than any publicly available source, but they're a single click away from their referencing patents and original research.

Coverage includes everything from the U.S. National Library of Medicine's (NLM) MEDLINE® and much more. In fact, SciFinder is the only single source of patents and journals worldwide.

Once you've found relevant literature, you can use SciFinder's powerful refinement tools to focus on a specific research area, for example: biological studies such as target organisms or diseases; expression microarrays; or analytical studies such as immunoassays, fluorescence, or PCR analysis. From each reference, you can link to the electronic full text of the original paper or patent, plus use citation tools to track how the research has evolved and been applied.

Visualization tools help you understand results at a glance. You can categorize topics and substances, identify relationships between areas of study, and see areas that haven't been explored at all.

Comprehensive, intuitive, seamless—SciFinder directs you. It's part of the process. To find out more, call us at 1-800-753-4227 (North America) or 1-614-447-3700 (worldwide) or visit www.cas.org/SCIFINDER.

SciFinder®

Part of the process.SM

CAS®

EDITORS' CHOICE

edited by Gilbert Chin

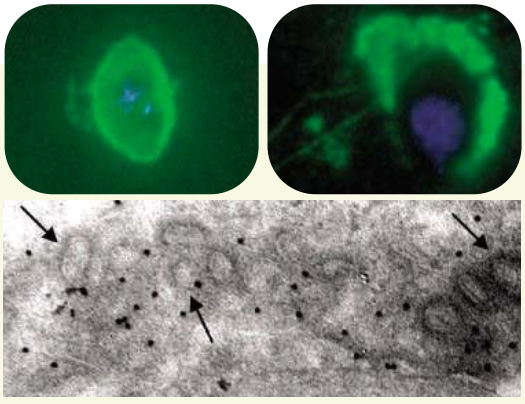

An early (top left) and late (top right) parasite (blue)–containing vacuole with p47 (green) localized at the membrane; p47 (bottom, black dots)–positive vesicles separating from the parasitophorous vacuolar membrane.

CREDITS: (TOP) MARTENS *ET AL.*, *PLOS PATHOG.* 1, E24 (2005); (BOTTOM) VINCENT *ET AL.*, *PROC. NATL. ACAD. SCI. U.S.A.* 10.1073/PNAS.0504499102 (2005)

PARASITOLOGY

Vacuolar Deconstruction

The protozoan parasite *Toxoplasma gondii* actively invades host cells during infection and sets up house within a cytoplasmic structure known as a parasitophorous vacuole, created from the host cell plasma membrane. The host cells repel the invader, of course, and mice display an interferon-γ–induced cell autonomous immunity that depends on a class of GTPases: the p47 GTPases.

Martens *et al.* describe the mechanism of protection conferred by the p47 GTPases. These proteins appear to promote the disruption of the parasitophorous vacuole and the enclosed parasites. After invasion, several p47 GTPases accumulate in a GTP-dependent fashion on the parasitophorous vacuole membrane, which then suffers vesiculation, and eventually the vacuole and the parasite are destroyed. Elevated expression of the GTPases accelerates the disruption process, and inhibition of the GTPase activity by the expression of a dominant negative form interferes with interferon-γ–induced killing of the pathogen.

In a separate study, Bekpen *et al.* looked at the species distribution of p47 GTPases and explain why humans are more susceptible than mice to *T. gondii* infections. Humans express only a single form of the p47 GTPase, compared with more than 20 in the mouse, and it is not induced in response to interferon-γ; hence, humans lack an innate form of defense against protozoan parasites.—SMH

PLoS Pathog. **1,** e24 (2005); *Genome Biol.* **6**, R92 (2005).

ECOLOGY

It's Not Always a Bed of Roses

Many plants maintain mutualisms with systemic fungi (endophytes): The fungi gain nutrients and the plants gain resistance via fungal alkaloids against stress, pathogens, and herbivores. But the benefit/cost equation can be pulled from mutualism toward antagonism by the effects of other variables in the community.

Lehtonen *et al.* found that when a hemiparasite, in this case yellow rattle, enters a grass/endophyte system, the yellow rattle becomes more successful at deterring aphid attack. Ultimately, the endophyte-positive grass suffered more from parasitism and grew less than similarly parasitized but endophyte-free grass. What seems to be happening is that the yellow rattle is not only taking nutrients from the grass but also obtaining the fungal alkaloids, which then repel the aphids. So together the yellow rattle and the fungus are sapping nutrients from the host grass, and the fungus no longer supplies as much protective benefit to its grass host. — CA

Ecol. Lett. **8**, 1256 (2005).

BIOCHEMISTRY

Controlled Combustion

Diatomic molecules are mostly not too different in size and shape, yet they can be vital nutrients, such as O_2, or inimical to aerobic energy metabolism, as when CO blocks O_2 binding to the heme Fe in hemoglobin or when CN^- poisons mitochondrial cytochrome c oxidase. Nevertheless, both CO and CN^- can be found as stable Fe ligands in the [NiFe] hydrogenases, which use a bimetallic cluster to extract energy from the oxidation of H_2. Most hydrogenases operate only in the absence of oxygen, but Vincent *et al.* use protein film voltammetry to show that the membrane-bound hydrogenase of the bacterium *Ralstonia eutropha* is essentially insensitive to CO and can still effect H_2 oxidation at ambient oxygen levels. As a preliminary indication of its potential use in fuel cells, two electrodes, one coated with the *Ralstonia* hydrogenase and the other with laccase, immersed in aqueous solution and flushed with H_2 and air, work together to convert H_2 into H_2O with an open-circuit voltage of almost 1 V. — GJC

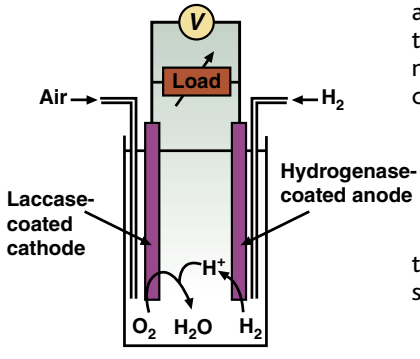

A simple fuel cell.

Proc. Natl. Acad. Sci. U.S.A. 10.1073/pnas.0504499102 (2005).

GEOCHEMISTRY

Shifting Grasses

One of the major ecological changes in the recent past in East Africa was a great expansion of grasslands from about 10 to 15 million years ago (Ma) to the present. This change had a pronounced effect on the evolution of many African species, including humans. Feakins *et al.* reveal some important details about this expansion by analyzing carbon isotope ratios in organic compounds derived uniquely from African terrestrial plants preserved in a marine core in the Gulf of Aden. Because grasses photosynthesize using the C_4 pathway, they produce a diagnostic shift in carbon isotopes in plant material when compared to C_3 plants—mostly trees and shrubs. The record, although discontinuous, shows that although some grasses were present by 9 Ma, the major expansion occurred after about 3.4 Ma. Interestingly, the detailed record shows dramatic oscillations in the abundance of grasses, likely tied to Milankovitch cycles, beginning about 3.8 Ma, before the onset of glacial cycles. Evolving African mammalian species would have to have adapted to these shifts. — BH

Geology **33**, 977 (2005).

CONTINUED ON PAGE 1249

Advanced Quality. Reliable Performance. Better Oligos.

QSR-773

For U.S. Certification Only

100% Quality Control, 100% of the Time

Our quality standards are so high, we guarantee every oligo will work, every time. Just choose your oligo, and we'll select the best quality control procedures to ensure both accuracy and consistency. When we synthesize complex oligos, we will use a combination of state-of-the-art analytical techniques to guarantee performance. Here are just a few of the ways we lead the world in quality control:

- ***MALDI-TOF Mass Spectrometry:*** *Verified composition.*
- ***Electrospray Ionization Mass Spectrometry (ESI-MS):*** *Validated composition for oligos longer than 50 bases*
- ***Capillary Electrophoresis (CE):*** *Guaranteed consistent measurement of purity.*
- ***Polyacrylamide Gel Electrophoresis (PAGE):*** *Quality tested purity and oligo length.*

What Does ISO Mean To You?

- **Consistent Product and Service through Well-Documented Processes**
- **Reduced Cost through Continual Process Improvement**
- **Reduced Cycle Time for Quick Delivery**

ISO 9001:2000 registered: Canada, Germany, Japan and the USA.

ISO 14001:1996 registered: UK

For our latest insights on oligo quality and our performance guarantee, please visit:
sigma-aldrich.com/oligos_iso

sigma-aldrich.com

YOUR GLOBAL PARTNER FOR INNOVATIVE CUSTOM GENOMIC AND PROTEOMIC SOLUTIONS
SIGMA-GENOSYS • 1442 LAKE FRONT CIRCLE • THE WOODLANDS • TEXAS 77380 • USA

SIGMA® GENOSYS

CHEMISTRY

Two-Handed Catalysts

Enzymes derive some of their effectiveness by orienting substrates into reactive conformations. This technique can be challenging to mimic using small molecule catalysts, which lack the structural complexity of a protein. However, hydrogen bonding has recently shown promise in achieving enzyme-like directing effects with a simpler scaffold, and Rajaram and Sigman have developed chiral oxazoline-derived catalysts with

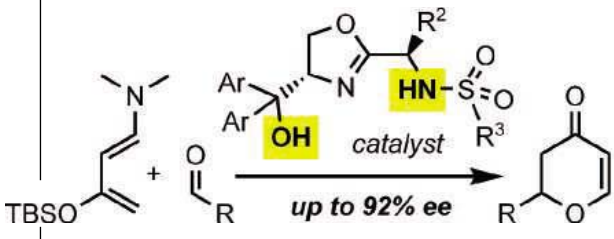

Catalyst structure and Diels-Alder reaction.

two proximal hydrogen bond donor sites: a hydroxyl group and a secondary amine. The catalysts are efficiently prepared from amino acids and feature tunable donor strength through variation of the nitrogen substituent. Initial work has produced an optimized structure for the catalytic asymmetric hetero Diels-Alder addition of aryl aldehydes to substituted dienes. Appending a camphor sulfonyl group to the amine drives the reaction with enantiomeric excesses up to 92%. Products of this reaction can then be efficiently elaborated to useful pyranone intermediates. The dual hydrogen-bonding sites proved crucial for grasping the substrates, because catalysts lacking either the hydroxyl or the amine group afforded significantly diminished yields and selectivities. — JSY

Org. Lett. 10.1021/ol052300x (2005).

CLIMATE SCIENCE

Estimates, Uncertainties, and Noise

Reconstructing a temperature record for the past from proxy data (e.g., tree rings, corals, and ice cores) is difficult because proxies are imperfect thermometers, and the noise that contaminates the temperature signal can introduce large uncertainties into any estimate. The two most common statistical techniques used to interpret these noisy data sets are the climate field reconstruction (CFR, well suited for spatial patterns) and composite-plus-scale (CPS, with a simpler statistical procedure) methods. Evaluating the fidelity of those approaches is difficult, however, because the direct observational temperature record is too short and too incomplete to allow them to be verified thoroughly. Climate models can be used to do this, though, because their temperature outputs can be made arbitrarily long and geographically complete, so that the CFR and CPS methods can be tested using a virtual climate record that is essentially perfect.

Mann *et al.* conducted such tests in order to address a recently made claim that real-world proxy-based temperature reconstructions might tend to systematically underestimate century-scale temperature variability. They find that neither method is prone to such behavior and that both can provide an accurate estimate of actual long-term hemispheric temperature histories, within estimated uncertainties. Therefore, although each method has its own strengths and weaknesses, some concerns about their basic utility seem unfounded. — HJS

J. Clim. **18**, 4097 (2005).

PSYCHOLOGY

A Dating Rating

Why people choose the mates they do can be a topic of endless discussion. Three of the best-known explanations are (i) that opposites attract; (ii) that we look for someone just like ourselves; and (iii) that there are cross-cultural attributes that everyone would like to have in their partners (but that only a lucky few do).

Zentner has developed an inventory to measure the personality characteristics of one's ideal mate and applied it to college students in conjunction with an established questionnaire for reporting one's own personality facets. He finds that there is roughly the same variability across individuals in the two measures, arguing against the existence of a universally desired set of attributes. Furthermore, in a longitudinal sampling, the similarity of one's actual mate and one's idealized choice along the dimensions of agreeableness and openness was important and predictive of satisfaction with the relationship. — GJC

J. Pers. Soc. Psych. **89**, 242 (2005).

CREDITS: RAJARAM AND SIGMAN, *ORG. LETT.* 10.1021/OL052300X (2005)

ScienceCareers.org is the leading careers resource for scientists. And now it offers even more. In addition to a brand new website with easier navigation, ScienceCareers.org now includes Next Wave, the essential online careers magazine. Next Wave is packed with features and articles to help advance your science career – all for free.

- Hundreds of job postings
- Career tools from Next Wave
- Grant information
- Resume/CV Database
- Career Forum

www.sciencemag.org

Science

1200 New York Avenue, NW
Washington, DC 20005
Editorial: 202-326-6550, FAX 202-289-7562
News: 202-326-6500, FAX 202-371-9227

Bateman House, 82-88 Hills Road
Cambridge, UK CB2 1LQ
+44 (0) 1223 326500, FAX +44 (0) 1223 326501

SUBSCRIPTION SERVICES For change of address, missing issues, new orders and renewals, and payment questions: 800-731-4939 or 202-326-6417, FAX 202-842-1065. Mailing addresses: AAAS, P.O. Box 1811, Danbury, CT 06813 or AAAS Member Services, 1200 New York Avenue, NW, Washington, DC 20005

INSTITUTIONAL SITE LICENCES please call 202-326-6755 for any questions or information

REPRINTS: Author Inquiries 800-635-7181
Commercial Inquiries 803-359-4578
Corrections 202-326-6501

PERMISSIONS 202-326-7074, FAX 202-682-0816

MEMBER BENEFITS Bookstore: AAAS/BarnesandNoble.com bookstore www.aaas.org/bn; Car purchase discount: Subaru VIP Program 202-326-6417; Credit Card: MBNA 800-847-7378; Car Rentals: Hertz 800-654-2200 CDP#343457, Dollar 800-800-4000 #AA1115; AAAS Travels: Betchart Expeditions 800-252-4910; Life Insurance: Seabury & Smith 800-424-9883; Other Benefits: AAAS Member Services 202-326-6417 or www.aaasmember.org.

science_editors@aaas.org (for general editorial queries)
science_letters@aaas.org (for queries about letters)
science_reviews@aaas.org (for returning manuscript reviews)
science_bookrevs@aaas.org (for book review queries)

Published by the **American Association for the Advancement of Science (AAAS)**, *Science* serves its readers as a forum for the presentation and discussion of important issues related to the advancement of science, including the presentation of minority or conflicting points of view, rather than by publishing only material on which a consensus has been reached. Accordingly, all articles published in *Science*—including editorials, news and comment, and book reviews—are signed and reflect the individual views of the authors and not official points of view adopted by the AAAS or the institutions with which the authors are affiliated.

AAAS was founded in 1848 and incorporated in 1874. Its mission is to advance science and innovation throughout the world for the benefit of all people. The goals of the association are to: foster communication among scientists, engineers and the public; enhance international cooperation in science and its applications; promote the responsible conduct and use of science and technology; foster education in science and technology for everyone; enhance the science and technology workforce and infrastructure; increase public understanding and appreciation of science and technology; and strengthen support for the science and technology enterprise.

INFORMATION FOR CONTRIBUTORS

See pages 135 and 136 of the 7 January 2005 issue or access www.sciencemag.org/feature/contribinfo/home.shtml

EDITOR-IN-CHIEF **Donald Kennedy**
EXECUTIVE EDITOR **Monica M. Bradford**
DEPUTY EDITORS **R. Brooks Hanson, Katrina L. Kelner**
NEWS EDITOR **Colin Norman**

EDITORIAL SUPERVISORY SENIOR EDITORS Barbara Jasny, Phillip D. Szuromi; SENIOR EDITOR/PERSPECTIVES Lisa D. Chong; SENIOR EDITORS Gilbert J. Chin, Pamela J. Hines, Paula A. Kiberstis (Boston), Beverly A. Purnell, L. Bryan Ray, Guy Riddihough (Manila), H. Jesse Smith, Valda Vinson, David Voss; ASSOCIATE EDITORS Marc S. Lavine (Toronto), Jake S. Yeston; ONLINE EDITOR Stewart Wills; CONTRIBUTING EDITOR Ivan Amato; ASSOCIATE ONLINE EDITOR Tara S. Marathe; BOOK REVIEW EDITOR Sherman J. Suter; ASSOCIATE LETTERS EDITOR Etta Kavanagh; INFORMATION SPECIALIST Janet Kegg; EDITORIAL MANAGER Cara Tate; SENIOR COPY EDITORS Jeffrey E. Cook, Harry Jach, Barbara P. Ordway; COPY EDITORS Cynthia Howe, Alexis Wynne Mogul, Jennifer Sills, Trista Wagoner; EDITORIAL COORDINATORS Carolyn Kyle, Beverly Shields; PUBLICATION ASSISTANTS Ramatoulaye Diop, Chris Filiatreau, Joi S. Granger, Jeffrey Hearn, Lisa Johnson, Scott Miller, Jerry Richardson, Brian White, Anita Wynn; EDITORIAL ASSISTANTS E. Annie Hall, Lauren Kmec, Patricia M. Moore, Brendan Nardozzi, Michael Rodewald; EXECUTIVE ASSISTANT Sylvia S. Kihara; ADMINISTRATIVE SUPPORT Patricia F. Fisher

NEWS SENIOR CORRESPONDENT Jean Marx; DEPUTY NEWS EDITORS Robert Coontz, Jeffrey Mervis, Leslie Roberts, John Travis; CONTRIBUTING EDITORS Elizabeth Culotta, Polly Shulman; NEWS WRITERS Yudhijit Bhattacharjee, Adrian Cho, Jennifer Couzin, David Grimm, Constance Holden, Jocelyn Kaiser, Richard A. Kerr, Eli Kintisch, Andrew Lawler (New England), Greg Miller, Elizabeth Pennisi, Robert F. Service (Pacific NW), Erik Stokstad; Carolyn Gramling (intern); CONTRIBUTING CORRESPONDENTS Marcia Barinaga (Berkeley, CA), Barry A. Cipra, Jon Cohen (San Diego, CA), Daniel Ferber, Ann Gibbons, Robert Irion, Mitch Leslie (NetWatch), Charles C. Mann, Evelyn Strauss, Gary Taubes, Ingrid Wickelgren; COPY EDITORS Linda B. Felaco, Rachel Curran, Sean Richardson; ADMINISTRATIVE SUPPORT Scherraine Mack, Fannie Groom BUREAUS: Berkeley, CA: 510-652-0302, FAX 510-652-1867, New England: 207-549-7755, San Diego, CA: 760-942-3252, FAX 760-942-4979, Pacific Northwest: 503-963-1940

PRODUCTION DIRECTOR James Landry; SENIOR MANAGER Wendy K. Shank; ASSISTANT MANAGER Rebecca Doshi; SENIOR SPECIALISTS Jay R. Covert, Chris Redwood **PREFLIGHT** DIRECTOR David M. Tompkins; MANAGER Marcus Spiegler; SPECIALIST Jessie Mudjitaba

ART DIRECTOR Joshua Moglia; ASSOCIATE ART DIRECTOR Kelly Buckheit; ILLUSTRATORS Chris Bickel, Katharine Sutliff; SENIOR ART ASSOCIATES Holly Bishop, Laura Creveling, Preston Huey; ASSOCIATE Nayomi Kevitiyagala; PHOTO RESEARCHER Leslie Blizard

***SCIENCE* INTERNATIONAL**

EUROPE (science@science-int.co.uk) EDITORIAL: INTERNATIONAL MANAGING EDITOR Andrew M. Sugden; SENIOR EDITOR/PERSPECTIVES Julia Fahrenkamp-Uppenbrink; SENIOR EDITORS Caroline Ash (Geneva: +41 (0) 222 346 3106), Stella M. Hurtley, Ian S. Osborne, Stephen J. Simpson, Peter Stern; ASSOCIATE EDITOR Joanne Baker EDITORIAL SUPPORT Alice Whaley; Deborah Dennison ADMINISTRATIVE SUPPORT Janet Clements, Phil Marlow, Jill White; NEWS: INTERNATIONAL NEWS EDITOR Eliot Marshall DEPUTY NEWS EDITOR Daniel Clery; CORRESPONDENT Gretchen Vogel (Berlin: +49 (0) 30 2809 3902, FAX +49 (0) 30 2809 8365); CONTRIBUTING CORRESPONDENTS Michael Balter (Paris), Martin Enserink (Amsterdam and Paris); INTERN Michael Schirber

ASIA Japan Office: Asca Corporation, Eiko Ishioka, Fusako Tamura, 1-8-13, Hirano-cho, Chuo-ku, Osaka-shi, Osaka, 541-0046 Japan; +81 (0) 6 6202 6272, FAX +81 (0) 6 6202 6271; asca@os.gulf.or.jp JAPAN NEWS BUREAU: Dennis Normile (contributing correspondent, +81 (0) 3 3391 0630, FAX 81 (0) 3 5936 3531; dnormile@gol.com); CHINA REPRESENTATIVE Hao Xin, + 86 (0) 10 6307 4439 or 6307 3676, FAX +86 (0) 10 6307 4358; haoxin@earthlink.net; SOUTH ASIA Pallava Bagla (contributing correspondent +91 (0) 11 2271 2896; pbagla@vsnl.com); ASIA Richard Stone +66 2 662 5818 (rstone@aaas.org)

EXECUTIVE PUBLISHER **Alan I. Leshner**
PUBLISHER **Beth Rosner**

FULFILLMENT & MEMBERSHIP SERVICES (membership@aaas.org) DIRECTOR Marlene Zendell; MANAGER Waylon Butler; SYSTEMS SPECIALIST Andrew Vargo; SPECIALISTS Pat Butler, Laurie Baker, Tamara Alfson, Karena Smith, Vicki Linton; CIRCULATION ASSOCIATE Christopher Refice

BUSINESS OPERATIONS AND ADMINISTRATION DIRECTOR Deborah Rivera-Wienhold; BUSINESS MANAGER Randy Yi; SENIOR BUSINESS ANALYST Lisa Donovan; BUSINESS ANALYST Jessica Tierney; FINANCIAL ANALYST Michael LoBue, Farida Yeasmin; RIGHTS AND PERMISSIONS: ADMINISTRATOR Emilie David; ASSOCIATE Elizabeth Sandler; MARKETING: DIRECTOR John Meyers; MARKETING MANAGERS Darryl Walter, Allison Pritchard; MARKETING ASSOCIATES Julianne Wielga, Mary Ellen Crowley, Catherine Featherston; DIRECTOR OF INTERNATIONAL MARKETING AND RECRUITMENT ADVERTISING Deborah Harris; INTERNATIONAL MARKETING MANAGER Wendy Sturley; MARKETING/MEMBER SERVICES EXECUTIVE: Linda Rusk; JAPAN SALES Jason Hannaford; SITE LICENSE SALES: DIRECTOR Tom Ryan; SALES AND CUSTOMER SERVICE Mehan Dossani, Kiki Forsythe, Catherine Holland, Wendy Wise; ELECTRONIC MEDIA: MANAGER Lizabeth Harman; PRODUCTION ASSOCIATES Sheila Mackall, Amanda K. Skelton, Lisa Stanford, Nichele Johnston; APPLICATIONS DEVELOPER Carl Saffell

ADVERTISING DIRECTOR WORLDWIDE AD SALES Bill Moran

PRODUCT (science_advertising@aaas.org); MIDWEST Rick Bongiovanni: 330-405-7080, FAX 330-405-7081 • WEST COAST/W. CANADA B. Neil Boylan (Associate Director): 650-964-2266, FAX 650-964-2267 • EAST COAST/E. CANADA Christopher Breslin: 443-512-0330, FAX 443-512-0331 • UK/EUROPE/ASIA Tracey Peers (Associate Director): +44 (0) 1782 752530, FAX +44 (0) 1782 752531 JAPAN Mashy Yoshikawa: +81 (0) 33235 5961, FAX +81 (0) 33235 5852 ISRAEL Jessica Nachlas +9723 5449123 • TRAFFIC MANAGER Carol Maddox; SALES COORDINATOR Deiandra Simms

CLASSIFIED (advertise@sciencecareers.org); U.S.: SALES DIRECTOR Gabrielle Boguslawski: 718-491-1607, FAX 202-289-6742; INSIDE SALES MANAGER Daryl Anderson: 202-326-6543; WEST COAST/MIDWEST Kristine von Zedlitz: 415-956-2531; EAST COAST Jill Downing: 631-580-2445; CANADA, MEETINGS AND ANNOUNCEMENTS Kathleen Clark: 510-271-8349; LINE AD SALES Emnet Tesfaye: 202-326-6740; SALES COORDINATORS Erika Bryant; Rohan Edmonson Christopher Normile, Joyce Scott, Shirley Young; INTERNATIONAL: SALES MANAGER Tracy Holmes: +44 (0) 1223 326525, FAX +44 (0) 1223 326532; SALES Christina Harrison, Svitlana Barnes; SALES ASSISTANT Helen Moroney; JAPAN: Jason Hannaford: +81 (0) 52 789 1860, FAX +81 (0) 52 789 1861; PRODUCTION: MANAGER Jennifer Rankin; ASSISTANT MANAGER Deborah Tompkins; ASSOCIATES Christine Hall; Amy Hardcastle; PUBLICATIONS ASSISTANTS Robert Buck; Natasha Pinol

AAAS BOARD OF DIRECTORS RETIRING PRESIDENT, CHAIR Shirley Ann Jackson; PRESIDENT Gilbert S. Omenn; PRESIDENT-ELECT John P. Holdren; TREASURER David E. Shaw; CHIEF EXECUTIVE OFFICER Alan I. Leshner; BOARD Rosina M. Bierbaum; John E. Burris; John E. Dowling; Lynn W. Enquist; Susan M. Fitzpatrick; Richard A. Meserve; Norine E. Noonan; Peter J. Stang; Kathryn D. Sullivan

AAAS
ADVANCING SCIENCE, SERVING SOCIETY

NetWatch

edited by Mitch Leslie

DATABASE

Another Day, Another Genome

For genome sequencers, it's just over 300 down and at least 1300 to go. Keep tabs on the progress of DNA sequencing projects at Genomes OnLine Database (GOLD), maintained by Nikos Kyrpides of the Joint Genome Institute in Walnut Creek, California, and colleagues. As of last week, scientists had polished off 319 genomes, including that of the sea squirt *Ciona intestinalis* (above), a close relative of vertebrates. The site lists information on these efforts, such as who performed the sequencing, where the results are housed, and whether they are public or proprietary. GOLD also tracks more than 1300 ongoing projects.

www.genomesonline.org

ONLINE JOURNAL

Bioethics Views From the Campus

This online journal lets undergraduate students intrigued by the interplay between science, society, and the law reach a national audience. *The Triple Helix* involves student chapters from Cornell University, the Massachusetts Institute of Technology, the University of Pennsylvania, and other schools. The site offers student-written features and news updates on topics such as the recently proposed home HIV tests. You can also download a PDF of the first print issue of the journal, which included articles on the Vioxx recall and the ethics of xenotransplantation. The next issue will appear on several campuses this month and online.

www.thetriplehelix.org

FUN

Turn That Down!

Brace yourself if you tune in to Bad Vibes from the University of Salford, U.K. The site is canvassing netizens to determine which noise people find most horrible. Visitors get to rate some 30 annoying, sickening, or grating recordings, from scraping Styrofoam to the yowls of Tasmanian devils. The results will not only nail down the most noisome sound, but they also might help scientists understand why we find some sounds offensive. So far, the top vote getter is audio of somebody retching, followed by microphone feedback and bawling babies.

www.sound101.org

WEB LOGS

The Darwin Brigade

Darwin's contemporaries Thomas Huxley and Joseph Hooker championed his theory in print and in lectures. If they were alive today and had a little attitude, they might craft something like The Panda's Thumb, a Web log in which a cadre of Darwin's modern-day defenders pummels antievolution pseudoscience such as "intelligent design" (ID). The site gets its name from a Stephen Jay Gould essay about the giant panda's adaptation for stripping bamboo leaves—it's a jury-rigged feature a clever designer wouldn't engineer. Panda's Thumb regulars—who range from Ph.D.s and grad students to a businessman and a lawyer—comb the news media for follies to expose and errors to correct. The site provided blanket coverage of the recent trial on the Dover, Pennsylvania, school board's decision to require teaching of ID (*Science*, 18 November, p. 1105). Panda's Thumb also highlights evolution-related research, such as a study showing that the antibiotics produced by our immune systems may not be a panacea for drug-resistant bacteria.

www.pandasthumb.org

EXHIBITS

Newton Confidential

Isaac Newton was up to something that he concealed from his scientific contemporaries. He was experimenting with alchemy—a mystical endeavor that sought to turn base metals into gold. To explore this little-known side of the great physicist, drop by The Chymistry of Isaac Newton, run by science historian William Newman of Indiana University, Bloomington.

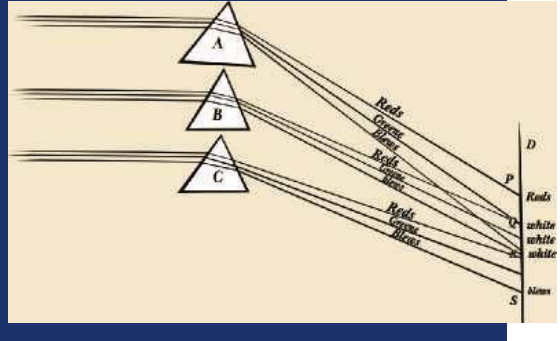

Newton pursued "chymistry," the 17th century term for alchemy, for some 30 years. At the time, alchemists undertook genuine chemistry but also pursued dubious projects such as transmuting metals, and the practice fell into disrepute. The site publishes the first complete transcript of one of Newton's key lab notebooks, which shows that his alchemy and science intertwined. The pages brim with alchemical recipes but also record some of his pioneering optical observations, such as his discovery that white light comprises a spectrum of colors (above). Newman plans to add annotated versions of all of Newton's writings on chymistry. To browse one of these manuscripts, link to the site for a PBS *NOVA* program on Newton that aired earlier this month.

webapp1.dlib.indiana.edu/newton/index.jsp

Send site suggestions to netwatch@aaas.org. Archive: www.sciencemag.org/netwatch

CREDITS (TOP TO BOTTOM): LAWSON WOOD/CORBIS; JUPITER IMAGES; DARICK CHAMBERLIN

NEWS

This Week

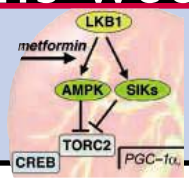

PAGE 1259
New findings explain old drug

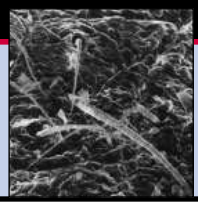

1260
News from neuroscience meeting

AVIAN INFLUENZA

China Will Attempt Largest-Ever Animal Vaccination Campaign

China watchers say it's no coincidence that the country announced a massive poultry-vaccination campaign just a day before confirmation of its first human fatality from the H5N1 strain of bird flu. "As long as it was in animals and not seen to be in humans, there was a certain complacency," says Roy Wadia, spokesperson for the World Health Organization (WHO) in Beijing.

Public health experts welcomed the announcement as a sign that China is getting serious about bird flu, which has led to the death of more than 150 million birds in Asia and 67 human fatalities. China recently set up a national bird flu task force with $247 million to finance initiatives such as rewards for people who report unusual poultry deaths and compensation for farmers who lose birds. China's decision to vaccinate its entire poultry population—some 5 billion chickens, geese, and ducks—seems to be a recognition that the best way to keep H5N1 out of humans is to keep it out of birds.

But as other countries in Asia have learned, there's more to vaccination than just jabbing chickens. Although experts increasingly agree that vaccination should be considered as a part of an H5N1 control strategy, it is hard to implement well. Countries must aggressively track circulating virus, for instance. And reaching every domestic bird, especially in a country like China, is difficult.

Hong Kong, where H5N1 was first identified in 1997, has become a poster child for the strategy. Since it began vaccinating all domestic birds in early 2003, the territory has remained free from H5N1 infection. Vietnam is now in the midst of a vaccination campaign that will cover nearly all of the country's 200 million birds.

Logistical challenge. China will have to vaccinate individually each of its more than 5 billion chickens, geese, and ducks, both in backyard and large commercial operations.

A challenge with vaccination is distinguishing vaccinated from infected birds. One solution is to use a vaccine based on a slightly different virus strain, such as H5N2, which provides protection against H5N1 but allows birds to be distinguished by simple lab tests. Hong Kong is using an H5N2 vaccine and also placing unvaccinated sentinel birds among each flock. Vietnam, relying on international support, has opted to use a vaccine based on the H5N1 virus and to upgrade its lab facilities to do the more sophisticated testing required. China has been mostly using H5N1 vaccines, but details of its ▶

U.S. BUDGET

NIH Set for Tiny Spending Hike in 2006

Despite a surprise legislative setback, the National Institutes of Health (NIH) appears likely to receive the president's budget request for 2006—a 0.7% increase to $28.6 billion that leaves the agency with what one lobbyist calls "unpalatable choices." However, biomedical community leaders are heartened that Congress rejected a proposal to revoke funds for two NIH grants and accepted language that bolsters the independence of scientific advisory panels.

Last week, as part of a larger spending bill, House and Senate conferees agreed to increase NIH's budget by $253 million. That amount falls far short of a $1.05 billion boost that the Senate had passed and marks the third year of increases below biomedical inflation. And once $97 million earmarked for biodefense is removed, the final figure reflects a 0.5% boost—the smallest increase in 36 years. A rare rejection of the entire conference report by the House left the bill in limbo at press time, although observers don't foresee any changes to NIH's portion.

Based on the conference report, Representative David Obey (D–WI) warned that NIH will be forced to fund 505 fewer new grants than in 2004. The agency also anticipates funding fewer training grants. "The agency is going to have to confront a series of unpalatable choices," says Dave Moore, head of governmental relations for the Association of American Medical Colleges. And the worst may not be over: Congress is weighing an across-the-board cut in all spending bills to pay for recovery costs from hurricanes Katrina and Rita and the president's proposed $7.1 billion pandemic flu plan, Moore says.

To the relief of biomedical scientists, the conference bill drops a House provision that would have revoked funds for two NIH grants studying visual perception in pigeons and factors involved in stable marriages (*Science*, 1 July, p. 29). And it retains a Senate amendment that would bar Health and Human Services (HHS) officials from asking candidates for scientific advisory committees about their political views—a response to such litmus tests earlier in the Bush Administration. The amendment also orders HHS not to use its budget "to disseminate scientific information that is deliberately false or misleading."

–JOCELYN KAISER

CREDIT: GREG BAKER/AP PHOTO

1264
Katrina's aftermath

1271
Clues to superconductivity mystery

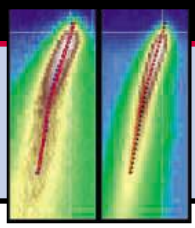

1272
Decision time for Europe's space plans

new campaign have not been released.

But "vaccination by itself is not enough," says Kitman Dyrting, senior veterinary officer with Hong Kong's Agriculture Fisheries and Conservation Department. It should be coupled with biosecurity measures, such as keeping domestic birds from contact with wild birds and sanitizing poultry farms—steps tricky to implement for backyard flocks. This is particularly relevant for mainland China, where an estimated 50% of all poultry are free ranging. Carolyn Benigno, a Bangkok-based animal health officer for the U.N. Food and Agriculture Organization, says that given the difficulty and expense of rapidly improving biosecurity for backyard holders, vaccination "could reduce the virus load in the environment."

China also plans to compensate farmers for losses, which will likely mean better reporting of outbreaks. Poorer farmers have been reluctant to tell authorities about sick birds, preferring to try to sell or eat them. And China will strengthen surveillance for human cases, particularly in provinces hit by outbreaks in poultry. A WHO expert team has been in China advising the country on field surveillance and lab work.

Tests at a national lab have confirmed that a poultry worker died of H5N1 on 10 November, and an infected 9-year-old boy is recovering. His sister almost certainly died of an H5N1 infection, but the body was cremated before samples were taken. It's a puzzle why China had not recorded any human cases previously, says Wadia, as the virus has been circulating there since at least early 2004. If cases were missed in the past, he says, they are less likely to be missed in the future.

–DENNIS NORMILE

With reporting by Gong Yidong of *China Features* in Beijing.

GENETICS

Expression of Endorphin Gene Favored in Human Evolution

Humans and chimpanzees share at least 98% of their DNA sequences. Yet chimps are an endangered species, whereas humans have used their superior cognition to transform the face of the earth. What makes the difference? Thirty years ago, geneticist Mary-Claire King and biochemist Allan Wilson proposed that changes in how genes are regulated, rather than in the proteins they code for, was the key (*Science*, 11 April 1975, p. 107). A new study of evolutionary changes in the regulation of a gene implicated in perception, behavior, and memory suggests that King and Wilson may have been at least partly right.

Other researchers say that the new study is one of the first human examples of selection acting on a regulatory element, and it adds to a short list of brain genes now known to have been favored during the evolution of humans. "The evidence is compelling," says evolutionary geneticist Bruce Lahn of the University of Chicago. But he and others note that it is not yet clear what mental or behavioral traits were favored by selection in this case.

An international team led by evolutionary biologist Gregory Wray of Duke University in Durham, North Carolina, focused on the gene that codes for the protein prodynorphin (PDYN), a precursor to a number of endorphins (opiatelike molecules involved in learning, the experience of pain, and social attachment and bonding). The *PDYN* gene is controlled by a promoter region just upstream from the gene's coding region. Earlier studies had highlighted a 68 DNA base pair (bp) segment of the promoter that varies among humans, who carry between one and four copies of it. It isn't clear how the number of copies and other variations in the segment affect the gene's function, although some variants have been linked to schizophrenia, cocaine addiction, and epilepsy.

Wray and his colleagues sequenced the promoter and some flanking DNA from 74 human chromosomes as well as 32 chromosomes from seven other primates, including chimps, gorillas, and orangutans.

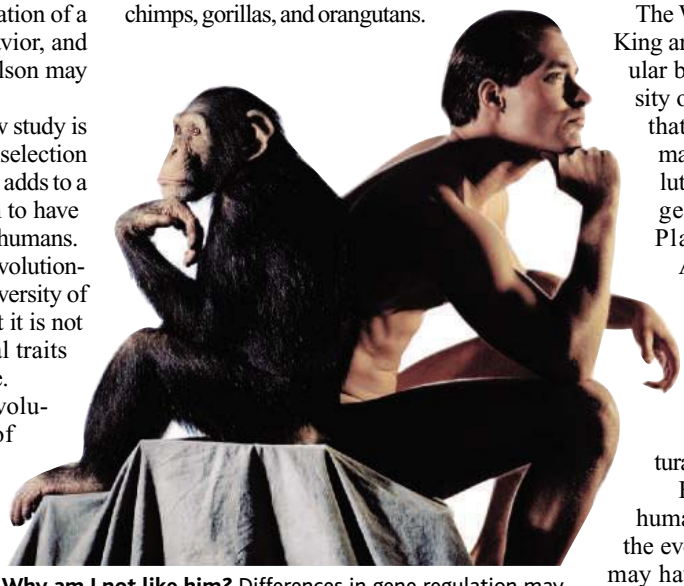

Why am I not like him? Differences in gene regulation may help set humans and chimps apart.

CREDIT: JAMES BALOG/GETTY IMAGES

As the team reports in the December issue of *PloS Biology*, none of the nonhuman primates had more than one copy of the 68-bp segment. In addition, all human segments had five DNA mutations not seen in the other primates. The team concludes that the pattern is a solid example of natural selection acting on the human lineage after it split from the chimp line about 5 million to 7 million years ago.

To see whether the differences in promoters actually altered gene expression, the team introduced either the chimp or human 68-bp segment into human neural cells. The human segment induced a 20% greater expression of the *PDYN* gene than did the chimp segment.

The Wray team's work "speaks directly to King and Wilson's hypothesis," says molecular biologist Sean Carroll of the University of Wisconsin, Madison. Carroll adds that the authors have provided a "road map" for experimental tests of the evolution of gene regulation. Evolutionary geneticist Svante Pääbo of the Max Planck Institute for Evolutionary Anthropology in Leipzig, Germany, agrees that the paper provides "convincing evidence for positive selection." But Pääbo cautions that this one example does not prove that regulatory mutations were more important than structural mutations during human evolution.

Because of *PDYN*'s importance in human biology, the authors suggest that the evolutionary changes in its regulation may have helped set chimps and humans apart. But Lahn says that such a conclusion is premature until researchers know more about why these changes were favored by natural selection. "It is a bit early to say that these changes were key to what makes us human," Lahn says. "But it seems like a reasonable hypothesis."

–MICHAEL BALTER

PIERCE

Grasp the Proteome®

Plant Cell Lysis

Is your plant cell lysis leafing you out in the cold?

The P-PER® Reagent Kit† (#89803) extracts maximum active protein from stem, root, seed and leaves in 10 minutes without liquid nitrogen.

You can trust the experts at Pierce to know how to get maximum protein extraction from your sample. We have been the protein people for over 50 years, providing the best solutions to extract, purify and quantify proteins from many types of cell lines and tissue.

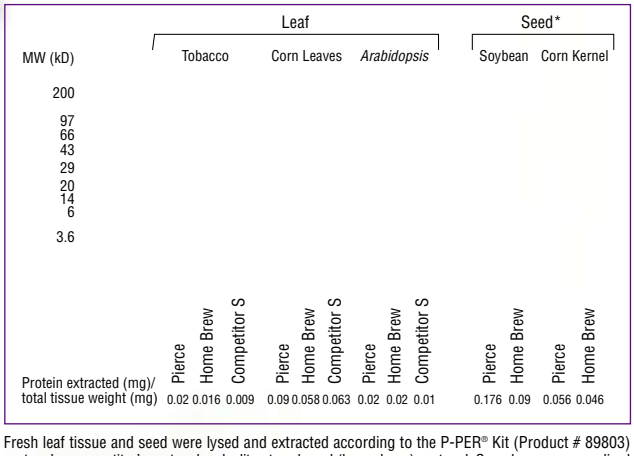

Fresh leaf tissue and seed were lysed and extracted according to the P-PER® Kit (Product # 89803) protocol, a competitor's protocol and a literature-based (home brew) protocol. Samples were normalized (weight tissue/volume extract), resolved on a 10% *Bis*-Tris gel and stained with Imperial™ Protein Stain† (Product # 24615). Samples were also quantified using the BCA™ Protein Assay Kit, Reducing Agent Compatible (Product # 23250).

*The Competitor S kit is not recommended for dried seed.

P-PER® Reagent Kit Highlights:

- **Convenient** – disrupts cells without harsh mechanical methods in 10 minutes
- **Compatible** – downstream applications include 1-D and 2-D gel electrophoresis, Western blotting, activity assays, and protein affinity purifications
- **Quantifiable** – use the BCA™ Protein Assay Kit, Reducing Agent Compatible†
- **Ready-to-use** – extract does not require filtration through cheesecloth or Miracloth
- **Provides active proteins** – extracted proteins are functional

New! Poppers™ Cell Lysis Solutions Handbook
Log on to our web site or call us to request your FREE handbook (#1601234). Outside the U.S., contact Perbio Science or your local distributor.

www.piercenet.com/pper22j

PIERCE

Tel: 815-968-0747 or 800-874-3723 • Fax: 815-968-7316 • Customer Assistance E-mail: CS@piercenet.com

Outside the United States, visit our web site or call 815-968-0747 to locate your local Perbio Science branch office (below) or distributor

Belgium & Dist.:	China:	France:	Germany:	Hong Kong:	The Netherlands:	United Kingdom:	Switzerland:
Tel +32 53 85 7184	Tel +86 10 8049 9033	Tel 0800 50 82 15	Tel 0228 9125650	Tel 852 2753 0686	Tel 076 50 31 880	Tel 0800 252185	Tel 0800 56 31 40
euromarketing@perbio.com	support@perbio.com.cn	euromarketing@perbio.com	de.info@perbio.com	SalesHK@perbio.com	euromarketing@perbio.com	uk.info@perbio.com	euromarketing@perbio.com

PERBIO

MEDICINE

Cancer-Suppressing Enzyme Adds a Link to Type 2 Diabetes

Every so often, research in one field suddenly bumps into another field. Take an enzyme known as LKB1. Discovered about 7 years ago as the product of a tumor-suppressor gene, LKB1 is now turning out to be a key regulator of the body's metabolic activities, including its handling of glucose—a discovery that connects LKB1 to type 2 diabetes and may explain its link to cancer.

The latest developments in the LKB1 saga, published online this week by *Science* (www.sciencemag.org/cgi/content/abstract/1120781), come from a team led by Reuben Shaw and Lewis Cantley of Beth Israel Deaconess Medical Center in Boston. Working with mice, the researchers have shown that the protein controls glucose production by the liver. In doing so, they've nailed down the mechanism of action for a drug that's been used to treat type 2 diabetes for nearly 50 years. Until now, it had been unclear how the drug, metformin, lowers a person's blood glucose.

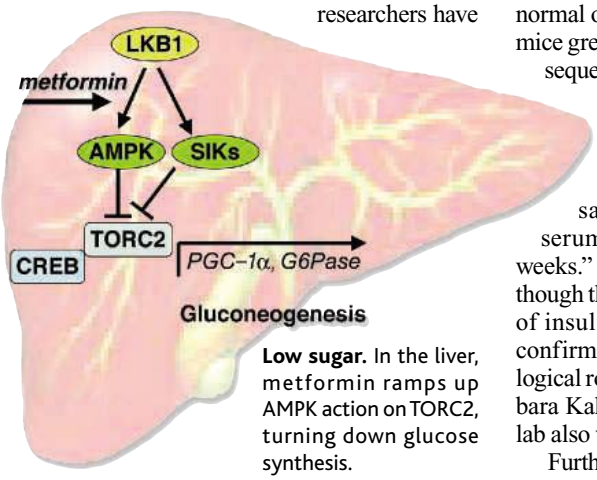

Low sugar. In the liver, metformin ramps up AMPK action on TORC2, turning down glucose synthesis.

The *LKB1* gene was originally discovered in 1998 as the gene mutated in Peutz-Jeghers syndrome, a rare hereditary form of cancer usually affecting the intestines. Because the causative mutations inactivate the gene, it appeared to be a tumor suppressor. The gene's sequence indicated that it produces one of the cell's many kinases—enzymes that regulate the activity of other proteins by attaching phosphate groups to them—but its targets were unknown.

About 2 years ago, the Beth Israel Deaconess team and those of David Carling at Imperial College School of Medicine in London and Grahame Hardie at the University of Dundee, U.K., showed that LKB1 phosphorylates—and thus activates—a protein called AMPK (for AMP-activated protein kinase) that may help protect the body from metabolic diseases such as type 2 diabetes. Activity of AMPK leads to decreased glucose production by the liver as well as increased uptake of the sugar by muscle—both actions that would help keep blood glucose levels down. Cantley points out that this activity may contribute to LKB1's tumor-suppressive effects by depriving tumor cells of the energy they need to grow.

Since discovering that LKB1 activates AMPK in cell culture experiments, investigators have sought to confirm the relationship in living animals. A few months ago, Hardie's team, working with that of Dario Alessi, also at Dundee, reported in the *EMBO Journal* that reducing *LKB1* gene expression to 10% of normal or less in the skeletal muscle of living mice greatly reduces AMPK activity, and consequently glucose uptake, in that tissue.

In the current work, Shaw genetically engineered mice so that the *LKB1* gene was turned off only in the liver. Those animals, Cantley says, "had extremely high levels of serum glucose that were maintained for weeks." The levels stayed up, he notes, even though the animals increased their production of insulin in response. These experiments confirm that LKB1 plays a "critical physiological role" in glucose metabolism, says Barbara Kahn of Beth Israel Deaconess, whose lab also works on AMPK.

Further experiments, performed in collaboration with Marc Montminy and colleagues at the Salk Institute for Biological Studies in San Diego, California, provided more information about how lack of LKB1, and the resulting decrease in AMPK activity, causes this persistent overproduction of glucose. Normally, AMPK phosphorylates a protein called TORC2, an alteration that keeps the protein in the cell cytoplasm. But when TORC2 is not phosphorylated, it enters the nucleus and turns on genes needed for glucose synthesis.

Previous work suggested that metformin works at least partly by stimulating AMPK activity in the liver. Shaw, Cantley, and their colleagues have now shown that although the drug stimulates AMPK phosphorylation in the livers of normal mice, it did not do so in mice whose livers could not produce LKB1. Nor did it decrease blood glucose concentrations in those animals. "This paper clinches" the idea that metformin exerts its effects through AMPK, Hardie says, although that enzyme apparently needs to be activated first by LKB1. And so a tumor-suppressor gene has solved a 50-year-old mystery about a diabetes drug.

–JEAN MARX

CREDIT: R. SHAW *ET AL.*, *SCIENCE*

ScienceScope

Rein In Patents, Panel Urges

It's relatively easy to claim ownership of biological information in the United States—perhaps too easy, says a National Academy of Sciences panel. "[F]uture discoveries in genomics and proteomics that would benefit the public health and well-being could be thwarted by an increasingly complex intellectual property regime," the panel warned in a report released last week.

The panel suggests that scientists limit their patent applications to "useful" proteins or nucleic acids. Basic scientists using patented material in their research—known as "experimental use"—should not be liable for patent infringement, said the panel, co-chaired by Princeton University President Shirley Tilghman and attorney Roderick McKelvie of Covington & Burling in Washington, D.C. The group also wants to raise the so-called obviousness bar that patents on genomic or proteomic sequences must clear. And the report calls for better ways to share sequence and structure data internationally.

Patent attorney Gerald Murphy of Birch, Stewart, Kolasch & Birch in Falls Church, Virginia, welcomes the call for closer scrutiny of applications on obviousness and more freedom for bench scientists. "Those are areas [of patent power] that should be weakened a bit," he says.

–ELI KINTISCH

European Parliament Crafts New Rules on Chemicals

After years of debate, the European Parliament last week approved a sweeping law to test most compounds used in commerce. The measure, as originally proposed, would have required countries in the European Union to test 30,000 common substances (*Science*, 7 November 2003, p. 969). But companies said it would cost too much. Parliament scaled back the rules last week, requiring safety tests for only about 10,000 of the most widely used substances over the next 11 years, starting with the most dangerous. But the law will require that all 30,000 chemicals flagged in the original draft be registered. And firms must replace hazardous chemicals with safe ones.

The European Environmental Bureau said the rules should be tighter and that they "would hamper the identification of harmful chemicals such as hormone disrupters." But a spokesperson with pro-business lobby Unice said the rules were "going in the right direction."

–XAVIER BOSCH

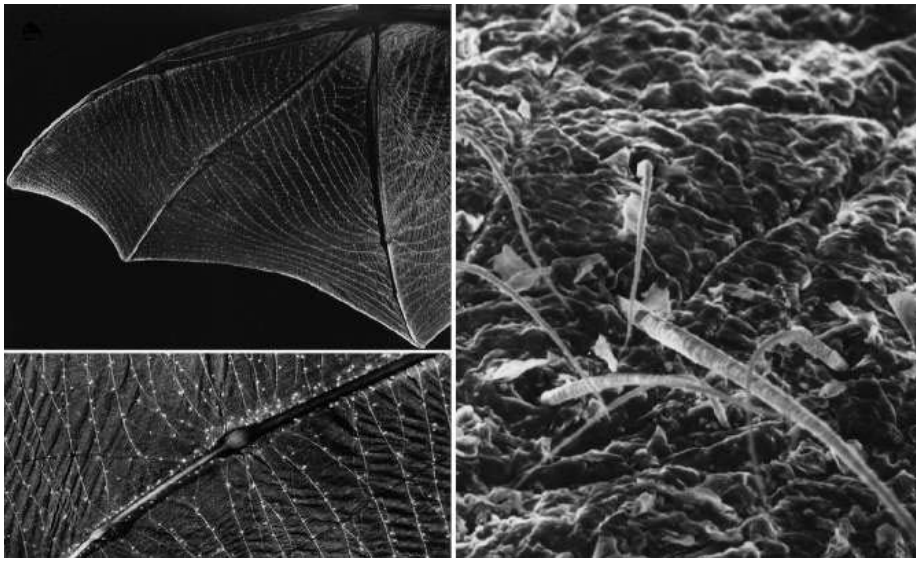

Skillful touch. Bat wings have tiny bumps (white dots) containing touch receptors that help sense in-flight turbulence.

Bats Have a Feel for Flight

Even in total darkness, bats can execute complex aerial maneuvers to capture prey, thanks to their famed sonarlike skill of echolocation. At the Society for Neuroscience meeting in Washington, D.C., however, a researcher suggested that a long-ignored feature of bats' wings also helps the creatures perform midair acrobatics and catch insects.

In the 1780s, noted French biologist Georges Cuvier proposed that bats use their sense of touch to fly adeptly in the dark. About a decade later, naturalist Lazaro Spallanzani suggested that bats instead depend upon echolocation, but Cuvier fiercely criticized this competing hypothesis, and his reputation swayed most people at the time. Moreover, 19th century anatomists described a latticework of tiny bumps on bat wings that contain tactile receptor cells. It wasn't until the 1930s, when researchers first recorded the high-pitched sounds bats use to echolocate, that Cuvier's idea was finally dismissed in favor of Spallanzani's.

But John Zook, a biologist at Ohio University in Athens, remained curious about the tactile receptor cells. Taking a look at the tiny bumps under a microscope, he discovered that the cells appear very similar to Merkel cells, a common type of touch-sensing cell in the skin of mammals. The bat Merkel cells, however, had an additional feature: a tiny hair poking out of the center. When Zook recorded the electrical activity of the nerves connected to the Merkel cells, he found that they were very sensitive to air flowing across the wing surface. Because air turbulence can signal that a wing is losing lift, Zook reasoned that the hairs on the Merkel cells might help tell bats when to adjust the angle and curvature of their wings during tight maneuvers to avoid stalling out in midair.

To test this hypothesis, Zook treated two bats with Nair, a depilating cream more commonly applied to the human bikini zone. Then he videotaped the bats in flight. "They flew perfectly well—in a straight line," he says. But when the bats had to make a 90-degree turn to avoid an obstacle, their elevation control was erratic. "Sometimes they hit the ▶

Neuroscience Society Plans to Leave New Orleans High and Dry

How soon can New Orleans be rebuilt? The Society for Neuroscience (SfN) has decided that the answer is probably not in time for its 2009 annual meeting. That decision doesn't sit well with local neuroscientists, who see it as kicking their flood-ravaged city when it's down.

Six weeks ago, the society, which has been meeting in New Orleans every 3 years, decided to move its 2006 meeting to Atlanta and its 2009 meeting to Chicago. "The devastation caused by recent hurricanes and worry about future hurricanes' effect on the low-lying city has created a high degree of uncertainty about the ability of the city's ... infrastructure to recover in time to host some 30,000 attendees," said a statement on the society's Web site. Officials also ruled out 2009 based on "what is foreseeable at this time."

Last week, the society's governing council voted to affirm the move but left open the possibility of revisiting the decision next spring after officials gather more information about the city's safety and redevelopment plans. "We were torn between ensuring that the meeting be held without snafus and sending a positive message to the New Orleans community," says Darwin Berg, a council member and biologist at the University of California, San Diego.

Local researchers say the loss of the 2006 meeting is bad enough. But relocating the 2009 event amounts to "abandoning the city not just in its greatest hour of need but well into the future," says Jeffrey Tasker of Tulane University. "It'll just make it more difficult to attract and retain scientific talent in New Orleans."

Although some organizations have chosen to relocate their meetings in late 2006 and early 2007, SfN is the only one to have canceled in 2009, says Jeff Anding of the New Orleans Metropolitan Convention and Visitors Bureau. (The convention center plans to reopen in April.) The American Chemical Society and the American Physical Society are still planning to come in 2008, and the American Psychological Association is on track for next August.

–YUDHIJIT BHATTACHARJEE

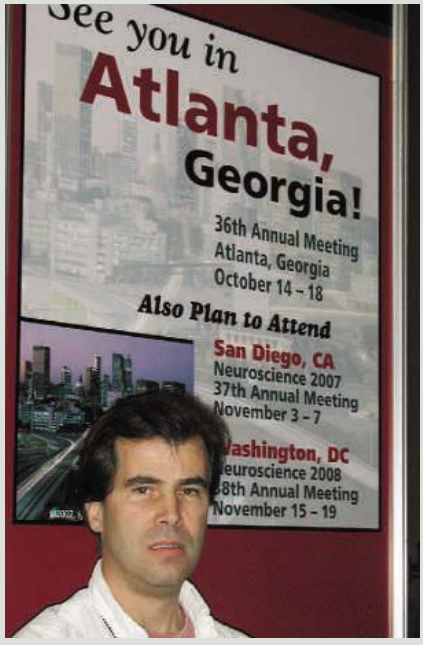

Fair-weather friends? Tulane University's Jeff Tasker says decision will hurt the city and its research community.

CREDITS (TOP TO BOTTOM): JOHN ZOOK/Y. BHATTACHARJEE

ceiling," Zook says. When the hairs grew back, the bats regained their aviation skills.

Zook also described another type of receptor in the membranous part of bats' wings. Nerve recordings revealed that these receptors respond when the membrane stretches, even slightly. The most sensitive parts of the wing turned out to overlap with the "sweet spots" where the bats prefer to hit the insects they scoop up in midflight. (Zook mapped the sweet spots by videotaping the bats as they gathered mealworms shot out of an air cannon.)

Other bat researchers are impressed. "This is good stuff," says neuroscientist James Simmons, who studies bat echolocation at Brown University. The work adds a new page to bats' remarkable résumé of sensory talents, he says. "It's very exciting work," agrees Cynthia Moss of the University of Maryland, College Park. Moss says the study provides convincing evidence that bats' long-ignored somatosensory system is important for behavior. It seems Cuvier wasn't entirely wrong after all.

–GREG MILLER

Computer Game Sharpens Aging Minds

Granny may not have the much-coveted Xbox 360 video game console on her Christmas list this year, but if a California company founded by neuroscientists has its way, computer games may soon become must-have items for seniors. Preliminary results presented at the meeting by company researchers suggest that a gamelike training program it has developed can improve memory and attention in elderly people.

The game, called HiFi, may lack the excitement of Grand Theft Auto, but it's designed to boost the function of the aging brain, says neuroscientist Henry Mahncke, vice president of research and outcomes for Posit Science, based in San Francisco, California. HiFi doesn't have a plot, per se, but offers several cartoonlike scenarios based on senior-friendly themes, including family and travel. In one part of HiFi, players collect photos of famous sites such as the Eiffel Tower by making increasingly difficult discriminations between whistling sounds that increase or decrease in frequency. The idea is to exercise and strengthen the neural circuits that process the acoustic building blocks of speech, Mahncke says. A similar approach has been used in computer games developed for children with language disabilities (*Science*, 5 January 1996, p. 27), several of which are now marketed by Scientific Learning Corp. of Oakland, California.

Older people often experience a decline in speech processing that can contribute to other types of problems, says Paula Tallal, a cognitive neuroscientist at Rutgers University in Newark, New Jersey, and co-director of Scientific Learning. (Tallal also sits on Posit Science's scientific advisory board, although she is not an author of the current study.) "If you can't process [speech] because it's going by too fast, you're not going to get it into memory," says Tallal.

In a randomized trial of 95 healthy older adults with an average age of 80, those who played HiFi for an hour a day for 8 weeks improved their scores on a standardized test of memory and attention by an average of 5.5 points. A similar group who used a computer for an hour a day to watch a lecture improved about 2 points, no better than a third group who made no change to their daily activities. The seniors in the HiFi group performed like people 10 years younger typically would, Mahncke says.

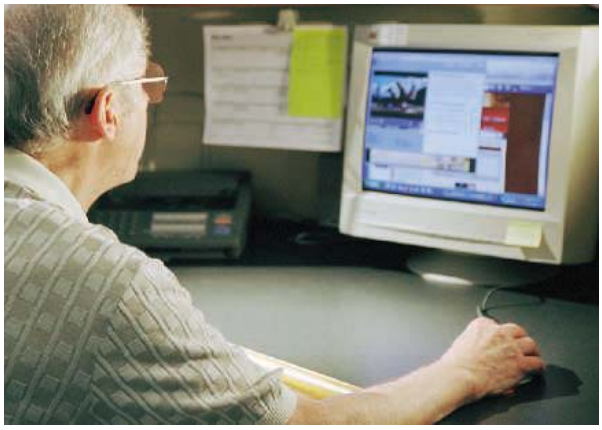

Turn back the years. A new computer game may improve cognition in older people.

But not everyone is convinced the improvement is all that dramatic. Dwight Dickinson, a neuropsychologist at the University of Maryland School of Medicine in Baltimore who uses computer training programs in his work with schizophrenia patients, suspects that the cognitive boosts reported so far aren't big enough to make much difference in people's day-to-day lives. It's analogous to getting a few extra IQ points, Dickinson says. Although he thinks the idea is worth pursuing, Dickinson is skeptical that computer training programs will undo time's inexorable toll on the brain. "You may be able to make changes around the edges, but you're not going to turn a 75-year-old back into a 40- or 50-year-old," he says. –GREG MILLER

CREDIT: BRAND X PICTURES/GETTY

ScienceScope

Weather Satellite Gap Looms

The United States could suffer a several-year hiatus in civilian weather data–gathering due to the slow development of an ambitious satellite. The National Polar-orbiting Operational Environmental Satellite System was supposed to be an economical replacement for two National Oceanic and Atmospheric Administration (NOAA) and military systems. The first of six satellites was scheduled to be launched in June 2008 at a system cost of $6.5 billion. But it's 3 years behind because of lagging sensor development and inept performance by project managers and contractors. The latest estimate is pushing $10 billion, a Government Accountability Office official told the House Science Committee this week. NOAA pledges a new plan following outside reviews. –RICHARD A. KERR

Fossils' Past Is Mysterious

The University of Washington's prestigious Burke Museum in Seattle is awaiting a report on potential problems with its vertebrate fossil collection. The concerns relate to nonhuman specimens dug up by curator John Rensberger, who retired last year. In 2003, a university investigation concluded that he had inadvertently removed fossils from federal land without a permit. With a new museum director at the helm, the university is now taking a broader look at the status of the discoveries. Three outside paleontologists recently examined the collections; their report is due out early next year. –ERIK STOKSTAD

No Sea Change on Fisheries Bill

Conservationists want science to play a greater role in fisheries policy, but they say a new proposal introduced last week by Senator Ted Stevens (R–AK) doesn't quite go far enough.

Stevens's bill gives more clout and independence to the scientific panels that currently advise fisheries councils, directing them to weigh advice on catch limits, health of fish stocks, and potential socioeconomic impacts when determining sustainable fish quotas—consideration now legally voluntary. But the new bill includes no mandates that managers must follow scientists' advice.

Marine scientist Andrew Rosenberg of the University of New Hampshire in Durham says the bill is a slight improvement on current law. "It's better," Rosenberg says. "But it's not there yet." A similar bill awaits House action. –CAROLYN GRAMLING

Mallinckrodt Baker.
We've been a hit with chemists for 130 years.

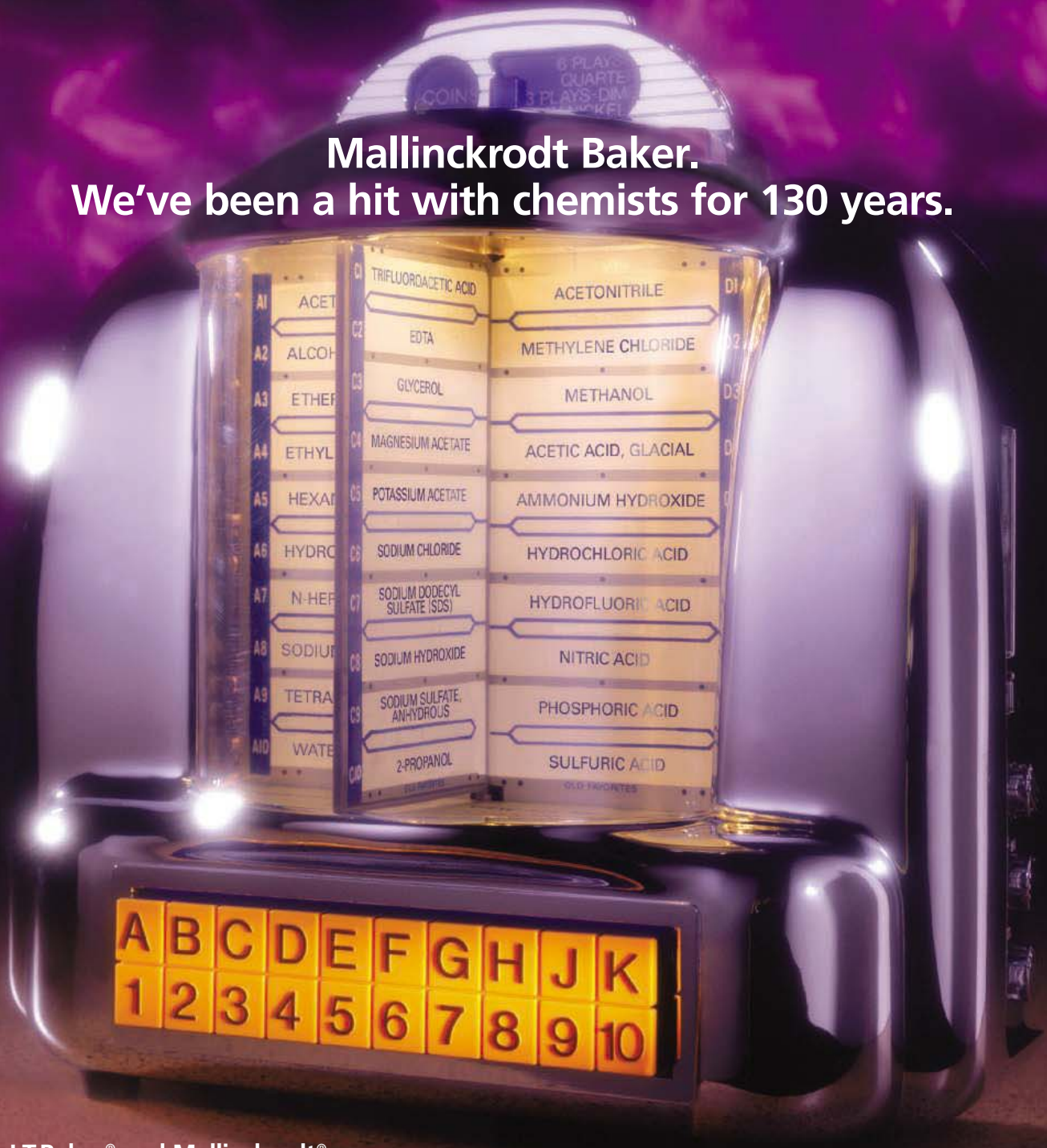

J.T.Baker® and Mallinckrodt®: Two great brands. One unique source for chemicals.

Every day, thousands of laboratories around the globe put their trust in chemicals from Mallinckrodt Baker. Our diverse product line offers a match for virtually any application you're working on. Plus, our chemicals deliver consistent results…time after time.

For details about the chemicals that are right for your application, visit www.mallbaker.com/lab

Mallinckrodt Baker

J.T.Baker® | Mallinckrodt® CHEMICALS

Quality ◆ Choice ◆ Value

CANADA

New Funding Schemes Aim to Retain Top Academic Talent

OTTAWA—As the general manager of a winning sports team knows, the secret to success is bringing on a superstar without losing existing talent. So too for university deans, who worry about raids from academic rivals while they are trolling for new talent.

To discourage such campus-hopping, the Canada Foundation for Innovation (CFI) has decided to give institutions a better chance of retaining their prized researchers. It's part of several programmatic changes at the foundation, an independent entity created by the government in 1997 to improve Canada's research infrastructure, as it prepares to spend the last billion dollars of a $3.1 billion endowment. One $262 million program has been tweaked to let universities—who receive block grants based on an assessment of faculty productivity—provide infrastructure for established as well as newly hired professors. CFI has also changed the rules for a core fund, which is preparing for a $276 million competition, to allow previous recipients to come back to the table for another bite.

"If we hadn't done this, the danger would be a bit of a revolving door," says CFI president Eliot Phillipson, who believes that retention of faculty has become as critical an issue in academia as recruitment. Allowing previous recipients to apply for upgrades, he adds, also acknowledges the rapid pace of technological change.

University officials say the changes are a sign that Phillipson, the former dean of medicine at the University of Toronto (U of T), has been listening since taking charge of CFI in February 2004. Other new wrinkles include a $51 million fund to establish a national high-performance computing system and, possibly, other platforms in so-called enabling technologies such as digital data storage, retrieval, and publication.

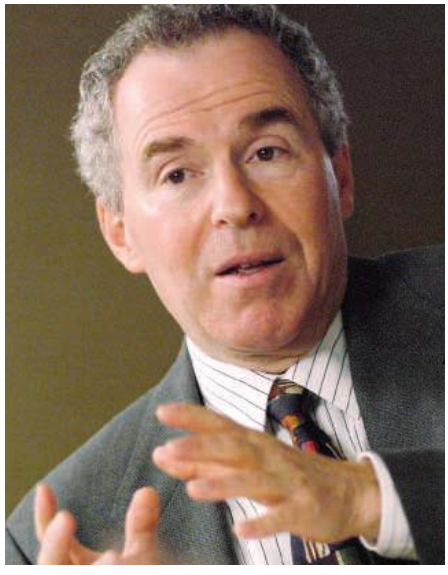

A moving foundation. Eliot Phillipson wants CFI to meet needs of university scientists.

CREDIT: CFI

James Turk, head of the Canadian Association of University Teachers, doubts that the changes will curb mobility. "A lot of academics look to move up the ladder," he says. "I don't think this is going to change that dynamic." But Michelle Gauthier of the Association of Universities and Colleges of Canada sees the changes as sound business practices that are long overdue. "If you look at any kind of standard for a solid management of an organization," she says, "keeping good people is as important as attracting new ones."

The new programs come with at least one string attached: Only 20% of an award will be available for operating and maintaining the new equipment, instruments, or research facility being funded. In the past, that share was 30%. Still, the approach "allows universities to customize their [spending] to [meet] their particular circumstances," says Judith Chadwick, director of U of T's government research infrastructure program. And because the size of U of T's block grant will more than double, to $33 million, Chadwick isn't complaining. "We're thrilled," she says. "I'm not looking a gift horse in the mouth."

–WAYNE KONDRO

Wayne Kondro writes from Ottawa.

HIGHER EDUCATION

U.S. Plans Suit to Stop Minority-Only Programs

Can a U.S. university participate in a federal program to increase the number of minority scientists without discriminating against the rest of the student population? That's the question facing Southern Illinois University (SIU) and the National Science Foundation (NSF) after the U.S. Department of Justice concluded this month that the university is violating the civil rights of Caucasian students by offering graduate fellowships to underrepresented minorities under an NSF program called "Bridges to the Doctorate."

The case is the latest skirmish in an ongoing battle over federal programs aimed at boosting the tiny percentage of Hispanics, African Americans, and Native Americans in the scientific workforce. Conservative groups such as the Virginia-based Center for Equal Opportunity (CEO), which flagged the SIU programs for the Justice Department, have pushed for the elimination of all racially exclusive programs at both the state and federal levels, and several universities have canceled such programs or changed their eligibility criteria (*Science*, 21 February 2003, p. 1167). But proponents say they are necessary to accomplish the goal of greater participation in science by minorities.

In a 4 November letter, the Justice Department informed SIU officials that they have "engaged in a pattern or practice of intentional discrimination against whites, nonpreferred minorities, and males" by offering the Bridges program and two university-funded graduate fellowships that serve underrepresented minorities and women. The department said SIU could avoid being taken to federal court by canceling the programs and providing "make-whole relief" to the "victims." It's the first such letter by the department to a university.

Some 27 students participate in the SIU Bridges program, one of 18 sites around the country. The $17.8-million-a-year NSF program is an extension of the foundation's Louis Stokes Alliance for Minority Participation (LS-AMP) that serves undergraduates majoring in science and engineering. The SIU case highlights what NSF spokesperson Curt Suplee calls "our two different legal mandates." Like every public agency, NSF swears it won't discriminate on the basis of race, religion, or national origin. Yet a 1980 law also gives it the authority to run programs to help minorities, women, and those with disabilities. "We are in compliance with both mandates," says Suplee.

And that's the rub. CEO's Roger Clegg says race cannot be used as the overriding criterion for participation in any campus program. But Representative Chaka Fattah (D–PA), a member of the spending panel that funds NSF and a vocal supporter of targeted programs, sees such programs as critical for achieving an adequate domestic scientific workforce. "The intervention of the Justice Department contradicts 40 years of federal efforts, by presidents of both parties, to improve access to higher education by disadvantaged groups," says Fattah.

SIU interim president Duane Stucky says the programs are part of the school's commitment to serving underrepresented students and that talks this week with the Justice Department are aimed at finding ways to preserve the programs.

–JEFFREY MERVIS

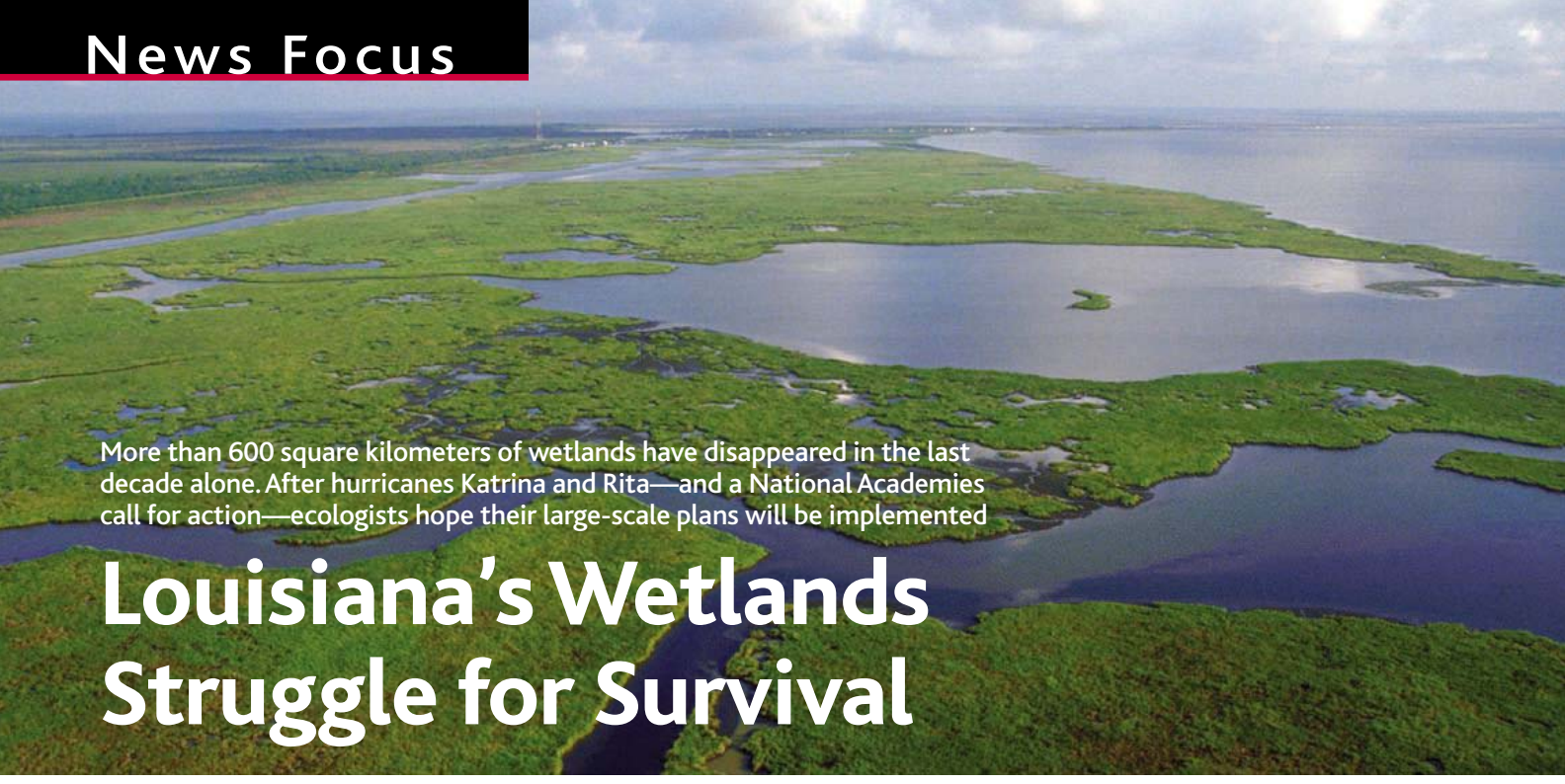

More than 600 square kilometers of wetlands have disappeared in the last decade alone. After hurricanes Katrina and Rita—and a National Academies call for action—ecologists hope their large-scale plans will be implemented

Louisiana's Wetlands Struggle for Survival

LULING, LOUISIANA—From its headwaters in Minnesota to the Gulf of Mexico, the Mississippi is lined with massive earthen levees designed to prevent the mighty river from flooding. But here, 37 kilometers upstream from New Orleans, the Army Corps of Engineers and the state of Louisiana have spent $120 million to get a little flooding back. On a sunny October afternoon, inside a control room, a technician presses a button, and hydraulics begin to whine. Deep within the concrete structure, four steel sluice gates slowly rise, and the Mississippi springs a leak.

With a gurgle, water from the Mississippi begins to flow through the four 16-square-meter culverts of the Davis Pond Freshwater Diversion Structure and into a 3-kilometer-long canal. Eventually, the water will reach the marshes of Barataria Bay, which, like much of coastal Louisiana, are starved of sediment. According to calculations by the corps, the water from Davis Pond should help preserve more than 13,000 hectares of Louisiana's endangered marshes—if it works, that is.

Three years into the project, engineers have realized it's not easy to mimic a flood. Since Davis Pond began operation in 2002, engineers have struggled to get the water to flow properly and enough sediments to accumulate in the right places (see sidebar, p. 1265). And this effort is just a tiny fraction of what's needed to restore the devastated Louisiana coastline, a National Academy of Sciences (NAS) panel said this month. "The challenge of protecting and restoring this wetland system is unprecedented," said the panel.

According to the report,* the corps' current plan—an unfunded, $1.9 billion, 10-year proposal to slow down the destruction—is generally a good start, but it's by no means comprehensive enough. "This is really [just] the first step," says Robert Dean, a civil and coastal engineer at the University of Florida, Gainesville, who chaired the committee. The academy is the latest in a long string of expert advisory bodies to call for urgent action. But its timing, less than 3 months after hurricanes Katrina and Rita devastated the coast and focused a spotlight on its problems, could make it the most influential. The question now is whether Louisiana, and the nation, will muster the political will and funds to set the course toward recovery.

* *Drawing Louisiana's New Map: Addressing Land Loss in Coastal Louisiana*, National Academies Press, 2005.

Small steps. Restoration happens at many scales, such as planting vegetation. Broader action is critically needed, scientists say.

Robbed of sediments

Coastal degradation was a problem long before Katrina roared into New Orleans. After the Army Corps tamed the Mississippi in the 1940s, the wetlands, deprived of the river's sediment, began to sink below sea level. Their health further deteriorated as extensive canals were dug, first to explore for oil and gas and then to pump them out. Adding insult to injury, a beaver-sized rodent called the nutria, introduced in the 1930s for its fur, turned out to have a voracious appetite for marsh plants. All told, more than 4000 square kilometers have been lost since 1950.

Faced with damage to marshes as well as impacts to wildlife, politicians began to address the problem in the 1960s. But despite many commissions and reports, there was little action until 1990, when federal legislation channeled about $50 million a year of funds to the state of Louisiana. Some 120 restoration projects are currently active, from hunting nutria to building new marshes with dredged silt. But these projects are small and piecemeal.

After years of debate, in 1998, a coalition of state, federal, and local officials finally settled on an ambitious blueprint for reclaiming the coast. Called Coast 2050 (*Science*, 15 September 2000, p. 1860), it would have cost $14 billion over 30 years.

CREDITS (TOP TO BOTTOM): ANNE MARINO/USACE; ERIK ZOBRIST/NOAA RESTORATION CENTER

Notably short on details, the proposal had the lofty goal of creating a "sustainable ecosystem that supports and protects the environment, economy, and culture of southern Louisiana." It won broad support, with 20 coastal parishes signing off on the concept.

But when the Army Corps presented its implementation plan to the Bush Administration in 2003, the White House balked at the cost. The corps was sent back to the drawing board with instructions to come up with something more modest to show that restoration was feasible. That irked leading restoration proponents, such as Robert Twilley of Louisiana State University (LSU) in Baton Rouge, who feel they already have the know-how to ramp up. "The science is there," he says.

It is this scaled-down version, called the Louisiana Coastal Area (LCA) study and released in November 2004, that the state and the corps asked NAS to evaluate. Weighing in at a more modest $1.9 billion over 10 years, the LCA plan would spend $864 million on five major projects, some already in early stages of operation, and another $762 billion for 10 smaller projects that haven't been as fully designed, among other things.

The NAS committee gave a thumbs-up to four of the five major projects, saying they were well conceived and technically feasible. These four included three sediment-diversion projects analogous to Davis Pond and an effort to restore an eroding headland and barrier island.

But, reflecting long-held concerns among the scientific community and environmentalists, NAS politely suggested the Army Corps "reconsider" a fifth project, a plan to reinforce a major navigational canal, called the Mississippi River Gulf Outlet (MRGO, known as "Mister GO"). Dredged in 1963 to shorten the distance that ships have to travel to New Orleans, this 122-kilometer-long canal was widely faulted post-Katrina for making the city more vulnerable to flooding. Paul Kemp of LSU says that computer models suggest that it and other canals helped channel storm waters into New Orleans and surrounding parishes.

MRGO has also been "an environmental nightmare," says Donald Boesch of the University of Maryland Center for Environmental Science in Cambridge, who was on an earlier technical review committee for the corps. NAS noted that the canal has allowed waves to erode 81 square kilometers of wetlands over the past 40 years. By ferrying in saltwater, it has killed marshes and cypress swamps, too.

NAS stopped short of recommending that MRGO simply be filled in, which John Day of LSU and many other scientists recommend. But it advises against spending $100 million to reinforce the shorelines, as the LCA proposal suggested. "We felt that that was probably not the best use of the available funds," Dean says.

Missing game plan

The main problem with the LCA study is that it is "too modest an effort," NAS concluded. By the corps' own calculations, the LCA study plan would slow the overall rate of land loss by only 20%, to 22.3 square kilometers per year. "It just isn't up to the massive deterioration of the Mississippi Delta," says Day.

A second criticism is that the five projects are spread out across the state. The report speculates that "small projects [were] selected in order to navigate through the political obstacles that might derail efforts if focus is shifted to larger, more significant projects." Although this may have political appeal, it's not a strategic approach that would place major projects in critical places where they would build on each other. Says Boesch: "You have to ask: What's the game plan?"

The Army Corps also needs to think bigger, the panel concluded. "There should be bolder, long-term sediment-delivery projects than were put forth in the [LCA study] plan," says Dean. In particular, NAS detailed two projects that state and federal authorities should consider for greater study. One would divert the final reach of the Mississippi River westward, abandoning the so-called Bird's Foot Delta. The committee couldn't say how much land this would create—in principle quite a bit—or how much it would cost, because the corps has not evaluated the concept.

Tapping a River to Restore And Build Up Wetlands

LULING, LOUISIANA—The Davis Pond diversion is just a small concrete building perched high on the riverbank. But it and another so-called freshwater diversion, located farther downstream, have sparked a huge controversy that demonstrates the political and technical challenges to restoring Louisiana's wetlands (see main text).

Authorized in 1965, the diversions were intended to help fisheries by channeling fresh water from the Mississippi River into the marshes to dilute the encroaching saltwater. But the plans gathered dust until coastal restoration issues moved to the front burner in the late 1980s. That's when scientists realized that the marshes needed not just the right salinity but also fresh doses of river sediment.

The Caernarvon Freshwater Diversion Project, located 24 kilometers downstream of New Orleans, was completed in 1991. But the large releases of water also triggered lawsuits over their impact on local oyster beds. The result was $1.3 billion of awards that were finally overturned last year by the state's Supreme Court. Scientists have determined that releasing pulses of river water can deliver sediment to the marshes while minimizing disruptions to other fisheries.

Test run. In early trials, sediment (brown) passes from the Davis Pond structure (arrow and detail below) into Lake Cataouatche.

Having learned the hard way, the state spent $4 million to buy out existing oyster leases while Davis Pond was under construction. Opened in 2002, the project immediately ran into trouble when the discharged water backed up in the holding ponds, endangering a bridge. "We never got to the full range of tests before they had to pull the plug," recalls Bill Good of Louisiana State University (LSU) in Baton Rouge, a former chair of the Davis Pond advisory committee.

But prototypes are meant to illuminate problems, says Paul Kemp of LSU: "We need to bite the bullet and do the hard things." And that, he says, should include an even more ambitious project to divert the entire Mississippi downstream of New Orleans.

–E.S.

CREDIT: USACE (BOTH)

But, acknowledging the complexity of the undertaking, the committee also detailed the substantial side effects of this project. It would require the construction of a new navigational entrance to the river, for instance, and might also threaten the Delta National Wildlife Refuge and oil infrastructure in the delta.

The other project would divert water from the Mississippi River from a point about 100 kilometers upstream of New Orleans after building an 88-km-long channel to carry the flow to Barataria and Terrebonne Basins, just west of the Mississippi River. Depending on how much water flows through, this could create (or prevent the loss of) 28 to 56 square kilometers of land per year. Before any of this could happen, the Army Corp would have to buy much real estate for the canal and figure out how to compensate farm owners and others whose lands would be flooded. NAS raised the prospect of decades of legal challenges from property owners that "could prove insurmountable."

Indeed, NAS didn't downplay the political or biological challenges facing the area. Parts of coastal Louisiana are in such bad shape that trying to fix some wetlands may be hopeless, and communities there may need to be abandoned. Picking which ones will not be easy. What's needed, according to NAS, is a new vision of what the Louisiana coast should look like. Such a map, drawn by federal, state, and local officials, would weigh the societal tradeoffs and chart where wetlands should be restored. Although the ambitious earlier plan, Coast 2050, had many of these elements, says Diane Reed of the University of New Orleans, it didn't explicitly spell out the consequences of the suggested actions, such as diversions changing oyster or shrimp habitat.

Gusher. Pumping sediment through pipelines can create tracts of wetlands, but ecologists doubt that the energy-intensive technique is sustainable.

It's also important to move quickly from planning to action, scientists say. If barrier islands disappear, waves will strike wetlands with more force. "I'm concerned that if we wait around, we'll jump to a new level of wetland loss," says Greg Stone of LSU. Furthermore, as energy costs increase, some restoration projects, such as dredging or pumping sediment through pipelines, may become too expensive.

Flood protection

The NAS report was almost completed when hurricanes Katrina and Rita hit, focusing national attention on how best to protect the city from future storms. While most of the attention has gone to investigating the failure of the levees (*Science*, 11 November, p. 953) and options for rebuilding them, many coastal scientists have plugged the role that healthy coasts could play in lessening storm damage. "If we don't restore the coast, any flood-protection system will function less well," says Day. "We can't engineer a system that will protect New Orleans through levees alone."

The report makes a brief nod in that direction: "To the extent that wetlands can offset a significant degree of storm impact, large-scale wetlands restoration projects can be an important component of national efforts to reduce future hazards from hurricanes." The problem, the panel notes, is that there's little empirical evidence of the exact benefit that wetlands provide. An oft-quoted figure is that every kilometer of wetland reduces the storm surge by 7 centimeters, which comes from a few measurements of one hurricane in the 1960s. Better data come from Hurricane Andrew, which suggests that each kilometer of wetlands lowers the surge by 5 cm. Although that again can't be generalized, "there's no question that wetlands are better than open water," Stone says.

Computer models are beginning to provide better estimates of the benefits. For example, Stone simulated a Category 3 hurricane hitting south-central Louisiana. He and his colleagues compared the effects of the storm on the coast, given the extent of wetlands in 1950, 1990, and 2020, if current losses continue. "There was a dramatic increase in storm surge," Stone says. The past 40 years of decline led to a 2.5- to 3-meter increase in the height of storm surges, he says.

Even so, Reed says, it's unlikely that wetlands restoration would have done much to lessen the brunt of Katrina or Rita. "A really big storm is still a really big storm," she says. Given the lack of evidence, Reed, for one, cautions against trying to persuade Congress to foot the restoration bill on these grounds. Levees will remain a key defense.

The importance of wetlands restoration, she and others say, is to ensure that coastal communities are still worth defending. And as the marshes go, so do habitats for oysters, shrimp, and fish that make up an industry valued at more than $3 billion—and the rich culture of the Bayou. Oil and gas infrastructure and jobs are threatened, too. As the coast slowly sinks and sea level rises, doing nothing means an inevitable retreat from the coast, says Bill Good of LSU: "Ultimately, the consequences are going to be worse than Hurricane Katrina."

—ERIK STOKSTAD

Coastal Land Loss in Southern Louisiana

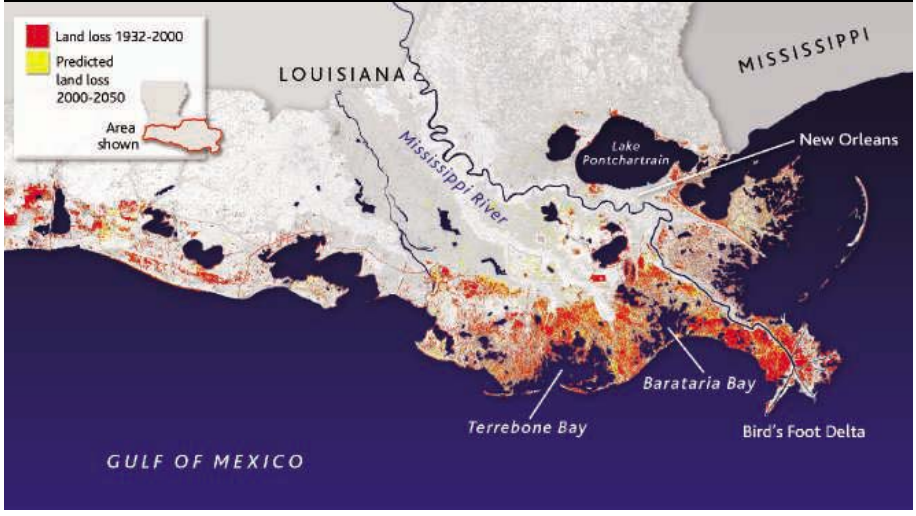

CREDIT: ERIK ZOBRIST/NOAA RESTORATION CENTER; SOURCE: USGS

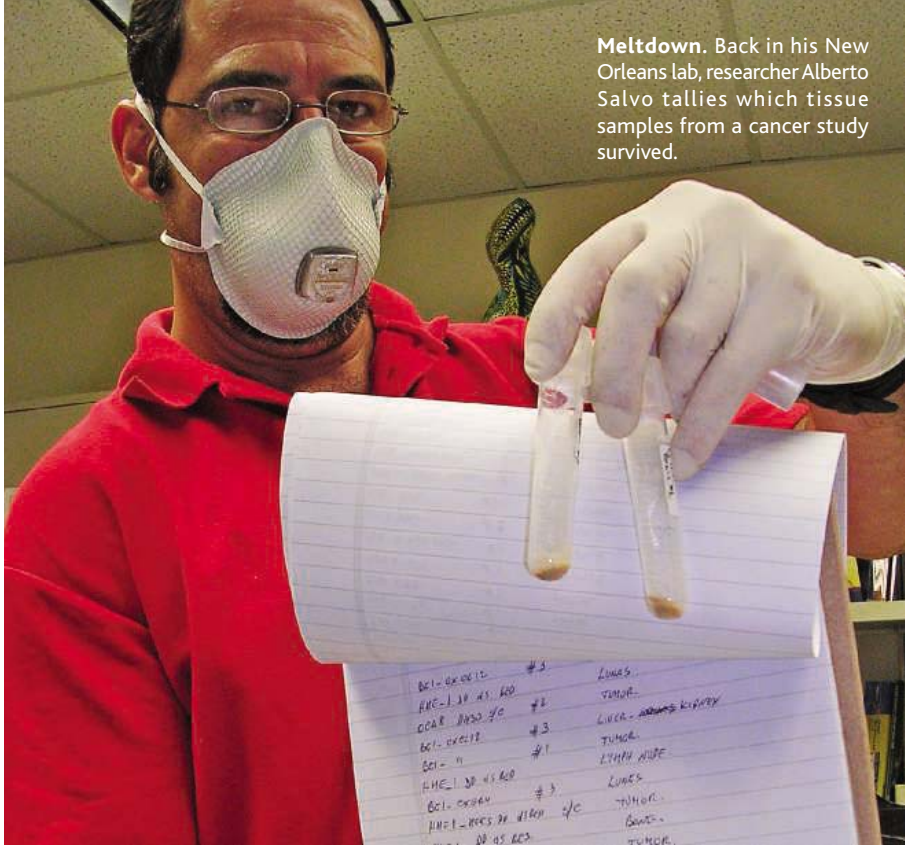

Meltdown. Back in his New Orleans lab, researcher Alberto Salvo tallies which tissue samples from a cancer study survived.

CREDIT: J. KAISER/*SCIENCE*

New Orleans Labs Start Their Uncertain Comeback

Putting on a brave face as they begin returning to their flood-ravaged city, researchers are trying to resurrect their personal lives and research careers

NEW ORLEANS, LOUISIANA—On the first full day in his lab after 10 weeks of hurricane-forced exile, Tulane University cancer researcher Matt Burow looks on with dismay as his gloved and masked research assistant Alberto Salvo holds out a scrap of brown tissue—a mouse tumor that sat at room temperature for weeks. "Everything liquefied. It just melted," Burow says of the sample, which is now useless for protein analysis. Burow's group also lost 200 costly mutant mice, including a half-dozen that had just been injected with a promising antitumor chemical that took 2 months to extract from soybeans. Burow, who is just 34 years old but already has independent funding from the National Institutes of Health (NIH), says his research has been set back a year. Yet he tries to remain hopeful. "The only way you can really function is on the premise of faith that there's going to be support," he says. "Because if [we] don't, we'll fall apart. Especially at this point in my career. You just have to hope we can catch up."

That forced optimism is shared by many researchers who began trickling back here earlier this month to restart their labs in the wake of the flooding caused by Hurricane Katrina. The city's two research powerhouses—Tulane University and Louisiana State University's (LSU's) Health Sciences Center (HSC)—don't expect to resume medical school classes in New Orleans before next summer, but administrators are scrambling to reopen laboratories, even in a city of boarded-up businesses, broken traffic lights, and armed patrols. The officials argue that opening labs quickly is necessary to hold on to faculty members who are now scattered at institutions across the country (*Science*, 23 September, p. 1980). Indeed, a few have already taken new positions elsewhere. "We need to secure the intellectual infrastructure of this place," says Paul Whelton, senior vice president for health sciences at Tulane Medical Center.

Those returning face a host of challenges, both professional and personal. Labs have lost many thousands of dollars' worth of biological samples, equipment, and research animals. New Orleans researchers are seeking funds to quickly replenish lost equipment and materials wherever they can, from federal agencies to scientific societies. They are also anxiously awaiting news that could prove crucial to their ability to resurrect their research: NIH and the National Science Foundation (NSF) must decide whether they can provide New Orleans investigators with 1-year funded extensions on expiring grants, given that the White House has already turned down NIH and NSF requests for additional funds to help Katrina-affected grantees. Numerous researchers, meanwhile, are struggling to rebuild or replace homes in neighborhoods devastated by floodwaters.

Still, some researchers are positive. "I think we'll ride it out. We may be a little leaner and meaner, but we'll be back stronger than before," says Tulane virologist Robert Garry. Others, however, are deeply worried about not only their own research but also whether new students, postdocs, and faculty members will commit to a devastated city with an uncertain future. "The ripple effect is going to be more painful to the institution than the initial shock was," predicts LSU cell biologist Mark Alliegro.

Lake LSU

From his corner office eight stories up in LSU's downtown HSC, neuroscientist Nicolas Bazan asks a visitor to look out the window and picture the complex in early September, during the days after the levees broke. "Imagine there was a lake," says the director of LSU's Neuroscience Center of Excellence. A roughly 2-meter high, black line is still visible on one of the white tiled buildings; it marks the high point of floodwaters in that part of the complex. Since mid-October, many of Bazan's 110 staff have been cleaning out their labs, wiping up mold, and tossing out spoiled cell cultures and reagents. "These floors were smelly; there were flies. It was extremely sad and overwhelming in many ways," he says.

Bazan is lucky: None of LSU's other downtown buildings is officially open yet. Scientists in those facilities have made forays into dark labs with flashlights to begin cleaning up and to retrieve computers. The biggest problem, say LSU officials, is that flooding damaged electrical switches and water pumps that now have to be repaired. LSU has also been slowed by state and Federal Emergency Management Agency (FEMA) rules requiring that rebuilding contracts be put up for bids. Plans now call for sealing off the first floors of buildings and allowing access to upper levels through walkways, says Joseph Moerschbaecher, vice chancellor for academic affairs at LSU's HSC. With the exception of the LSU-affiliated Children's Hospital in uptown New Orleans, which wasn't flooded and has taken in about 60 displaced researchers, the school has not yet set any firm date for fully reopening research labs—they're shooting for January to spring. Some researchers are "frustrated," Moerschbaecher acknowledges.

The recovery is further along at Tulane, a private university that doesn't have to follow the same bidding rules. In Tulane's main bio-

medical research buildings, a few blocks from LSU and on the university's uptown campus, yellow tubes attached to dehumidifiers pump cold, dry air into the damp buildings around the clock. Researchers began coming back to a relatively unscathed building the week of 8 November and, once a damage inventory was done, set to work again. "There's an enormous sense of relief. We can make some of the pieces move forward," says Donald Krogstad, Tulane's chair of tropical medicine.

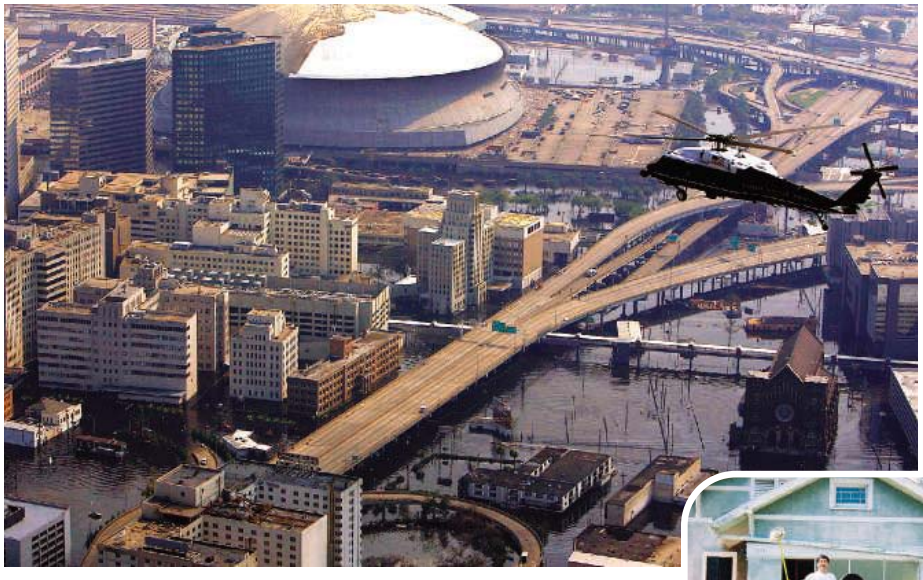

Muddy waters. LSU's and Tulane's downtown research buildings near the Superdome suffered severe flooding. Cell biologist David Mullin (*inset*) tackles cleaning up his house near Tulane's main campus.

As they return, researchers are benefiting from some heroic efforts in the days after the flooding. Teams at both universities retrieved priceless cell lines, and many of Tulane's transgenic mice survived trips to temporary homes elsewhere. Accompanied by armed guards, some scientists went back to labs multiple times to keep Dewars stocked with nitrogen to preserve other materials. Indeed, tales of dedication and ingenuity abound: the maintenance worker who hot-wired a flooded elevator to get 135-kg Dewars moved and the staff at Tulane's suburban primate center who camped on the grounds and ate military rations for weeks to keep the center going, for example. Tulane saved its four nuclear magnetic resonance machines, whose magnets have to be kept close to 0 kelvin, thanks to an act of charity: A scientist described the problem to his neighbor, a welder, who had liquid helium flown in from one of his contacts.

Still, there were huge losses. At Tulane, for example, one failed Dewar held 4 years' worth of cell lines of developmental biologist YiPing Chen, who has about $1 million in NIH grants. And LSU was forced to kill most of its mice, rabbits, dogs, and monkeys, which were largely kept on ground floors. The loss of thousands of animals and supplies and equipment for caring for them adds up to an estimated $10.5 million, says Moerschbaecher. At both campuses, anything in electricity-dependent refrigerators and –70°C freezers spoiled during weeks-long power outages—enzymes, antibodies, plasmids, bottles of serum, as well as pig hearts used by biomedical engineers. Some labs are also finding that equipment such as centrifuges and incubators didn't survive power surges and the soaring temperatures and humidity experienced by labs that were without air conditioning for weeks. Researchers estimate anywhere from $50,000 to hundreds of thousands of dollars in damages per lab.

Those conducting basic research aren't the only scientists who suffered losses. "Clinical and population researchers are very badly disrupted," Whelton says. Twenty-seven freezers holding blood and urine samples from population studies were lost; the only studies that can probably be rescued will involve analyses of the stored DNA, which survived warm temperatures. The projects affected include a 33-year heart study following 8000 subjects and a multicenter chronic renal insufficiency study for which Tulane had the largest site. And given the citywide evacuation, clinical researchers have also lost their patients, many of whom need medications they were receiving for AIDS, cancer, or diabetes, says Laura Levy, Tulane University associate senior vice president for research. Universities are scrambling to track them down by telephoning contacts and placing ads in newspapers. They are also trying to decide what to do about the loss of Charity Hospital, the main site for Tulane and LSU clinical studies, which is now boarded up and too badly damaged to be saved.

Universities are still tallying the total damages to laboratories. But the cost will clearly be high: When Baylor College of Medicine's main medical school building in Houston, Texas, was hit by a flood 4 years ago, it sustained research damages of more than $100 million. "I wouldn't be surprised if it's hundreds of millions," says Levy. Even at the University of New Orleans (UNO)—a state university that had a "growing research program" with about 28 NSF grants, says graduate school dean Robert Cashner—losses will total $5 million to $6 million dollars at a minimum.

Officials say they expect to incorporate lessons from Katrina into future disaster plans. With the next hurricane season just 6 months away, LSU immunologist Seth Pincus is already taking preventive steps. For example, he learned that samples adequately stocked with liquid nitrogen can last for weeks—so he will make sure more large Dewars are on hand for cell lines and reagants. LSU's Iris Lindberg has also called for revising disaster plans so that LSU scientists, who were barred from their labs for 6 weeks, can have earlier access to retrieve valuable materials (*Science*, 11 November, p. 971).

Still waiting for help

Planning for future Katrinas could take significant amounts of money, but New Orleans institutions are finding it hard simply to cover the costs of bringing labs back to life. Insurance and FEMA will cover much of the damages, officials say. But getting the checks could take a long time—at Baylor, it took up to 4 years. "We need help right now," says Whelton of Tulane. Many investigators have applied for supplemental grants from NSF and NIH. Some are accepting donations—a pharmacology society, for example, has given grad students $2000 stipends and exempted LSU researchers from paying meeting and journal fees, says Moerschbaecher. Drug companies have donated compounds, and vendors are offering discounts as high as 75% on reagents and research equipment.

Getting labs up and running is only half the battle. The other is making up for lost time. With many experiments destroyed, it will take months for scientists to get back to where they were. Institutions are asking federal research agencies to provide a year of additional funding for their grantees. After 15 years of NIH support, "I would hope I'd be given some time to make myself competitive again," says Tulane's Steve Hill, who was on the verge of starting a clinical trial for a breast cancer treatment he had spent years studying in animals.

CREDITS (TOP TO BOTTOM): AP; COURTESY OF DAVID MULLIN

Set back. Infectious disease researcher Donald Krogstad and graduate student James Colborn lost samples from a malaria study.

Whether that funding will come through is unclear, however. Federal agencies have been "so compassionate and responsive," readily granting unfunded extensions for expiring grants, says Levy. But there's been no extra money yet. NIH Deputy Director for Extramural Research Norka Ruiz Bravo says the agency is waiting for scientists to fully assess damages and is working with FEMA on how to avoid duplicating reimbursement funds. How much overall funding is available may depend on NIH's 2006 budget—unlikely to be much higher than this year's—and whether NIH receives any money from Katrina relief bills passed by Congress. NIH has already asked the White House to request $150 million in post-Katrina recovery funds but has been turned down, according to biomedical lobbyists; a similar request from NSF was also rejected. If no extra money comes through, New Orleans's researchers will have to compete with other priorities. "We're very aware that there's a great need there. We'll keep that in mind," Ruiz Bravo says. But she acknowledges that NIH had more resources to help researchers at Baylor, where flooding occurred when NIH's budget was booming. "It's a different budget environment," she says.

The disruption, meanwhile, has stalled expansion plans at both universities. Tulane "had been moving at a fantastic pace pre-Katrina," says Whelton. It tripled its NIH grants over the past 5 years, rising to 86th among institutions with the most NIH funding, he notes. The university had hoped to double such funding again, but that strategic plan is now on hold. LSU, which had also been on a recruiting drive, hiring 100 faculty and three new department chairs in the last 4 years, is in even worse shape. HSC is losing revenue from a lack of patients, and the state is considering cutting money for higher education by at least 5%. LSU staff have already been laid off, and faculty could come next, says spokesperson Leslie Capo. "Money for recruiting's going to be very scarce," says Pincus.

Homeless but hopeful

Even as they try to resurrect their labs, many investigators are dealing with staggering personal property losses. A number lived in flooded suburbs such as Lakeview, which is next to the failed 17th Street levee. A drive through this neighborhood is shocking—block after block of middle-class homes marked halfway up with flood lines, some with caved-in walls and roofs and muddy yards littered with overturned cars and fallen trees. Researchers who have salvageable homes are spending weekends cleaning up, often while putting in grueling commutes to teach medical students in Baton Rouge, where LSU is holding classes, or at Tulane's temporary campus in Houston—5 to 6 hours away. Some have sent spouses and children to live with relatives in distant cities.

Fungal fright. Mold in a basement chemistry lab at Tulane.

Universities are scrambling to locate places for faculty and lab workers to stay. UNO plans to find a place to put nearly 400 trailer homes provided by FEMA. LSU is considering cruise ships. Tulane, meanwhile, is hoping to entice back faculty members with families by co-launching a new charter school near campus.

Still, scientists expect that some of their colleagues won't stay long or return at all, especially because most research grants are given to individuals and are not tied to an institution. "They're portable," says Bazan. Tulane has already lost at least two researchers, a husband-wife couple. LSU has seen a half-dozen faculty members take slots elsewhere. Others aren't ruling out a move. "I'm keeping my options open. I can't afford to lose another 2 to 3 months of research time," says LSU neuroscientist Jeffrey Magee, who is 40. Another worry is that graduate students and postdocs will no longer come.

Any abandonment of New Orleans is premature, say some. Students and scientists don't realize that New Orleans is not the "hell on Earth" portrayed on television, says Tulane developmental biologist Peter Cserjesi, noting that restaurants are reopening, the French Quarter is coming alive at night, and crime is at an all-time low because so few people are left and the National Guard and police are patrolling the streets. But concerns about future hurricanes and the city's infrastructure are tough to shed, especially for outsiders. Some New Orleans researchers, for example, are protesting the Society for Neuroscience's decision to move its 2009 meeting from New Orleans (see News story, p. 1260).

Among those who have returned, many share a sense of mission. "It's almost like people are coming back because they want to make a difference," says molecular biologist John McLachlan, who runs a joint environmental center with Xavier University in New Orleans that has received a $200,000 NSF grant to coordinate post-Katrina research. "They want to save Tulane. They want to save the city. I think that's palpable and real." But whether that goodwill will be enough to salvage science in New Orleans may not be known for a long time.

–JOCELYN KAISER

CREDITS (TOP TO BOTTOM): P. BURCH/TULANE UNIVERSITY; J. KAISER/*SCIENCE*

"I think the dosage needs adjusting. I'm not nearly as happy as the people in the ads."

It's time for genetics.

What if you could use DNA to identify patients who respond well to your drug? You might use that knowledge to reach more patients and expand your market, or to get a drug to market faster. Either way – patients win. Perlegen is helping drug companies do just that – today.

Working with you, we can comprehensively analyze the DNA from hundreds of patients taking your drug. Out of the millions of genetic variations between patients, we help you identify the ones that are associated with strong efficacy, poor efficacy, or side effects. Perlegen's unparalleled coverage of the genome and experienced team of analysts mean you get clinically relevant answers, not just data, in a matter of months.

We partner with the top pharmaceutical companies around the world. We also license late-stage drugs. If you have a drug that can benefit from our approach, please contact us.

Patients are waiting.

genetics@perlegen.com
Mountain View, California • 650-625-4500
Tokyo, Japan • +81 (0)3 3444-6080
www.perlegen.com

Targeting today's drugs. Discovering tomorrow's.™

PERLEGEN SCIENCES®

Researchers Turn Up the Heat In Superconductivity Hunt

Physicists still can't explain why some ceramic materials lose electrical resistance at relatively balmy temperatures, but they think they're on the right track

When Peter Johnson and colleagues set out to study the behavior of electrons in high-temperature superconductors, their experiments raised more than a few eyebrows. In 1999, Johnson, a physicist at Brookhaven National Laboratory in Upton, New York, systematically blasted electrons out of a superconductor with bursts of photons. The technique, called angle-resolved photoemission (ARPES), can reveal intricate details about how electrons behave inside a material. The Brookhaven team's results, however, flew in the face of other ARPES results as well as other types of electron-tracking experiments.

Today, things are falling into line. Armed with more-precise electron detectors, Johnson and his colleagues say the bumps and wiggles in their data better match other experimental results. Other photoemission experimenters, such as Z. X. Shen's group at Stanford University in Palo Alto, California, report a similar swerve toward consensus. "We are correcting ourselves, and Z. X. is happy to correct us as well," Johnson quips.

That turnabout and others have convinced a number of researchers that they are closing in on what many view as the biggest mystery in condensed-matter physics: the mechanism that causes certain ceramics to superconduct at unusually high critical temperatures (T_c). But as experimental results grow ever more precise and convincing, just what they all mean remains highly contested. "There has been a tremendous amount of progress in the experiments," says Mike Norman, a high-T_c theorist at Argonne National Laboratory in Illinois. "The data are pretty clear. But there is a lot of controversy about the interpretation,"

Controversy has been in steady supply since 1986, when Swiss physicists Georg Bednorz and Alex Müller discovered a class of copper-and-oxygen–containing ceramics called cuprates. The materials have since been shown to conduct electricity without resistance at temperatures as high as 138 kelvin—more than three times the temperature of the best metallic superconductors. As in those conventional superconductors, electrons in the cuprates pair up into "Cooper pairs" and surf through the material without the electrical friction typical of electrons traveling through other materials. Because all electrons carry a negative charge, they usually repel one another and don't want to pair up. But the rules change for superconductors. In the low-temperature metallic variety, a moving electron creates vibrations in the material's atomic lattice that pull another electron in its wake. It's these lattice vibrations, also known as phonons, that glue Cooper pairs together.

So what glues Cooper pairs together in high-temperature superconductors? After nearly 20 years of searching, physicists continue to battle over the answer. Perhaps the most prevalent view is that this pairing is driven by the magnetic behavior of the copper atoms in the atomic lattice of the cuprates: The presence of an electron on one copper atom causes nearby magnetic "spins" to align in a way that attracts another electron to sit nearby. Plenty of other researchers, however, argue in favor of phonons or some still more exotic mechanism.

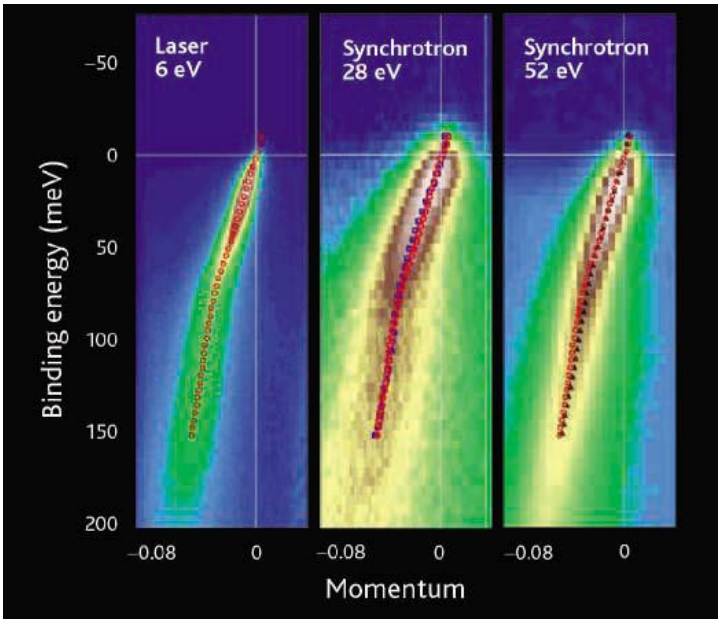

Signpost? "Kinks" in photoemission data may show that electrons interact with vibrations of the crystalline lattice—a possible clue to high-T_c superconductivity.

Sorting out what is going on has been a headache in part because of the odd way in which the cuprates superconduct. In traditional superconductors, Cooper pairs surf through the material with the same ease in all directions. That's not the case with the cuprates. These materials have a complex layered structure that forces Cooper pairs to travel in the flat planes that contain copper and oxygen atoms. And even within these planes, they travel only along the two axes of the crystal, not along the 45° angles. When researchers map out the energy that binds Cooper pairs together versus their momentum (a product of their mass and velocity), they see a cloverleaf pattern, very different from what is seen in metallic superconductors.

Researchers initially turned to ARPES because it can track both the energy level of liberated electrons—which is determined in part by what other players the electrons are interacting with—and how this behavior changes with the electron's momentum. Other techniques reveal only the energy. But although early ARPES experiments did a fair job of nailing down the momentum, they couldn't come close to the energy resolution of other types of experiments. Over the past several years, the ability of the detectors to gauge the particular track of the electrons has improved 40-fold, and the energy resolution has skyrocketed as well. "The measurements are vastly superior to 10 years ago," which has made ARPES an essential tool for investigating high-T_c materials, Norman says.

In Johnson's early photoemission experiments, he and his colleagues found that the electrons evicted from the cuprates had a broad range of energies. As they lowered the temperature of their sample from above the superconducting temperature to below it, the spread stayed about the same. That stability muddied the waters by suggesting that the researchers weren't seeing excited electrons interacting with any specific player in the material, such as a lattice vibration or type of magnetic fluctuation. In the parlance of physicists, they didn't see any "quasiparticles" in the superconducting state, which are essentially the combination of excited electrons together with the forces exciting them. Superconductivity in cuprates, it seemed, was due to a jumble of influences instead of a specific one.

CREDIT: D. DESSAU/UNIVERSITY OF COLORADO AND NATIONAL INSTITUTE OF STANDARDS AND TECHNOLOGY, BOULDER

That picture soon began to change when a company called Scienta came out with new, more-sensitive electron detectors, and it has been growing sharper ever since. Researchers led by Juan Campuzano at Argonne National Lab, for example, reported evidence in 2000 that quasi-particles were in fact present below the material's superconducting temperature. And this summer, after a series of very precise measurements, Johnson's team reported at a meeting that it largely agrees. Still, Johnson and others say that just what influences those quasi-particles represent remains unclear. But they're offering new hope that experimenters and theorists will soon pin them down. "It offers a signpost that we might be seeing something important," says Daniel Dessau, a photoemission expert at the University of Colorado, Boulder, and the National Institute of Standards and Technology.

Another set of key signposts gives added reason for cheer. When researchers plot the energy of electrons liberated by a photoemission experiment against their momentum, they now regularly see what looks like a straight line with a kink in it, reminiscent of the bend in a flexible drinking straw. "The kink is an indication of a sudden change in the electron's velocity at a particular energy," Shen explains. "There must be something making that change." And the energy signature of that something is conspicuously close to the amount of energy that binds Cooper pairs together—suggesting that whatever gives rise to the kinks also acts as the mysterious glue for Cooper pairs.

In results reported at an American Physical Society meeting in March, for example, Dessau's team, working with photons from a high-power laser, sees a crystal-clear kink at 70 milli–electron volts (meV), an energy level that is most commonly associated with a phonon (see figure, p. 1271). Shen and colleagues working at the Hiroshima Synchrotron Radiation Center in Japan see a similar kink as well, which these and other groups had spotted with less resolution before. The catch is these electrons are traveling at a 45° angle to the crystal lattice—a direction, called the "node," in which Cooper pairs can't travel. Because the electrons couldn't have been paired before being blasted out of the material, many researchers question how relevant this phonon is to the glue that holds Cooper pairs together. "This is not the node to study pairing," Shen says.

Along the "antinode," the 0° and 90° axes of the crystalline lattice, the picture is more confusing. Several groups, including Dessau's, see a kink there as well, at 40 meV. That suggests a different influence is acting on the electron. Shen and colleagues argue that their data point to a separate phonon from the 70-meV version present along the node. But for now, many other researchers don't agree. "The other groups are fairly insistent that it is not a phonon effect along the antinode," Norman says. Most of these teams suggest that the kink is caused by a collective magnetic behavior of the electrons. The wrinkle, Johnson says, is that both the phonons and the magnetic excitations would likely have about the same energy signature, so it is hard to tell which one is playing the key role. But the recent progress in ARPES and other experiments has many high-T_c researchers feeling more confident than ever that they will find the answer soon. Says Norman: "I think it will be sorted out in the next couple of years."

–ROBERT F. SERVICE

Space Science

The Question on the Table: Will Europe Go to Mars?

At a meeting in Berlin next month, members of the European Space Agency will be asked to invest in Aurora, a still-evolving scheme to explore the solar system

CAMBRIDGE, U.K.—Next month, when ministers from the 15 member states in the European Space Agency (ESA) meet in Berlin to discuss the next 5-year chunk of funding, they will face an important question: Is it time for Europe to forge its own path among the planets? European governments made a tentative move in this direction in 2000—several years before President George W. Bush committed the United States to going to the moon and Mars—by asking ESA to lay the groundwork for human exploration of the solar system. In 2001, this program got a name—Aurora—and some seed money. Now it is time to write a big check.

Aurora, if it goes, will be small by NASA's standards. In its first decade, it will consist principally of a single robotic mission, known as ExoMars, and technology development for a future Mars sample-return mission and human exploration. ESA next month will request a budget in the region of $800 million to $950 million for Aurora over the next 5 years.

Although the program is beginning modestly, it is symbolic of the agency's burgeoning ambitions and Europe's desire to assert its independence in space. "Europe now has greater confidence and capability in planetary exploration," says astrophysicist Ken Pounds of the University of Leicester, a former chief executive of the United Kingdom's Particle Physics and Astronomy Research Council. And to underline this new spirit of bravado, ESA also wants to collaborate with Russia to build a minishuttle called Clipper that would carry up to six astronauts into space.

As a rule, space agencies' plans tend to outrun their available budgets. Whereas NASA must go to Congress every year to get its budget approved and make good the cost overruns, ESA walks a different financial tightrope: It must persuade 15 governments to agree on its funding once every 5 years or so—as it hopes to do in Berlin on 5 to 6 December.

ESA's science missions often fare badly in this process because science is one of the

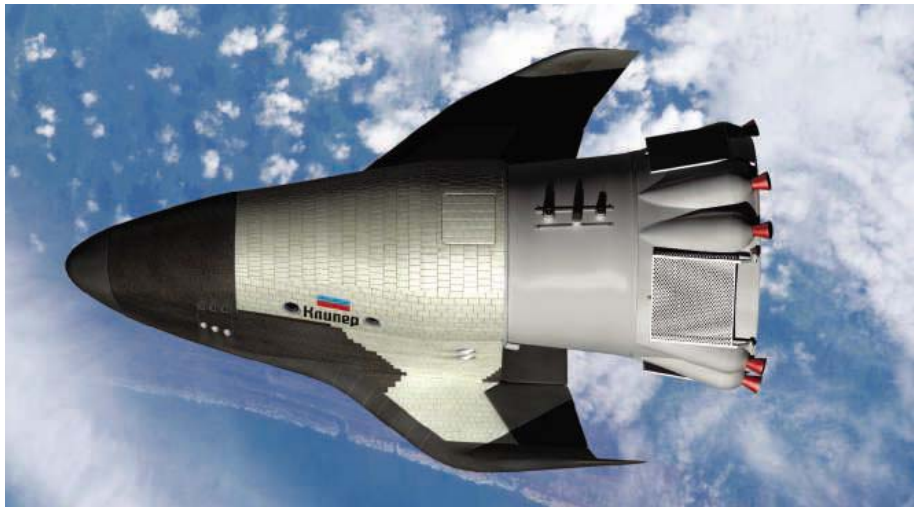

CREDIT: ANATOLY ZAK/RUSSIANSPACEWEB.COM

Shuttle-lite. ESA is interested in Russia's design for a six-person exploration vehicle.

agency's few mandatory programs, to which every member state contributes in proportion to its gross national product. That may seem like a formula for assured funding, but because all the members have to agree on the total sum, the science budget has remained static for about a decade. ESA officials aim to break Aurora out of that straitjacket by casting it as an optional program: Each member can contribute as much or as little as it likes and receive back funding for its researchers or industry contracts in proportion to its contribution. ESA's leaders hope Aurora will be attractive enough to win funding in its own right, and they are busy selling the concept.

"We've been working closely with most of the delegations with an interest in ExoMars," says Piero Messina of the exploration program at ESA headquarters in Paris. "We hope this will pay off." ExoMars is something of a carrot to lure member states into Aurora. Following on from ESA's successful Mars Express orbiter, the baseline version of ExoMars will consist of two parts: a rover that will be able to drill into rocks and burrow beneath the surface in search of samples, which can then be analyzed onboard for signs of life, and a static base station with environmental and geophysics instruments.

ExoMars will also be a test bed for essential technologies, including hardware for descent and landing, power supply, and communications. Finally, it will assess what sorts of hazards future human visitors might face. "We sense that the interest in ExoMars is such that it may attract more money than the baseline," Messina says. If member states pledge more than the $700 million ESA is seeking for ExoMars, the agency may be able to add an orbiter that will act as a communications relay while studying the planet's surface from space.

The potential sticking point in next month's negotiations is that member states are divided on the long-term goal of sending human beings to explore the solar system. ESA already has a corps of astronauts, but no vehicle to carry them in: They must travel as guests aboard the shuttle or Soyuz. The United Kingdom has a decades-long policy of not participating in programs involving humans in space because of the huge investment required, and sources say Germany, too, may be reluctant to join Aurora if it emphasizes human exploration.

Earlier this year, the United Kingdom's Royal Astronomical Society asked a panel of three prominent scientists, including Pounds, to investigate the case for human exploration of the solar system. They were skeptical from the start, having seen the billions squandered on the international space station produce little scientific return. But after 9 months of investigation, they were convinced that for the foreseeable future, robots would be unlikely to be adept enough to provide answers to important questions such as the history of the solar system and the existence, or not, of life on Mars. The United Kingdom, they concluded, should abandon its policy of avoiding all human missions. "Do we want to be in there, or standing by watching?" asks Pounds.

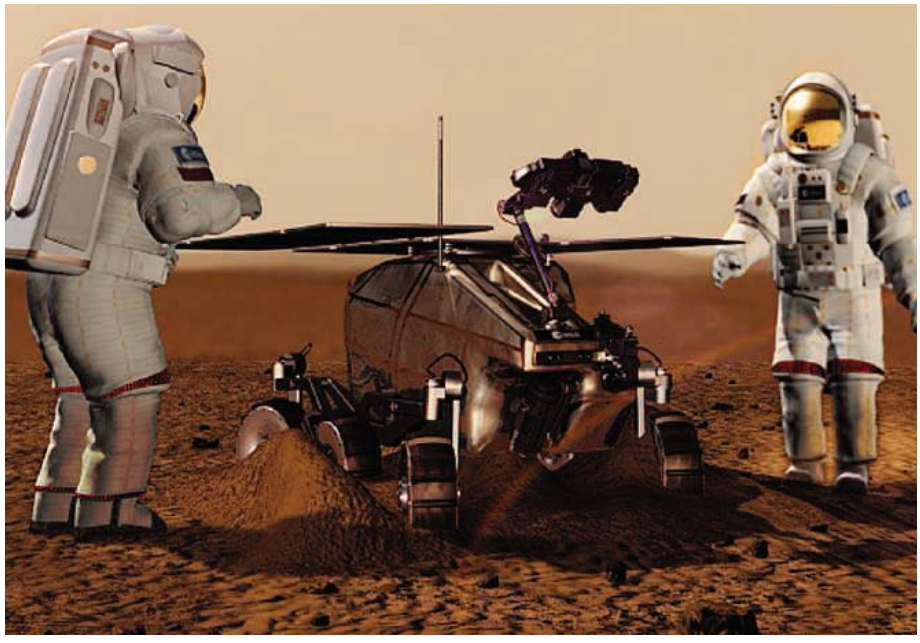

CREDIT: ESA

Far out. Europe may be ready to embrace a new vision for human space exploration, setting aside disappointments with the U.S.-led international space station.

Despite such encouragement, ESA foresaw that the human issue would continue to be a problem for some member states, and it has toned down those parts of the Aurora proposal, for the early years at least. "For the moment, there is no human element," says Roger Bonnet, former director of science at ESA, who now heads the International Space Science Institute in Bern, Switzerland.

Another potential area of uncertainty is the extent to which Aurora will require collaboration with other space agencies. ExoMars "is clearly an ESA mission," says Messina. The sample-return mission that is to follow it "was always conceived as an international endeavor, but [whether] partners will be ready or willing is uncertain" because "calendars have to match," he explains. Aurora officials and their opposite numbers at NASA have had regular meetings, but Messina says U.S. plans are still in flux. Although ESA officials may talk big, realistically Europe is never going to send astronauts to Mars on its own. "Aurora is about enhancing our knowledge of Mars, getting technology ready, keeping an eye on the plans of other nations, and identifying the building blocks that ESA can contribute," Messina says.

While ESA is keeping an eye on NASA to set the pace for a visit to Mars, it is looking to the East in search of a vehicle to get astronauts into space. NASA has made it clear that it does not want any international help in developing its Crew Exploration Vehicle, the successor to the shuttle. However, earlier this year, the Russian space agency approached ESA to suggest teaming up to develop Clipper, which Russia has been working on since 2000 as a replacement for the venerable Soyuz capsule. In June, the two agencies inked an agreement to carry out 2 years of joint studies beginning in January 2006, assuming that ESA members agree to the $60 million price tag at the Berlin meeting.

Clipper would be lofted into space with an existing launcher, such as Russia's Angara or Ukraine's Zenit, and it would glide down to land on a runway. The aim is to have an initial unpiloted flight in 2011 and to carry the first passengers in 2012 or 2013. Initially, it will take over from Soyuz in ferrying crew back and forth to the international space station, but, says Manuel Valls of ESA's Human Spaceflight Directorate, it is not designed to provide a taxi service: "It's an exploration vehicle. It could go to the moon, provided with appropriate propulsion." The agencies are reluctant to talk about the total cost of development, but it is likely to be somewhere in the region of $2 billion to $3.5 billion. Russia has also asked Japan to join the collaboration; a decision from Tokyo is expected during December.

Next month's meeting will reveal whether European politicians share ESA's enthusiasm for sending their citizens into the final frontier. Buying into the Aurora program would be the down payment.

–DANIEL CLERY

Random Samples

Edited by Constance Holden

Fight or Flight

Anger is better for your health than fear, say researchers. The two emotions are generally lumped together when it comes to stress-related health risks. But psychiatrist Jennifer Lerner of Carnegie Mellon University in Pittsburgh, Pennsylvania, and colleagues have devised a way to sort them out through analysis of facial expressions.

The researchers studied 92 subjects who counted backward and did math problems while an experimenter verbally harassed them. To determine the participants' emotions during testing, the researchers used a system that tracks facial muscle movements known to be correlated with fear or anger.

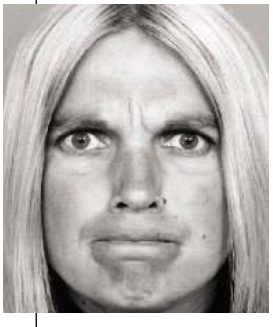

Measurements taken during the testing showed that blood pressure and saliva levels of the stress hormone cortisol went up in all participants expressing fear from the unreasonable pressure. But those physiological responses were much less pronounced among those whose faces indicated anger instead, the researchers reported in last month's issue of *Biological Psychiatry*. This makes sense to Lerner: Whereas fear implies loss of control, anger suggests that action can be taken, she explains.

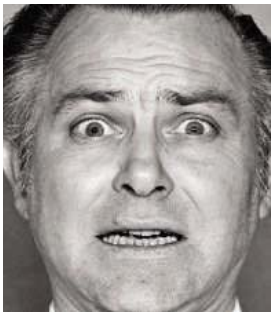

Because it's hard to trust the emotions described by a participant under stress, Lerner says, the facial-analysis technique has "enormous potential for getting a window on emotion." Correlating facial expressions with biological responses to stress is "really cool," says psychiatrist Reginald Adams of Pennsylvania State University, University Park. "It's such a versatile tool. It's going to open up some very exciting directions for future research."

Two Views Better Than One?

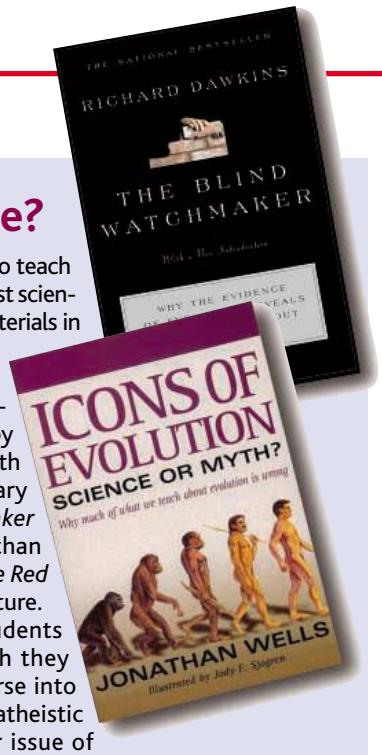

The demand by intelligent design (ID) proponents to teach the scientific "controversy" about evolution riles most scientists. But a new study suggests that including ID materials in biology classes may help open minds to evolution.

During the fall of 2003, 103 freshman biology majors at Central Washington University in Ellensburg were divided into four sections. Two, taught by biologist Steven Verhey, learned arguments for both ID and evolution, with readings from evolutionary biologist Richard Dawkins's *The Blind Watchmaker* and *Icons of Evolution* by ID proponent Jonathan Wells. The other two read only Matt Ridley's *The Red Queen*, about the evolution of sex and human nature.

At the end of the semester, 66 of the students agreed to take an anonymous survey in which they classified their beliefs before and after the course into six categories, ranging from biblical literalism to atheistic evolutionism. Verhey reports in the November issue of *BioScience* that 61% of the respondents exposed to both ID and evolution indicated a change of mind, as opposed to 21% in the control sections. The great majority of shifters moved toward evolution. For example, four of six in the experimental group who identified themselves as biblical literalists moved in the "rationalist" direction, Verhey reports.

The study provides "powerful evidence" that directly engaging students' beliefs, rather than ignoring them, may be an effective way to teach evolution, writes biologist Craig Nelson of Indiana University, Bloomington, in an accompanying editorial. But he agrees with evolutionary geneticist Jerry Coyne of the University of Chicago that this strategy wouldn't be appropriate for high school students, who, says Coyne, "are not intellectually equipped to deal with such [a] controversy."

Flying Noses

Hunting for dead bodies or hidden explosives? A tube of wasps may be the answer for both types of unusual searches. In the wild, the tiny parasitic wasp *Microplitis croceipes* can smell not only nectar but also airborne chemical signals from plants being eaten by its host caterpillar.

Entomologist W. Joe Lewis of the U.S. Department of Agriculture's Agricultural Research Service found he could train the wasps to link many scents with a sugar-water reward. But "you can't put a wasp on a leash and take it around" like a bomb-sniffing dog, he says. So engineer Glen Rains of the University of Georgia, Tifton, designed a portable "Wasp Hound": a device outfitted with a fan that pulls air through a cartridge holding five wasps. When they catch a whiff of a target scent, say, 2,4-dinitrotoluene from explosives, they crowd around the air holes, looking for a reward.

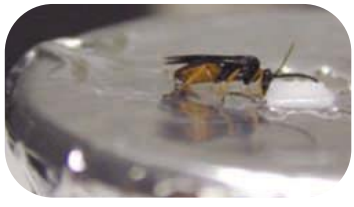

Wasp in training.

In a recent test using five different smells, the device far outperformed an electronic nose and was as good as a dog, the researchers report in an upcoming issue of *Biotechnology Progress*. But wasps are cheaper than bloodhounds and need only 5 minutes of training, Lewis says. Now, Rains and Lewis are working on a mass wasp-training regimen and on new applications including finding dead bodies from scents such as cadaverine and putrescene.

Bees are also joining the olfactory workforce. Bee specialist Mathilde Briens, of Inscentinel in Harpenden, U.K., says they're working on a system in which bees stick out their tongues in response to a scent.

CREDITS (TOP, MIDDLE LEFT, BOTTOM): PAUL EKMAN/UNIVERSITY OF CALIFORNIA, SAN FRANCISCO; GLEN RAINS

Edited by Yudhijit Bhattacharjee

AWARDS

Qubits for dollars. Quantum computing guru David Deutsch is the first recipient of the $100,000 Edge of Computation Science Prize for researchers whose computer-related ideas touch on broader questions about life, the universe, and everything.

The 52-year-old Deutsch, at the University of Oxford, U.K., provided the first blueprints for a universal quantum computer in 1985, bringing to life an earlier suggestion from physicist Richard Feynman. Quantum computation, which theoretically is exponentially faster than classical computing, could potentially speed up calculations that currently hamper fields such as physics, biology, and nanotechnology.

"Deutsch clearly deserved the prize because of his seminal role in creating and furthering quantum computation," says physicist and computer scientist Seth Lloyd of the Massachusetts Institute of Technology in Cambridge, who was a judge.

But it's an unusual reward that transcends disciplines; other nominees were from fields of computational biology, software development, and communications, he notes. "I'll be very interested to see who wins it next," says Lloyd.

The prize is funded by philanthropist Jeffrey Epstein.

ON THE JOB

A green NSF. The National Science Foundation's system of hiring "rotators"—academics who take a few years' leave to work at NSF—seems to be spinning out of control. The problem: So much new blood threatens to leave the agency with little institutional memory at the top.

By next summer, it's possible that only one of the agency's seven research directorates will be headed by someone with even 1 year of experience on the job. Last month, Michael Turner, head of mathematics and physical sciences, announced he would be returning to the University of Chicago in the spring. And this month, NSF is convening search committees to find successors for engineering's John Brighton, who left this summer, and computer sciences' Peter Freeman, who next spring completes a 3-year stint. A search to replace education's Judith Ramaley, now president of Winona State University in Minnesota, has dragged on for more than a year, with Don Thompson filling in since January.

NSF Director Arden Bement has recently filled two slots: Jim Collins came on board last month to succeed longtime biology head Mary Clutter, and David Lightfoot arrived in June to lead the social, behavioral sciences, and economics program. That leaves only geosciences' boss Margaret Leinen, who came to NSF in 2000, with significant time in her position. Bement is also sifting through applicants to fill two other senior posts: the heads of international affairs and legislative/public affairs.

THEY SAID IT

"Twenty-eight billion dollars is a lot of money. It's ridiculous to ask for more given all the problems the country is facing. The question is how to spend it."

—Steven Heinemann, president-elect of the Society for Neuroscience, on whether biomedical lobbyists should be trying to boost the president's request for only a $146 million increase in 2006 for the National Institutes of Health.

Got any tips for this page?
E-mail people@aaas.org

MOVERS

Magnetic draw. The promise of constructing a high-field magnet from a new type of superconductor is shifting the landscape among superconductivity experts. Researchers at the Applied Superconductivity Center (ASC) at the University of Wisconsin, Madison, announced last month that they're moving their operations to Florida State University in Tallahassee, which is also home to the National High Magnetic Field Laboratory. About 22 ASC members will relocate by July 2006, forming a materials research division of the magnet lab.

Physicist David Larbalestier (left), one of ASC's leaders, cites the growing promise of a metallic superconductor called MgB_2 that could be used for making more powerful magnets that work at warmer temperatures than traditional metallic superconductors.

Bob Hawsey, who runs the superconductivity program at Oak Ridge National Laboratory in Tennessee, says the move is a big loss for the University of Wisconsin, which has been home to ASC for more than 20 years.

Leaving the garden. Saying that great institutions need "a regular infusion of new ideas and energy to stay at the top of their game," paleobotanist Peter Crane announced last week that he will step down after 7 years as director of the Royal Botanic Gardens, Kew, in London. Next summer, he will join the geophysics department at the University of Chicago.

Before Kew, Crane was director of the Field Museum of Natural History in Chicago, Illinois, for 7 years, and he says he's looking forward to working with an "enormously strong group of paleontologists" in a city where his wife, Elinor Hamer Crane, grew up. Kew, which last year attracted a record 1.35 million visitors, acquired a new molecular mycology lab and became a UNESCO-designated World Heritage Site during Crane's tenure.

CREDITS (TOP TO BOTTOM): LUJE TAYLOR; DAVID NEVALA/UNIVERSITY OF WISCONSIN; ROYAL BOTANIC GARDENS, KEW

LETTERS

Making a Rebuilt New Orleans Sustainable

THE TRAGIC EVENTS RESULTING FROM Hurricane Katrina have seen a major U.S. city almost totally destroyed, and it is 100 years of human activity that have created the conditions leading to this inevitable tragedy.

The dramatic, human-driven deterioration of 25% of the wetlands of the Mississippi delta has removed an important buffer against storms. The river that built and nourished the delta over thousands of years has been leveed to its mouth, preventing the freshwater, silts, and nutrients that nourished and sustained the delta from flowing over the wetlands. The natural subsidence that delta soils undergo continues, and without river input, most wetlands sink below the water and die. Within the delta plain, there have been enormous changes in the natural hydrology as more than 15,000 km of canals have been dredged through the marshes. Barrier islands that helped protect the wetlands have fragmented and disappeared.

A broken levee on the east side of the London Avenue Canal in the Gentilly neighborhood of New Orleans, 11 September 2005.

One of the most notable of the canals is the Mississippi River Gulf Outlet (MRGO), which runs southeast from New Orleans to the Gulf of Mexico. It was constructed by the Corps of Engineers in the 1950s as a shorter shipping route to the gulf; however, it has never carried more than a small percentage of the shipping that comes to New Orleans. Saltwater intrusion through the MRGO killed extensive freshwater cypress wetlands in St. Bernard Parish just downriver from New Orleans. Thus, MRGO has been an economic and environmental disaster.

The levees of the MRGO, when combined with those along the Gulf Intracoastal Waterway and the Mississippi River, form a funnel drawing the surge into the heart of New Orleans. Paul Kemp and Hassan Mashriqui, researchers with the LSU Hurricane Center, published surge simulation results days before the storm hit that showed the city flooding (www.hurricane.lsu.edu/floodprediction) through the funnel. Early availability of the results is believed to have played an important role in convincing both civic leaders and the citizenry to begin an unprecedented evacuation, estimated at over 85%. As Katrina approached, the storm surge was forced into the funnel and built up to levels that overtopped levees in eastern New Orleans and St. Bernard Parish. This is not the first time that this has happened. In 1965, Hurricane Betsy followed a similar path that led to extensive flooding in the same area of eastern New Orleans.

What should be done now? The City of New Orleans should be rebuilt, but not as it was, or the inevitable will happen again. New Orleans and South Louisiana can be reborn in a way that is sustainable and serves as an example to the rest of the nation. The living spaces of homes need to be above maximum flood level. These buildings need to be strong enough to survive hurricane force winds and should be super-efficient and constructed to use renewable energy such as solar and wind power. As the city rebuilds, efficient mass transit and use of wetlands for assimilation can contribute to sustainability. All of this should be done in a way that engages and enables the poor and marginalized citizens of the city.

New Orleans sits in the middle of the largest and most productive coastal wetland ecosystem in the United States, the Mississippi delta. Louisiana and the federal government have begun a joint effort to restore the delta, and the first significant funding has been approved this year in the Energy Bill. Restoration of the delta is critical for the protection of a rebuilt New Orleans because of the storm buffer that wetlands provide.

New Orleans and the surrounding region must be rebuilt in a way that is sustainable and energy efficient. In this way, out of this tragedy, a new vision for the future can emerge, not only for south Louisiana, but for the nation as a whole.

JOHN W. DAY

Distinguished Professor Emeritus, Louisiana State University, Baton Rouge, LA 70803, USA.

Problems of Studying Extinction Risks

M. CARDILLO *ET AL.*'S ANALYSIS OF MAMmalian extinction biology ("Multiple causes of high extinction risk in large mammal species," Reports, 19 Aug., p. 1239) uses data from the IUCN Red List of Threatened Species (*1*). I believe that conservationists should be much more circumspect than we currently are about conclusions based on such analyses of the Red List.

The Red List is not managed as a database for biological analysis. Many problems are inherent in using threatened species lists for purposes for which they were not designed (*2*). The Red List's categorizations are largely informed guesswork by experts. That guesswork is vital and appropriate, given how little we know of most of the world's species and how little would be done about them if we insisted on full knowledge before action. Nevertheless, what is going to inform guesswork but knowledge of extinction biology?

Consequently, the biology of extinction is being investigated by the use of data that are (properly) fundamentally affected by knowledge of extinction biology. I cannot see that the inevitable circularity is removed by use of, for example, only species categorized on the basis of only population size or rate of decline [(*3*); Cardillo *et al.*]: The expert does not know the rate of decline (*4*) but does know that large-bodied, slow-reproducing species that live in small geographic ranges are more likely to be threatened than are small-bodied, fast species in large ranges—and so suggests a faster decline for the former.

How can use of Red Lists to investigate extinction biology avoid such circularity, especially when the IUCN does not yet have the resources to make available the data on which the categorizations are based?

A. H. HARCOURT

Department of Anthropology, Graduate Group in Ecology, University of California, Davis, CA 95616, USA. E-mail: ahharcourt@ucdavis.edu

References

1. IUCN, *2003 IUCN Red List of Threatened Species* (International Union for Conservation of Nature and

Natural Resources, Gland, Switzerland, 2003) (available at www.redlist.org/).
2. H. P. Possingham *et al.*, *Trends Ecol. Evol.* **17**, 503 (2002).
3. A. Purvis, J. L. Gittleman, G. Cowlishaw, G. M. Mace, *Proc. R. Soc. London Ser. B* **267**, 1947 (2000).
4. S. Blake, S. Hedges, *Conserv. Biol.* **18**, 1191 (2004).

M. CARDILLO *ET AL.* APPLY PHYLOGENETICALLY controlled comparative analyses to investigate patterns of extinction risk in large mammals ("Multiple causes of high extinction risk in large mammal species," Reports, 19 Aug., p. 1239). Similar analyses have been reported elsewhere (*1*–*3*). Although it is obviously important to understand the factors affecting extinction risk, these techniques are being applied beyond their intended application and may not be providing meaningful results.

The technique of independent contrasts is designed to control for nonindependence among traits resulting from shared phylogenetic history or common descent (*4*). However, extinction risk is not a phenotypic trait and has no shared phylogenetic history with any trait. For most mammal species, the external threats or processes promoting higher risk of extinction (e.g., habitat loss, alteration or fragmentation, exploitation, etc.) are often very recent in origin and have no phylogenetic history at all, shared or otherwise. In these cases, it is meaningless to infer values for such recent and externally driven factors at deeper (i.e., ancestral) nodes of a phylogeny. As a result, the calculated contrast values of extinction risk are potentially misleading.

Although extinction risk may indeed vary across a phylogeny, this phylogenetic signal is not the same as nonindependence resulting from shared phylogenetic history. A possible association with phylogeny is something for which we should test, not something to assume a priori. We need to develop and employ more appropriate methods for investigating associations between traits that are linked by phylogeny (e.g., life history variables) and other factors that are not (e.g., extinction risk). The big danger for conservation biology is that the continued use of inappropriate techniques may lead to erroneous conclusions and poor decisions.

DAVID PUTLAND
School of Integrative Biology, The University of Queensland, St. Lucia, QLD 4072, Australia.

References
1. M. Cardillo, *Anim. Conserv.* **6**, 63 (2003).
2. D. O. Fisher, S. P. Blomberg, I. P. F. Owens, *Proc. R. Soc. London Ser. B* **270**, 1801 (2003).
3. M. Cardillo *et al.*, *PloS Biol.* **2**, 909 (2004).
4. P. H. Harvey, M. D. Pagel, *The Comparative Method in Evolutionary Biology* (Oxford University Press, Oxford, 1991).

Response

USING THE IUCN RED LIST (*1*) WE HAVE shown that body mass strongly mediates the effects of biological and environmental factors on mammal species extinction risk. Our extinction risk measure was conservative in only including threatened species listed under criterion A of the Red List, which is based on rates of population decline.

Despite Harcourt's concerns about circularity, biological traits do not form part of the process of categorizing species under criterion A. Categorizations of extinction risk are made under explicit, objective, and quantitative criteria (*2*). For example, under criterion A1, a species is listed as Vulnerable, Endangered, or Critically Endangered if the rate of population decline has been 50 to 70%, 70 to 90%, or >90%, respectively, over a period of 10 years or three generations, whichever is longer (*3*). Rates of decline may be assessed from direct observations or inferred from indirect evidence such as catch statistics or habitat loss. If the latter, there are explicit guidelines for inferring population decline rates from indirect evidence (*3*), and assessors must present the evidence they have used to conclude that a population has declined by the amount claimed. Before listing, assessments are

reviewed by independent Red List Authorities. Species listings are accompanied by a justification giving support for the listing, together with relevant data and references, thus making the process as repeatable and transparent as possible. Species for which too little data exist to assign to an extinction risk category are listed as Data Deficient.

Our comparative analysis used phylogenetically independent contrasts (PICs) to eliminate the pseudoreplication that would otherwise result from the phylogenetic nonindependence of the observations in our data set (*4*). A phylogenetically nonrandom distribution of extinction risk among mammals and other taxa is well established, has long been recognized as a noteworthy and important phenomenon (*5*, *6*), and appears to be the rule rather than the exception (*7*). Despite the case for using PICs in extinction risk studies having recently been clearly and elegantly made (*6*), Putland is skeptical about the need to employ such methods. However, as we and many others have shown, extinction risk is correlated with many different factors, some of which (e.g., body mass) are strongly heritable and closely associated with phylogeny. Whether or not it is itself heritable, extinction risk shows a phylogenetic signal. Comparative tests that fail to account for this signal suffer from pseudoreplication, with potentially misleading results (*7*, *8*).

MARCEL CARDILLO,[1]
GEORGINA MACE,[2] ANDY PURVIS[1]

[1]Division of Biology, Imperial College London, Silwood Park Campus, Ascot SL5 7PY, UK. [2]Institute of Zoology, Zoological Society of London, Regent's Park, London NW1 4RY, UK.

References

1. IUCN, 2003 *IUCN Red List of Threatened Species* (IUCN, Gland, Switzerland, 2003).
2. A. S. L. Rodrigues, J. D. Pilgrim, J. F. Lamoreaux, M. Hoffmann, T. M. Brooks, *Trends Ecol. Evol.*, in press.
3. IUCN, www.iucn.org/webfiles/doc/SSC/RedList/RedListGuidelines.pdf (2005).
4. P. H. Harvey, M. D. Pagel, *The Comparative Method in Evolutionary Biology* (Oxford Univ. Press, Oxford, 1991).
5. M. L. McKinney, *Annu. Rev. Ecol. Syst.* **28**, 495 (1997).
6. A. Purvis, P.-M. Agapow, J. L. Gittleman, G. M. Mace, *Science* **288**, 328 (2000).
7. D. O. Fisher, I. P. F. Owens, *Trends Ecol. Evol.* **19**, 391 (2004).
8. A. Purvis, M. Cardillo, R. Grenyer, B. Collen, in *Phylogeny and Conservation*, A. Purvis, J. L. Gittleman, T. Brooks, Eds. (Cambridge Univ. Press, Cambridge, 2005), pp. 295–316.

Benefits of a Regional Climate Model

THE EDITORIAL BY C. HUNTINGFORD AND J. Gash encouraging regional climate modeling studies in developing countries ("Climate equity for all," 16 Sept., p. 1789) perfectly captures the objectives of the Regional Climate Network (RegCNET) (see www.ictp.trieste.it/RegCNET/). Based

at the International Centre for Theoretical Physics (ICTP) in Trieste, Italy, F. Giorgi, J. Pal, X. Bi, and others have developed and supported the use of the regional climate model RegCM via a listserv, workshops around the world, time on ICTP computers, and personal correspondence with users. At last count, RegCM is used by scientists in over 40 mostly developing countries or countries with economies in transition, including Egypt, Iran, Pakistan, India, Nigeria, Cameroon, Ghana, Bangladesh, China, Vietnam, the Philippines, Estonia, Peru, and Brazil. The benefits of support to these climate scientists cannot be overstated, as many of the smaller countries would not even show up in the geography of a global climate model, yet they are at considerable risk from climate change. Furthermore, the model itself benefits as developers strive to make it perform in regions influenced by monsoons, tropical convection, dramatic topography, and large lakes. Funding the efforts of climate scientists already working at the regional level and encouraging them to collaborate with those assessing impacts would be an expedient way to achieve more local capacity for climate prediction and adaptation.

LARA M. KUEPPERS
Department of Earth Sciences, University of California, Santa Cruz, 1156 High Street, Santa Cruz, CA 95064, USA.

Proposed Changes to Biomedical Funding

THE EDITORIAL "NIH FUNDING REFORM" (J. F. Strauss III, 5 Aug., p. 851) correctly identifies many of the problems facing the biomedical research community. To the proposed solutions, I would add two more. First, institutional indirect costs should be capped at a reasonable level for all institutions. As institutions can collect up to 100% in indirect costs, a limit of 25% would free many billions of dollars to fund additional investigators. Indeed, the rush to generate more indirect costs has been a driving force behind expansion at many medical schools. Second, universities should provide a larger fraction of salary support for their faculty. The Principal Investigator's salary and benefits eat up another large portion of the research budget. At a time when NIH paylines are nearing 10%, from 25 to 30% just a few years ago, we need to ask why our most prestigious universities are sitting on billion-dollar endowments while the taxpayers, through the NIH, support the salaries of their faculty and the expansion of their research enterprises.

GREGORY R. DRESSLER
University of Michigan, Ann Arbor, MI 48109, USA.

The Paradox of Radiation's Effects

PARADOXES ARE VERY OFTEN INDICATIVE OF our inadequate insight into natural phenomena rather than being features of the phenomena themselves. C. Dissanayake's description of the intimate entanglement of human health with mankind's local material basis ("Of stones and health: medical geology in Sri Lanka," Essays, 5 Aug., p. 883) provides another example of this rule. His "radiation paradox" (that people living in certain areas with high levels of background radiation do not seem to suffer adverse effects from exposure to radiation) resides entirely in the minds of those who are convinced that any small amount of chronic exposure to ionizing radiation constitutes a health risk, a notion devoid of any empirical corroboration. Most fittingly, Dissanayake's Essay actually already spells out the solution to this putative "paradox" by quoting Paracelsus's nearly 500-year-old dictum "The right dosage differentiates a poison and a remedy." This dictum seems to apply to ionizing radiation, one of the most persistent and ubiquitous environmental toxins of the biosphere, much as it applies to virtually any other substance that pharmacology or toxicology has studied so far.

RAINER FACIUS
Institute of Aerospace Medicine, DLR, German Aerospace Center, Linder Hoehe, Cologne 51147, Germany.

CORRECTIONS AND CLARIFICATIONS

Reports: "Inner core differential motion confirmed by earthquake waveform doublets" by J. Zhang *et al.* (26 Aug., p. 1357). In Fig. 1B, Mw = 5.5 and Mw = 5.6 should be m_b = 5.5 and m_b = 5.6, respectively. In reference (*30*) on page 1360, Air Force Tactical Applications Center was incorrect. It should be Air Force Technical Applications Center.

News of the Week: "Earth's inner core is running a tad faster than the rest of the planet" by R. A. Kerr (26 Aug., p. 1313). The figure caption should read "Seismic waves from a later quake follow the same path but arrive earlier because the inner core has rotated more than the rest of the planet."

Letters to the Editor

Letters (~300 words) discuss material published in *Science* in the previous 6 months or issues of general interest. They can be submitted through the Web (www.submit2science.org) or by regular mail (1200 New York Ave., NW, Washington, DC 20005, USA). Letters are not acknowledged upon receipt, nor are authors generally consulted before publication. Whether published in full or in part, letters are subject to editing for clarity and space.

PSYCHOLOGY

The Outer Limits of Belief

Stuart Vyse

Sometimes important things are found in unusual places. Generally, it is not considered a wise career move for a behavioral scientist to pursue research on ghosts, extrasensory perception, or communication with the dead. Becoming an expert in these matters may get you interviewed on cable television, but it is rarely the path to academic promotion, prestige, or professional honor. Fortunately, these concerns did not deter Susan Clancy (a postdoctoral fellow in psychology at Harvard University) and her colleagues from trying to understand how people come to believe they have been abducted by aliens.

Clancy stumbled onto the alien abduction phenomenon while studying something else. As a psychology graduate student at Harvard, she worked with a group of colleagues on recovered memories of sexual abuse, a highly charged and controversial issue within clinical psychology. Childhood sexual abuse is a real and very troubling concern, but when the victim's memory of the abuse emerges for the first time in therapy many years later, a serious scientific and clinical dilemma results. Many therapists argue that traumatic events are often forgotten or repressed, which makes their subsequent retrieval in therapy credible, but memory researchers have also demonstrated that, under the right conditions, many people can be convinced they remember things that never happened. The problem for therapists and memory researchers alike is that often the validity of the memories cannot be verified. Years have passed since the abuse was purported to have occurred, and little evidence remains. Mental health professionals are often inclined to believe their clients' memories are genuine, but because criminal charges have been brought and court cases conducted on the basis of recovered memories of sexual abuse, the scientific issues loom large.

Abducted
How People Come to Believe They Were Kidnapped by Aliens
by Susan A. Clancy

Harvard University Press, Cambridge, MA, 2005. 191 pp. $22.95, £14.95, €21.20. ISBN 0-674-01879-6.

It occurred to Clancy and her colleagues that people who believed they had been abducted by aliens might represent a useful comparison group. Here was a category of people who had memories of being kidnapped by visitors from other worlds—or, in some cases, believed they had been kidnapped in the absence of clear memories—and yet, the Harvard research team could be fairly certain the kidnappings had never occurred. Furthermore, the alien abductees shared other similarities with people who had recovered memories of sexual abuse. The majority of abductees reported that they had been sexually or in some other way physically violated by their alien kidnappers. Some of them believed that hybrid alien-human children had resulted from these unions. Furthermore, both groups had been aided by a caring person in their quest to uncover their pasts. Memories of sexual abuse were typically revealed in psychotherapy, and most of the alien abductees had uncovered their memories under hypnosis.

Abduction scar. Bruce May shows his shoulder, where he believes aliens entered his body to experiment after they abducted him. (The 1996 photograph was taken at Rachel, Nevada, the "UFO capital of the world.")

Clancy chronicles her experiences in *Abducted: How People Come to Believe They Were Kidnapped by Aliens*, a book that is a combination of science journalism and personal memoir. Clancy's research has taken her to places few of us will ever visit, and she brings us along to gatherings of abductees and to her interviews with some of the unusual characters she encountered. Naturally, this material makes for interesting reading, but it also helps to dispel the common view that these people are crackpots and crazies. Yes, they hold weird beliefs—very weird beliefs—but in the final analysis, she concludes they are not weird people.

Therein lies the challenge for behavioral science. If these people are not mentally ill, how do they come to embrace such unusual ideas? First, Clancy must dispense with the issue of whether alien abduction could possibly be a valid phenomenon. Many scientists, most notably Carl Sagan, have believed the sheer number of environments in the universe makes it possible that life has developed elsewhere. But as Clancy points out, "It's one thing to believe that life might exist on other planets, and quite another to believe that it is secretly examining your private parts." Nonetheless, having concluded that valid abductions are extremely unlikely, Clancy is left with the problem of explaining how such vivid memories are produced.

The author and her colleagues found that both groups—those who had recovered memories of sexual abuse and those who believed they were abducted by aliens—were prone to create false memories in a laboratory test. When asked to memorize a group of related words ("sugar," "candy," "sour," and "bitter"), they were more likely to later say they also remembered the target word "sweet" (which was deliberately omitted from the original list) than people who did not report memories of either alien abduction or sexual abuse. On the other hand, when asked to recall their experiences with aliens, the abductees produced physiological reactions that were similar to those of people who had experienced verified traumas. So, if the abductees had constructed these memories out of the psychic ether of their imaginations, they had managed to summon very powerful and evocative visions.

Unfortunately, there is a limit to what the laboratory can yield in cases like these. The belief that one has been kidnapped by beings from another world develops gradually in the uncontrolled spaces of everyday life, and as a result the investigator who hopes to explain this phenomenon must become a kind of psychological detective in search of reasonable hypotheses. As Clancy gathered information in her many interviews of alien abductees, she found no shortage of plausible candidates. Most of her abductees had their extraterrestrial encounters at night while on the edges of sleep. Many reported feeling pinned down in their beds, unable to move, an experience that can be caused by sleep paralysis (a common phenomenon that results when sleep cycles become desynchronized). By the time they agreed to be hypnotized in an effort to better understand the strange experiences they had encountered, most abductees were well versed in the

The reviewer is in the Department of Psychology, Box 5621, Connecticut College, New London, CT 06320, USA. E-mail: stuart.vyse@conncoll.edu

lore of alien visitation and abduction, and many had read popular books about the phenomenon, such as Whitley Strieber's *Communion* (*1*).

At its core, *Abducted* is a story about scientific thinking. In some respects, Clancy finds her subjects to be somewhat logical and scientific. The abductees were often aware of the alternative explanations that have been proposed for their experiences, but some of their memories were so real that alien abduction appeared to be the best fit for the data. In other respects, Clancy's abductees failed to adopt many of the basic principles of scientific reasoning. They frequently misplaced the burden of proof, arguing there was no evidence alien abduction was not real. Most important, Clancy's abductees did not apply the test of parsimony to their beliefs. Many people who feel temporarily paralyzed upon waking might reasonably be surprised and worried about their health, but the alien abductees appeared to have constructed a much more elaborate and unlikely explanation for this experience.

Clancy is a skeptic who mounts a strong case for terrestrial rather than extraterrestrial explanations, but she does so while maintaining a steadfast compassion for her subjects. The story is told with great humor, often at the author's expense as she finds herself in unlikely predicaments. Despite these lighter moments, Clancy never loses sight of the serious questions raised by the alien abduction phenomenon, nor does she waver in her respect for the abductees. Having concluded that these people are not dismissible as ignorant or crazy, she is left with a more unsettling truth: under the right circumstances, normal people can come to hold very bizarre beliefs. Furthermore, the imagined experience of being kidnapped by aliens, while traumatic and frightening, often seemed to provide Clancy's abductees with a kind of spiritual meaning they had not found elsewhere. Unlike people who recover memories of sexual abuse, many alien abductees said that, given the choice, they would still want to be abducted.

The history of psychological science is replete with unusual and controversial experiments that have yielded secrets of lasting value. Some of them, like Phineas Gage's encounter with the tamping iron, were natural experiments that helped etch the limits of human behavior. Susan Clancy's study of alien abductees is a natural experiment that explores the outer limits of human belief and serves as a useful reminder of the importance of scientific thinking.

Reference

1. W. Strieber, *Communion: A True Story* (Beech Tree, New York, 1987).

10.1126/science.1121309

BROWSINGS

The Science of False Memory. *C. J. Brainerd and V. F. Reyna*. Oxford University Press, Oxford, 2005. 573 pp. $79.95, £49. ISBN 0-19-515405-3. Oxford Psychology.

Brainerd and Reyna offer an authoritative overview of contemporary research on "errors of commission in memory reports." After sketching the historical roots of the field, they discuss the varied methods that have been used in studies of false memories. Their consideration of basic laboratory research emphasizes the predictive power of opponent-processes theories. The authors pay particular attention to three areas in which the consequences of false memories can be particularly horrendous: suggestive interviewing of victims and suspects in criminal investigations, the identification of suspects by victims and witnesses, and psychotherapy. They cap their account by exploring emerging work on mathematical models, the effects of aging, and cognitive neuroscience. The book will interest the authors' fellow memory researchers, but it will also reward anyone curious as to why people often remember events differently from how they actually happened and why some people have vivid memories of events that never happened.

Human Bones. A Scientific and Pictorial Investigation. *R. McNeill Alexander; photography by Aaron Diskin*. Pi (Pearson Education), New York, 2005. 208 pp. $37.50, C$54.50, £26.99. ISBN 0-13-147940-7.

This account of skeletal anatomy, written for a popular audience, begins with a consideration of bones as living organs, which grow, are damaged, and repair themselves. Alexander then surveys the form and function of the skeletal elements that compose the skull, arms and legs, and the torso. He also discusses the effects of disease and injury. After looking at how the bones of different people differ, he summarizes the adaptations and constraints that have shaped the evolution of the human skeleton. Supplementing Alexander's accessible prose, Diskin's color photographs emphasize aesthetic aspects of our dry bones.

The Human Bone Manual. *Tim D. White and Pieter A. Folkens*. Elsevier Academic, Amsterdam, 2005. 484 pp. Paper, $29.95, £19.99. ISBN 0-12-088467-4.

Archaeologists, paleontologists, anthropologists, forensics workers, and anyone seeking to identify human bones will find this handbook helpful. It begins with brief overviews of procedures for discovering and retrieving skeletal remains, ethical aspects of forensic and archaeological osteology, and bone biology and variation. Other introductory chapters cover postmortem modification and anatomical terminology. The authors then turn to the anatomy, growth, and identification of every bone in the body—from the frontal in the skull to the distal foot phalanges. Their concise text is accompanied by multiple 1:1 photographs of every bone and 2:1 images of each tooth. White and Folkens conclude the book with discussions of skeletal and dental pathologies, laboratory procedures, and means of determining age, sex, stature, and ancestry.

Garbage Land. On the Secret Trail of Trash. *Elizabeth Royte*. Little, Brown, New York, 2005. 320 pp. $24.95, C$33.95. ISBN 0-316-73826-3.

Science writer Royte explores the routes wastes take after they leave her Brooklyn apartment. She follows the trails of used bottles, cans, plastic bags, old newspapers, worn clothes, discarded toys, sewage, and the like. Escorting readers along paths linking trash cans, garbage trucks, transfer stations, landfills, incinerators, and recycling centers as well as toilets, treatment tanks, and sludge depots, she introduces a collection of colorful characters. Statistics and findings from earlier books and studies reinforce her personal perspective on America's garbage problems. Royte also incorporates self-deprecating accounts of her efforts to reuse, recycle, and compost. Despite the often humorous descriptions of the smells and sights she takes in on her tour, the volume and potential hazards of the wastes leave one rather discouraged. Nonetheless, the author may convince members of her intended audience (the general public) to take actions to reduce their "garbage footprint."

PUBLIC HEALTH

Violence Against Women

Claudia Garcia-Moreno,[1*] Lori Heise,[2] Henrica A. F. M. Jansen,[1] Mary Ellsberg,[2] Charlotte Watts[3]

The Millennium Development Goals commit the 191 member states of the United Nations to sustainable, human development and recognize that equal rights and opportunities for women and men are critical for social and economic progress (*1*). This must include addressing violence against women—a concrete manifestation of inequality between the sexes. Policies to prevent this violence should be implemented as part of the agendas for equality, development, public health, and human rights (*2*). Although statements and international declarations have called for the eradication of violence against women (*3*, *4*), many agencies, governments, and policy-makers view it as a relatively minor social problem.

There is a growing body of evidence from research that suggests that violence against women is highly prevalent, with an estimated one in three women globally experiencing some form of victimization in childhood, adolescence, or adulthood (*5*–*10*). This violence has a direct economic impact along with the human and emotional costs. A study in the USA estimated the costs of intimate partner rape, physical assault and stalking as exceeding $5.8 billion each year, nearly $4.1 billion of which is for direct medical and mental health care services (*11*).

Violence against women also has a substantial impact on health (*12*–*15*). In the Australian state of Victoria, violence by intimate partners is calculated to result in more ill health and premature death among women of reproductive age than any other risk factor, including high blood pressure, obesity, and smoking (*16*). Intimate partner violence is also an important cause of death, accounting for 40 to 60% of female homicides in many countries, and an important portion of maternal mortality in India, Bangladesh, and the United States (*17*).

The evidence suggests that violence can be prevented. Policies to prevent violence include promoting social awareness to change norms that condone violence against women; equipping young people with skills for healthy relationships; expanding women's access to economic and social resources and to support services; providing training for health services to better identify and support women experiencing violence and to integrate violence prevention into existing programs, including for HIV prevention; and promotion of adolescent health. States must take responsibility for the safety and well-being of their citizens and must tackle the problem with the urgency it requires.

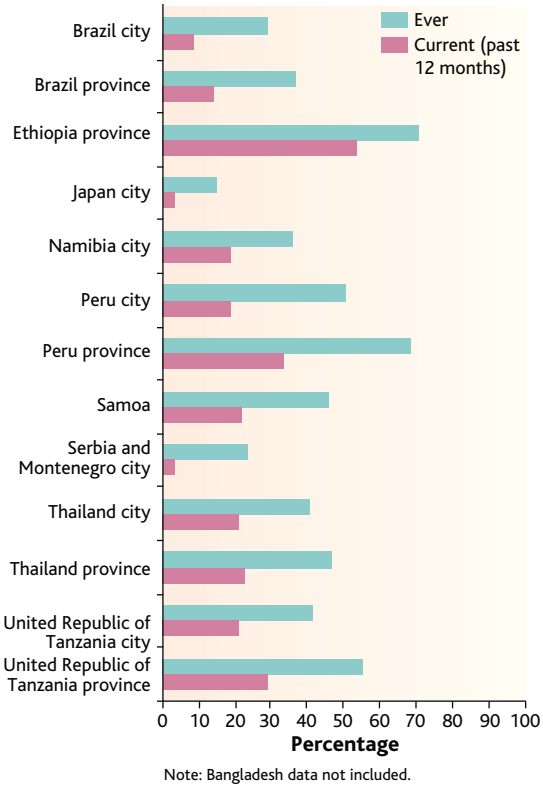

Note: Bangladesh data not included.

Percentage of ever-partnered women reporting physical or sexual violence, or both, by an intimate partner, by site.

The results from the WHO Study on Women's Health and Domestic Violence against Women released this week (*18*) greatly extend the geographic range and scope of available data. The results in this report are based on over 24,000 interviews with 15- to 49-year-old women from 15 sites in 10 countries: Bangladesh, Brazil, Ethiopia, Japan, Peru, Namibia, Samoa, Serbia and Montenegro, Thailand, and the United Republic of Tanzania (*19*). In 13 of the 15 sites studied, between one-third and three-quarters (35 to 76%) of women had been physically or sexually assaulted by someone since the age of 15. In all the settings but one, the majority of this violence was perpetrated by a current or previous partner, rather than by other persons.

Overall, 15 to 71% of women who ever had a partner had been physically or sexually assaulted by an intimate partner (see figure, this page). In most settings, about a half of these respondents reported that the violence (*20*) was currently ongoing (occurred in the past 12 months preceding the interview). In the majority of settings, too, a greater proportion of women had experienced "severe" physical violence than those suffering "moderate" physical violence (*21*). Much of the violence reported was hidden: More than one-fifth (21 to 66%) of women reporting physical violence in the study had never told anyone of their partner's violence before the study interview.

The study findings confirm that women around the world are at significant risk of physical and sexual violence from their partner, but also highlight that there is substantial variation both within and between countries. In the WHO study, the lowest prevalence of lifetime and current partner violence was found in urban Japan and Serbia and Montenegro, which suggests that rates of abuse may reflect, in part, different levels of economic development. However, a study in two sites in New Zealand that replicated the WHO methodology found lifetime prevalence of partner violence as high as that found in many WHO developing country sites (*22*). The rates of current violence were much lower (less than 6% in both sites), which suggests that women in industrialized nations may find it easier to leave abusive relationships.

Assault by a partner was a direct cause of injuries, with between one in five and one-half of women reporting that they had been injured as a result of physical violence, often more than once. In addition, women who experienced violence by a partner were more likely to report poor general health and greater problems with

[1]Department of Gender, Women and Health, World Health Organization, Geneva, Switzerland. [2]PATH, Washington, DC; [3]London School of Hygiene and Tropical Medicine, London, UK. The authors write on behalf of the WHO Multi-Country Study on Women's Health and Domestic Violence against Women. *Author for correspondence. E-mail: garciamorenoc @who.int

walking and carrying out daily activities, pain, memory loss, dizziness, and vaginal discharge in the 4 weeks before the interview. The study also found that abused women were more likely to experience emotional distress and to have considered or attempted suicide. An association between recent ill health and lifetime experience of violence suggests that physical and mental effects may last long after the violence has ended.

Although pregnancy is often considered a time when women are more likely to be protected from harm, 1 to 28% of women who had ever been pregnant reported being beaten during pregnancy. More than 90% of these women were abused by the father of the unborn child, and between a quarter and half of them had been kicked or punched in the abdomen. In most cases, the abuse during pregnancy was a continuation of previous violence. However, for some women, the abuse started during pregnancy. Intimate partner violence was also associated with an increased number of induced abortions and, in some settings, with miscarriage. In all sites except urban Thailand and Japan, women who experienced violence were significantly more likely to have more children than other women.

Despite these health associations, over half of physically abused women (55 to 95%) reported that they had never sought help from formal services or from people in positions of authority. Only in Namibia and in both sites in Peru had more than 20% of women contacted the police, and only in Namibia and in urban Tanzania had about 20% sought help from health-care services. Family, friends, and neighbors, rather than more formal services, most often provide the first point of contact for women in violent relationships.

The study also demonstrates the remarkable degree to which women in some settings have internalized social norms that justify abuse. In about half of the sites, 50 to >90% of women agreed that it is acceptable for a man to beat his wife under one or more of the following circumstances: if she disobeys her husband, refuses him sex, does not complete the housework on time, asks about other women, is unfaithful, or is suspected of infidelity. This was higher among women who had experienced abuse than among those who had not, and may indicate either that women experiencing violence learn to "accept" or rationalize this abuse, or that women are at greater risk of violence in communities where a substantial proportion of individuals condone abuse.

The association between the prevalence of partner violence and women's belief that such violence is normal or justified constitutes one of the most salient findings of the WHO study. The data also highlight the degree to which women in some settings feel that it is unacceptable for women to refuse sex with her husband, even in circumstances where it could put them at risk. In three of the rural provincial sites, as many as 44 to 51% of women believe that a woman is not justified in refusing her husband sex if he mistreats her. The fact that the association is particularly marked in rural and more traditional societies reinforces the hypothesis that traditional gender norms are a key factor in the prevalence of abuse and that transforming gender relations should be an important focus of prevention efforts.

Violence against women is a complex social problem, and our knowledge on how to address it is evolving. Tackling the problem requires coordinated action that engages communities and many different sectors—including health, education, and justice—to challenge the inequities and social norms that give rise to violence and to provide emotional and physical support for victims. Early intervention, particularly targeting children who witness violence or are abused, is a promising yet underdeveloped area for action. Developing curricula for children and young people to learn emotional and social skills, including nonviolent methods of conflict resolution, could be an important contribution to violence prevention. Support services for abused women and programs to sensitize legal systems are also needed.

Health providers need to be trained to identify women experiencing violence and to respond appropriately to those who disclose abuse. Health services that women are most likely to use, such as those for family planning, prenatal care, or post-abortion care, offer potential entry points for providing care, support, and referral to other services. Existing programs, particularly those involved in prevention of HIV, promotion of adolescent health, and reduction of teenage pregnancy, need to address women's and girl's vulnerability to abuse.

Many local and national organizations exist to combat violence against women and to promote gender equality, and these vital efforts deserve increased support. At the international level, the WHO Global Campaign for the Prevention of Violence aims to increase awareness about the impact of violence on public health and the role of public health in its prevention, and seeks to support governments in their efforts to prevent violence and to develop policies and programs for this (*23*).

There is nothing "natural" or inevitable about men's violence toward women. Attitudes can and must change; the status of women can and must be improved; men and women can and must be convinced that violence is not an acceptable part of human relationships.

References and Notes

1. Resolution A/55/2, The United Nations Millennium Declaration [United Nations (UN), New York, 8 September 2000]; (www.un.org/millennium/declaration/ares5552e.htm).
2. "Addressing violence against women and achieving the Millennium Development Goals" [World Health Organization (WHO), Geneva, 2005].
3. "Declaration on the elimination of violence against women" (UN General Assembly resolution, document A/RES/48/104, UN, New York, 1993).
4. The Fourth World Conference on Women, Beijing, China, 4 to 15 September 1995 (document A/CONF.177/20, UN, New York, 1995).
5. L. Heise, M. Ellsberg, M. Gottemoeller, *Ending Violence Against Women* (Johns Hopkins Univ. Press, Baltimore, MD, 1999).
6. L. Heise, C. Garcia-Moreno, in *World Report on Violence and Health*, E. G. Krug *et al.*, Eds. (WHO, Geneva, 2002).
7. H. Johnson, *Dangerous Domains: Violence Against Women in Canada* (International Thomson, Ontario, 1996).
8. P. Tjaden, N. Thoennes, "Extent, nature and consequences of intimate partner violence: Findings from the National Violence Against Women Survey" (National Institute of Justice, Washington, DC; Centers for Disease Control and Prevention, Atlanta, GA, 2000).
9. F. Hassan *et al.*, *Inj. Control Saf. Promot.* **11**, 111 (2004).
10. S. Kishor, K. Johnson, "Profiling domestic violence: A multi-country study" (ORC MACRO, Calverton, MD, 2004).
11. National Center for Injury Prevention and Control "Costs of intimate partner violence against women in the United States" (Centers for Disease Control and Prevention, Atlanta, GA, 2003).
12. J. C. Campbell, *Lancet* **359**, 1331 (2002).
13. S. B. Plichta, M. Falik, *Womens Health Issues* **11**, 244 (2001).
14. S. B. Plichta, C. Abraham, *Am. J. Obstet. Gynecol.* **174**, 903 (1996).
15. H. S. Resnick, R. Acierno, D. G. Kilpatrick, *Behav. Med.* **23**, 65 (1997).
16. "The health costs of violence: Measuring the burden of disease caused by intimate partner violence: A summary of findings" (VicHealth, Carlton South, Australia, 2004).
17. E. G. Krug *et al.*, Eds., *World Report on Violence and Health* (WHO, Geneva, 2002).
18. C. Garcia-Moreno, H. A. F. M. Jansen, M. Ellsberg, L. Heise, C. Watts, "WHO multi-country study on women's health and domestic violence against women: Initial results on prevalence, health outcomes, and women's responses" (WHO, Geneva, 2005).
19. In Bangladesh, Brazil, Peru, Thailand, and the United Republic of Tanzania two sites were studied: the capital and a province with a rural-urban mix. The remaining countries had one study site only: in Ethiopia, a rural province; in Japan and Serbia and Montenegro, an urban site; and in Samoa, the whole country was included.
20. The term "violence" without further qualification refers to physical (either moderate or severe) or sexual violence, or both.
21. A woman was said to have experienced severe physical violence if she reported that she had been kicked, dragged or beaten up; hit with a fist or something else that could hurt; choked or burned on purpose; or if her partner had threatened to use or had actually used a gun, knife, or other weapon against her. A woman is considered to have experienced moderate violence if she has only been slapped, pushed, shoved, or had something thrown at her.
22. J. Fanslow, E. Robinson, *J. N.Z. Med. Assoc.* **117**, 341 (2004).
23. "Milestones for a global campaign for violence prevention" (WHO, Geneva, 2005).

Supporting Online Material

www.sciencemag.org/cgi/content/full/310/5752/1282/DC1

10.1126/science.1121400

CELL SIGNALING

Frizzled at the Cutting Edge of the Synapse

Alfonso Martinez Arias

Signaling by the Wnt family of secreted proteins provides a molecular means to process information during animal development and morphogenesis. The first molecular event in Wnt signaling is the interaction of Wnt proteins with members of the Frizzled family of seven-transmembrane cell surface receptors (*1*, *2*). There are different modes of Wnt signaling, and that which ensues in a particular situation is determined by the interaction between individual Frizzled receptors and particular Wnt proteins (*2*). Although most work on Wnt signaling has focused on its effects on cell fate assignation or cytoskeletal organization, there is increasing evidence that Wnt signaling also plays a role in the architecture of synaptic terminals and the activity of the nervous system (*3*, *4*). On page 1344 of this issue, Mathew *et al*. (*5*) describe a previously unknown mechanism of action for DFrizzled2, a Wnt receptor of the fruit fly *Drosophila melanogaster*. They demonstrate that at the neuromuscular junction, cleavage of the intracellular domain of DFrizzled2, and its translocation to the nucleus, occurs upon receptor association with Wingless (the fly ortholog of Wnt1) and that this event is required for synapse formation. Although it is well established that members of the same subfamily of seven-transmembrane receptors undergo cleavage of their extracellular domains to generate a functional ligand (*6*), Mathew *et al.* provide an intriguing report of an alternate, intracellular cleavage of these receptors.

The development of the neuromuscular junction has been exploited as an excellent experimental system for the study of synapse formation, a multistep architectural process crucial for coordinating sensory inputs and motor neuron outputs (*7*, *8*). The major features of synapse construction are conserved, and *Drosophila* has been an excellent model system for the detailed analysis of this process (*8*). In recent years, it has become clear that in addition to synapse-specific molecules and processes, some "generic" signaling systems that control diverse biological processes, such as those controlled by bone morphogenetic protein/transforming growth factor–β and Wnt, are also used to modulate synapse construction (*3*, *4*).

Wingless plays a central role in synapse maturation at the larval neuromuscular junction where it is secreted by presynaptic neurons and is required for the differentiation of pre- and postsynaptic structures (*9*). In their study, Mathew *et al*. used amino terminus– and carboxyl terminus–specific antibodies to analyze the distribution of the Wingless receptor DFrizzled2 in postsynaptic structures. Both antibodies detected DFrizzled2 at the surface and in intracellular structures of the muscle cell. In addition, the carboxyl terminus–specific antibody detected small areas of localized expression in the nuclei of muscle cells. This nuclear presence was not observed in other cell types and was greater in nuclei adjacent to the synapse—the site of Wingless release—suggesting a correlation between this localization and Wingless signaling.

Biochemical analysis of the receptor in vivo and in tissue culture revealed an 8-kD carboxyl-terminal fragment corresponding to the intracellular domain of DFrizzled2 that is released upon Wingless signaling. A comparison of the sequence of multiple Frizzled receptors revealed a conserved glutamyl-endopeptidase cleavage site located in the carboxyl-terminal tail of DFrizzled2 near the transmembrane domain (see the figure). Mutations of this domain abolished the cleavage and the nuclear accumulation of the carboxyl-terminal domain. To rule out that the cleavage is a by-product of the synthesis and secretion of DFrizzled2, the authors examined larval muscles to show that the cleavage event requires Wingless-induced endocyto-

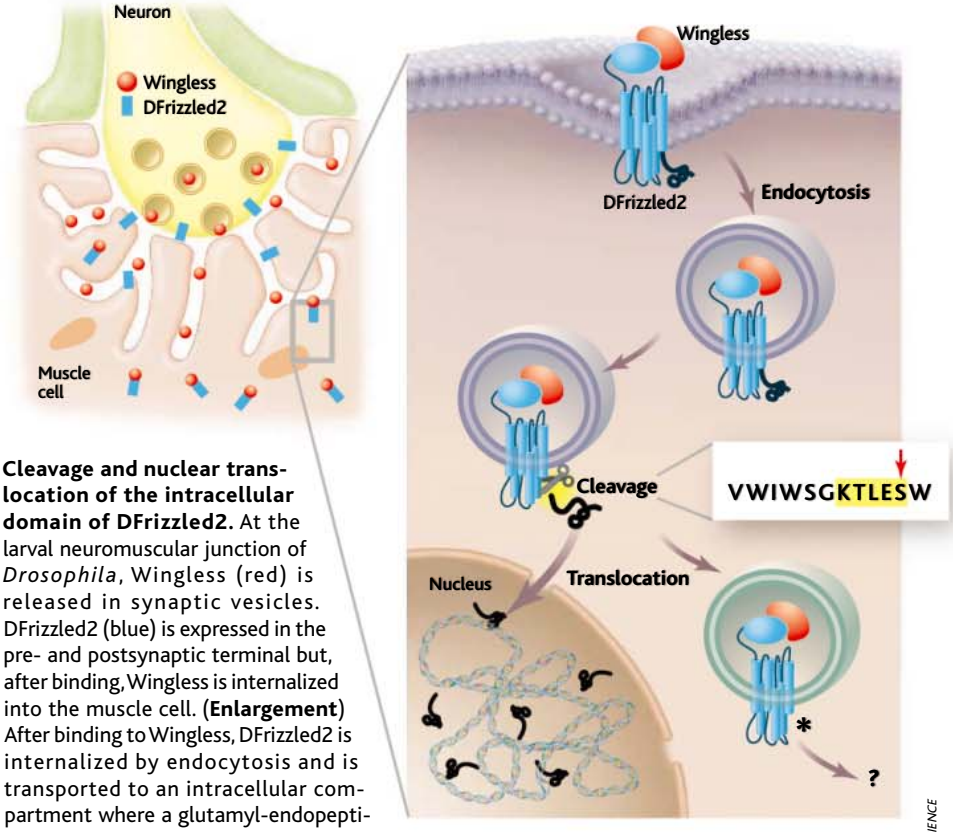

Cleavage and nuclear translocation of the intracellular domain of DFrizzled2. At the larval neuromuscular junction of *Drosophila*, Wingless (red) is released in synaptic vesicles. DFrizzled2 (blue) is expressed in the pre- and postsynaptic terminal but, after binding, Wingless is internalized into the muscle cell. (**Enlargement**) After binding to Wingless, DFrizzled2 is internalized by endocytosis and is transported to an intracellular compartment where a glutamyl-endopeptidase of the tumor necrosis factor–α converting enzyme family cleaves the intracellular domain. The cleaved fragment enters the nucleus and appears to associate with transcriptionally active DNA. The cleaved receptor (asterisk) is presumably translocated into an endocytic compartment, and its fate remains unknown. (**Inset**) Consensus sequence for the cleavage site of Frizzled receptors. The arrow indicates the site for glutamyl-endopeptidase cleavage.

CREDIT: K. SUTLIFF/*SCIENCE*

The author is in the Department of Genetics, University of Cambridge, Cambridge CB2 3EH, UK. E-mail: ama11@hermes.cam.ac.uk

sis of the receptor. Although they could not pinpoint the intracellular location of the cleavage event, an intense perinuclear accumulation of the DFrizzled2 extracellular domain is intriguing and raises the possibility that the cleavage and/or delivery of the intracellular fragment occurs at or near the nuclear membrane.

A correlation does not prove function, however, so the authors tested the requirement for receptor cleavage in Wingless signaling at the synapse. For multiple Wingless-mediated signaling events, DFrizzled2 activity is redundant with that of *Drosophila* Frizzled1 (*10*). However, synaptic maturation at the neuromuscular junction only requires DFrizzled2, and this allowed Mathew *et al.* to perform genetic studies and show that forms of DFrizzled2 that cannot be cleaved do not provide effective rescue of the *DFrizzled2* mutant phenotype.

These observations are surprising and raise several questions. In the past few years, cleavage of the intracellular domain of some cell surface receptors (e.g. Notch) has emerged as a way of modulating their activity (*11*, *12*). In all known cases, this is mediated by the γ-secretase complex and usually involves cleavage within the transmembrane domain. The observations of Mathew *et al*. (*5*) uncover a previously unknown mechanism that invites a closer examination of the activity and mode of action of the Frizzled receptor family. A second question concerns the exact role of the cleaved fragment. Although its presence in the nucleus in transcriptionally active areas suggests a role in gene expression, this remains to be shown. Mathew *et al*. have shown that cleavage is necessary for DFrizzled2 function at the neuromuscular junction—that is, to promote synapse maturation. However, they did not show that the intracellular domain itself provides that function, because expression of a soluble version of this domain has no activity. Perhaps the cleaved receptor is recycled to the cell surface or to some intracellular compartment where it acts in a functionally altered manner, and the carboxyl-terminal fragment is merely a by-product of the process.

The observation that cleavage is triggered by Wingless echoes the unsolved question of how interactions between particular Wnt proteins and specific Frizzled receptors can elicit different molecular and mechanistic responses. Given the versatility of Frizzled-Wnt interactions in controlling signaling events and biological processes, it is not surprising that at the synapse, a highly specialized structure, these receptors and ligands exert their functional potential with an unexpected molecular twist.

References

1. T. Reya, H Clevers, *Nature* **343**, 843 (2005).
2. H. C. Huang, P. S. Klein, *Genome Biol*. **5**, 234 (2004).
3. L. Ciani, P.C. Salinas, *Nat. Rev. Neurosci*. **6**, 351 (2005).
4. M. Packard M. D. Mathew D. V. Budnik, *Nat. Rev. Neurosci.* **4**, 113 (2003).
5. D. Mathew *et al*., *Science* **310**, 1344 (2005).
6. F. Schmidlin, N. W. Bunnett, *Curr. Opin. Pharmacol*. **1**, 575 (2001).
7. J. R. Sanes, J.W. Lichtman, *Nat. Rev. Neurosci*. **2**, 791 (2001).
8. H. Keshishian *et al.*, *Annu. Rev. Neurosci.* **19**, 545 (1996).
9. M. Packard *et al*., *Cell* **111**, 319 (2002).
10. P. Banhot *et al*,. *Development* **126**, 4175 (1999).
11. M. S. Wolfe, R. Kopan, *Science* **305**, 1119 (2004).
12. M. E. Fortini, *Nat. Rev. Mol. Cell. Biol*. **3**, 673 (2002).

10.1126/science.1121906

ATMOSPHERIC SCIENCE

Tiny Bubbles Tell All

Edward J. Brook

During the past 200 years, humans have caused a remarkable change in the levels of several atmospheric greenhouse gases. We know this from direct measurements that started in the latter half of the 20th century, but for earlier times we rely on tiny samples of the atmosphere trapped in polar ice. Coring the polar ice sheets provides access to these samples and allows us to place modern changes in the context of long-term natural cycles in greenhouse gases. Until recently, the longest of these ice core records (from Vostok Station in Antarctica) extended back 440,000 years (*1*). Now, reports by Siegenthaler *et al*. on page 1313 (*2*) and by Spahni *et al*. on page 1317 (*3*) extend our window into the past an additional 210,000 years.

The new ice core records come from the European Project for Ice Coring in Antarctica (EPICA) (see the figure). EPICA, an international collaboration of scientists, engineers, and drillers, made a major contribution to the study of past climates by recovering this deep ice core in East Antarctica where low snowfall rates allow the accumulation of an extremely old section of ice (*4*). One of the new findings from this project concerns the nature of long-term glacial-interglacial climate cycles. Ice core scientists use the ratio of deuterium to hydrogen in ice as a proxy for temperature. Records from EPICA Dome C show a strong 100,000-year periodicity for the past 740,000 years (*4*). The existence of this cycle is well known from ocean sediments and other types of climate records. Its origin is enigmatic, because external climate forcing caused by changes in Earth's orbit is weak on this time scale. In the Dome C record the oldest three cycles are of lower amplitude than their later cousins. The reason for the shift from low- to high-amplitude cycles is not clear, but an obvious question concerns the behavior of the major greenhouse gases during the older time period (*4*).

Siegenthaler *et al*. (*2*) and Spahni *et al*. (*3*) address this issue with new records of atmospheric carbon dioxide, methane, and nitrous oxide, created through the collaborative efforts of two European research groups. They combine their work on Dome C with previous work on Vostok and other ice cores to create records of these gases covering the past 650,000 years. These new records will no doubt become canonical figures in the global change literature, as did the Vostok records before them (*1*).

Two basic messages are apparent in this extended history of the atmosphere. First, even with this longer perspective, the modern atmosphere is still highly anomalous. At no time in the past 650,000 years is there evidence for levels of carbon dioxide or methane significantly higher than values just before the Industrial Revolution. Second, the covariation of carbon dioxide and methane with climate, strikingly evident in the Vostok record, follows essentially the same pattern in the earlier time period. The muted climate cycles (as indicated by the deuterium content of the ice) are accompanied by equally muted cycles of carbon dioxide and methane (see the figure). This relationship reinforces the view that the large-scale cycles in Antarctic temperature have global importance, and that climate and greenhouse gas cycles are intimately related.

For nitrous oxide, the picture is slightly less clear. The record is not complete, making it difficult to judge how or whether the amplitude of 100,000-year cycles changed with time, and anomalous levels of nitrous oxide appear to be related to high levels of dust in the ice. This had been observed before and was attributed to microbial activity in ice with high levels of terrigenous dust (*5*). Spahni *et al*. argue plausibly that the enrichment is significant only in very dusty ice, and use dust records to determine which samples they feel are reliable (*3*). This is probably the

The author is in the Department of Geosciences, Oregon State University, Corvallis, OR 97331, USA. E-mail: brooke@geo.oregonstate.edu

best that can be done at this point, but it is less than satisfying, as one wonders about smaller levels of contamination at lower dust levels.

What causes the glacial-interglacial variations in these gases? For carbon dioxide, this question has been a grand challenge in geochemistry for decades. The answer most likely lies in the ocean, and the tight coupling with Antarctic climate suggests that high-latitude Southern Ocean processes are important. Dome C gives us more data to reinforce these thoughts, but convincing explanations are still elusive. Methane variations are widely believed to result from climate driven changes in emissions from tropical and boreal wetlands (*6*). The new methane data reinforce the climate-methane connection but leave on the table lingering questions about methane hydrates (*7*) and new ones about the atmospheric methane sink (*8*). For nitrous oxide, climate-driven variations in both marine and terrestrial sources are probably the dominant factors (*9*, *10*). Another challenge is to understand the feedbacks that control the rather uniform upper and lower limits of the natural concentration cycles. The Dome C record lengthens the target for biogeochemical modelers bold enough to accept these challenges. In fact, some have already risen to the bait, and the first evaluation of modeling skill will come when the results of the "EPICA Challenge," a contest of sorts to predict the Dome C greenhouse gas records (*11*), are evaluated.

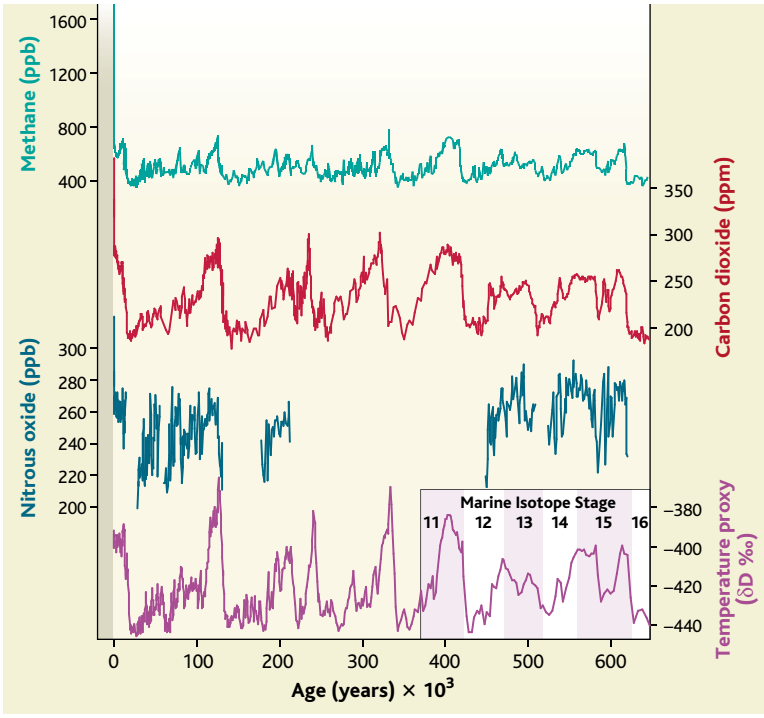

The long view. The greenhouse gas (CO_2, CH_4, and NO_2) and deuterium (δD) records for the past 650,000 years from EPICA Dome C and other ice cores, with marine isotope stage correlations (labeled at lower right) for stages 11 to 16 (*2*, *3*). δD, a proxy for air temperature, is the deuterium/hydrogen ratio of the ice, expressed as a per mil deviation from the value of an isotope standard (*4*). More positive values indicate warmer conditions. Data for the past 200 years from other ice core records (*20*–*22*) and direct atmospheric measurements at the South Pole (*23*, *24*) are also included.

The new results also provide a tantalizing view of greenhouse gas variations within the older climate cycles. These cycles have been correlated with marine isotope stages (MISs) of the oceanic oxygen isotope record, used by paleoceanographers. For both methane and carbon dioxide there are millennial-scale variations in cold stages that presage similar variability during the last ice age (*6*, *12*, *13*), known to be related to abrupt climate shifts recorded in Greenland ice cores and other archives. There are also interesting variations in warm stages. During MIS 11, an interglacial period between about 420,000 to 370,000 years ago, methane reached typical maximum levels, fell by about 100 parts per billion over 5000 years, then rose again toward the end of the interglacial period. This is similar to the pattern over the past 10,000 years (*14*), which has been the subject of an interesting argument over the impact of early human activities on the atmosphere (*15*, *16*). Apparently, natural variability can also result in relatively large oscillations in greenhouse gases during interglacial periods. MIS 11 has previously been identified as an exceptionally long interglacial (*17*), but the Dome C record now suggests that MISs 13 and 15 were similarly long, with surprisingly constant levels of carbon dioxide, methane, and nitrous oxide in MIS 15. Although this suggests that interglacial periods can last for quite a long time, and may assuage fears about the demise of the current one, there are complications. Isotopic records from benthic-dwelling foraminifera—which record a combined signal of temperature and continental ice volume change, and provide, to first order, a global record of climate change—don't support the long MIS 15, raising the possibility of some uncertainty in this part of the Dome C time scale.

Chronological uncertainties also may be apparent in MIS 14, where the temporal phasing of methane, nitrous oxide, and carbon dioxide are different than expected, and in MIS 13, where the Dome C temperature proxy appears to lag the benthic oxygen isotope signal (the reverse is expected because of the slow response of the ice sheets to climate change). The Dome C time scale is based on ties to the marine isotope record, but also on glaciological calculations of ice flow, thinning, and densification (*4*). (The latter is particularly important for estimating the age difference between gases and ice—and therefore the age difference between these gases and the temperature record—because of bubble close-off at depth in the snowpack.) These are in turn based on assumptions about ice thickness history, basal melting, and snow accumulation (derived from the temperature proxy). There are no ties to the marine record within MISs 13 to 15 (*4*), so inaccuracies in glaciological parameters, possibly anomalies in ice flow, may explain the chronological mismatches. It is worth pointing out that the entire pre-Vostok section of the Dome C core is in the bottom ~400 m of a 3200-m ice core (*4*). There is no evidence of large-scale irregularities in the stratigraphy of the record, but the risk of glaciological anomalies clearly increases as one approaches bedrock. Sorting out the chronological details related to these issues will take time, but these uncertainties in no way diminish the importance of the Dome C records, which set a new standard for ice core science.

What's next for old ice core gases? Further analysis of the Dome C and other cores, including stable isotopic composition of the three gases, will help establish the patterns and causes of variability more firmly. We also may go deeper and thus older. The Dome C ice record may ultimately extend to 900,000 years (*4*). Interpreting the bottom section of an ice core is a tricky business, however, because melting, folding, and other processes can distort the stratigraphic order and contaminate the record. Getting back this far is a tantalizing goal, though, because it is at about this time (the so called "mid-Pleistocene transition") when marine sediment records indicate a change in the period of Earth's major climate cycles, from a dominance of ~40,000-year cycles (the "40 k" world) to the 100,000-year cycles (the "100 k" world). This transition is not well understood. One commonly cited hypothesis involves long-term cooling and increasing ice volume due to a decrease in average atmospheric carbon dioxide levels over the past 2 million years (*18*). Many competing mechanisms have been invoked, however, and even the existence of a global long-term cooling trend is not clear (*19*).

In reality, it is likely that an even older ice core record will be needed to adequately address this question, because even a 900,000-year record would probably end in the middle of the 40 k–100 k transition. Such a core is in the works. International Partnerships in Ice Coring Science, a diverse group of ice coring scientists and drillers, has been planning major drilling projects. An ice core record through the mid-Pleistocene transition and into the 40 k world was high on the agenda at the most recent meeting in Brussels, in October 2005. Careful survey work and logistics planning will be necessary, as the most probable locations for cores of this age are in the coldest and remotest parts of Antarctica. Nonetheless, as the new EPICA records show, the payoff of deep ice coring is a dramatically improved understanding of the coevolution of climate and greenhouse gases. Explaining the origins of these relationships remains a major goal of global Earth science.

References

1. J. R. Petit *et al.*, *Nature* **387**, 359 (1999).
2. U. Siegenthaler *et al.*, *Science* **310**, 1313 (2005).
3. R. Spahni *et al.*, *Science* **310**, 1317 (2005).
4. EPICA Community Members, *Nature* **431**, 147 (2004).
5. T. Sowers, *J. Geophys. Res.* **106**, 31903 (2001).
6. E. Brook, S. Harder, J. Severinghaus, E. Steig, C. Sucher, *Global Biogeochem. Cycles* **14**, 559 (2001).
7. J. P. Kennett, K. G. Cannariato, I. L. Hendy, R. J. Behl, *Methane Hydrates in Quaternary Climate Change: The Clathrate Gun Hypothesis* (American Geophysical Union, Washington, DC, 2003).
8. J. O. Kaplan, *Geophys. Res. Lett.* **29**, 10.1029/2001GL013366 (2002).
9. T. Sowers, R. B. Alley, J. Jubenville, *Science* **301**, 945 (2003).
10. J. Flückiger *et al.*, *Global Biogeochem. Cycles* **18**, GB1020 (2004).
11. E. Wolff *et al.*, *EOS* **86**, 341 (2005).
12. J. Chappellaz *et al.*, *Nature* **366**, 443 (1993).
13. A. Indermühle, E. Monnin, B. Stauffer, T. Stocker, M. Whalen, *Geophys. Res. Lett.* **27**, 735 (2000).
14. T. Blunier, J. Chappellaz, J. Schwander, B. Stauffer, D. Raynaud, *Nature* **374**, 46 (1995).
15. W. Ruddiman, *Clim. Change* **61**, 261 (2003).
16. G. Schmidt, D. Shindell, S. Harder, *Geophys. Res. Lett.* **31**, L23206 (2004).
17. D. Raynaud *et al.*, *Nature* **436**, 39 (2005).
18. A. Berger, X. S. Li, M.-F. Loutre, *Quat. Sci. Rev.* **18**, 1 (1999).
19. T. de Garidel-Thoron, Y. Rosenthal, F. Bassinot, L. Beaufort, *Nature* **433**, 294 (2005).
20. D. Etheridge *et al.*, *J. Geophys. Res.* **101**, 4115 (1996).
21. D. Etheridge, L. P. Steele, R. J. Francey, R. L. Langenfields, *J. Geophys. Res.* **103**, 15979 (1998).
22. T. Machida, T. Nakazawa, Y. Fujii, S. Aoki, O. Watanabe, *Geophys. Res. Lett.* **22**, 2921 (1995).
23. C. D. Keeling, T. P. Whorf, In *Trends: A Compendium of Data on Global Change* (Carbon Dioxide Information Analysis Center, Oak Ridge National Laboratory, Oak Ridge, TN, 2005).
24. CH_4 and N_2O data from South Pole courtesy of the Global Monitoring Division of NOAA's Earth System Research Laboratory (www.dmdl.noaa.gov/infodata/ftpdata.html).

10.1126/science.1121535

PLANETARY SCIENCE

Saturn's Strangest Ring Becomes Curiouser and Curiouser

Mark R. Showalter

The Cassini spacecraft continues to send back astounding images of Saturn and its retinue of rings and moons. We have become so accustomed to new wonders that it is hard to remember the shock of seeing Saturn's F ring up close for the first time (see the figure). On 12 November 1980, Voyager 1 sent back its first closeup images of this faint and narrow ring orbiting just outside Saturn's main rings. The image revealed what were variously described as kinks, clumps, strands and, most famously, "braids" in the ring. On page 1300 of this issue, Charnoz *et al.* (*1*) offer a new and perhaps even more puzzling description of the F ring thanks to Cassini: It is a spiral.

The Voyager images showed features that deviated substantially from those of a simple ellipse, so concerns were initially raised that the F ring might violate Kepler's basic laws of orbital motion. Luckily, we have come to understand that Kepler's laws still apply: Each particle in the F ring follows its own elliptical orbit about Saturn. The kinks and so-called braids do not represent the paths of individual particles; they are instantaneous snapshots of a ring containing particle orbits that vary from place to place.

The ring's nearby "shepherding" moons, Prometheus and Pandora, have long been recognized as providing the gravitational tugs that continuously regenerate some of this ring's curious patterns. Because Keplerian orbits are closed, encounters between a moon and a ring recur each time the moon circles the planet. The effect on the ring is a pattern that roughly repeats, with a characteristic spacing proportional to the difference in orbital speeds between the ring and the moon. The length scale of most F-ring structures indicates that Prometheus, the larger and closer of the two moons, is the major "braid-maker."

However, perturbations by nearby moons are insufficient to explain many of the ring's other curiosities. The Voyager images showed that the brightest clumps are not periodic (*2*, *3*). Some of these, the so-called "bursts," appear suddenly and then spread out over time scales of days to weeks. Others evolve more slowly but still last no longer than months. What can cause such rapid changes? One hypothesis is that the most rapid "bursts" are dust clouds arising when a meteoroid hits the ring; the other is that all the clumps arise from mutual impacts among ring bodies (*4*). The debate hinges on whether mutual collisions can occur at high enough speeds to produce the bursts. In this regard, the discovery of the object designated S/2004 S6, which is either a small moon or a long-lived clump, is of particular interest. Its orbit can intersect the F ring at very high speeds, perhaps making mutual collisions a more viable explanation.

As far as F-ring structures go, the newly reported spiral is in a class by itself. It is clearly evolving according to the laws of Kepler, so that between November 2004 and May 2005 it has wound itself into a tighter spiral. By running the kinematics

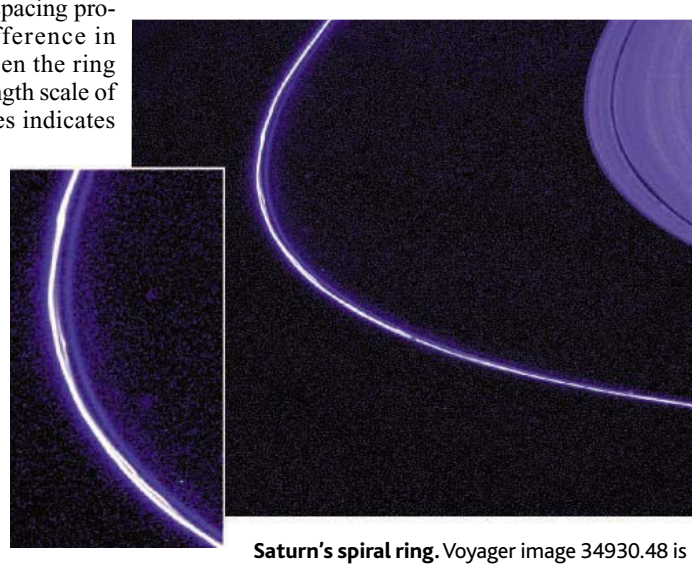

Saturn's spiral ring. Voyager image 34930.48 is one of two that first revealed the kinks, clumps, and "braids" of Saturn's F ring. The faintest features have been enhanced in blue to make them more visible. The inset shows the ring's peculiar structures in finer detail. New Cassini data continue to challenge our understanding of how such surprising structures are able to form.

CREDIT: NASA

The author is at the SETI Institute, Mountain View, CA 94043, USA. E-mail: mshowalter@seti.org

backward in a computer simulation, Charnoz *et al.* (*1*) demonstrate that the spiral arose as a localized cloud, about 300 km in radial extent, in early 2004. In other words, the spiral began with an event. But whereas the clumps imaged by Voyager dissipated on time scales of months or less, this pattern has persisted for at least 1.5 years and is likely to continue for years more. (The spiral strands will continue to wind ever tighter until, eventually, they blend into a more uniform skirt around the F ring.)

The discovery of spiral structure reopens the debate over external versus internal collisions. Charnoz *et al.* (*1*) emphasize the role of S/2004 S6, although they acknowledge that its mass is far too small to create such an immense pattern. They suggest instead that scattering of ring particles off the surface of S/2004 S6 may be the cause of the spiral. As for interactions of the ring with other moons, Prometheus is large enough, but we know that it has not collided with the F ring in the recent past.

So what is left as an explanation? When particles collide, the energy of impact is distributed among particles typically comprising 10 to 100 times as much mass as that of the impactor. As a result, any impactor that produced the spiral probably came from a distance far greater than 300 km. So an alternative to the model of Charnoz *et al.* (*1*) is that we are seeing the outcome of a rare, very large impact into the F ring. By this argument, S/2004 S6 may still play a role but, as a consequence, not a cause—it may be a particularly large shard left over from the impact, which now finds itself on a very different orbit from the rest of the ring.

Further monitoring by Cassini should enable us to distinguish between these models. If S/2004 S6 has a continuing role, then we would expect a new spiral to form when its orbital orientation again intersects the ring's core. If Cassini is still operational in 2009, then we might observe the formation of something similar when Prometheus begins to skim the inner edge of the F ring. On the other hand, meteoroid impacts would be expected to occur randomly, with a broad distribution of sizes from the numerous small, clump-forming events to the very rare, large, spiral-forming events.

Perhaps the most fundamental questions concern how the F ring came to exist and why it is so strange. A few factors are important. First, the ring orbits at the edge of the Roche limit, the boundary that separates rings from moons. Inside the Roche limit, Saturn's tidal forces overcome self-gravity, preventing moons from accreting. In the F ring, some reaccretion is possible, so ring bodies are continuously breaking up and joining back together. Second, it is faint and narrow, so that small injections of new dust are quite noticeable; in the A ring, the equivalent of a spiral-forming event might pass unnoticed. Third, the ring and its nearby "shepherds" all follow highly eccentric orbits, which means that the ring is perturbed quite radically as the moons approach and recede on each orbit. (Here "shepherd" is probably a misnomer; elsewhere in the solar system, nearby moons act to confine rings, whereas the perturbations by Prometheus and Pandora are quite disruptive.) The ring also presumably contains a large mass of its own; how else could it maintain a fixed eccentricity against the tendency of ring particles to precess at different speeds? The picture that emerges is that of a ring that arose from the disruption of a small moon—perhaps the size of Prometheus—that lives in an environment too severely perturbed to ever settle down into a uniform, circular ring. If history is any guide, the F ring harbors a few more surprises that are awaiting Cassini's instruments and science teams.

References

1. S. Charnoz *et al.*, *Science* **310**, 1300 (2005).
2. M. R. Showalter, *Science* **282**, 1099 (1998).
3. M. R. Showalter, *Icarus* **171**, 356 (2004).
4. J. M. Barbara, L. W. Esposito, *Icarus* **160**, 161 (2002).

10.1126/science.1121223

DEVELOPMENTAL BIOLOGY

Encountering MicroRNAs in Cell Fate Signaling

Xantha Karp and Victor Ambros

Organisms must tightly regulate where and when each of their genes is expressed, lest their development goes awry with potentially lethal consequences. The mechanisms that control these important time and place decisions have been of great investigative interest. Hence, it came as a huge surprise that a major level of gene regulation was completely unknown until the recent discovery of a class of small regulatory RNA molecules known as microRNAs (*1*, *2*). Ever since, we have been racing to understand microRNA function during the development of multicellular animals and plants. On page 1330 in this issue, Yoo and Greenwald (*3*) describe a direct connection between the miR-61 microRNA and LIN-12/Notch, the cell surface receptor that controls a fundamental and highly conserved signaling pathway. The link marks an important advance in our understanding of the role of microRNAs in developmental processes.

Enhanced online at www.sciencemag.org/cgi/content/full/310/5752/1288

The authors are in the Department of Genetics, Dartmouth Medical School, Hanover, NH 03755, USA. E-mail: victor.r.ambros@dartmouth.edu; xantha.e.karp@dartmouth.edu

Mature microRNAs are small RNAs, about 22 nucleotides in length, that are encoded in the genomes of every multicellular organism examined so far. MicroRNAs block gene expression by binding to complementary sequences in the 3′ untranslated region (3′ UTR) of messenger RNAs and directing either degradation of the messenger RNAs or inhibition of their translation (*2*). MicroRNAs were first discovered in the microscopic roundworm *Caenorhabditis elegans* as important regulators of developmental timing. They have since been implicated in other aspects of development in plants (*4*) and animals, including vertebrates and invertebrates (*1*, *5*). However, little is known about the precise role that microRNAs play in many important developmental decisions. For example, communication between cells via molecular signals is a universal mechanism to coordinate cell fate decisions during animal development. What role do microRNAs play, if any, in signaling pathways? Using *C. elegans* vulval development as a model system, Yoo and Greenwald provide an answer.

The vulva is a specialized adult structure that provides a connection from the uterus of the worm to the external environment (*6*) (see the figure). In wild-type larvae, three vulval precursor cells, called P5.p, P6.p, and P7.p, are specified to eventually form the adult vulva. Each of these cells adopts one of two vulval cell fates—primary (1°) or secondary (2°)—in the precise spatial pattern 2°-1°-2° (see the figure). LIN-12 (the worm homolog of Notch) specifies the 2° fate in P5.p and P7.p, whereas the epidermal growth factor signaling pathway specifies the 1° fate in P6.p. Cross-talk between the two pathways ensures the spatial precision of these cell fate decisions (*6*). To understand how LIN-12 signaling specifies the 2° fate, one must identify the target

genes whose transcription is turned on in response to LIN-12 activation. The LIN-12 target genes identified previously seemed to function by keeping epidermal growth factor signaling turned off in P5.p and P7.p (*7*, *8*). Yoo and Greenwald now identify a target gene that promotes the 2° fate apparently independently of epidermal growth factor signaling. Interestingly, this gene encodes a microRNA, miR-61 (*3*).

Using computational methods, Yoo and Greenwald identified *mir-61* as a potential transcriptional target of LIN-12 signaling. Specifically, the *mir-61* locus was found to contain DNA sequences typical of those to which LIN-12/Notch receptors and their cofactors bind to regulate transcription of a target gene. The authors verified that *mir-61* is a true LIN-12 target gene in P5.p and P7.p by using a fluorescent reporter protein whose expression was driven by the *mir-61* regulatory region, including the predicted target sites. The reporter protein was visible in P5.p and P7.p, but was no longer expressed in those cells when the predicted target sites were mutated. When miR-61 was expressed in P6.p, where it is not normally expressed, the microRNA was sufficient to cause P6.p to adopt 2°, rather than 1°, cell fate characteristics (*3*). These results show that expression of a microRNA can be directly activated by a signaling pathway and that this can influence cell fate decisions (see the figure).

Yoo and Greenwald found that the worm gene *vav-1*, homologous to the vertebrate oncogene *Vav*, contains sequences in its 3′ UTR that are complementary to miR-61, and predicted that miR-61 could promote the 2° fate by repressing the production of VAV-1 protein (*3*). They confirmed this with two elegant experiments, again using fluorescent reporter proteins. The authors first showed that fusing the 3′ UTR of *vav-1* to the messenger RNA encoding the reporter protein is sufficient to down-regulate expression of the reporter when miR-61 was present in the same cell. They then showed that the miR-61 binding sites in the *vav-1* 3′ UTR are critical for down-regulating *vav-1* expression in P5.p and P7.p. When *vav-1* regulatory sequences were used to express the reporter, fluorescence was observed in vulval precursor cells but not in P5.p and P7.p, where endogenous miR-61 is expressed. However, when the miR-61 binding sites in the 3′ UTR were mutated, the fluorescent protein became visible in P5.p and P7.p.

Finally, when Yoo and Greenwald lowered *vav-1* activity, LIN-12 was better able to specify the 2° fate, indicating that *vav-1* antagonizes *lin-12* activity in vulval precursor cells (*3*). Importantly, *vav-1* does not accomplish this by promoting the 1° fate, because in this experiment, epidermal growth factor signaling was removed.

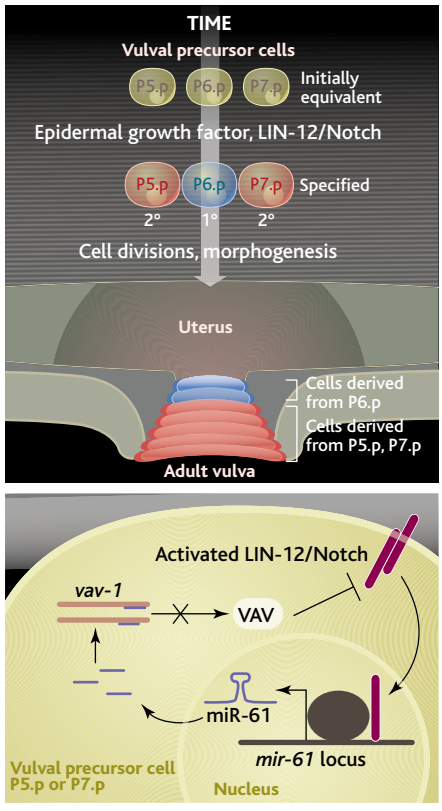

A microRNA, miR-61, regulates a major developmental signaling pathway. (Top) Simplified schematic view of *C. elegans* vulval development. Vulval precursor cell specification during larval development leads to the formation of an adult vulva. (**Bottom**) Signaling feedback loop proposed by Yoo *et al*. (*3*). The LIN-12/Notch receptor is activated in the vulval precursor cells P5.p and P7.p, resulting in the translocation of the receptor intracellular domain to the nucleus. There, it binds to cofactors and activates *mir-61* expression. miR-61 blocks expression of its target, messenger RNA encoding VAV-1, to promote 2° fate.

Together these observations suggest a feedback loop in P5.p and P7.p in which LIN-12 signaling directly activates expression of miR-61, thereby preventing the expression of VAV-1 protein, which could otherwise interfere with *lin-12* activity (see the figure). The precise molecular mechanism whereby *vav-1* opposes *lin-12* activity should prove to be interesting.

Yoo and Greenwald therefore show a new role for a microRNA in an important signaling pathway—in this case, as a direct target of LIN-12/Notch and as a determinant of the 2° cell fate. This is one of the very first descriptions of microRNA involvement in a signaling pathway. The only other study implicating microRNAs in the LIN-12/Notch pathway was carried out by Lai *et al*., although in fruit flies (*9*). Lai *et al*. found that many protein-encoding genes whose transcription is up-regulated by Notch signaling are also posttranscriptionally repressed by certain ubiquitously expressed microRNAs, and that this repression is important to prevent overexpression of the Notch targets. Lai *et al*. suggested a model whereby these microRNAs help dampen or "tune" expression of these target genes in Notch-responsive cells.

The evidence provided by Yoo and Greenwald points to a more specific role for *mir-61* in influencing a cell fate decision compared with the proposed "tuning" role of microRNAs in fly Notch signaling. This highlights a major question in the micro RNA field: How is it that microRNAs seem to be so remarkably versatile? For example, why do some microRNAs seem to function as developmental switches, controlling cell fate decisions by turning off a few key target genes, whereas other microRNAs seem to function more globally to modulate many target genes in many cells, apparently to ensure the precision of gene expression patterns?

In theory there are several factors that may contribute to these diverse roles. First may be the specificity of the expression of the microRNA; thus, a microRNA that is expressed in response to a particular signal may have a more specific function than a microRNA that is more ubiquitously expressed. Second, the number of target messenger RNAs that a microRNA finds is also likely to be important. A microRNA with very few critical targets, such as the canonical worm microRNA *lin-4* (*1*), is likely to act in a more specific manner than a microRNA with many targets. Finally, it is worth noting that a single microRNA may in fact function as a developmental switch in some circumstances and in "tuning" expression in other circumstances. For example, *mir-61* appears to be a LIN-12 target in some cells, but not others (*3*), so the role *mir-61* plays in these various cells may be quite different. Careful analysis of loss-of-function microRNA mutants, including *mir-61*, will be important to address this question. Such analysis may be complex because of redundancy between microRNAs that target the same messenger RNA (*10*).

References

1. V. Ambros, *Nature* **431**, 350 (2004).
2. D. P. Bartel, *Cell* **116**, 281 (2004).
3. A. S. Yoo, I. Greenwald, *Science* **310**, 1330 (2005); published online 20 October 2005 (10.1126.science.1119481).
4. C. A. Kidner, R. A. Martienssen, *Curr. Opin. Plant Biol.* **8**, 38 (2005).
5. B. D. Harfe, *Curr. Opin. Genet. Dev.* **15**, 410 (2005).
6. P. W. Sternberg, in *Wormbook*, B. J. Meyer, Ed. (2005), www.wormbook.org/chapters/www_vulvaldev/vulvaldev.html.
7. T. Berset, E. F. Hoier, G. Battu, S. Canevascini, A. Hajnal, *Science* **291**, 1055 (2001).
8. A. S. Yoo, C. Bais, I. Greenwald, *Science* **303**, 663 (2004).
9. E. C. Lai, B. Tam, G. M. Rubin, *Genes Dev.* **19**, 1067 (2005).
10. A. Abbott *et al*., *Dev. Cell* **9**, 403 (2005).

10.1126/science.1121566

CREDIT: P. HUEY/*SCIENCE*

edited by Edward W. Lempinen

SCIENCE CAREERS

Bold Change, New Energy for *Science*/AAAS Career Resources

A decade after their first career aids went online, *Science* and AAAS have moved to dramatically update their programs, retooling them for a mobile, global 21st-century science and technology workforce.

The new ScienceCareers.org debuted on 15 November, consolidating its powerful recruitment and job search features with *Science*'s Next Wave, GrantsNet, the Minority Scientists Network, and other features—all at one fresh-looking, easy-to-navigate site.

The changes at ScienceCareers are a central part of a sweeping redesign of the *Science* family of Web sites that has given the sites a clean, integrated look; easier access; and more intuitive navigation. One key change: The *Science*NOW daily news Web site will for the first time be available to all readers, without charge.

At the new ScienceCareers site, visitors will find the single most comprehensive, freely accessible source of online S&T career support in the world, serving scientists, engineers, and others at every level.

"Combining services for those who need to fill jobs with those who need help with their careers is a terrific idea," said Donald Kennedy, editor-in-chief of *Science*. "Young scientists need the kind of help Next Wave has given them about building their own professional futures, and they will continue to get it in an editorially independent way at the new site. They will also find *Science*'s unmatched inventory of new opportunities."

Added *Science* Publisher Beth Rosner: "We are enthusiastic that this site will be the most heavily visited career Web site for scientists worldwide and will allow our users to find not only their first job, but the tools and resources to advance in every stage of their careers."

Readers can find the full menu of *Science*'s job and C.V. listings, career resources, and grant information at the new www.sciencecareers.org.

Science has been responsible for bringing together employers and jobseekers through its classified listings for decades, Rosner said, and has long had the largest recruitment section of any scientific journal. But the increasing use of the Internet in the mid-1990s brought new opportunities and new challenges.

Science had a job Web site on the Internet in early 1995; the journal Web site and Next Wave debuted later that year, with GrantsNet following in 1998. NextWave is a career site geared toward young scientists in North America and Europe, while ScienceCareers has offered job listings and materials oriented more to mid-career scientists. Taken together, the sites attract more than three-quarters of a million visitors every month.

The journal's Web site also has been an important vehicle for *Science's* knowledge environments on signal transduction (STKE) and aging (SAGE), as well as for the journal itself.

Stewart Wills, the online editor of *Science*, said surveys, focus groups, and usability testing indicated that readers value the information on the sites but are put off by the complex navigation and varying access controls.

ScienceCareers.org Editor Jim Austin and Sales Director Gabrielle Boguslawski led the team that worked for over a year to study how to merge the sites in a way that kept core audiences satisfied while providing content to new audiences. Wills and *Science*'s electronic media manager, Betsy Harman, worked with a group of stakeholders from Careers, Next Wave, and GrantsNet to help shape the new one-stop career shop, and AAAS Technology Director Rose Futchko supervised the process of building a working site out of that vision.

Wills and others suggest that traffic at www.sciencemag.org and at the new careers site will likely increase as a result of the consolidation, the improved ease of use, and the free access to ScienceNOW.

"We also expect that ScienceNOW will enjoy a broad general readership," said *Science* News Editor Colin Norman. "The stories are accessible accounts of cutting-edge science that should appeal to scientists and high school students alike."

Meanwhile, AAAS named Richard Weibl, a former U.S. editor for *Science*'s Next Wave, as project director of the Center for Careers in Science and Technology. Returning to AAAS after more than 2 years with the Peace Corps in South Africa, Weibl will serve as a linchpin for AAAS's comprehensive efforts to provide career information to students, postdocs, and professionals.

Weibl said the center would propel new collaboration and synergy among different departments and projects at AAAS and *Science*. The center might seek to develop services that now are in short supply. Among the possibilities: career guidance for pre-college students, their parents, and their teachers and information on new opportunities for late-career scientists.

KATHY WREN CONTRIBUTED TO THIS REPORT.

2006 ANNUAL MEETING

An Affair to Remember

The AAAS Annual Meeting will convene on 16 February in St. Louis, Missouri. Over the course of 5 days, the meeting will feature more than 200 symposia, lectures, seminars, and other sessions. For more information about the program and registration, see www.aaasmeeting.org.

SCIENCE EDUCATION

Project 2061: 20 Years of "Science Literacy for All"

On a cool autumn evening at the U.S. Capitol, some of Congress's most influential science and technology advocates joined with AAAS officials to mark the 20th anniversary of Project 2061, the AAAS science literacy project.

They used the briefing to celebrate the project's accomplishments and growing global influence. But they also shared a sense of concern at the challenges confronting the nation as it works to nurture new generations of scientists and engineers and to prepare young people to ad-

AAAS GOVERNANCE

AAAS 2005 Election of Officers

The deadline for return of ballots has been extended to 16 December.

dress complex science-related issues.

"We are falling behind the rest of the world in teaching our students math and science concepts," warned Representative Vernon Ehlers (R–MI). "It's urgent that AAAS and Project 2061 continue to do what you are doing."

Ehlers was joined by Representative Mark Udall (D–CO), his partner in launching the bipartisan Science, Technology, Engineering and Mathematics (STEM) Education Caucus in 2004. U.S. Representative Sherwood Boehlert (R–NY), the chair of the House Science Committee, was there, as were Representatives Rush Holt (D–NJ), a physicist and former AAAS Science and Technology Policy Fellow, and Donald Payne (D–NJ).

The anniversary celebration "gave us a chance to look back and to see how far we've come and how much has been accomplished," said Project 2061 Director Jo Ellen Roseman. "At the same time, it renewed our commitment to the work ahead—there is still so much to be done, and Project 2061 clearly has an important role to play."

As its core mission, Project 2061 advocates that science education is essential for all students, not just for those going on to technical or research careers. The arrival of Halley's Comet in 1985 served as an inspiration to the founders, who envisioned a reform of K–12 education so that broad science, mathematics, and technology literacy is a reality when the comet reappears in 2061.

"No organization had previously addressed the issue of what was needed in K–12 schooling by putting aside the traditional curriculum and starting by debating and deciding what every adult citizen needed to know and be able to do," said AAAS President Gilbert S. Omenn, a member of Project 2061's original advisory group.

Project 2061's *Science for All Americans*, published in 1989, and its 1993 *Benchmarks for Science Literacy* have set standards and goals that have had a deep influence on education not just in the U.S., but as far away as China and Japan. In addition to setting goals for science and mathematics learning, Project 2061 is equally committed to helping educators use those goals to make changes in what and how they teach.

One recent project that showcases the Project's ambition is a study of middle-school mathematics now under way in Delaware and Texas.

The study, involving 9 school districts and 85 middle-school math teachers and their students, is exploring how to improve teachers' classroom instruction through the use of professional development that is tied closely to specific learning goals and the lessons in their textbooks that target those goals. By watching videotapes of themselves teaching selected lessons, teachers are able to judge whether they and their students are progressing toward the goals.

"It was extremely enlightening," said Laura Conner, a sixth-grade math teacher in Middletown, Delaware.

The anniversary events from 17 to 19 October also included a workshop for teachers and a program of speakers from science and science education. The events brought former and current staff members, past collaborators, and current Project 2061 postdoctoral fellows to Washington, D.C., for a look at the project's past and its future challenges.

Project 2061 founder F. James Rutherford was honored with a framed poster displaying the covers of Project books that were published during his tenure as director. He is currently a distinguished visiting professor at Mills College in Oakland, California, and is working on several projects involving science and environmental education.

"Project 2061 can be proud of the unrivaled contributions it made to the advancement of science education during its first 20 years," Rutherford said, "and now, in the next 20, it must continue to press forward with the same strategy, energy, and inventiveness in its crucial effort to make nationwide science literacy a reality in America."

LONNIE SHEKHTMAN AND PAM GEORGE CONTRIBUTED TO THIS REPORT.

SCIENCE COMMUNICATION

Learning to Think Like a Harried News Editor

The space devoted to news in most American newspapers is shrinking. Television often seems uninterested in science news. In any given day, thousands of messages are competing for the attention of consumers, and attention spans seem to be getting shorter.

That's the difficult environment that news editors face. And when it comes time to get news or ideas to the public, science and medical researchers would do well to think like news editors.

That was a central message of the third annual EurekAlert! seminar for public information officers, "Communicating Science & Health News Across the Media Spectrum." The seminar was short on sugarcoating but rich with advice for navigating the hypercompetitive media landscape.

"The media is very much like a prom queen," quipped moderator and TV show host Rea Blakey. "You must seek us. We have 600 e-mails a day, we have 200 people calling, we are bombarded with your press releases…. We need immediacy, we need timeliness, we need you to respond to our needs."

A panel of six journalists joined Blakey, detailing strategies for capturing a news editor's interest. John Timpane, op-ed editor for the *Philadelphia Inquirer*, said it's helpful to focus on subjects that are high on the national news agenda—avian flu or evolution, for example. Others expressed an interest in scientists who are good storytellers, or in good photo or video options.

Rea Blakey

Blakey is president and founder of TV Talks Inc.; host of a national medical show, "Discovery Health CME," which airs on the Discovery Health Channel; and a media training consultant for Spectrum Science Communications, which co-sponsored the event. The event was organized by Cathy O'Malley, project director of EurekAlert! at AAAS, in collaboration with Spectrum President John Seng.

EurekAlert!, a service of AAAS, is the premier service of its kind in the world, a site where journalists, educators, students, and others come for the latest science and engineering news. EurekAlert! counts 5,000 reporters from 50 countries as registered users and receives 900,000 visits every month from 500,000 unique visitors.

To access seminar materials and presentations, visit www.eurekalert.org/seminar.

2006 ELECTION

A Call for Nominations

AAAS members may suggest nominees (including themselves) for president-elect and the Board of Directors for election in the fall of 2006. For a list of this year's candidates, see "AAAS News and Notes" in the 29 July 2005 issue of *Science*; for a list of current Board members, see the masthead page of any recent issue of *Science*. Please send the suggested nominee's curriculum vitae no later than 30 December to Gretchen Seiler, AAAS Executive Office, 1200 New York Avenue, NW, Washington, DC 20005. Suggested nominees will be considered by the AAAS Committee on Nominations at their winter meeting.

IS YOUR

hot-start method giving you more questions

THAN ANSWERS?

Results clearly demonstrate a shift from predominantly primer-dimers to the specific target when HotStart-IT is included in the reactions.

"Are my PCR reactions specific enough? Will my experiment be contaminated from animal-sourced antibodies? Will the DNA be damaged from extensive heat denaturation? Will my results be compromised?" If these are some of the questions you're asking yourself, try HotStart-IT.™ Developed by USB scientists, HotStart-IT is an elegant new method that doesn't use antibodies or chemically modified enzymes. Instead, HotStart-IT relies on a unique protein that binds and sequesters primers at lower temperatures which prevents mispriming and the formation of primer-dimers. When PCR is initiated, the protein is inactivated during the heat denaturation step and the primers are free to participate in the subsequent amplification cycles. The result? Higher specificity. Higher yield. And, most importantly, a higher level of confidence for you.

usb®
Fueling Innovation™

For a FREE sample of new HotStart-IT, call 800.321.9322 or visit www.usbweb.com/hotstart

The Phanerozoic Record of Global Sea-Level Change

Kenneth G. Miller,[1]* Michelle A. Kominz,[2] James V. Browning,[1] James D. Wright,[1] Gregory S. Mountain,[1,3] Miriam E. Katz,[1] Peter J. Sugarman,[4] Benjamin S. Cramer,[1,5] Nicholas Christie-Blick,[3] Stephen F. Pekar[3,6]

We review Phanerozoic sea-level changes [543 million years ago (Ma) to the present] on various time scales and present a new sea-level record for the past 100 million years (My). Long-term sea level peaked at 100 ± 50 meters during the Cretaceous, implying that ocean-crust production rates were much lower than previously inferred. Sea level mirrors oxygen isotope variations, reflecting ice-volume change on the 10^4- to 10^6-year scale, but a link between oxygen isotope and sea level on the 10^7-year scale must be due to temperature changes that we attribute to tectonically controlled carbon dioxide variations. Sea-level change has influenced phytoplankton evolution, ocean chemistry, and the loci of carbonate, organic carbon, and siliciclastic sediment burial. Over the past 100 My, sea-level changes reflect global climate evolution from a time of ephemeral Antarctic ice sheets (100 to 33 Ma), through a time of large ice sheets primarily in Antarctica (33 to 2.5 Ma), to a world with large Antarctic and large, variable Northern Hemisphere ice sheets (2.5 Ma to the present).

Fluctuations in global sea level (eustasy) result from changes in the volume of water in the ocean or the volume of ocean basins (Fig. 1) (*1–4*). Water-volume changes are dominated by growth and decay of continental ice sheets, producing high-amplitude, rapid eustatic changes [up to 200 m and 20 m per thousand years (ky)]. Other processes that affect water volume occur at high rates (10 m/ky) and low amplitudes (~5 to 10 m): desiccation and inundation of marginal seas, thermal expansion and contraction of seawater, and variations in groundwater and lake storage. Changes in ocean basin volume are dominated by slow variations in sea-floor spreading rates or ocean ridge lengths (100 to 300 m amplitude, rates of 10 m/My). Variations in sedimentation cause moderate amplitude (60 m), slow changes (10 m/My). Emplacement of oceanic plateaus produces moderately rapid rises (60 m/My) but slow falls due to thermal subsidence (10 m/My).

Eustatic variations can be estimated from satellite measurements, tide gauges, shoreline markers, reefs and atolls, oxygen isotopes ($\delta^{18}O$), and the flooding history of continental margins and cratons. Satellite measurements are limited to the past 10 years (*5*), whereas tide gauge records extend back only ~150 years (*3*). The most recent pre-anthropogenic sea-level rise began at about 18 ka and can be measured by directly dating shoreline markers (fig. S1). Tropical reefs and atolls (fig. S2) provide the most reliable geological estimates by dating "fossil sunshine" (e.g., shallow-dwelling corals) and have provided a precise estimate for the last sea-level lowstand (120 ± 5 m below present at 18 ka) (fig. S2) (*6*, *7*). However, most coral records are from regions with complicated uplift/subsidence histories, are difficult to recover and date (particularly beyond a few 100 ky), and have poorly preserved lowstand deposits.

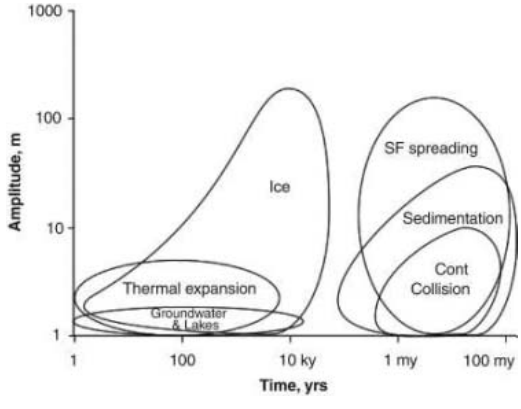

Fig. 1. Timing and amplitudes of geologic mechanisms of eustatic change derived from (*1–4*). SF, sea floor; Cont, continental.

The growth and decay of continental ice sheets causes eustatic changes that are indirectly recorded in the chemistry of foraminifera because ice has lower $\delta^{18}O$ values than seawater (fig. S2) [e.g., (*8*, *9*)]. Oxygen isotope values provide a proxy for glacioeustasy, but $\delta^{18}O$-based reconstructions are subject to several uncertainties: (i) Calcite $\delta^{18}O$ values also vary as a function of temperature. (ii) Surface-ocean $\delta^{18}O$ values are influenced by local evaporation-precipitation effects on seawater. (iii) Postdepositional alteration (diagenesis) may overprint original $\delta^{18}O$ values, limiting useful records to sediments younger than 100 My.

Continents have been flooded many times in the geologic past (Fig. 2). However, the flooding record is not a direct measure of eustatic change because variations in subsidence and sediment supply also influence shoreline location. Regional unconformities (surfaces of erosion and nondeposition) divide the stratigraphic record into sequences and provide a key to eustatic change. Unconformities result from sea-level fall or tectonic uplift (*10–12*). Similar ages of sequence boundaries on different continents have been interpreted as indicating that the surfaces were caused by a global process, eustasy [e.g. (*10*, *11*)]. The linkage with $\delta^{18}O$ increases for the past 40 My (*13*) indicates that most sequence boundaries resulted from eustatic falls driven by the growth of continental ice sheets.

Although unconformities potentially provide the timing of eustatic lowstands, extracting global sea-level history from the stratigraphic record requires a quantitative method that distinguishes the contributions of eustasy, subsidence, and sediment accumulation. Backstripping is an inverse technique that can be used to quantitatively extract sea-level change amplitudes from the stratigraphic record. It accounts for the effects of sediment compaction, loading (the response of crust to overlying sediment mass), and water-depth variations on basin subsidence (*14*). Tectonic subsidence at a passive margin is modeled with thermal decay curves and removed

[1]Department of Geological Sciences, Rutgers University, Piscataway, NJ 08854, USA. [2]Department of Geosciences, Western Michigan University, Kalamazoo, MI 49008–5150, USA. [3]Lamont-Doherty Earth Observatory of Columbia University, Palisades, NY 10964, USA. [4]New Jersey Geological Survey, Post Office Box 427, Trenton, NJ 08625, USA. [5]Department of Geological Sciences, University of Oregon, Eugene, OR 97403–1272, USA. [6]School of Earth and Environmental Sciences, Queens College, 65-30 Kissena Boulevard, Flushing, NY 11367, USA.

*To whom correspondence should be addressed: kgm@rci.rutgers.edu

to obtain a quantified eustatic estimate in the absence of local tectonic complexities.

We review the record of and uncertainties in eustatic changes over the past 543 My on three time scales: (i) a long-term trend (10^7 to 10^8 years) that has been attributed largely to variations in sea-floor spreading; (ii) the 10^6-year scale that is among the most prominent features of the stratigraphic record; and (iii) the 10^4- to 10^5-year scale that is dominated by changes in ice volume and controlled by astronomical variations in insolation. We present a new eustatic record for the past 100 My, with implications for causal mechanisms for both 10^7- and 10^6-year changes.

Long-Term Flooding of Continents

Sloss (*15*) recognized that North America experienced five major Phanerozoic floodings (Fig. 2) and attributed these changes to subsidence and uplift of the craton. Vail and colleagues at Exxon Production Research Company (EPR) recognized similar 10^7- to 10^8-year scale "supersequences" that they attributed to global sea-level changes (*10*, *11*, *16*). Others have reconstructed continental flooding history on the 10^7- to 10^8-year scale (*4*, *17*–*19*) (Fig. 2) and inferred eustatic changes from commonalities among continents.

High Late Cretaceous sea level has been attributed to high ocean-crust production rates that resulted in more buoyant ridges displacing seawater onto low-lying parts of continents ("tectonoeustasy") (*20*). This concept has been extended to the Paleozoic through Early Mesozoic by assuming that 10^7- to 10^8-year scale continental flooding was caused by high sea-floor spreading rates, even though direct evidence for sea-floor spreading rates is absent owing to subduction.

Our sea-level record for the past 100 My has much lower amplitudes on the 10^7- to 10^8-year scale than previously inferred (Figs. 2 and 3 and fig. S3), with implications for sea-level change from 543 to 100 Ma. Our 100 to 7 Ma record (Fig. 2) is based on backstripping stratigraphic data from five New Jersey coastal plain coreholes (*21*, *22*). Similar estimates obtained for each site suggest that we successfully accounted for the effects of thermal subsidence, sediment loading, compaction, and water-depth variations. Our long-term trend indicates that sea level was 50 to 70 m above present in the Late Cretaceous (~80 Ma), rose to 70 to 100 m from 60 to 50 Ma, and fell by ~70 to 100 m since 50 Ma (*23*). This contrasts with previously reported Late Cretaceous sea-level peaks of about 250 to 320 m based on sea-floor spreading reconstructions (*2*), although it is within error estimates of 45 to 365 m (best estimate 230 m) (*24*). It is lower than global continental flooding estimates [150 m (*19*), 80 to 200 m (*18*)].

Our results are similar to backstripped estimates from the Scotian and New Jersey continental shelves (*14*), although the Late Cretaceous peak is lower (50 to 70 m versus ~110 m) (fig. S3). One-dimensional (1D) backstripping may underestimate the Late Cretaceous peak because coastal plain subsidence results from a thermoflexural effect (*14*), and thermal subsidence curves may slightly overestimate the tectonic portion of subsidence of the older section. Considering backstripping and continental flooding estimates (*18*, *19*) and errors in our paleowater depth estimates (eustatic error of ±10 to 35 m), we conclude that sea level in the Late Cretaceous was 100 ± 50 m higher than it is today.

Using new sea-floor age data, Rowley (*25*) suggested that there have been no changes in sea-floor spreading rates over the past 180 My. Our record implies a modest decrease in the rate of ocean-crust production because the long-term eustatic fall of 70 to 100 m since the early Eocene (Fig. 3) cannot be totally ascribed to permanent growth of ice sheets (*26*).

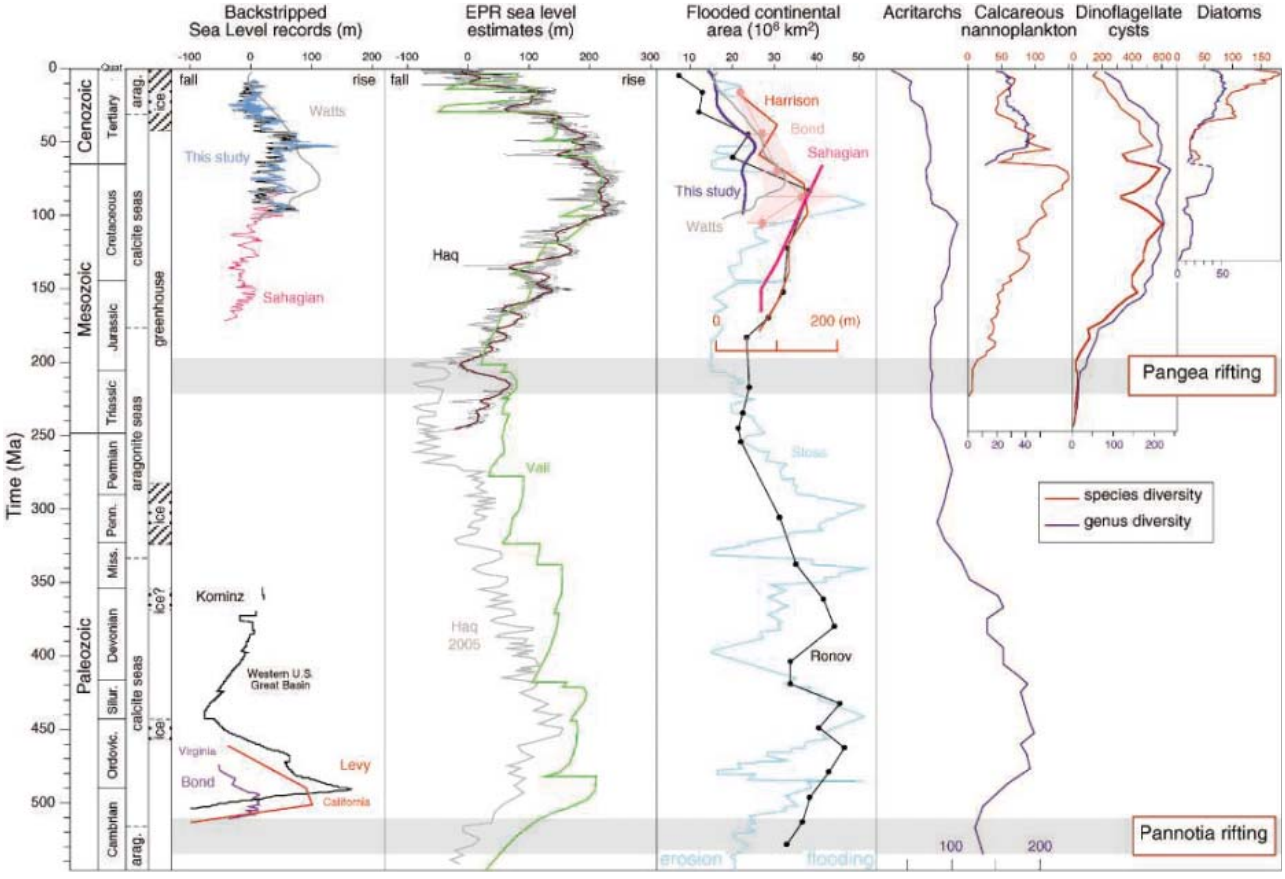

Fig. 2. Comparison of Phanerozoic backstripped eustatic estimates of this study, Watts (*14*), Sahagian (*35*), Kominz (*29*), Levy (*30*), and Bond (*18*); EPR records of Vail (*10*) and Haq (*11*, *16*); continental flooding records of Sloss (*15*) and Ronov (*17*) plotted versus area, and Bond (*18*), Harrison (*19*), and Sahagian (*4*) plotted versus sea level; and evolutionary records compiled by Katz (*52*).

Our observation that long-term eustatic changes were appreciably smaller than previously thought has implications for geochemical models [e.g., (*27*)] that have used sea-level records to scale ocean production rates. Estimates derived from backstripping from the past 170 My (Fig. 2) show much lower long-term amplitudes than those published by EPR. Backstripped sea-level records from the Cambrian-Devonian of the western United States show ~200-m amplitudes on the 10^7-year scale (*28*–*30*) (Fig. 2), although a Cambrian-Ordovician backstripped data set from the Appalachians shows a lower (~70 m) amplitude (Fig. 2) (*28*). The sea-level rise in the Cambrian is attributed to the generation of new ocean ridges with the breakup of Pannotia (*29*), but the amplitude of this rise is still uncertain. Although the jury is still out on the amplitudes of Paleozoic sea level on the 10^7-year scale, our work suggests that the EPR records cannot be used to scale past spreading rates.

Sea-level changes on very long time scales (250 My) are related to the assembly and breakup of supercontinents. Formation of the supercontinents Pannotia (late Proterozoic to Early Cambrian) and Pangea (Permian to early Triassic) was associated with low levels of continental flooding (Fig. 2). This may be attributed to (i) a eustatic effect due to thickening of continents during orogeny resulting in increased oceanic area (*2*) and/or (ii) higher elevations that result when trapped heat builds up below the supercontinents (*31*).

Million-Year Scale Changes

In 1977, EPR surprised academic and industrial colleagues with the publication of a Phanerozoic eustatic record that showed more than 50 falls, some as large as 400 m (*10*). In 1987, the EPR group published a series of papers, including a synthesis in *Science* (*11*) that reported more than 100 sea-level falls during the past 250 My, with a maximum fall of 160 m. The EPR studies came under intense scrutiny because of the novel suggestions that (i) sequence boundaries are time-important features that could be recognized on seismic profiles and (ii) seismic profiles could be used to determine the history of sea level. The EPR curves have been strongly criticized for their methodology (*12*, *32*), with critics suggesting that coastal onlap curves presented cannot be translated into a eustatic estimate.

Drilling on the New Jersey margin has provided new insights into the amplitudes of and mechanisms for 10^6-year scale sea-level changes. Fourteen Late Cretaceous sequences and 33 Paleocene-Miocene sequences were identified in New Jersey coastal plain coreholes (*13*, *33*) and dated by integrating biostratigraphy, Sr-isotopic stratigraphy, and magnetostratigraphy to produce a chronology with age resolution of better than ±0.5 My for the Cenozoic (*13*) and ±1.0 My for the Late Cretaceous (*33*). Onshore New Jersey sequence boundaries correlate with sequence boundaries in the Bahamas, northwest Europe, the U.S. Gulf Coast, Russia, offshore New Jersey, and those of EPR, which suggests that they are global and formed in response to eustatic falls (*13*, *33*). Thus, drilling has validated the number and timing, although not the amplitude, of many of the EPR sea-level events for the past 100 My (*13*, *33*). Oligocene-Miocene sequence boundaries can be firmly linked with global $\delta^{18}O$ increases, demonstrating a causal relation between sea level and ice volume (*13*, *33*), as expected for the Icehouse world of the past 33 My.

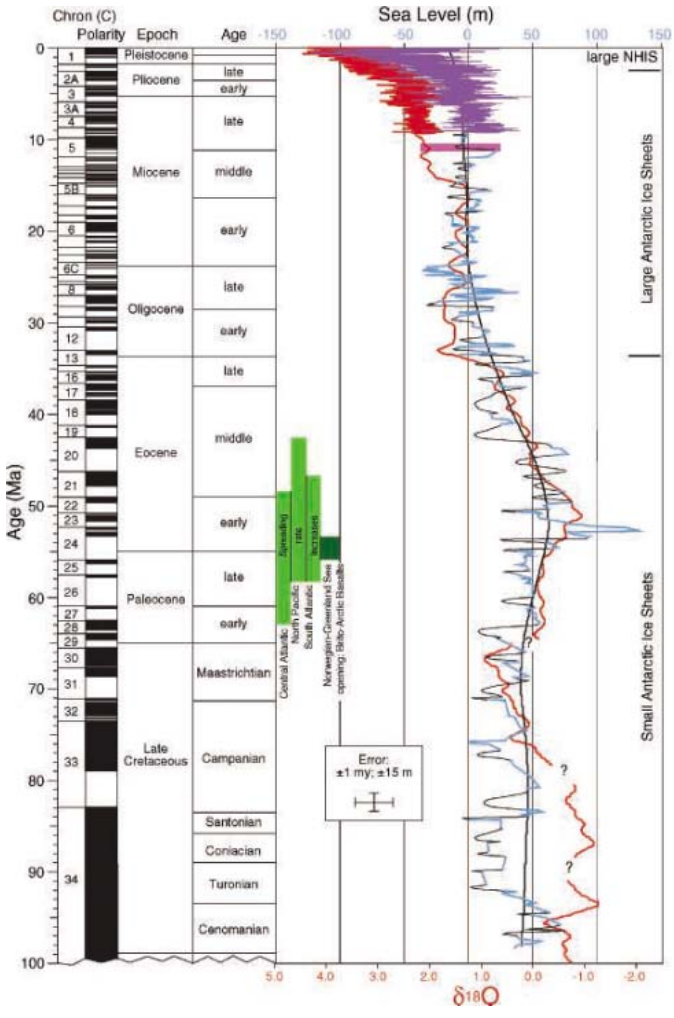

Fig. 3. Global sea level (light blue) for the interval 7 to 100 Ma derived by backstripping data (*21*). Global sea level (purple) for the interval 0 to 7 Ma derived from $\delta^{18}O$, shown in detail on Fig. 4. Shown for comparison is a benthic foraminiferal $\delta^{18}O$ synthesis from 0 to 100 Ma (red), with the scale on the bottom axis in ‰ [reported to *Cibicidoides* values (0.64‰ lower than equilibrium)]. The portion of the $\delta^{18}O$ curve from 0 to 65 Ma is derived using data from Miller (*44*) and fig. S1 recalibrated to the time scale of (*71*). The $\delta^{18}O$ curve from 65 to 100 Ma is based on the data compiled by Miller (*36*) calibrated to the time scale of (*72*). Data from 7 to 100 Ma were interpolated to a constant 0.1-My interval and smoothed with a 21-point Gaussian convolution filter using Igor Pro. Pink box at ~11 Ma is sea-level estimate derived from the Marion Plateau (*51*). Heavy black line is the long-term fit to our backstripped curve (*23*). Light green boxes indicate times of spreading rate increases on various ocean ridges (*57*). Dark green box indicates the opening of the Norwegian-Greenland Sea and concomitant extrusion of the Brito-Arctic basalts.

Backstripping of the New Jersey records provides eustatic estimates from ~100 to 7 Ma (Fig. 3). Paleocene-Eocene and Miocene estimates are derived from 1D backstripped records from five sites and Late Cretaceous sequences from two sites (*34*). Several Upper Cretaceous onshore sections capture full amplitudes of change; however, many Cretaceous and most Cenozoic onshore sections do not record sea-level lowstands. Eustatic estimates for the latest Eocene to earliest Miocene are derived from 2D backstripping (*22*) that addressed this problem.

Our backstripped eustatic estimate (table S1) shows that global sea level changed by 20 to 80 m during the Late Cretaceous to Miocene (this study) and the Middle Jurassic to Late Cretaceous (*35*). Our comparison shows that the amplitudes of the EPR sea-level curve, including the most recent update (*16*), are at least 2.5 times too high (Fig. 2 and fig. S3).

Eustatic changes with amplitudes of 10s of meters in less than 1 My pose an enigma for a supposedly ice-free Greenhouse world, because ice-volume changes are the only known means of producing such large and rapid changes. Our record (Fig. 3) quantifies high amplitudes and rates of eustatic change (>25 m in < 1 My) in the Late Cretaceous to Eocene Greenhouse world. Based on the sea-level history, we have proposed that ice sheets existed for geologically short intervals (i.e., lasting ~100 ky) in the previously assumed

ice-free Late Cretaceous-Eocene Greenhouse world (*36*). This view can be reconciled with previous assumptions of an ice-free world. Sea-level changes on the 10^6-year scale were typically ~15 to 30 m in the Late Cretaceous-Eocene (~100 to 33.8 Ma), suggesting growth and decay of small- to medium-sized (10 to 15×10^6 km^3) ephemeral Antarctic ice sheets (*36*). These ice sheets did not reach the Antarctic coast; as a result, coastal Antarctica and deep-water source regions were warm even though there were major changes in sea level as the result of glaciation (*36*). These ice sheets existed only during "cold snaps," leaving Antarctica ice-free during much of the Greenhouse Late Cretaceous to Eocene (*36*).

Sea-level changes on the 10^6-year scale occurred throughout the Phanerozoic. Studies from the Russian platform and Siberia provide backstripped records of 10^6-year sea-level changes that are remarkably similar to New Jersey in the interval of overlap and extend to the Middle Jurassic (~170 Ma) (*35*). The stratigraphic record before 170 Ma is replete in 10^6-year sea-level changes (*16*, *37*). However, it is unclear whether these variations represent global changes in sea level. Eustatic estimates have been extracted from backstripping of Paleozoic strata (*28*, *29*) (Fig. 2), although differences in the Appalachian versus the western U.S. Cambrian-Ordovician sea-level amplitude estimates are large, and thus the eustatic imprint is ambiguous.

Eustatic changes on the 10^4- to 10^6-year scales were controlled primarily by variations in ice volume during the past 100 My and may be expected to be modulated by both short-period [19/23 (precession), 41 (tilt), and ~100 ky (precession)] and long-period [1.2 (tilt) and 2.4 My (precession)] astronomical variations (*38*). Spectral analysis of our sea-level records shows that variations occur with an as-yet-unexplained, persistent 3-My beat and a second primary period varying from 6 to 10 My (fig. S4). Amplitudes in the ~3-My bandwith are ~10 m from 60 to 20 Ma, with lower amplitude from 90 to 60 Ma.

The existence of continental ice sheets in the Greenhouse world is a controversial interpretation, but the study of ice-volume history has progressively tracked ice sheets back through the Cenozoic (*36*). After extensive debate, a consensus has developed that ice volume increased markedly in the earliest Oligocene (*8*, *9*). We suggest that, at that time, the Antarctic ice sheet began to be a forcing agent of, and not just a response to, ocean circulation (*36*). The Antarctic continent (including west Antarctica) (*39*) was entirely covered by ice, and sea level was lower by ~55 m (*22*). As a result, latitudinal thermal gradients (*40*) and deep-water circulation rates increased [with pulses of Southern Component and Northern Component Water (*41*)]. Diatoms diversified rapidly in response to increased surface-water circulation and nutrient availability (Fig. 2), resulting in increased export production and a positive feedback on CO_2 drawdown and cooling.

The earliest Oligocene event represented a major change in climate state from a Greenhouse world with cold snaps to the Icehouse world that continues today. Sea-level changes from the Oligocene to the early Pliocene (~33.8 to 2.5 Ma) were ~30 to 60 m (Figs. 3 and 4), with growth and decay of a large (up to present volumes of 25×10^6 km^3) ice sheet mostly in Antarctica. A middle Miocene $\delta^{18}O$ increase is associated with deep-water cooling and two ice-growth events that resulted in the permanent development of the East Antarctic ice sheet (*40*). Northern hemisphere ice sheets (NHIS) have existed since at least the middle Miocene (*41*), but large NHIS with sea-level changes of 60 to 120 m only began during the late Pliocene to Holocene (~2.5 to 0 Ma) (Fig. 4).

Milankovitch Scale Changes

The growth and decay of NHIS (the late Pliocene-Holocene "ice ages") and attendant sea-level changes were paced by 10^4- to 10^5-year scale Milankovitch changes. The $\delta^{18}O$ record shows a dominant 100 ky (eccentricity) beat over the past 800 ky, with secondary 19/23 (precession) and 41-ky (tilt) periods (*42*). Before ~800 ky, the tilt cycle dominated $\delta^{18}O$ (*43*) and sea-level records. Although strong precessional and eccentricity beats occur in the carbon system, the tilt cycle has dominated $\delta^{18}O$ and ice-volume records for much of the past 33.8 My (*9*). Growth and decay of small- to medium-sized ice sheets in the Late Cretaceous-Eocene on the Milankovitch scale probably lie near or below the detection limit of $\delta^{18}O$ records [~ 0.1 per mil (‰) = 10-m eustatic change].

Continental margins record 10^4- to 10^5-year scale sea-level changes only in very high sedimentation rate settings. Foraminiferal $\delta^{18}O$ records reflect ice volume in addition to temperature changes and potentially provide a proxy for sea-level changes on the 10^4- to 10^5-year scale. The $\delta^{18}O$ record provides continuity and excellent age control, although assumptions about thermal history must be made to use it as a sea-level proxy. In addition, diagenesis complicates planktonic foraminiferal $\delta^{18}O$ records, although benthic foraminifera generally show little evidence for diagenesis at burial depths less than 400 to 500 m (*44*).

We derive sea-level estimates from 9 to 0 Ma using benthic foraminiferal $\delta^{18}O$ records because the New Jersey record is incomplete from 7 to 0 Ma (table S1). We scaled the benthic foraminiferal $\delta^{18}O$ record (*45*) to sea level by making minimum assumptions about ocean thermal history (Fig. 4). The resultant sea-level curve (Fig. 4) aligns remarkably well with the backstripped record from 9 to 7 Ma (Fig. 3).

Our $\delta^{18}O$-derived sea-level estimate for the past 9 My (Fig. 4) shows that the record is dominated by the response to the 41-ky period tilt forcing, which increases in amplitude toward the present, and a low-amplitude ~21-ky precession response. The major 100-ky events of the past 900 ky stand out in the sea-level record (Fig. 4). There are prominent 10^6-year scale sea-level falls (the 2.5, 3.3, 4.0, 4.9, 5.7, and 8.2 Ma events) (Fig. 4), but these are not obviously paced by amplitude modulations of either precession or tilt (fig. S4).

Suborbital Scale

Very large (>100 m) sea-level rises are associated with glacial terminations of the past 800 ky (fig. S1) (*6*). The most recent rise that followed the last glacial maximum at 18 ka occurred as two major steps associated with meltwater pulses (MWP) 1a (13.8 ka) and 1b (11.3 ka), punctuated by a slowing at ~12 ka (*6*). Sea-level rise slowed at about 7 to 6 ka (fig. S1). Some regions experienced a mid-Holocene sea-level high at 5 ka, but we show that global sea level has risen at ~1 mm/year over the past 5 to 6 ky. We present new core data from New Jersey covering the past 6 ky that show a rise of 2 mm/year over the past 5 ky (fig. S1). This New Jersey curve is remarkably similar to sea-level records from Delaware (*46*) and southern New England (*47*), with a eustatic rise of 1 mm/year over the past 5 ky once corrected for subsidence effects (*48*), virtually identical to that obtained from Caribbean reef localities (*49*) (fig. S1) accounting for subsidence.

Error Estimates

Long-term sea-level estimates show considerable differences, with a large range of Late Cretaceous sea-level estimates: ~110 m (*14*), 150 m (*19*), 250 m (*4*), and 80 to 200 m (*18*), and our best estimate of 100 ± 50 m. We conclude that sea-level amplitudes on this scale were substantially lower than generally believed (100 versus 250 m) over the past 170 My, with uncertain amplitude before this (Fig. 2).

Sea-level estimates on the 10^6-year scale have an uncertainty, typically, of at best ±10 to ±50 m. The two main sources of errors in backstripping relate to hiatuses (time gaps) and paleowater depth estimates. New Jersey coastal plain sequences represent primarily inner-shelf to middle-shelf environments, with eustatic errors from paleowater depth estimates of ±10 to 20 m (*50*). Hiatuses in our record potentially explain why amplitudes of change might not be fully recorded, and the effect of hiatuses can be evaluated only by comparing our record with other regions. Drilling on the Marion Plateau (offshore northeast Australia) targeted an ~11 Ma eustatic lowering (*51*); backstripping yields a sea-level estimate of 56.5 ± 11.5 m for this event (pink bar on Fig. 3). Our estimate for this event is ~40 ± 15 m (Fig. 1); these estimates are consistent, within error, but suggest that we may underestimate sea-level falls by 5 to 30 m.

The record of the past 130 ky illustrates the errors in converting a $\delta^{18}O$ record into a sea-level proxy (fig. S1). Benthic foraminiferal $\delta^{18}O$ records can be scaled to a faithful proxy for glacial to cool interglacials [Marine Isotope Chron (MIC) 2d to 5d] (fig. S2), with sea level and $\delta^{18}O$ in phase and lagging insolation. However, large deviations of the $\delta^{18}O$-based sea-level curve occur during peak warm intervals (Holocene and MIC 5e) (Fig. 2), with a hint that deep-sea temperature change leads sea level. We have attempted to correct for this temperature effect by scaling to the Barbados sea-level record (*6*). However, this results in underestimating amplitudes of glacials and overestimating amplitudes of interglacials, with a resultant 20% uncertainty.

Relation of Sea Level to Evolution and Climate Changes

Episodes of supercontinent rifting and sea-level rise on the 10^7- to 10^8-year scale played a role in phytoplankton evolution since the Proterozoic by flooding continental shelves and low-lying inland areas and increasing the total length of coastline. The resulting increases in habitat heterogeneity, ecospace, and nutrient availability favored plankton that lived along continental margins. Accordingly, diversity increases in phytoplankton (Fig. 2) appear to correlate with continental rifting of Pannotia (Early Paleozoic) and Pangea (Jurassic) (Fig. 2), ultimately resulting in the three groups of eukaryotic phytoplankton (coccolithophores, diatoms, and dinoflagellates) that dominate the modern ocean (*52*).

Sea-level changes are expected with beats of 19/23, 41, and 100 ky, but similar changes on the 10^6-year scale (Fig. 3) have puzzled geologists. Sea-level cyclicity on the 10^6-year scale can be explained by a modulation of the shorter term Milankovitch-scale sea-level events (fig. S5). For example, a prominent seismic disconformity spanning the Oligocene/Miocene boundary (~23.8 Ma) on the New Jersey slope (*13*) can be correlated to a detailed $\delta^{18}O$ record at deep-sea Site 929 (*53*), showing that the 10^6-year scale sea-level fall at the Oligocene/Miocene boundary occurred as a series of 41-ky $\delta^{18}O$ increases and sea-level changes. The 41-ky sea-level falls are reflected in core photographs by a series of dark-light changes (fig. S5), resulting from variations in glauconite transported downslope during lowstands. The seismic reflection is a concatenation of these beds and the ice-volume events that caused them.

The high sea levels of the Late Cretaceous and early Eocene are associated with peak benthic foraminiferal $\delta^{18}O$ values (Fig. 3) (table S1), and it has long been suggested that sea level covaries with $\delta^{18}O$ on the 10^7-year scale [e.g., (*54*)]. On the 10^5- to 10^6-year scales, such covariance can be explained by ice-volume changes in concert with temperature changes (*8*, *13*). However, this cannot be true on the 10^7- to 10^8-year scale because most of the $\delta^{18}O$ signal must be attributed to temperature changes. For example, 3.6‰ of the 4.4‰ increase from 50 to 0 Ma (Fig. 3) must be attributed to deep-water cooling (15°C overall) rather than to ice storage (*55*). The link between sea level and temperature on the 10^7- to 10^8-year scale cannot be due to cooling alone, because this would explain only ~15 m of eustatic fall since 50 Ma. The link between $\delta^{18}O$ and sea-level variations on the 10^7- to 10^8-year scale can be explained by CO_2 variations controlled by tectonics (changes in ocean-crust production and mountain uplift).

High ocean-crust production rates have long been linked to high sea level, high CO_2, and warm global temperatures [e.g., (*54*)]. Warm Late Cretaceous climates and elevated sea level may be attributable to moderately higher sea-floor production rates, although our results require that crustal production rates were lower than previously thought. However, the intensity of spreading ridge hydrothermal activity (a major source of CO_2 outgassing) appears also to correlate with times of major tectonic reorganizations (*56*). We propose that the early Eocene peak in global warmth and sea level (Fig. 3) was due not only to slightly higher ocean-crust production but also to a late Paleocene-early Eocene tectonic reorganization. The largest change in ridge length of the past 100 My occurred ~60 to 50 Ma (*57*), associated with the opening of the Norwegian-Greenland Sea, a significant global reorganization of spreading ridges, and extrusion of 1 to 2 × 10^6 km^3 of basalts of the Brito-Arctic province (*58*). A late Paleocene to early Eocene sea-level rise coincides with this ridge-length increase, suggesting a causal relation. We suggest that this reorganization also increased CO_2 outgassing and caused global warming to an early Eocene maximum. Subsequent reduced spreading rates and hydrothermal activity resulted in lower long-term sea level, reduced CO_2 outgassing, and a cooling of deep-water by ~8°C (*44*). CO_2 may have been further lowered by an increase in continental weathering rates during the remainder of the Cenozoic (*59*), explaining an additional deep-water cooling of 7°C to 9°C (*44*).

Our studies of the past 100 My provide clues to the tempo of climate and ice-volume changes for other Icehouse and Greenhouse worlds of the Phanerozoic (Fig. 2). Icehouse worlds of the past 33 My, the Pennsylvanian to Early Permian, Late Devonian, and Late Ordovician (*60*), can be characterized by ice-volume changes that caused sea-level variations up to 200 m. Greenhouse worlds characterize much of the Phanerozoic, but we note that small (10 to 15 × 10^6 km^3), ephemeral ice sheets occurred in the Greenhouse of the Late Cretaceous to Eocene. This raises the question as to whether any portion of the

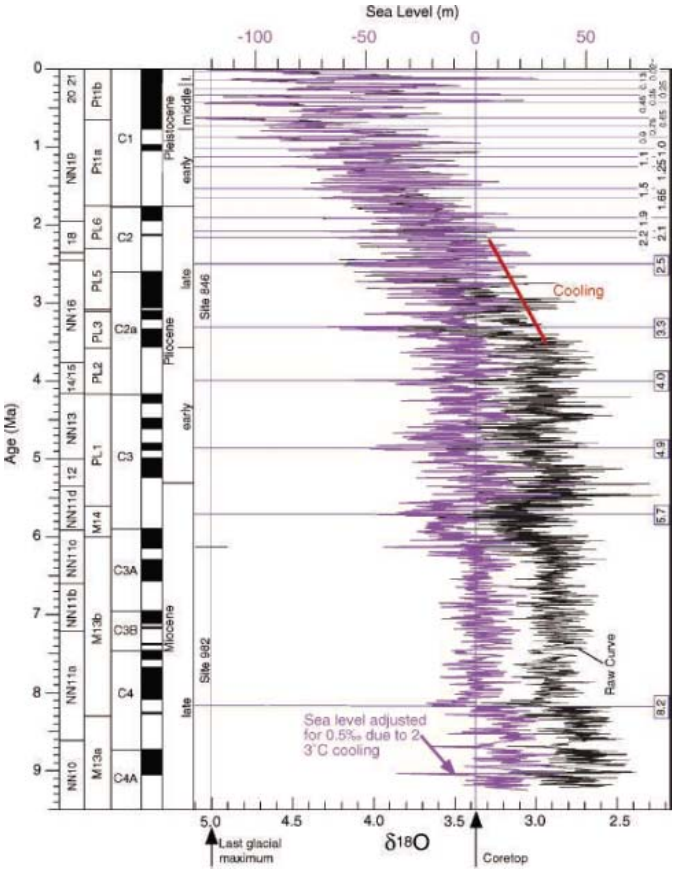

Fig. 4. Oxygen isotopic-based sea-level estimate for the past 9 My. Isotopic values are reported to equilibrium, with coretop and last glacial maximum values indicated with arrows and thin vertical green lines. Thin black line is raw data plotted versus the $\delta^{18}O$ scale (bottom). The purple line is the sea-level estimate (top scale), which is derived by correcting the $\delta^{18}O$ data by 0.5‰ due to a ~2°C cooling between 3.3 and 2.5 Ma (red line), scaling by $\delta^{18}O$ to sea level using a calibration of 0.1‰/10 m, and scaling the result by 0.8 (*45*).

Phanerozoic was ice-free. The Triassic and Cambrian pose two of the best candidates for an ice-free world (*60*), yet Haq (*11*, *16*) noted numerous 10^6-year scale sea-level variations at these times (Fig. 2). If corroborated, these changes suggest the presence of ephemeral ice sheets even in the warmest of the Greenhouse periods.

References and Notes

1. D. T. Donovan, E. J. W. Jones, *J. Geol. Soc. (London)* **136**, 187 (1979).
2. W. C. Pitman III, X. Golovchenko, *Soc. Econ. Paleontol. Mineral. Spec. Publ.* **33**, 41 (1983).
3. R. Revelle, Ed., *Sea-Level Change* (National Academy Press, Washington, DC, 1990).
4. D. Sahagian, M. Jones, *Geol. Soc. Am. Bull.* **105**, 1109 (1993).
5. A. Cazenave, R. S. Nerem, *Rev. Geophys.* **42**, RG3001 (2004).
6. R. G. Fairbanks, *Nature* **339**, 532 (1989).
7. J. Chappell *et al.*, *Earth Planet. Sci. Lett.* **141**, 227 (1996).
8. K. G. Miller, J. D. Wright, R. G. Fairbanks, *J. Geophys. Res.* **96**, 6829 (1991).
9. J. Zachos, M. Pagani, L. Sloan, E. Thomas, K. Billups, *Science* **292**, 686 (2001).
10. P. R. Vail *et al.*, *Am. Assoc. Petrol. Geol. Mem.* **26**, 49 (1977).
11. B. U. Haq, J. Hardenbol, P. R. Vail, *Science* **235**, 1156 (1987).
12. N. Christie-Blick, G. S. Mountain, K. G. Miller, in *Sea-Level Change*, R. Revelle, Ed. (National Academy Press, Washington, DC, 1990), pp. 116–140.
13. K. G. Miller *et al.*, *Rev. Geophys* **36**, 569 (1998).
14. A. B. Watts, M. Steckler, *Ewing Series* **3**, 218 (1979).
15. L. L. Sloss, *Geol. Soc. Am. Bull.* **74**, 93 (1963).
16. B. U. Haq, A. M. Al-Qahtani, *GeoArabia* **10**, 127 (2005).
17. A. B. Ronov, *Am. J. Sci.* **294**, 802 (1994).
18. G. C. Bond, *Tectonophys* **61**, 285 (1979).
19. C. G. A. Harrison, in *Sea-Level Change*, R. Revelle, Ed. (National Academy Press, Washington, DC, 1990), pp. 141–158.
20. J. D. Hays, W. C. Pitman, *Nature* **246**, 18 (1973).
21. W. A. Van Sickel, M. A. Kominz, K. G. Miller, J. V. Browning, *Basin Res.* **16**, 451 (2004).
22. M. A. Kominz, S. F. Pekar, *Geol. Soc. Am. Bull.* **113**, 291 (2001).
23. The long-term record was computed as follows: (i) The median was interpolated at a 0.2 My interval. (ii) A singular spectrum transform following the description of the VG algorithm in (*61*) was applied using a window length of 65 points (13 My window). (iii) The curve was reconstructed from the first empirical orthogonal function resulting from singular spectrum analysis, which accounts for 58% of total variance in the interpolated series.
24. M. A. Kominz, *Am. Assoc. Petrol. Geol. Mem.* **36**, 108 (1984).
25. D. B. Rowley, *Geol. Soc. Am. Bull.* **114**, 927 (2002).
26. The development of an ice sheet the size of modern ice sheets would cause an 80-m fall (*62*), but this would only explain a ~54-m eustatic fall after accounting for isostatic adjustment.
27. R. A. Berner, Z. Kothavala, *Am. J. Sci.* **301**, 182 (2001).
28. G. C. Bond, M. A. Kominz, M. S. Steckler, J. P. Grotzinger, *Soc. Econ. Paleontol. Min. Spec. Publ.* **44**, 39 (1989).
29. M. A. Kominz, *Basin Res.* **7**, 221 (1995).
30. M. Levy, N. Christie-Blick, *Geol. Soc. Am. Bull.* **103**, 1590 (1991).
31. D. L. Anderson, *Nature* **297**, 391 (1982).
32. A. D. Miall, *J. Sed. Petrology* **61**, 497 (1991).
33. K. G. Miller *et al.*, *Geol. Soc. Am. Bull.* **116**, 368 (2004).
34. Water-depth changes were inferred from lithofacies and benthic foraminiferal biofacies studies of (*63*–*66*).
35. D. Sahagian, O. Pinous, A. Olferiev, V. Zakaharov, A. Beisel, *Am. Assoc. Petrol. Geol. Bull.* **80**, 1433 (1996).
36. K. G. Miller, J. D. Wright, J. V. Browning, *Mar. Geol.* **218**, 215 (2005).
37. A. Hallam, *Phanerozoic Sea Level Changes* (Columbia Univ. Press, New York, 1992).
38. J. Laskar *et al.*, *Astron. Astrophys.* **428**, 261 (2004).
39. R. V. Dingle, J. M. McArthur, P. Vroon, *J. Geol. Soc. (London)* **154**, 257 (1997).
40. N. J. Shackleton, J. P. Kennett, *Init. Repts. Deep Sea Drilling Project* **29**, 743 (1975).
41. J. D. Wright, in *Tectonic Boundary Conditions for Climate Reconstructions*, T. J. Crowley, K. Burke, Eds. (Oxford Univ. Press, New York, 1998), pp. 192–211.
42. J. D. Hays, J. Imbrie, N. J. Shackleton, *Science* **194**, 1121 (1976).
43. M. E. Raymo, B. Grant, M. Horowitz, G. H. Rau, *Mar. Micropaleontol.* **27**, 313 (1996).
44. K. G. Miller, R. G. Fairbanks, G. S. Mountain, *Paleoceanography* **2**, 1 (1987).
45. Benthic foraminiferal $\delta^{18}O$ records from 846 [0 to 6.136 Ma, equatorial Pacific (*67*)] and 982 [6.139 to 9 Ma, northern North Atlantic (*68*)] were spliced to create a high-resolution $\delta^{18}O$ composite record with a sample resolution of 3 ky for the late Miocene to the present. Although they are located in different deep-water masses, the records yield similar values across the splice. The pre–late Pliocene $\delta^{18}O$ record has average values (2.9‰) that are 0.5‰ lower than modern values (3.4‰). Ice volumes during the late Miocene to early Pliocene were similar to the modern (*69*), indicating that this long-term $\delta^{18}O$ offset reflects deep-water temperatures that were warmer relative to the modern. Thus, we incrementally added 0.5‰ to the values older than 3.5 Ma as a linear function from 2.5 to 3.5 Ma. We converted the adjusted $\delta^{18}O$ composite record to a sea-level estimate (Fig. 2) by scaling to a calibration of 0.1‰/10 m. Our initial sea-level and $\delta^{18}O$ estimates showed a change from the last glacial maximum to modern changes of 1.5‰; this change has been calibrated in Barbados as 1.2‰. The difference is due to glacial-interglacial deep-sea temperature changes of ~2°C (*6*), as illustrated on Fig. 3. We scaled the sea-level curve by 0.8 to account for this difference (Fig. 4).
46. K. W. Ramsey, *Delaware Geol. Surv. Rept. of Investigations* **54**, 1 (1996).
47. J. P. Donnelly, P. Cleary, P. Newby, R. Ettinger, *Geophys. Res. Lett.* **31**, L05203 (2004).
48. W. R. Peltier, *Rev. Geophys.* **36**, 603 (1997).
49. R. G. Lighty, I. G. Macintyre, R. Stuckenrath, *Coral Reefs* **1**, 125 (1982).
50. Paleowater depth estimates are a critical data set needed for backstripping. Paleowater depth estimates of shallow-shelf (neritic) environments are relatively precise (±15 m), but uncertainties increase into middle-shelf (±30 m), outer-shelf (±50 m), and slope (±200 m) environments. The errors in paleowater depth estimates correspond to eustatic errors correcting for loading of ±10, 20, 35, and 120 m, respectively. Most of our sections are inner to middle neritic, with eustatic errors of ±10 to 20 m.
51. C. M. John, G. D. Karner, M. Mutti, *Geology* **32**, 829 (2004).
52. M. E. Katz, Z. V. Finkel, D. Grzebyk, A. H. Knoll, P. G. Falkowski, *Annu. Rev. Ecol. Evol. Syst.* **35**, 523 (2004).
53. J. C. Zachos, B. P. Flower, H. Paul, *Nature* **388**, 567 (1997).
54. R. L. Larson, *Geology* **19**, 547 (1991).
55. This assumes that a global equivalent of 0.9‰ is stored as ice today (*70*).
56. M. Lyle, M. Leinen, R. Owen, D. K. Rea, *Geophys. Res. Lett.* **14**, 595 (1988).
57. S. C. Cande, D. V. Kent, *J. Geophys. Res.* **97**, 13917 (1992).
58. D. G. Roberts, A. C. Morton, J. Backman, *Init. Rept. Deep Sea Drilling Proj.* **81**, 913 (1984).
59. D. L. Royer, R. A. Berner, I. P. Montañez, N. J. Tabor, D. J. Beerling, *GSA Today* **14**, 4 (2004).
60. L. A. Frakes, E. Francis, J. I. Syktus, *Climate Modes of the Phanerozoic* (Cambridge Univ. Press, Cambridge, 1992).
61. M. R. Allen, L. A. Smith, *J. Climate* **9**, 3373 (1996).
62. R. S. Williams, J. G. Ferrigno, *U.S. Geol. Surv. Prof. Pap.* 1386-A (1999).
63. K. G. Miller, S. W. Snyder, *Proc. ODP, Scientific Results* **150X**, 1 (1997).
64. K. G. Miller *et al.*, *Proc. ODP Init. Rep.* **174AX**, 43 (1998).
65. K. G. Miller *et. al.*, *Proc. ODP Init. Rep.* **174AXS**, 1 (1999).
66. K. G. Miller *et. al.*, *Proc. ODP Init. Rep.* **174AXS**, 1 (2001).
67. N. J. Shackleton, M. A. Hall, D. Pate, *Sci. Res. ODP* **138**, 337 (1995).
68. D. A. Hodell, J. H. Curtis, F. J. Sierro, M. E. Raymo, *Paleoceanography* **16**, 164 (2001).
69. D. R. Marchant, G. H. Denton, C. C. Swisher, *Geografiska Annaler* **75A**, 269 (1993).
70. N. J. Shackleton, J. P. Kennett, *Initial Rep. Deep Sea Drill. Proj.* **29**, 743 (1975).
71. W. A. Berggren, D. V. Kent, C. C. Swisher, M.-P. Aubry, *Soc. Econ. Paleontol. Mineral. Spec. Publ.* **54**, 129 (1995).
72. F. M. Gradstein *et al.*, *J. Geophys. Res.* **99**, 24051 (1994).

73. We thank W. Van Sickel and A. Stanley for contributions to development of the sea-level curves, D. Sahagian for reviews, P. Falkowski and D. Kent for comments, and the members of the Coastal Plain Drilling Project (ODP Legs 150X and 174AX) who are not listed here for contribution of critical data sets that led to the curve. Supported by NSF grants OCE 0084032, EAR97-08664, EAR99-09179, and EAR03-07112 (K.G.M.); EAR98-14025 and EAR03-7101 (M.A.K.); and the New Jersey Geological Survey. Samples were supplied by the Ocean Drilling Program.

Supporting Online Material

www.sciencemag.org/cgi/content/full/310/5752/1293/DC1
Figs. S1 to S5
Table S1

10.1126/science.1116412

Singing Icebergs

Christian Müller,[1,2]* Vera Schlindwein,[2] Alfons Eckstaller,[2] Heinrich Miller[2]

From July until November 2000, several episodes of sustained seismic tremor were recorded at the seismological network at Neumayer Base near the continental margin of Dronning Maud Land, Antarctica (Fig. 1A) (*1*). The signals resemble harmonic volcanic tremor in terms of their duration, magnitude, and spectral features (*2*). The most spectacular tremor event, which spanned 16 hours, was recorded on 22 July 2000 (Fig. 1B). The spectrum of parts of this event consisted of narrow peaks with a fundamental frequency around 0.5 Hz and more than 30 integer harmonic overtones (Fig. 1B, between times E and F). The spectral peaks varied slightly with time (frequency gliding), and amplitude was inversely proportional to frequency (times C to F). The tremor signals change from harmonic to nonharmonic and vice versa (times D and E) and show period-doubling phenomena, as do volcanic tremors (*3*). The spectra of the tremor episodes show the same fundamental frequencies, harmonic overtones, and simultaneous gliding of the spectral peaks at all four stations of the network with an aperture of 280 km, suggesting a source effect (fig. S2).

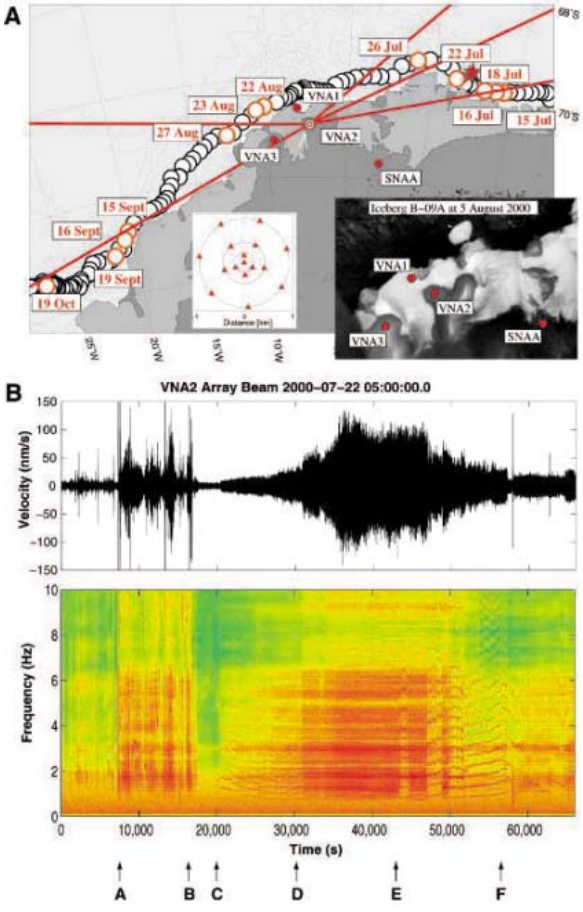

Fig. 1. The stations of the Neumayer Base seismological network, the iceberg B-09A, its track, tremor location, example tremor seismogram, and corresponding spectrogram of the event recorded on 22 July 2000. (**A**) Western Dronning Maud Land, showing daily averaged positions of B-09A from Quik-SCAT satellite radar backscatter images (*5*). Its position at the times of harmonic tremors are shown in red. The left inset shows the geometry of the small aperture array VNA2. The backazimuths of the tremor signals are shown as red lines. The two stars indicate the epicenters of the two events preceding the strong tremor of 22 July 2000. The right inset shows a satellite image (*6*) of B-09A on 5 August 2000. (**B**) VNA2 array beam seismogram (top) and corresponding spectrogram (bottom) of the 22 July 2000 tremor (Audio S1).

To identify the source, we estimated backazimuths from array frequency–wave number (fk) analysis for harmonic tremor episodes for nine events, and we obtained systematically changing directions pointing to a moving source. In addition, the 22 July signals were preceded by two local earthquakes, which we located to offshore the continental margin (Fig. 1A). These two events resembled volcanic "tornillo" events, characterized by a slowly decaying, peaked frequency coda (fig. S3). Comparing the earthquake epicenters with satellite images, we recognized iceberg B-09A as the source of the tremors and earthquakes. The backazimuths of the tremor signals followed the track of the iceberg as it moved westward (Fig. 1A). The tremors were recorded up to 820 km away. We calculated the reduced displacement (*4*) to estimate the strength of the tremor signals and obtained values comparable to strong volcanic tremors observed, for example, at Kilauea and Mount St. Helens.

We propose that, analogous to the sources of volcanic tremors, the iceberg tremor signals represent elastic vibrations of the iceberg produced by the flow of water through its tunnels and crevasses. A scenario for tremor evolution on 22 July 2000 is that the iceberg drifted westward with the Antarctic Coastal Current at ~0.23 m/s. At time A (Fig. 1B), the iceberg collided with the shallow sea floor of a northward-protruding escarpment of the continental margin, causing a seismic shock with an estimated local magnitude $M_l = 3.6$, equivalent to a seismic energy release of $E = 2.7 \times 10^9$ J. Assuming an elliptical shape with half-axes of 15 and 25 km, a height of 400 m, and density of ice equivalent to 915 kg/m^3, iceberg B-09A has a kinetic energy of 1.1×10^{13} J, which is converted to only a small amount of seismic energy during the initial collision. The collision continued as the iceberg slid along the continental shelf, pushed by the coastal current. This sliding and eventual catastrophic collapses explain the diffuse spectral features during times A to B. During the quiescence period B to C, water flow may have pushed the iceberg northward around the escarpment. The following episode of harmonic and chaotic tremor C to F may reflect fluid flow through the iceberg from ongoing oscillations after the collision, the changed orientation of the iceberg relative to the coastal current, or differential flow as the iceberg accelerated.

References and Notes

1. The four stations of the network consist of one short-period seismometer (VNA1) close to Neumayer Base on the floating Ekström Ice Shelf, two remote broadband sensors, VNA2 and VNA3, deployed on grounded ice, and SNAA at the South African base Sanae IV on solid rock (Fig. 1A). VNA2 is the central sensor of a small-aperture detection array, consisting of 16 sensors on three concentric rings with diameters of 2 km (Fig. 1A, left inset) (*7*).
2. K. I. Konstantinou, V. Schlindwein, *J. Volcanol. Geotherm. Res.* **119**, 161 (2002).
3. B. Julian, *J. Geophys. Res.* **99**, 11859 (1994).
4. K. Aki, R. Koyanagi, *J. Geophys. Res.* **86**, 7095 (1981).
5. D. G. Long, J. Ballantyne, C. Bertoia, *Eos* **83**, 469 (2002).
6. T. Scambos, B. Raup, J. Bohlander, Advanced Very High Resolution Radiometer (AVHRR) thermal image, available at http://nsidc.org/data/iceshelves_images/fimbul.html (2004).
7. T. Büsselberg, C. Müller, A. Eckstaller, *Terra Antarctica* **8**, 41 (2001).
8. We thank the Alfred Wegener Institute for Polar and Marine Research for support.

Supporting Online Material
www.sciencemag.org/cgi/content/full/310/5752/1299/DC1
Figs. S1 to S3
Audio S1

8 July 2005; accepted 14 September 2005
10.1126/science.1117145

[1]FIELAX Gesellschaft für wissenschaftliche, Datenverarbeitung mbH, Schifferstraße 10-14, 27568 Bremerhaven, Germany. [2]Alfred Wegener Institute for Polar and Marine Research, Columbusstraße, 27568 Bremerhaven, Germany.

*To whom correspondence should be addressed. E-mail: mueller@fielax.de

Cassini Discovers a Kinematic Spiral Ring Around Saturn

S. Charnoz,[1]* C. C. Porco,[2] E. Déau,[1] A. Brahic,[1]
J. N. Spitale,[2] G. Bacques,[1] K. Baillie[1]

Since the time of the Voyager flybys of Saturn in 1980–1981, Saturn's eccentric F ring has been known to be accompanied on either side by faint strands of material. New Cassini observations show that these strands, initially interpreted as concentric ring segments, are in fact connected and form a single one-arm trailing spiral winding at least three times around Saturn. The spiral rotates around Saturn with the orbital motion of its constituent particles. This structure is likely the result of differential orbital motion stretching an initial cloud of particles scattered from the dense core of the F ring. Different scenarios of formation, implying ringlet-satellite interactions, are explored. A recently discovered moon candidate, S/2004 S6, is on an orbit that crosses the F-ring core at the intersection of the spiral with the ring, which suggests a dynamical connection between S/2004 S6 and the spiral.

Saturn's F ring has been one of the most intriguing structures around Saturn since it was first imaged by Voyager in 1980 (*1*). Its time-changing appearance and diversity of transient embedded structures (e.g. "clumps," "braids," "kinks," etc.), with short lifetimes on the order of several weeks, have challenged researchers for decades. High-resolution images (3 km per pixel) taken by Voyager 2 revealed the ring to be composed of a primary bright narrow ring, called the core, surrounded by dimmer strands on either side (Fig. 1). The number of strands and their shapes seemed to vary with time and longitude of observation. However, the Voyager images revealed only local portions of the F ring; it was not imaged over 360° with high resolution. Different models were proposed that suggested that the strands are eccentric and concentric ring segments extending ~45° in longitude (*2*), or are alternatively a collection of clumps of material orbiting near the F-ring core (*3*).

High-resolution "movie" sequences obtained by the Cassini Narrow Angle Camera (NAC) in November 2004, April 2005, and May 2005, covering 360° of orbital motion of the F-ring material, reveal that the strands are each one coil of a one-armed spiral that crosses the core of the main ring. In these sequences, the camera's field of view was positioned at the ansa of the F ring and the camera was shuttered with a frequency sufficiently high (table S1) to capture all the material passing through the field of view. The ring material was observed as if by scrolling with a fixed observation window in a Saturn-centered inertial frame for a full orbital period of 15 hours. We observed the ring this way three times, centered at 160°, 49°, and 135° longitude in November, April, and May, respectively. Note that in such a sequence, the eccentric nature of the F ring is not evident: Its precession rate is only 2.7° per day (*4*), and throughout these fixed-longitude sequences its orbital distance from Saturn changes little.

Data processing. These observations produced high-resolution (<10 km per pixel), nearly 360° "movie maps" of Saturn's F ring. A movie map is a mosaic of images showing one portion of the ring in Saturn's inertial frame at different consecutive epochs (whereas a "snapshot map" would be a mosaic showing the full ring at 360° but at a single epoch). The images' absolute positions were determined by measuring the position of either the A ring edge or stars in the images as fiducial features. The navigation was deemed accurate because of the proper coincidence (within 2 pixels) of the predicted and observed positions of satellites such as Prometheus and Pandora (*5*). All images were then reprojected and reconstructed so that the eccentric F-ring core became a line of constant radius centered on the core. This transformation preserves the scale of structures. These reconstructed maps were finally assembled into a continuous mosaic, with image time increasing to the left (Fig. 2). Assuming a constant F-ring mean motion of 582.05° per day (*6*), the time elapsed from the beginning of the observation was converted into a longitude system corotating with the motion of the F-ring particles, such that orbital longitude increases to the right. The origin of longitude is the intersection of the ascending node of Saturn's ring plane on Earth's equator at the J2000 epoch. For direct comparison, all maps have been precessed to the epoch of 1 July 2004 18:00:00 UTC. Each map is duplicated and repeated across 2 × 360° of longitude to aid examination of the azimuthal structure of the ring (Fig. 2) (fig. S1).

A spiral structure revealed. The F-ring core appears as a bright horizontal ribbon at the center of the three maps, with an irregular shape usually believed to be the consequence of the gravitational influence of nearby satellites (*5*, *7*–*9*). The strands appear as dim inclined features above and below the F-ring core. Three characteristics are striking: (i) The strands appear differently in the three maps, which suggests either a rapid evolution or a changing shape with the longitude of the observation; (ii) they do not appear as concentric ringlets (in which case they would be horizontal and parallel to the F ring) but rather connect to each other at 0° and 360°, suggesting a spiral structure (see table S1 for starting and ending longitude of each sequence of observation); and (iii) they seem to cross the core between 0° and 100° longitude.

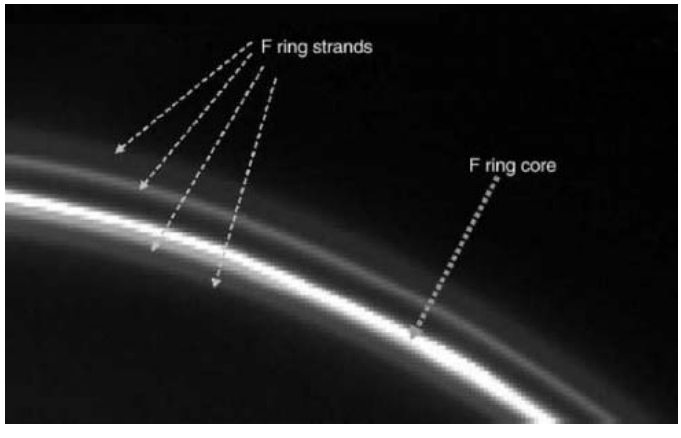

Fig. 1. The F ring as seen by Cassini on 15 November 2004, with ~35° of longitudinal extension and radial resolution of ~27 km per pixel. This image is located at 100° corotating longitude in the November map (Fig. 2).

[1]Astrophysique Interactions Multi-échelles (CEA/Université Paris 7/CNRS), DSM/DAPNIA/SAp, CEA Saclay, 91191 Gif-sur-Yvette, France. [2]Cassini Imaging Central Laboratory for Operations (CICLOPS), Space Science Institute, 4750 Walnut Street, Suite 205, Boulder, CO 80301, USA.

*To whom correspondence should be addressed. E-mail: charnoz@cea.fr

In the November maps, two strands separated by ~200 km are visible above (outside) the core and two other strands below (inside) the core, with radial separation of ~100 km. The upper strands extend longitudinally over ~750° with a full radial extension of ~500 km. Lower strands have a comparable azimuthal extension and a radial extension of 300 km. In the April and May mosaics, the strands above the core are more tightly wound with similar radial extensions (300 km), azimuthal extensions (~800°), and radial separations (~80 km), whereas strands below the core look more widely spread (500 km). All values may be inaccurate by 10% to 20% because of the diffuse nature the structure. The strands seem to cross the core around longitude 0° in November and 100° in April and May. In the latter maps, with better resolution, the core is severely distorted at this location, which suggests a real physical connection with the strands and not a simple visual superposition of two separated objects. Note also that the crossing region has an extension of 50° to 100° longitude and that several arms seem to originate from this point. This may suggest the presence of some periodic production mechanism at work. Wavy patterns are also visible; they could be real structures, or they may be artifacts attributable to an inaccuracy in the spacecraft position or in the orbital plane of the strands, inducing absolute radial displacement about ±50 km. However, this is a large-scale effect that does not affect relative distances and cannot explain why the strands appear physically connected. In addition, the continuity of brightness of the strands over their full extension implies that they are indeed a single object.

A rotating spiral. Examination of the movie maps also reveals the kinematics of the spiral structure: The overall pattern is not fixed in the inertial frame of Saturn, nor is it rotating with the precession rate of the F ring. The fact that the radial position of the strands changes with time implies that the strands are moving in Saturn's inertial frame. The rotation period of the spiral should be close to the F ring's orbital period in order to explain the reconnection of the arm with itself exactly after one F-ring orbital period (at 210° longitude in the November map). Strong similarities between the relative position of the spiral arm with respect to the F-ring core in April and in May strengthen this conclusion. Note that a simple fixed eccentric ring would not appear like this, because a piece of elliptical ring observed at the same inertial longitude always appears with the same radius. A precessing elliptical ring could explain the observations. However, at the distance of the F ring, the precession rate (2.7° per day) can only account for a radial shift of 3 to 4 km, much less than the observed 300-km radial extent of strands.

In an attempt to understand the origin of this structure, we have examined the idea that the spiral form derives from simple orbital motion (Keplerian) shear such that particles closer to the planet have larger orbital speed. Particles orbiting at different distances from Saturn have different orbital speeds according to the law $\omega(r) = (GM_p/r^3)^{1/2}$ (without considering planetary oblateness), where ω is angular speed, G is the gravitational constant, M_p is the mass of Saturn, and r is the distance to Saturn. So if, by some mechanism, a collection of particles has been scattered from a narrow ring into a cloud with Δr radial extent, it will be sheared by Keplerian motion over an angular distance α in a time $T = 2\alpha r/3\omega\Delta r$ into the shape of a trailing spiral. From the April and May observations, we measure $\Delta r \sim$ 300 km and $\alpha \sim 800°$, giving $T \sim 1.2$ years. The observed spiral might have been first generated around the beginning of 2004 (also consistent with November observations). If Keplerian shear is really the key mechanism that drives the evolution of these structures, this time scale is a strong constraint, because shear alone causes the number of arms within a fixed radial width to increase at a rate of one new arm every ~190 days. This is roughly what is observed above the ring core when comparing April and November maps (separated by 149 days) and November and May maps (separated by 170 days). However, the lifetime of a spiral structure is limited; as the material is spread over more and more arms, brightness should decrease linearly with

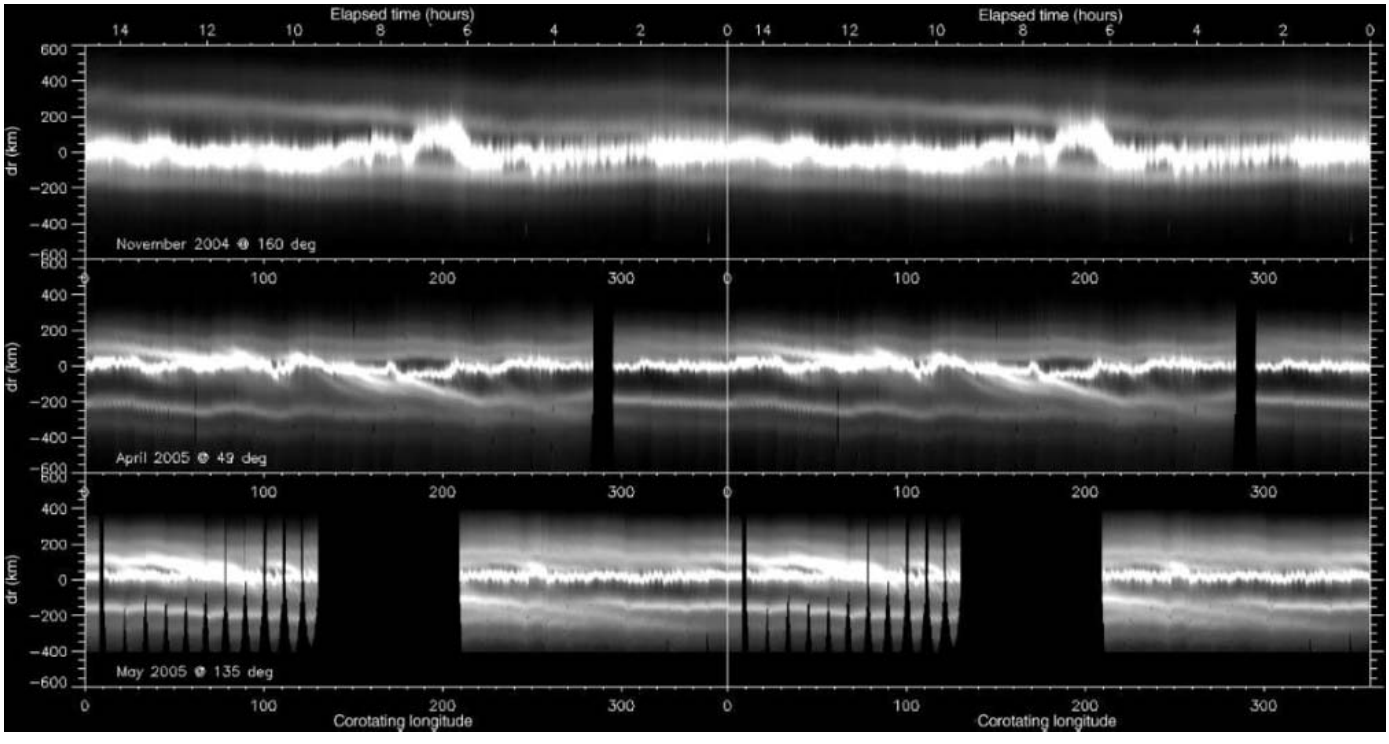

Fig. 2. Maps of the F ring in November (upper) with radial resolution of ~27 km per pixel, April (middle) with radial resolution of ~6.5 km per pixel, and May (bottom) with radial resolution of ~5 km per pixel. All maps are precessed to the epoch 1 July 2004 18:00:00, using a mean motion of 582.05° per day. The *x* axis is the corotating longitude; the *y* axis is the distance from the F-ring core in kilometers. The F-ring core is the bright horizontal line in the center of all maps. The strands appear as dimmer inclined lines below and above the core. Faint structures may be more visible in fig. S1.

time, and the structure might be expected to fade away.

What mechanism might scatter particles out of the F-ring core? If the spiral is made of micrometer-sized particles, what would regenerate and maintain it against radiative effects, such as Poynting-Robertson drag or light pressure (*10*), that sweep small particles into the planet? The F-ring strands have been observed since the Voyager epoch, so a regeneration mechanism is required. Impacts with meteoroids or micrometer-sized particles released by Enceladus (*10*–*13*) are not implausible, but these are intrinsically random events that likely cannot explain the constant regeneration of a coherent structure like the observed spiral. Because such a temporally limited data set does not allow us to dismiss random impacts, we instead investigated the scenario of a close interaction between the F-ring core and a satellite on an eccentric orbit. We considered this scenario for two reasons: (i) Satellite-ringlet interactions are known to play a major role in the dynamical evolution of ringlets (*7*, *8*, *14*), and (ii) a satellite on an eccentric orbit can interact periodically with a nearby ringlet, constantly generating new structures longitudinally spaced by $3\pi\Delta a/a$ [where a and $a + \Delta a$ are the semimajor axes of the F-ring core and of the satellite, respectively (*15*)]. In addition to Prometheus and Pandora, the F ring has long been suspected to shelter a population of small unseen moons (*16*, *17*).

A simple numerical model. Simulations of a satellite interacting with the F-ring strands have been performed for Prometheus in the past (*8*) and more recently (*9*) over a few orbital periods. Our simulations extended over 2000 orbital periods to follow the Keplerian shear of particles in a narrow ring intersected every orbital period by a massive satellite. Including the effect of Saturn's oblateness, we computed the trajectories of 10^4 test particles in orbit around Saturn, gathered into a longitudinally limited ringlet and perturbed by a satellite. At the beginning, the particles were given the same orbital parameters as the F-ring core (*4*), with semimajor axis at 140,223 km. To test the code, we reproduced the formation of drapes in the F ring as seen on 1 July 2004 in earlier Cassini images (fig. S2) (*9*). To follow the interaction in detail, we gathered all particles at the beginning of the simulation in a small segment extending 0.5° in longitude and on a trajectory intersecting the satellite's orbit. Because we wanted to simulate a strong interaction to test the basic mechanisms of the ring-satellite scenario, the satellite's semimajor axis was set at 139,600 km (120 km closer to the F ring than today's Prometheus), its eccentricity at 0.0023, and its orbit anti-aligned with the F ring's so that it crosses the ring at the ring's pericenter (the location where the ring is closest to Saturn). In such a simulation, the mass of the required satellite is critical: After a single encounter, a satellite scatters neighboring particles over a distance of a few Hill's radii. The Hill's radius is the typical distance of gravitational influence of a satellite, given by $a(M_s/3M_p)^{1/3}$, where a is the satellite's semimajor axis, M_p is Saturn's mass, and M_s is the satellite's mass (*18*). Therefore, in these simulations the satellite's mass was set to 2×10^{17} kg (comparable to that of Prometheus) in order to scatter particles over the radial extent of the spiral (~300 km). Whereas the simulated satellite's characteristics were similar to those of Prometheus, the latter is not currently on an intersecting orbit with the F-ring core. However, in 2009 its orbit will be anti-aligned with the orbit of the F ring because of the precession induced by Saturn's oblateness (*2*, *8*).

Immediately after the simulated satellite encounter (Fig. 3A) (fig. S3), particles are scattered out of the ringlet over ~300 km, in agreement with the prediction. They are separated into three groups because in these simulations the satellite crosses the ring twice: before and after its apocenter (the place where the body reaches its maximum distance from Saturn). Those groups are subsequently stretched and sheared by Keplerian motion. After 300 orbits (~6 months), they have differentially spread over 360°, producing a trailing spiral structure. After 700 orbits of evolution (~1.2 years), the spiral structure is clear and extends below and above the original location of the ring (Fig. 3B). It winds around the planet about three times. The arms are discontinuous because of the original division into three groups.

To illustrate the motion of the spiral, Fig. 3C shows the configuration of particles just half a period after Fig. 3A. Although the overall shape is the same, the radial structure of the spiral has changed. Inspection of the particles' orbital elements reveals that the shape and orientation of their orbits remain very close to those of the original ring. The greatest change occurring from the interaction with the satellite is the alteration of the particles' semimajor axes by about ±200 km (eccentricities vary by about ±0.001 only). As a consequence, on short time scales the spiral is carried along by the particles' orbital motions. Moreover, because the particles retain values of eccentricity and apse locations close to that of the F ring, the arms will be more separated near the apocenter of the F ring than near the pericenter. This effect is clearly visible in Fig. 3, B and C. On longer time scales (~1800 orbits, 3 years) the spiral structure will disappear because of multiple reinteractions with the satellite that randomly scatter the already scattered particles. Note also that the strands remain parallel with the F-ring core as a result of initial conditions (this was a major issue in previous work on the F-ring strands) (*2*). Numerous other configurations were investigated by varying the mass and location of the satellite or assuming that particles are scattered from the

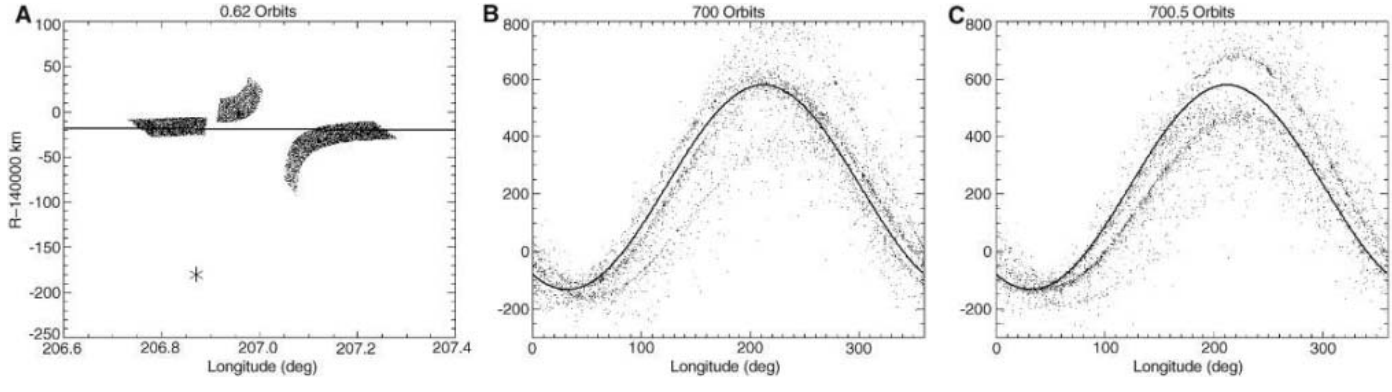

Fig. 3. Simulation of a piece of ringlet, with 0.5° starting extension, interacting with a satellite on a crossing orbit at three different epochs. The *x* and *y* axes are the longitude and distance to Saturn, respectively. Particles are represented by dots; the perturbing satellite is denoted by an asterisk. The center of the F-ring core is represented by the solid back curve. (**A**) Just after the close interaction with the satellite. (**B**) 700 orbits after the interaction; the scattered particles have spread at 360° around the planet and the material is now organized as a spiral arms winding three or four times. (**C**) Same as previous, but half an orbit later to reveal the rotation of the spiral. The satellite's apocenter is located at 65° longitude. See fig. S3 for a color version of the plot.

strands themselves. All such simulations show that a smaller satellite (with radius of a few kilometers) is not massive enough to gravitationally scatter material over 300 km, and that the source of the particles must be the F-ring core itself in order to reproduce both exterior and interior spirals, as seen in the images.

Reproducing observations. We simulated the conditions of Cassini observations to examine and compare our model results with the movie maps. Three observing windows were defined in Saturn's inertial frame (each extending 30° longitude) to reproduce the November, April, and May conditions of observation. We found qualitative agreement for the November and April maps (Fig. 4, A and B), whereas we were less successful for the May map (Fig. 4C), in which the spiral seemed more tightly wound than in the simulation, perhaps because of the great simplicity of this model. An interesting aspect of these synthetic observations is that they show how different the spiral may appear when observed at different longitudes: As a result of its complex longitudinal and radial structure (Fig. 3, B and C), the spiral may appear with varying numbers of branches with different radial locations, depending on the longitude of observation (Fig. 4).

These results clearly show that a massive satellite, after a single interaction, can scatter particles efficiently from a narrow ring, after which orbital shear can then draw them into a rotating spiral. However, our simulations followed only a 0.5°-wide portion of the F ring encountering the satellite. The effect of the satellite over the full ring is not clear because multiple mechanisms are at work with opposite effects. On one hand, the lifetime of a single spiral arm is limited by repeated encounters with the satellite and by the natural fading away of the structure as a result of Keplerian shear. On the other hand, multiple encounters of the same satellite with the F-ring core would trigger the formation of additional spirals—one new spiral for every orbital period of the satellite—longitudinally spaced by $3\pi\Delta a/a$ (in radians). Whether or not successive spirals merge together (to form a featureless cloud) or enhance each other would depend on the orbital separation of the satellite and ring: If successive spirals have very small longitudinal separations, as they would in the case of a perturbing satellite with a semimajor axis very close to the F ring's, then they could combine into a single bright arm. Complicating things further, new spirals may differ in brightness because the F-ring core exhibits strong density variations, and at some longitudes, passage through the ring may not scatter much material. The combination of all these effects is obviously difficult to anticipate, and a full simulation is not possible because of computer limitations.

The role of a new satellite. The recent Cassini discovery of objects in the F-ring region (*5*, *19*) has proved promising. One of them, S/2004 S6, is relatively long-lived (more than 1 year) and may be a moon or an extended clump. It is on an eccentric, inclined orbit that crosses the F ring at 16°, 86°, and 96° in the November, April, and May maps, respectively, matching well the location where the spiral intersects the F-ring core. Its radial excursions beyond the ring, both interior and exterior, are several hundred kilometers, comparable to the radial extent of the spiral. These coincidences strongly suggest that S6 may be involved in the formation of the spiral. S/2004 S6 is much smaller than Prometheus and so cannot gravitationally scatter particles over 300 km. However, it may be possible that S6 drags particles out of the ring via nongravitational effects such as physical rebound at the satellite's surface. The magnitude of a perturbation on a particle's orbit may be roughly measured by the variation of its orbital speed, Δv. To scatter particles radially from the F-ring core over 300 km requires a Δv in the range of 25 m/s (from simple comparison of orbital velocities). Gravitational scattering by tiny S6 would give a Δv of only ~2 m/s, well below the required value (assuming a mass density of 0.8 g/cm^3 and a diameter of 5 km). However, on its present orbit, S6 encounters the F ring with a relative speed of ~30 m/s. Particles suffering inelastic collisions on its surface may undergo a Δv comparable to, although lower than, their impact velocity, which is roughly what is needed to scatter them over 300 km. Note also that S6 likely has a very low density, comparable to that of other ring-region moons (*5*), and may not be massive enough to accrete particles colliding with it because of its very low escape velocity (~2 m/s). In addition, S6 is very close to the F-ring region [$3\pi\Delta a/a \sim 0.34°$ (*19*)], and it may be possible that its repeated passages through the ring's core enhance the spiral (see above). This very rough calculation needs further investigation with a detailed model.

Whatever the mechanism that removes particles from the F-ring core, the Keplerian shear of scattered particles supplies a natural explanation for the variations in the appearance and in the number of arms observed as a function of longitude and time. Other effects, such as radiative forces or plasma drag, may in principle affect the particles' orbits. Whereas the core of the F ring seems to be made of big and small particles (*4*, *11*), the surrounding region seems populated by micrometer-sized particles (*12*, *20*) that will be sensitive to radiation effects (*10*). For the moment, no dynamical model of the F ring including radiative effects has been published. However, radiative effects act on time scales that are long relative to the observed evolution time of the spiral and are not likely to be important.

This interpretation of the F-ring strands should be compared to two previous investigations of the F ring based on Voyager images (*2*, *3*) with partial azimuthal coverage. In the first study, strands are envisioned as four nonintersecting and concentric arc-like rings extending ~45° in longitude with orbits aligned with the F-ring core. They were so described because of the changing number of visible strands in images. In the spiral model, the changing number of visible strands

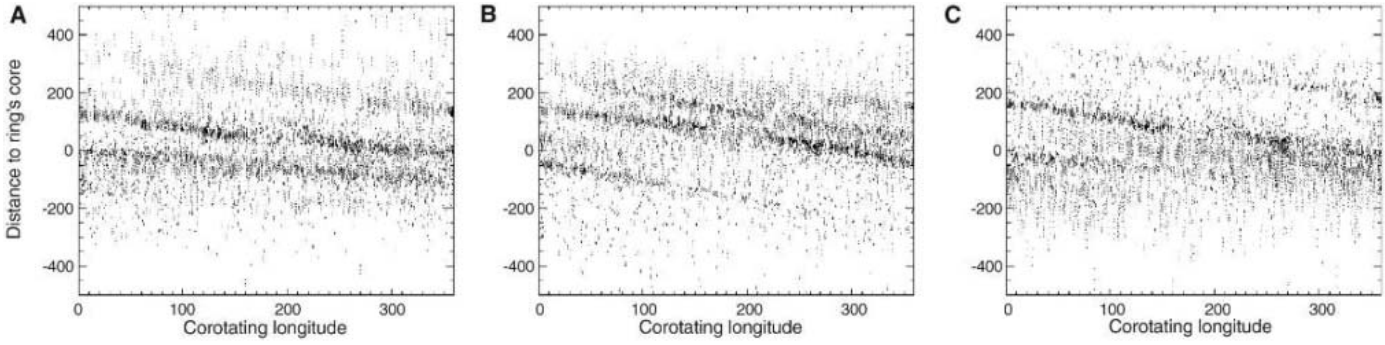

Fig. 4. The simulated spiral as if seen by Cassini. The spiral (Fig. 3) is observed passing through a constant observation window in Saturn's inertial frame during one orbital period. The results from three different observation windows are shown (at longitudes 300°, 189°, and 275° in Fig. 3, from left to right) to reproduce the conditions of observation in (**A**) November 2004, (**B**) April 2005, and (**C**) May 2005. The *x* axis is longitude; the *y* axis is the distance to the ring's core (in kilometers).

is a natural consequence of the longitude of observation, and the spreading by Keplerian shear explains also why they all appear concentric. In the second study, several clumps were tracked around Saturn, indicating a full 90-km range in semimajor axes (with a standard deviation of 45 km). The observations reported here show that the strands, organized as a rotating spiral, have a wider range of semimajor axes (300 km); however, it may be possible that the tracked clumps were only the brightest ones, naturally located closer to the core in the spiral model.

By the end of 2009, Prometheus and the F ring will be in a close-encounter configuration because of the precession of their orbits resulting from Saturn's oblateness (*2*, *8*). It is very probable that additional spirals will then be created by Prometheus and could be observed in an extended Cassini mission.

References and Notes

1. B. A. Smith *et al.*, *Science* **212**, 163 (1981).
2. C. D. Murray, M. K. Gordon, S. M. G. Winter, *Icarus* **129**, 304 (1997).
3. M. R. Showalter, *Icarus* **171**, 356 (2004).
4. A. S. Bosh, C. B. Olkin, R. G. French, P. D. Nicholson, *Icarus* **157**, 57 (2002).
5. C. C. Porco *et al.*, *Science* **307**, 1226 (2005).
6. P. D. Nicholson *et al.*, *Science* **272**, 509 (1996).
7. M. R. Showalter, J. A. Burns, *Icarus* **52**, 526 (1982).
8. C. D. Murray, S. M. G. Winter, *Nature* **380**, 139 (1996).
9. C. D. Murray *et al.*, *Nature* **437**, 1326 (2005).
10. J. A. Burns, D. P. Hamilton, M. R. Showalter, in *Interplanetary Dust*, E. Grün, B. A. S. Gustafson, S. F. Dermott, H. Fechtig, Eds. (Springer-Verlag, Berlin, 2001), pp. 641–725.
11. M. R. Showalter, *Science* **282**, 1099 (1998).
12. M. R. Showalter, J. B. Pollack, M. E. Ockert, L. Doyle, J. B. Dalton, *Icarus* **100**, 394 (1992).
13. D. P. Hamilton, J. A. Burns, *Nature* **365**, 498 (1993).
14. M. C. Lewis, G. R. Stewart, *Astron. J.* **120**, 3295 (2000).
15. S. F. Dermott, *Nature* **290**, 454 (1981).
16. R. A. Kolvoord, J. A. Burns, M. R. Showalter, *Nature* **345**, 695 (1990).
17. J. Hänninen, *Icarus* **103**, 104 (1993).
18. C. C. Porco *et al.*, *IAU Circ. 8432*, 1 (2004).
19. J. N. Spitale, unpublished data.
20. F. Poulet, B. Sicardy, P. D. Nicholson, E. Karkoschka, J. Caldwell, *Icarus* **144**, 135 (2000).

21. We thank H. Throop, J. Cuzzi, J. Decriem, C. Ferrari, M. Hedman, C. Murray, P. Nicholson, M. Tiscareno, and three anonymous referees for useful comments and discussions. We also acknowledge the work of the CICLOPS operations group in making the observations described here possible.

Supporting Online Material

www.sciencemag.org/cgi/content/full/310/5752/1300/DC1
Table S1
Figs. S1 to S3

26 August 2005; accepted 19 October 2005
10.1126/science.1119387

REPORTS

Encoding Electronic Properties by Synthesis of Axial Modulation-Doped Silicon Nanowires

Chen Yang,[1]* Zhaohui Zhong,[1]* Charles M. Lieber[1,2]†

We describe the successful synthesis of modulation-doped silicon nanowires by achieving pure axial elongation without radial overcoating during the growth process. Scanning gate microscopy shows that the key properties of the modulated structures—including the number, size, and period of the differentially doped regions—are defined in a controllable manner during synthesis, and moreover, that feature sizes to less than 50 nanometers are possible. Electronic devices fabricated with designed modulation-doped nanowire structures demonstrate their potential for lithography-independent address decoders and tunable, coupled quantum dots in which changes in electronic properties are encoded by synthesis rather than created by conventional lithography-based techniques.

A wide range of nanoscale electronic and photonic devices have been made with carbon nanotube and nanowire functional elements (*1*–*4*). Although the nanomaterials are important for achieving observed functional properties in these nanodevices, many of the most critical features have been defined with the use of similar lithographic approaches that drive and ultimately limit the planar semiconductor industry. The current dependence on lithography thus could reduce advantages of these nanoscale elements in proposed applications and suggests that nonlithographic approaches for encoding key features or information are needed.

Modulation of the composition has been demonstrated recently in relatively simple nanorod and nanowire structures to yield functional structures (*5*–*8*). For example, gold grown on the tips of cadmium selenide nanorods provides specific points for self-assembly and electrical contact (*5*). Modulation of the dopant or composition of nanowires during synthesis also has been used to define functional *p*-type/*n*-type diodes (*6*) and single quantum dots (*8*). These studies show the potential for synthesis to define function without lithography, yet the level of information and function encoded in the materials has been very limited. We now describe selective dopant modulation during the growth of silicon nanowires with essentially complete control over the size, spacing, and number of modulated regions.

Applications of nanowires in conventional electronics could be facilitated by using synthesis to define the aspects of transistors that are currently enabled by lithographic and ion-beam processing, such as feature uniformity and controlled doping. For example, the high sensitivity of carbon nanotubes to adsorbed gases and solid coatings, along with lithographic patterning, has been exploited in transistor structures (*9*, *10*). Greater ease of circuit assembly could be afforded by the ability to create semiconductor nanowires that are uniform in shape and that can be doped selectively along their length, in that the formation of regions with different electronic properties would be intrinsic to nanowire synthesis and would not require intermediate lithographic patterning and/or electrical contacts. Many of the wiring steps normally created by lithography can be encoded by varying the doping sequence of the nanowires so that the only postfabrication lithographic steps would be those involved in making external input and output contacts to individual nanowires.

Synthesis of dopant-modulated nanowire structures in which function can be predicted on the basis of the encoded axial sequence of doping is challenging: It requires effectively pure axial or one-dimensional (1D) growth without simultaneous radial or 2D growth (Fig. 1A), because even a few atomic layers of dopant deposited on the surface of a nanowire can dominate its overall electronic properties (*11*). In the metal nanocluster-catalyzed vapor-liquid-solid growth process (*3*–*5*), which has been widely used to prepare nanowires, the dopant must be added exclusively at the nanocluster catalyst without reaction and deposition at the much larger area of the exposed solid

[1]Department of Chemistry and Chemical Biology, [2]Division of Engineering and Applied Sciences, Harvard University, Cambridge, MA 02138, USA.

*These authors contributed equally to this work.
†To whom correspondence should be addressed. E-mail: cml@cmliris.harvard.edu

surface of the growing nanowire in order to encode electronic function. Simultaneous radial growth with axial elongation, which would obscure modulation of electronic properties along the nanowire axis, is likely more common than recognized (*11*) and is apparent in extreme cases as visible tapering seen in nanowire structures.

In nanocluster-catalyzed growth of Si nanowires with silane as a reactant, homogeneous gas-phase decomposition produces reactive species that can lead to uncontrolled and deleterious radial overcoating of the nanowire during elongation (*11*, *12*). To control radial deposition down to the atomic level, we used a local substrate heater (versus a tube furnace reactor) and carried out growth in a H_2 atmosphere (*13*), which suppresses the decomposition of silane and inhibits deposition on the nanowire surface (*14*, *15*). Transmission electron microscopy (TEM) studies of modulation-doped n^+-n-n^+ silicon nanowires (Fig. 1B), where n^+ and n represent the heavily and lightly n-type regions, respectively, show that the nanowires prepared in this way have uniform diameters for lengths of >10 μm. High-resolution TEM analysis of the opposite ends of a representative n^+-n-n^+ silicon nanowire (Fig. 1B) further demonstrate that the diameters are 17.4 and 17.1 nm. This 0.3-nm variation is on the order of a single atomic layer and shows that radial overcoating has been effectively eliminated during growth of these modulation-doped structures.

To determine whether the n^+-n-n^+ nanowires exhibit expected variations in the electronic properties associated with modulated dopant concentration, we used scanning gate microscopy (SGM) (*6*, *13*, *16*). In these measurements, a conducting atomic force microscopy probe with an applied voltage (V_{tip}) functions as a spatially localized gate, which enables the conductance of the nanowire with fabricated source and drain contacts to be varied and mapped (*13*). Data acquired from a n^+-n-n^+ nanowire device with a 555-nm-long n-type segment (length based on growth time) exhibits localized variations in conductance between the source and drain (Fig. 1, C and D). When $V_{tip} = -9$ V the conductance of this region is reduced, and when $V_{tip} = +9$ V the conductance is enhanced. The changes in conductance are consistent with the expected depletion or accumulation of carriers in the lightly doped n-type region, and moreover, the ~525-nm length of this region agrees well with that expected of 555 nm. No SGM response was observed from other regions of the nanowire, and is consistent with heavily doped n^+ regions connected to the source and drain in the n^+-n-n^+ device. These data thus confirm that our synthetic approach yields spatially and electrically well defined n^+-n-n^+ nanowire structures.

We explored limits to these modulated nanowires by preparing and characterizing structures of the general form n^+-$(n$-$n^+)_N$, where N is the number of repeat units. Representative SGM data (Fig. 2, A to C) show that N and the repeat spacing can be varied over a wide range. Specifically, the SGM results show n^+-$(n$-$n^+)_N$ modulated structures with $N = 3$, 6, and 8 and repeat spacings of 3.20, 1.55, and 0.75 μm, respectively. The observed number of repeats and spacing between repeats agrees well with that designed through synthesis (3.12, 1.56, and 0.78 μm, respectively).

To further explore the synthetic control of these modulated structures, we also prepared structures with variable repeat lengths, where the separation between fixed-length n-type segments is varied by the n^+ growth time. The SGM data show that the designed $N = 5$ structure has separations of 0.80, 1.15, 1.85, and 3.43 μm, which are consistent with the variation in growth times (Fig. 2D). These data and measurements from a number of additional samples (>15) have been summarized as a plot of n-n^+ length versus growth time (Fig. 2E) and demonstrate the linear dependence that is essential for predictable dopant modulation during synthesis.

The potential for scaling n-n^+ features to smaller sizes was also probed by reducing the nanowire growth rate. We found that the growth rate decreased linearly to ~2.9 nm/s when the pressure was reduced from 320 to 80 torr (Fig. 2F). Notably, reproducible $N = 3$ structures prepared at 160 and 80 torr exhibited average repeat spacings of 180 nm

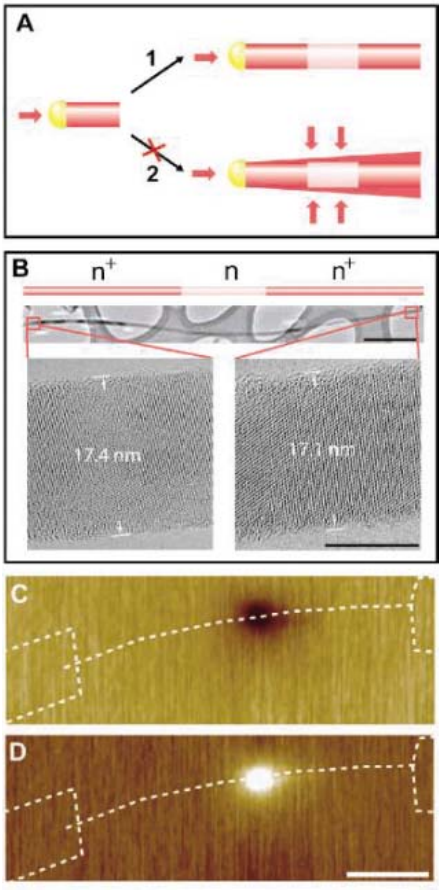

Fig. 1. Synthesis and characterization of modulation-doped nanowires. (**A**) Illustrations of (1) pure axial and (2) simultaneous axial and radial growth occurring during gold nanocluster (yellow) catalyzed nanowire synthesis. Simultaneous radial growth (2) leads to undesirable deposition of high dopant concentration material over the entire nanowire. (**B**) (Top) Schematic and low-resolution TEM image of a representative n^+-n-n^+ modulation-doped silicon nanowire. Scale bar, 500 nm. (Bottom) High-resolution TEM images recorded at the two ends indicated by red boxes. Scale bar, 10 nm. (**C** and **D**) SGM images of a n^+-n-n^+ modulation-doped nanowire recorded with a V_{tip} of –9 and +9 V, respectively, and $V_{sd} = 1$ V. The dark and bright regions correspond to reduced and enhanced conductance, respectively. The white dashed lines highlight the positions of source-drain electrodes and nanowire. Scale bar, 1 μm.

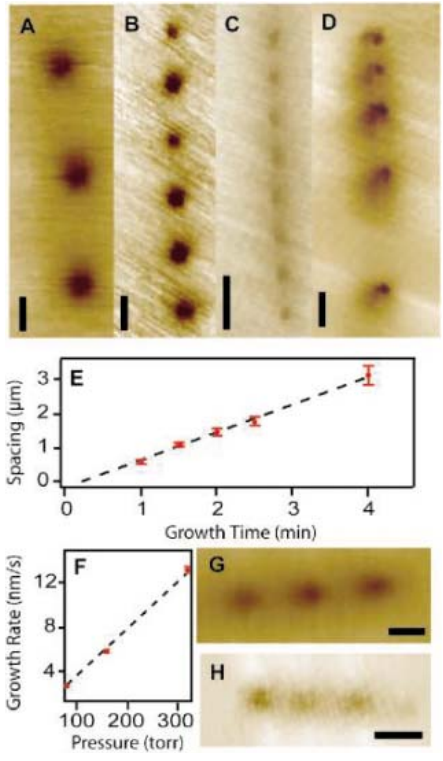

Fig. 2. Scalable synthesis of modulation-doped nanowires. SGM images of n^+-$(n$-$n^+)_N$ nanowires where (**A**) $N = 3$, (**B**) $N = 6$, and (**C**) $N = 8$, and the growth times for the n/n^+ regions are 1/3, 1/1, and 0.5/0.5 min, respectively. (**D**) SGM image of $N = 5$ nanowire, where the growth time for the n regions is 0.5 min, and n^+ sections are 0.5, 1, 2, and 4 min. Scale bars, 1 μm. (**E**) Repeat spacing versus growth time at total pressure of 320 torr. (**F**) Growth rate versus growth pressure. SGM images of n^+-$(n$-$n^+)_3$ modulation-doped nanowires synthesized with total pressures of (**G**) 160 torr and (**H**) 80 torr. The growth time for each n and n^+ region is 15 s. Scale bars, 100 nm. Error bars in (E) and (F) show means ± SD.

(Fig. 2G) and 90 nm (Fig. 2H), respectively, where the average section length in each structure was only 90 and 45 nm, respectively. These values do not represent a lower limit of the feature size. Because dopant diffusion is negligible at the growth temperature (*17*), it should be possible to reduce the feature size to at least that of the diameter of the nanowire (*6*), which for molecular-scale Si nanowires (*18*) is 3 to 5 nm.

The substantial differences in nanowire conductance resulting from locally gating *n* and n^+ segments can be used as a general method for addressing individual nanowires in an array when the nanowires have different n/n^+ sequences or codes. To test this idea, we first fabricated n^+-*n*-n^+ Si nanowire transistors with three equally spaced top metal gates (Fig. 3A). The nanowire transistor is easily turned off by gate 2 (–1 V), whereas the other gates produce only small conductance changes. Because the three gates are fabricated at the same time in a parallel process, the observed address selectivity is intrinsic to the differences in dopant concentration of *n* and n^+ sections of the Si nanowire and is distinct from lithographically defined steps previously used (*19*) to create differential responses in a specific nanowire region.

We have extended this basic approach to arrays (Fig. 3B). Two metal top gates, In1 and In2, were deposited directly on two modulation-doped silicon nanowires configured as outputs, Out1 and Out2. Conductance versus applied gate voltage (V_g) data measured at the four cross points show that Out1 and Out2 can only be turned off by In1 and In2, respectively (fig. S1), and thus, these inputs can selectively address Out1 and Out2 (Fig. 3B); that is, the array functions as an address decoder circuit for multiplexing and demultiplexing signals. A key point in our approach is that lithography is only used to define a regular array of microscale gate wires and is not needed to create a specific address code at the nanoscale as in previous work (*19*). Because synthesis is used to define the code required for nanoscale addressing (not lithography), we call this a "lithography-independent" addressing scheme. In the demonstration example of Fig. 3B, we took advantage of stochastic end-to-end nanowire alignment to produce distinct codes from a single type of nanowire. Indeed, the general case of a stochastic addressing with modulation-doped nanowires has been analyzed and shown to be an efficient approach for addressing dense nanoscale arrays; that is, it requires ~2.2ln(*N*) nanowires for addressing *N* lines when *N* is large (*20*).

Control of the size and separation of modulation-doped regions also enables synthesis to define quantum dot (QD) structures, in which the Fermi level offset caused by variations in dopant concentration produces potential barriers confining the QD (Fig. 4A). Conductance versus V_g and bias voltage (V_{sd}) studies of n^+-*n*-n_{QD}^+-*n*-n^+ modulation-doped silicon nanowires—in which the lightly doped *n*-type regions define barriers for a variable length QD, n_{QD}^+—reveal well-defined diamond structures (Fig. 4B); the single-period diamond shows that transport occurs through a single QD structure (*21*). Notably, the geometry-dependent gate capacitance, C_g, determined from these data, 23.5 aF, agrees well with the value, 24.1 aF, calculated from the ~500-nm QD size determined by SGM imaging (Fig. 4B, inset). In addition, current (*I*) versus V_g data for this nanowire and a structure in which the n_{QD}^+ section is reduced by half to ~250 nm (Fig. 4C) show single-

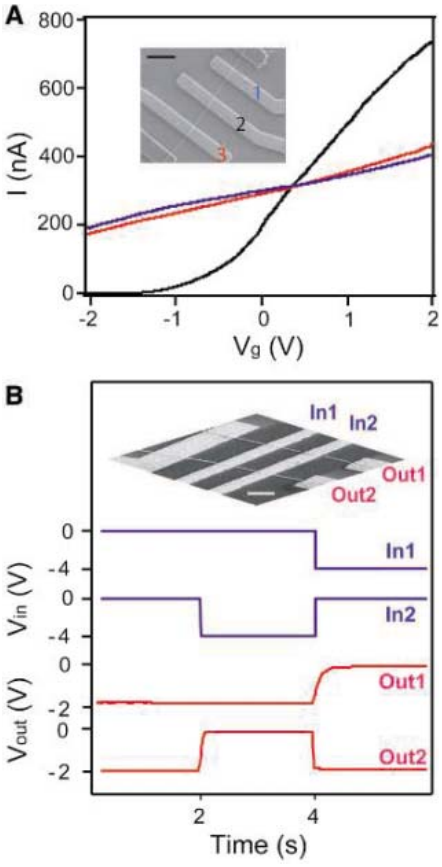

Fig. 3. Modulation-doped address decoder. (**A**) *I* versus V_g (V_{sd} = 1 V) measured for an n^+-*n*-n^+ silicon nanowire device, where gates 1, 2, and 3 (inset) correspond to blue, black, and red curves, respectively. The native silicon oxide was used as a gate dielectric with Au metal gates. (Inset) Scanning electron microscopy (SEM) image of the device. Scale bar, 1 μm. (**B**) SEM image of a 2-by-2 decoder configured using two modulation-doped silicon nanowires as outputs (Out1 and Out2) and two Au metal gates, which were deposited over a uniform Si_3N_4 dielectric as inputs (In1 and In2). Scale bar, 1 μm. Plots of input (blue) and output (red) voltages for the 2-by-2 decoder. Supply voltage is –2 V.

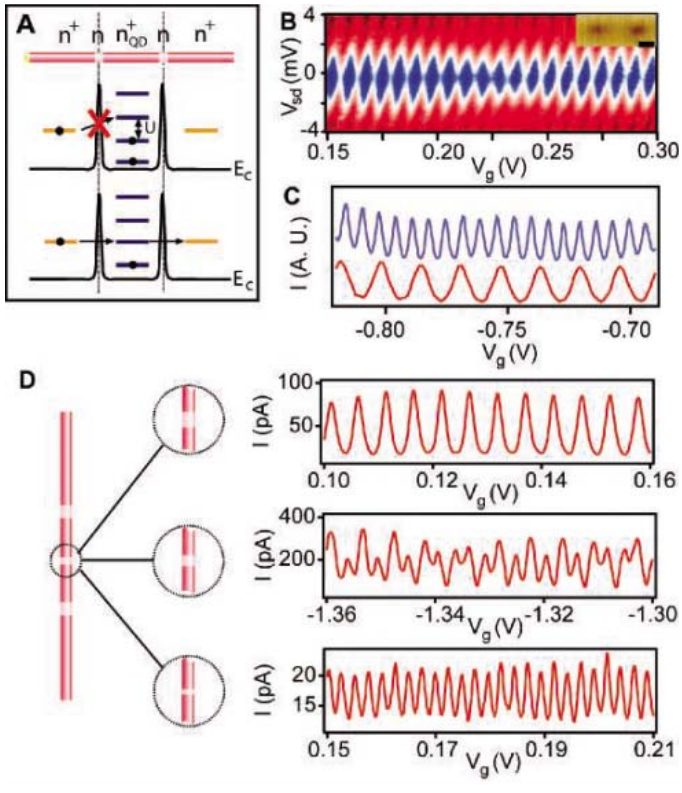

Fig. 4. QD structures defined by synthesis. (**A**) Schematic of n^+ QD structure confined by two *n*-type barriers within a modulation-doped nanowire. The conduction band (E_c) offset of the n^+ and *n* sections induce tunneling barriers with Coulomb blockade phenomenon observed when thermal energy is $\ll U$, the charging energy (*21*). The red X indicates blockage of charge transport. (**B**) Plot of $\partial I/\partial V_{sd}$ versus V_{sd} and V_g recorded at 1.5 K on a n^+-*n*-n_{QD}^+-*n*-n^+ device. The blue regions correspond to low values of $\partial I/\partial V_{sd}$, and the red regions correspond to high values; the red color corresponds to 1.8 μS. The middle n_{QD}^+ and two *n* sections were grown for 3 and 0.5 min, respectively, at 80 torr. (Inset) SGM image of the same device. Scale bar, 200 nm. (**C**) $I - V_g$ data taken at 1.5 K on the device in (B) (blue curve) and another device with the n_{QD}^+ section grown for 1.5 min (red curve). V_{sd} = 0.2 mV. A.U., arbitrary units. (**D**) Coupled double-QD structure with variable-width n_2 section between the two QDs. (Right) $I - V_g$ data recorded at 1.5 K on three devices with n_2 sections grown for 15, 10, and 5 s (top to bottom).

period oscillations in both devices, although the period ΔV_g is approximately doubled in the 250- versus 500-nm QD. Because ΔV_g is inversely proportional to the gate capacitance, $\Delta V_g = e/C_g$, and QD size, this comparison shows that the true size of the confined QD can be controlled in a predictable manner in these modulation-doped nanowires (*22*).

The potential of our approach for encoding coupled quantum structures has been explored in modulation-doped silicon nanowires that have structures of the form n^+-n_1-$n_{QD}{}^+$-n_2-$n_{QD}{}^+$-n_1-n^+, where n_1 are fixed-width tunnel barriers that weakly couple the structure to source and drain electrodes, and n_2 is a variable-width barrier that couples the two QDs (Fig. 4D, left panel). The $I - V_g$ data recorded from representative nanowire devices with three different n_2 barrier widths coupling the QDs (Fig. 4D, right panel) demonstrate several key points. First, the device with the largest barrier exhibits a single Coulomb oscillation period that yields a capacitance consistent with the size of each individual QD determined from SGM measurements. This result shows qualitatively that the two QDs are weakly coupled, and moreover, have sizes that are similar. Second, the data from the device with an intermediate-width n_2 barrier exhibits a splitting of each of the Coulomb oscillation peaks into doublets, which is the signature of enhanced tunneling conductance between the QDs (*23*, *24*). This observation agrees with previous studies (*23*, *25*, *26*) where coupled dots were defined by lithographically patterned gate electrodes. Last, as the barrier width is reduced further, a single Coulomb oscillation period is again observed, although the capacitance shows that the effective QD size is twice that of the individual $n_{QD}{}^+$ regions; that is, the structures are fully delocalized.

These studies demonstrate the ability to synthesize coupled QDs within nanowires, where the interaction between quantum structures is defined by synthesis not lithography. More generally, this work demonstrates the potential of encoding functional information into nanostructures during synthesis, which we believe will open up opportunities for conventional and quantum electronic devices and circuits in the future.

Reference and Notes

1. P. L. McEuen, M. S. Fuhrer, H. Park, *IEEE Trans. Nanotechnology* **1**, 78 (2002).
2. H. Dai, *Acc. Chem. Res.* **35**, 1035 (2002).
3. C. M. Lieber, *Mater. Res. Soc. Bull.* **28**, 486 (2003).
4. L. Samuelson *et al.*, *Phys. E* **25**, 313 (2004).
5. T. Mokari, E. Rothenberg, I. Popov, R. Costi, U. Banin, *Science* **304**, 1787 (2004).
6. M. S. Gudiksen, L. J. Lauhon, J. Wang, D. C. Smith, C. M. Lieber, *Nature* **415**, 617 (2002).
7. M. T. Bjork *et al.*, *Appl. Phys. Lett.* **80**, 1058 (2002).
8. M. T. Bjork *et al.*, *Nano Lett.* **4**, 1621 (2004).
9. C. Zhou, J. Kong, E. Yenilmez, H. Dai, *Science* **290**, 1552 (2000).
10. V. Derycke, R. Martel, J. Appenzeller, Ph. Avouris, *Nano Lett.* **1**, 453 (2001).
11. A. B. Greytak, L. J. Lauhon, M. S. Gudiksen, C. M. Lieber, *Appl. Phys. Lett.* **84**, 4176 (2004).
12. L. J. Lauhon, M. S. Gudiksen, D. Wang, C. M. Lieber, *Nature* **420**, 57 (2002).
13. Materials and methods are available as supporting material on *Science* Online.
14. J. M. Jasinski, S. M. Gates, *Acc. Chem. Res.* **24**, 9 (1991).
15. R. T. White, R. L. Espino-Rios, D. S. Rogers, M. A. Ring, H. E. O'Neal, *Int. J. Chem. Kinet.* **17**, 1029 (1985).
16. A. Bachtold *et al.*, *Phys. Rev. Lett.* **84**, 6082 (2000).
17. P. M. Fahey, P. B. Griffin, J. D. Plummer, *Rev. Mod. Phys.* **61**, 289 (1989).
18. Y. Wu *et al.*, *Nano Lett.* **4**, 433 (2004).
19. Z. Zhong, D. Wang, Y. Cui, M. W. Bockrath, C. M. Lieber, *Science* **302**, 1377 (2003).
20. A. DeHon, P. Lincoln, J. E. Savage, *IEEE Trans. Nanotechnology* **2**, 165 (2003).
21. L. P. Kouwenhoven *et al.*, in *Proceedings of Advanced Study Institute on Mesoscopic Electron Transport*, L. L. Sohn, L. P. Kouwenhoven, G. Schön, Eds. (Kluwer, Dordecht, Netherlands, 1997).
22. Recent studies have demonstrated the formation of single quantum dots in InP/InAs composition-modulated nanowires, where InP is used to produce confining barriers for an InAs QD (*8*).
23. F. R. Waugh *et al.*, *Phys. Rev. B* **53**, 1413 (1996).
24. The tunneling conductance for the strongly coupled QDs was estimated to be 0.9 G_0, where $G_0 = 2e^2/h$, e is the elementary charge, and h is Planck's constant, assuming that interdot capacitance is negligible compared with individual QD capacitances (*23*).
25. N. Mason, M. J. Biercuk, C. M. Marcus, *Science* **303**, 655 (2004).
26. C. Fasth, A. Fuhrer, M. T. Bjork, L. Samuelson, *Nano Lett.* **5**, 1487 (2005).

27. We thank H. Park and A. DeHon for discussion. C.M.L. acknowledges support of this work by the Defense Advanced Research Projects Agency.

Supporting Online Material

www.sciencemag.org/cgi/content/full/310/5752/1304/DC1
Materials and Methods
Fig. S1

12 August 2005; accepted 24 October 2005
10.1126/science.1118798

Super-Compressible Foamlike Carbon Nanotube Films

Anyuan Cao,[1]* Pamela L. Dickrell,[2] W. Gregory Sawyer,[2] Mehrdad N. Ghasemi-Nejhad,[1] Pulickel M. Ajayan[3]*

We report that freestanding films of vertically aligned carbon nanotubes exhibit super-compressible foamlike behavior. Under compression, the nanotubes collectively form zigzag buckles that can fully unfold to their original length upon load release. Compared with conventional low-density flexible foams, the nanotube films show much higher compressive strength, recovery rate, and sag factor, and the open-cell nature of the nanotube arrays gives excellent breathability. The nanotube films present a class of open-cell foam structures, consisting of well-arranged one-dimensional units (nanotube struts). The lightweight, highly resilient nanotube films may be useful as compliant and energy-absorbing coatings.

Structural foams (*1*, *2*) have a variety of applications in modern society such as in construction, energy dissipation, cushioning, and packaging. Mechanical strength (compressive stress) and compressibility (strain) are two important factors that determine the performance and applications of foams; however, these two properties are of opposing nature. Increasing the volume of the cells (i.e., the void area) in a foam results in higher compressibility (up to 75%) but causes rapidly decreasing strength (*2*–*4*). For the foam at a fixed chemical composition, its modulus (E_f) decreases with increasing relative cell volume (ϕ) as $E_f = CE(1 - \phi)^2$, where C is a constant (close to unity) and E is the cell edge modulus (*1*). Metallic (e.g., Al) foams have higher compressive strength than polymeric foams, but the plastic deformation of cell structures results in little resilience upon load release (*5*). The elastic segments (struts) between adjacent cells form the architecture of a foam, and it is the bending and buckling of these struts that allows the foam to be compressed; the property of a strut (determined by its composition, geometry, and dimension) dictates the compressive behavior (*6*, *7*).

A carbon nanotube (*8*, *9*) is perhaps the best strut to make ultralight yet strong foams, considering its exceptional mechanical strength, low density, and high elasticity (*10*). In particular, the nanotube exhibits extreme structural flexibility (*10*–*12*) and can be repeatedly bent through large angles and strains without structural failure (*13*). The ability of nanotubes to adopt and switch between various buckled morphologies makes them capable of accommodating and sustaining large local strains while maintaining structural integrity (*14*, *15*).

We show that vertically aligned nanotubes (*16*) form a highly resilient open-cell

[1]Department of Mechanical Engineering, University of Hawaii at Manoa, Honolulu, HI 96822, USA. [2]Department of Mechanical and Aerospace Engineering, University of Florida, Gainesville, FL 32611, USA. [3]Department of Materials Science and Engineering, Rensselaer Polytechnic Institute, Troy, NY 12180, USA.

*To whom correspondence should be addressed. E-mail: anyuan@hawaii.edu (A.C.); ajayan@rpi.edu (P.M.A.)

foam system, with individual nanotubes acting as strong nanoscale struts and the internanotube space acting as interconnected open-air cells. Repeated compression tests showed that these nanotube struts can be squeezed to less than 15% of their free lengths by buckling and folding themselves like springs, collectively. After every cycle of compressive loading, the nanotubes unfold the buckles and recover to their near original lengths, resulting in a strong cushioning effect.

Vertically aligned, multiwalled nanotube arrays were produced by chemical vapor deposition (CVD), with ferrocene and xylene as the precursors (*17*). Freestanding nanotube films that peeled off from the substrate (with typical areas ranging from 0.5 to 2 cm^2) were compressed along the film-thickness direction (along nanotube axis) (Fig. 1) at a set constant strain, repeatedly for thousands of cycles. Two nanotube films squeezed to 15% of their original thickness recovered fully at the end of each cycle (movies S1 and S2). The porosity of the (as-grown) nanotube films is ~87% (*18*), potentially allowing a large volume reduction (up to 85%) when compressed. The near-full thickness recovery lasted hundreds of cycles before we saw a small reduction in thickness (gap between the top of the film and the compression stage) (fig. S1); however, the gap was stabilized at <20% of the total film thickness even after 10,000 cycles. The nanotube film did not fracture, tear, or collapse under compression, but remained at a constant width during the cycles (fig. S1). Previous work on nanotube brushes indicated that the shear resilience of aligned nanotubes is high, because no shedding of nanotubes was observed when the brushes were swept over solid surfaces (*19*).

Nanotube film-thickness recovery (back to its original morphology) during the compression-release period happens very fast. The compression head was set to retreat at a speed of 120 mm/min (upper limit of the instrument), and the film was observed to follow the returning head closely until it reached its maximum height (movie S2). Therefore, the film expansion rate on recovery can be considered to be at least the same speed as the receding head (>120 mm/min, or 2000 μm/sec). This is much faster than the general recovery rate for conventional flexible foams and spongy structures, especially those made of polymers with viscoelasticity that prevents instantaneous recovery at large strain rates.

Scanning electron microscopy (SEM) images show that the thickness of compressed nanotube films (>1000 cycles) decreases from the original 860 μm to around 720 μm. There are also ordered wavelike folds along the nanotubes, which are formed across the film section and correspond to the uniform horizontal lines seen in low magnification (Fig. 2A). The SEM image shows that repeated compression has converted initially straight nanotubes into buckled folds, with an average wavelength of ~12 μm (fig. S2). However, the buckles near the film's bottom side are heavily folded and gradually released when approaching the middle part of the film, where the slight buckles are almost undistinguishable (Fig. 2B). The buckling wavelength increases with increasing original film thickness, with 25-μm buckling

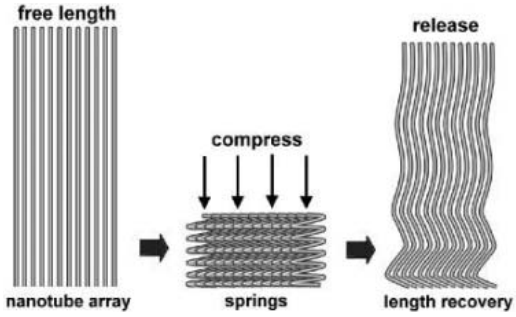

Fig. 1. Compression testing of aligned carbon nanotube films. A schematic illustration shows a nanotube array compressed to folded springs and then regaining the free length upon the release of compressive load.

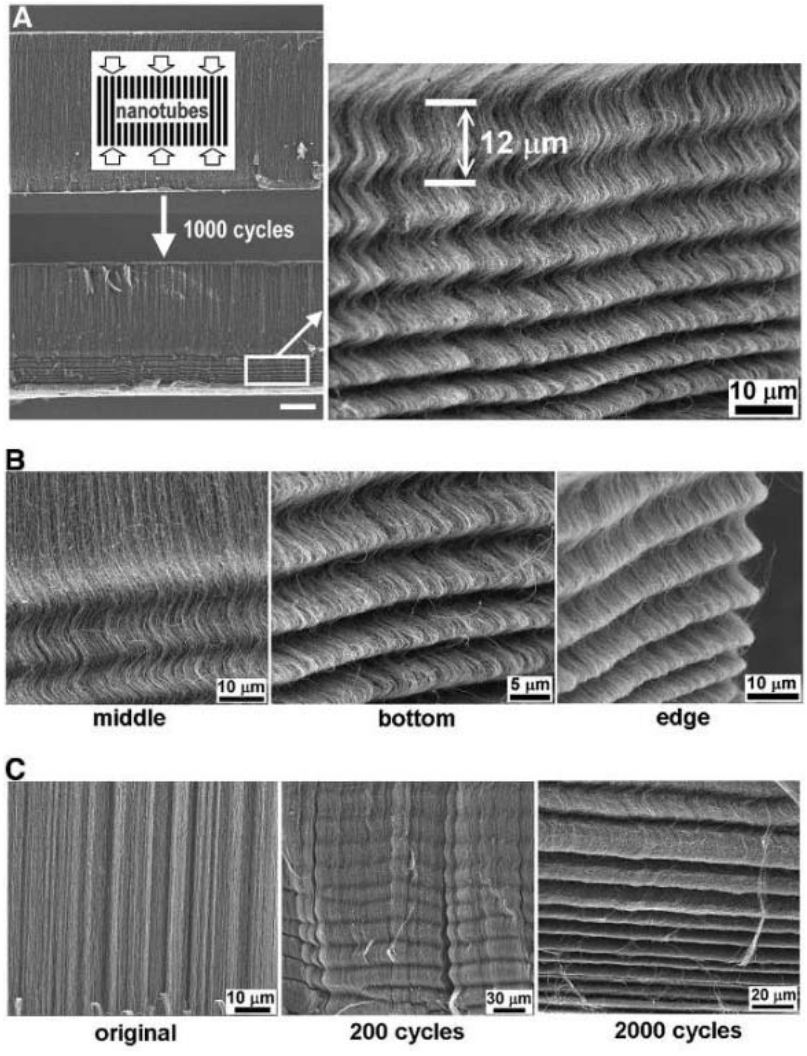

Fig. 2. SEM characterization of buckled carbon nanotubes under compression. (**A**) SEM of an original freestanding film (left, top) (thickness 860 μm) and a compressed film (left, bottom) (ε = 85%, 1000 cycles), with a reduced thickness of 720 μm, showing horizontal lines (wavelike buckles) uniformly distributed across the film section. Left scale bar, 200 μm. (Left, inset) Illustration of compression along the axis of nanotubes. (**B**) Slight buckles in the middle section, heavy buckles (almost completely folded) near the bottom of film, and the zigzag edge of the compressed film. (**C**) SEM image of a 1.2-mm-thick film before and after compression, showing the evolution of buckles with increasing compression cycles.

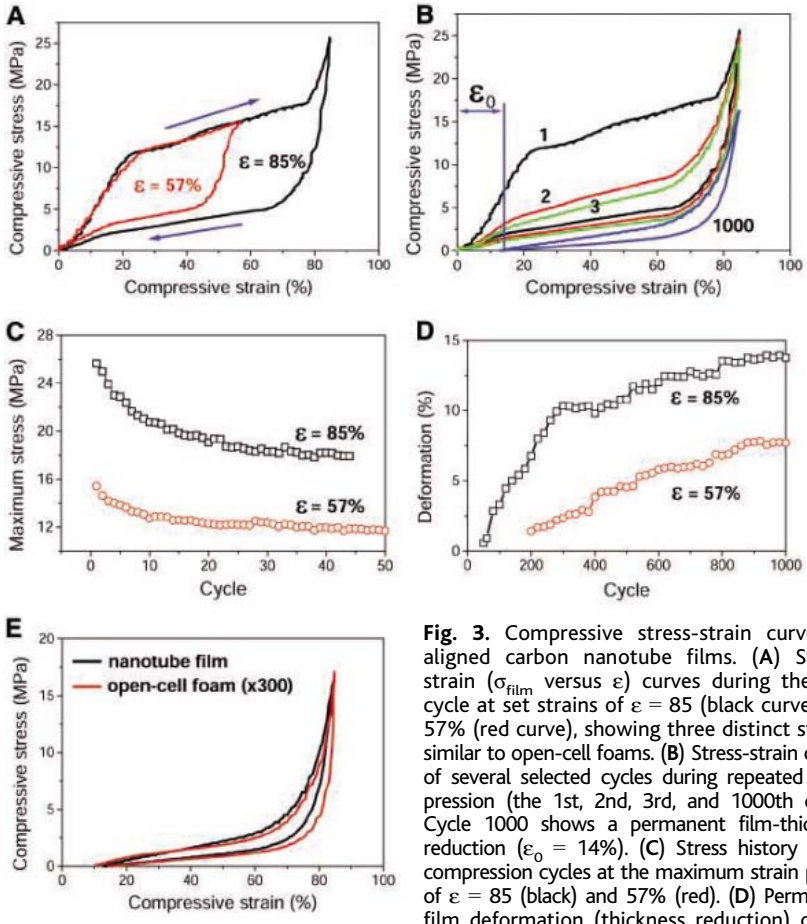

Fig. 3. Compressive stress-strain curves of aligned carbon nanotube films. **(A)** Stress-strain (σ_{film} versus ε) curves during the first cycle at set strains of ε = 85 (black curve) and 57% (red curve), showing three distinct stages, similar to open-cell foams. **(B)** Stress-strain curves of several selected cycles during repeated compression (the 1st, 2nd, 3rd, and 1000th cycle). Cycle 1000 shows a permanent film-thickness reduction (ε_0 = 14%). **(C)** Stress history of 50 compression cycles at the maximum strain points of ε = 85 (black) and 57% (red). **(D)** Permanent film deformation (thickness reduction) occurs over 1000 compression cycles. **(E)** Stress-strain curves of a nanotube film (black) at cycle 1000 and an open-cell cushion foam (red) at cycle 10. The latter was multiplied by 300 for comparison.

for a 1.2-mm-thick film after compression. We still observe the same tendency to buckle more heavily at the bottom of the film (the side adjacent to the substrate during the growth of the films) (Fig. 2C). When the film is flipped during compression, the pattern also flips, with heavy folds appearing at the top, suggesting that the bottom of the film has slightly different mechanical characteristics (difference in density, stiffness) compared with the rest of the film (*20*). For an as-grown film consisting of nearly straight nanotubes, we observed slight buckles at the beginning compression cycles, which gradually became heavily folded after thousands of cycles (Fig. 2C). Because the buckles near the film bottom are always compressed earlier during each cycle, they are subjected to large-angle folding for a much longer time, compared with the buckles that develop later at the top portion of film. This time difference consequently aggravates the waviness difference observed here.

In a dense aligned nanotube array, it is difficult for nanotubes to buckle independently (randomly) at an appreciable length scale because of the proximity of the neighboring tubes. The cooperative nature of the buckling results in a self-organized, zigzag-folded morphology seen from the edge of the compressed film (Fig. 2B), which is the most space-efficient and energetically favorable configuration for huge numbers of nanotubes to adopt under large compressive strains. The folding of these zigzag buckles allows for the maximum volume reduction under the smallest compressive load and does not require any extra space to accommodate the vertical deformations.

Figure 3A shows the plots of compressive stress (σ_{film}, the applied force divided by the film area) versus strain (ε, the compressed distance relative to film thickness) during the first compression cycle for the nanotube films (thickness ~860 μm) at set maxima ε of 57 and 85%. During the cycles, the stresses remain above zero until ε = 0, in agreement with the full recovery of nanotube films from experimental observation. Three distinct stages are observed during the loading process, including an initial Hookean region at ε < 22% with an elastic modulus just over 50 MPa, a plateau (buckling of cell struts) at 22% < ε < 79% with a reduced modulus of approximately 12 MPa, and final densification, marked by rapid rise of stress as ε approaches 85% (near monolith because of the large volume reduction). Representative open-cell foams have shown similar three characteristic regions (*5*–*7*). Nanotube films subject to a moderate compression (ε = 57%) show similar elastic behavior. The stress loops in both curves indicate that a large portion of energy (64%) is absorbed during compression. The energy dissipation is most likely caused by the friction between nanotubes (*21*) or movement of air through the porous nanotube arrays (which could be useful in damping applications).

Because nanotubes only occupy 13% of the film, the actual stress on each carbon nanotube (σ_{cnt}) is several times higher than the as-measured film stress (σ_{film}); that is, $\sigma_{cnt} = \sigma_{film}/0.13$ = 12 MPa/0.13 = 92 MPa at ε = 22%. Under Euler beam theory, the critical compression stress (σ_{crit}) beyond which a nanotube strut becomes unstable (starts to buckle) can be expressed as $\sigma_{crit} = E_{CNT}(\pi r/L_{HW})^2$, where E_{CNT} denotes the Young's modulus of nanotubes, r is the nanotube radius (20 nm), and L_{HW} is the half wavelength of the buckle along nanotubes (*15*, *22*). We used an average modulus of multiwalled nanotubes (E_{CNT}) of 1 TPa, based on both experimental measurements and theoretical calculations (*23*–*25*). The critical stress necessary to enable the formation of 12-μm buckles (half wavelength of 6 μm) as seen in Fig. 2A is σ_{crit} = 1 TPa × $(\pi 20/6000)^2$ = 110 MPa, which is only slightly larger than the transition stress observed during the first loading curve (σ_{cnt} = 92 MPa). Thus we believe the nanotubes at first are subject to elastic bending and then form wavelike folds at ε = 22%, when the compressive stress is large enough to make them buckle collectively. The slightly lower critical stress for buckling may due to the structural defects in CVD-produced nanotubes. The Euler instability only permits a semiquantitative analysis on these naturally grown nanotube arrays. According to Hooke's law, the compression rate (force divided by displacement) of the whole film (R_{film}) is determined by $R_{film} = \sigma_{film}/\varepsilon L$, where L is the original film thickness (860 μm), and was calculated to be 26.5 kPa/μm at ε < 79%. Correspondingly, the compression rate of individual nanotubes ($R_{cnt} = \sigma_{cnt}/\varepsilon L$) with 12-μm buckles is 204 kPa/μm.

Once the nanotubes have developed the self-organized folded patterns and have buckled collectively, the whole film becomes softer, which is seen by the loss of elasticity and decreased compressive stress in the cycles afterward (Fig. 3B), similar to the rapid stress decrease in the first several cycles of open-cell foams (*26*). The observed hysteresis is probably caused by the entanglement of nanotubes resulting in the impedance/friction during their movement. The stress at the maximum strain drops rapidly in the first 10 cycles (from 25.6 to 20 MPa at ε = 85%) and then stabilizes at ~18 MPa in the subsequent cycles (Fig. 3C).

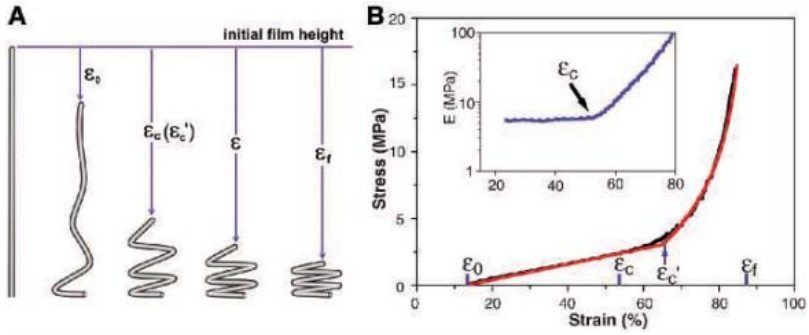

Fig. 4. Modeling of nanotube behavior under large strain compression. (**A**) Illustration of nanotubes buckling under compression, where ε_0 is the permanent initial strain (14% at cycle 1000), ε_c is the critical strain where the buckled nanotube folds begin to collapse from the bottom side, ε is the strain relative to initial film, and ε_f is the final strain where all folds are fully collapsed. (**B**) Experimental data of cycle 1000 (black curve) and the model (red curve) fit to this data. The experimental results show a critical strain (ε_c) of 53% from the differential curve (inset), whereas the model generates a critical strain (ε_c') of 65%.

The maximum degradation in compressive strength of the nanotube film is <30% after 1000 cycles. The thickness reduction of the nanotube film can be derived from the intersection of stress curve with the strain coordinate (ε_0 = 14% for cycle 1000, as marked in Fig. 3B). For a repeated compression at a high strain of ε = 85%, the nanotube film shows high resistance to any further structural deformation, because the film height became subsequently stabilized at a deformation of <15% approaching 1000 cycles (Fig. 3D). Compression of films at smaller strains (e.g., ε = 57%) resulted in smaller thickness reduction (~7.5%) after thousands of cycles.

The compressive strength (stress corresponding to the plateau region) of nanotube films (12 to 15 MPa) is much higher than typical low-density flexible foams that are capable of sustaining large strains (e.g., latex rubber, polyurethane), which generally have a plateau stress of only 20 to 30 kPa (*3*, *26*). Measurements on several types of compressible foams and sponges (e.g., cushioning package foam, Gymboree, USA) revealed a maximum compressive stress of 0.02 to 0.1 MPa at a comparable strain (~85%), which is two to three orders lower than the strength of nanotube films (Fig. 3E). The thickness deformation (which can't be recovered immediately) of such cushion foams is severe (>10%) within the first 10 cycles, and the thickness-regaining process is much slower (on the order of 1 mm/hour), compared with the fast unfolding rate of nanotubes (>2 mm/min). The sag factor, which is the relative ratio of stresses at two deflections of 65 and 25%, is an important criteria for cushioning foams (*26*). This criteria represents how much "fight back" will be encountered upon continued compression. For nanotube films (at cycle 1000, σ = 3.55 MPa at ε = 65% and σ = 0.84 MPa at ε = 25%), the sag factor is higher than 4. The resilience of nanotube films is 25 to 30%, measured by dropping a glass ball (1 to 2 mm in diameter) from zero speed onto the film and calculating the ball rebounce height relative to the initial ball-to-film distance before dropping. In addition, the open-cell nature of nanotube films also provides good breathability (allowing high-rate compression and recovery). The high compressive stress, sag factor, resilience, and breathability make nanotube films suitable for applications requiring strong cushioning effects.

Considering compression cycle 1000 shown in Fig. 3B, the derivative of its stress-strain curve depicts an initial linear elastic stage up to a critical strain ε_c = 53% (inset of Fig. 4B) with a single modulus of E = 5.85 MPa, after which the modulus increases exponentially with increasing strain. The exponential increase in stiffness can be explained through a complete collapse of individual nanotube folds starting from the bottom of film, thus reducing the number of folds participating in further deformations, until all the folds have been fully compressed (corresponding to a final strain of ε_f) (Fig. 4A). The stress of the initial linear stage is $\sigma = E(\varepsilon - \varepsilon_0)$, and the second stage can be expressed differentially as $d\sigma/d\varepsilon = E/(\varepsilon_f - \varepsilon)$. Figure 4B shows that the model featured by these two equations (red curve) fits quite well with the experimental data (black curve) of cycle 1000, yielding a critical strain of ε_c' = 65% (*18*). The earlier collapse of nanotube buckles (ε_c = 53%) in experimental results is attributed to the mechanically weaker region of the film near the bottom surface of the film, where the heaviest buckles were observed in Fig. 2.

Carbon nanotube films behave as open-cell foams with nanotubes as elastic struts. The high compressibility (~85%), recovery rate (>2000 μm/sec), sag factor (~4), and fatigue resistance (<15% deformation during thousands of cycles) make nanotube arrays/films potential foamlike structures with much improved strength/weight ratio, dimensional stability (at elevated temperature or humidity), and resistance to chemical environments. Aligned single-walled nanotubes are expected to have better performance (strength, resilience). In addition, the compressive strength of nanotube films could be tailored by controlling the wavelength of buckles. Such resilient nanotube systems could have many applications, such as flexible electromechanical systems, compliant interconnect structures, actuators, and coatings for mechanical damping and energy-absorbing services.

References and Notes

1. L. J. Gibson, M. F. Ashby, *Cellular Solids, Structure and Properties* (Pergamon, New York, 1997).
2. N. C. Hilyard, A. Cunningham, *Low Density Cellular Plastics, Physical Basis of Behavior* (Chapman and Hall, London, UK, 1994).
3. D. Klempner, K. C. Frisch, in *Handbook of Polymeric Foams and Foam Technology* (Hanser, New York, 1991), chaps. 4, 6, and 9.
4. H. X. Zhu, J. F. Knott, N. J. Mills, *J. Mech. Phys. Solids* **45**, 319 (1997).
5. L. J. Gibson, *Annu. Rev. Mater. Sci.* **30**, 191 (2000).
6. J. H. Kinney, G. W. Marshall, S. J. Marshall, D. L. Haupt, *J. Appl. Poly. Sci.* **80**, 1746 (2001).
7. H. X. Zhu, N. J. Mills, J. F. Knott, *J. Mech. Phys. Solids* **45**, 1875 (1997).
8. M. S. Dresselhaus, G. Dresselhaus, P. C. Eklund, *Science of Fullerenes and Carbon Nanotubes* (Academic, San Diego, 1996).
9. R. H. Baughman, A. A. Zakhidov, W. A. de Heer, *Science* **297**, 787 (2002).
10. D. Qian, G. J. Wagner, W. K. Liu, M. F. Yu, R. S. Ruoff, *Appl. Mech. Rev.* **55**, 495 (2002).
11. S. Iijima, C. Brabec, A. Maiti, J. Bernholc, *J. Chem. Phys.* **104**, 2089 (1996).
12. V. Sazonova *et al.*, *Nature* **431**, 284 (2004).
13. M. R. Falvo *et al.*, *Nature* **389**, 582 (1997).
14. B. I. Yakobson, C. J. Brabec, J. Bernholc, *Phys. Rev. Lett.* **76**, 2511 (1996).
15. O. Lourie, D. M. Cox, H. D. Wagner, *Phys. Rev. Lett.* **81**, 1638 (1998).
16. Z. F. Ren *et al.*, *Science* **282**, 1105 (1998).
17. R. Andrews *et al.*, *Chem. Phys. Lett.* **303**, 467 (1999).
18. Materials and methods are available as supporting material on *Science* Online.
19. A. Cao *et al.*, *Nat. Mater.* **4**, 540 (2005).
20. When we immersed a nanotube film in organic solvents (e.g., acetone) and then took it out, the condensed film after acetone evaporation was slightly curled toward the bottom side (more shrinkage near the bottom). Thus we believe that the bottom part of a film is less dense (strong), compared with its top part.
21. J. Suhr, N. Koratkar, P. Keblinski, P. Ajayan, *Nat. Mater.* **4**, 134 (2005).
22. S. Timoshenko, in *Theory of Elastic Stability* (McGraw-Hill, New York, 1936), chap. 2.
23. M. M. J. Treacy, T. W. Ebbesen, J. M. Gibson, *Nature* **381**, 678 (1996).
24. M. F. Yu *et al.*, *Science* **287**, 637 (2000).
25. J. P. Lu, *Phys. Rev. Lett.* **79**, 1297 (1997).
26. N. C. Hilyard, in *Mechanics of Cellular Plastics* (Macmillan, New York, 1982), pp. 103 and 226.

27. A.C. acknowledges the start-up funding from the College of Engineering and the Mechanical Engineering Department of the University of Hawaii at Manoa. P.M.A. thanks the Interconnect Focus Center New York.

Supporting Online Material

www.sciencemag.org/cgi/content/full/310/5752/1307/DC1
Materials and Methods
Figs. S1 and S2
Movies S1 and S2

16 August 2005; accepted 21 October 2005
10.1126/science.1118957

The Nature of Aqueous Tunneling Pathways Between Electron-Transfer Proteins

Jianping Lin, Ilya A. Balabin, David N. Beratan*

Structured water molecules near redox cofactors were found recently to accelerate electron-transfer (ET) kinetics in several systems. Theoretical study of interprotein electron transfer across an aqueous interface reveals three distinctive electronic coupling mechanisms that we describe here: (i) a protein-mediated regime when the two proteins are in van der Waals contact; (ii) a structured water-mediated regime featuring anomalously weak distance decay at relatively close protein-protein contact distances; and (iii) a bulk water–mediated regime at large distances. Our analysis explains a range of otherwise puzzling biological ET kinetic data and provides a framework for including explicit water-mediated tunneling effects on ET kinetics.

Protein ET reactions play a critical role in biologically vital processes in living cells, most notably photosynthesis and respiration (*1*). Describing the structure dependence of intermolecular ET reactions is particularly challenging because of the wide range of the accessible docking geometries, and several studies have addressed these reaction mechanisms (*2*–*8*). The factors that control unimolecular ET rates, namely the donor-to-acceptor (D to A) distance and energies, the structure of the ET-mediating protein matrix, and the thermal atomic motion, have been extensively explored both experimentally (*4*–*6*) and theoretically (*9*–*14*).

Intermolecular ET reactions, however, remain a challenge. In addition to the above factors, the rate depends on the D-to-A docking geometry, as well as on the structure and thermal motion of the solvent (*2*–*7*). The number of structural degrees of freedom makes quantitatively reliable theoretical calculations extremely difficult. We show that the intervening water structure leads to one of three distinctly different ET tunneling regimes, in contrast to the common assumption of single-exponential distance decay (*2*, *5*–*7*). The identification of these three regimes provides a framework for understanding the mechanisms that underlie several unexplained and seemingly unrelated water-mediated biological ET rate processes (*7*, *15*–*19*), as well as providing a strategy for making theoretical estimates of bimolecular rates that take these water-mediation effects into account.

Water can influence the ET reaction rates by mediating ET coupling pathways, as well as by controlling activation free energies (*5*, *9*). In the past decade, the distance dependence of water-mediated ET reaction rates has become the focus of intensive experimental (*4*–*7*, *13*, *15*–*17*, *20*, *21*) and theoretical (*18*, *19*, *22*–*24*) investigation. Until recently, experimental and theoretical analysis suggested a single-exponential decay of the ET rates with distance through water, with a characteristic decay constant of about 1.6 to 1.7 $Å^{-1}$ (*5*, *20*, *21*). In comparison with proteins that exhibit decay constants of about 1.0 to 1.2 $Å^{-1}$ (*5*), water appeared to be a rather poor ET mediator because of extensive through-space links in tunneling pathways (*20*).

In the past few years, however, a number of important experimental observations emerged that are inconsistent with the single-exponential decay model for water and with the generality of rapid distance decay for ET through water molecules. In crystals, ET across thin aqueous interfaces was found to be facile (*7*). In covalently cross-linked azurin complexes, water dimers that formed between the redox centers appeared to increase the ET rate substantially (*15*). In DNA, the influence of water (and counterions) may be even more pronounced, and fluctuations in hydration were proposed to gate ET (*16*). In small water clusters in gas phase or on TiO_2 surfaces, hydrated electrons were suggested to facilitate water-mediated ET reactions (*25*, *26*). These recent experiments all suggest the need for a deeper unifying theoretical framework to describe the distance and structure dependence of water-mediated ET reaction rates.

Here, we use computation to explore how the aqueous protein environment influences ET rates as a function of distance. Coupling interactions and rates were computed for the trypsin-solubilized bovine liver cytochrome b_5 [(*27*), Protein Data Bank (PDB) entry 1CYO] self-exchange ET reaction (*27*–*33*), which represents a broad class of solvent-mediated ET reactions involving α-helical redox proteins. To explore the influence of protein orientation, we constrained the cytochrome b_5 heme-heme angles to 0°, 45°, or 90°.

For each orientation, the molecules were also constrained to a specified distance between the porphyrin-ring edges between 6 and 16 Å. For each of the geometries, the protein molecules were solvated in the TIP3 (*34*) water; Na^+ and Cl^- counterions were added to establish an ionic strength of 0.2 M, and the system was equilibrated for 200 ps using the Charmm27 forcefield, constant pressure (NpT) ensemble, periodic boundary conditions, and particle-mesh Ewald full electrostatics (*35*). After equilibration, another 100-ps molecular dynamics (MD) simulation was performed, and the system conformation was saved every 1 ps, yielding 100 "snapshots." The D-to-A electronic coupling T_{DA} was computed for each snapshot with an extended–Hückel-level (XH) electronic Hamiltonian; the ET rate was estimated from the mean-square electronic coupling $\langle T_{DA}^2 \rangle$ in the non-adiabatic Fermi's golden rule expression (*10*, *11*). The T_{DA} calculations included the protein atoms and the interfacial water molecules. For comparison, these calculations were repeated without the interfacial water (*34*). This computational approach provides a reasonable qualitative estimate of the D-A couplings in proteins and small molecules (*10*, *11*, *36*, *37*). The coupling was also estimated using the empirical Pathways model (*38*) and atomic packing density analysis (*13*). Finally, bimolecular self-exchange ET rates were estimated by using the computed mean square donor-acceptor interactions (as a function of distance) in Brownian dynamics simulations (*28*, *29*).

The dependence of $\langle T_{DA}^2 \rangle$ on the distance between porphyrin-ring edges is essentially orientation independent (*35*); Fig. 1 shows the distance dependence for the 90° orientation between the porphyrin rings. Most important, rather than finding single-exponential decay with distance, the XH results reveal three distinct ET regimes at distances of 7 to 9 Å, 9 to 12 Å, and >12 Å, respectively. At 7 to 9 Å, the distance decay is similar to that for intramolecular ET (*5*); that is, the tunneling is facilitated primarily by the protein atoms, and water has little effect on the electronic coupling. In the distance range from 9 to 12 Å, the coupling decay is anomalously weak, and water is the principal mediator of tunneling across the protein-protein interface (i.e., the plateau regime). At distances >12 Å, the distance decay is consistent with tunneling through liquid water.

The empirical Pathways-level analysis of the $\langle T_{DA}^2 \rangle$ distance dependence also captures the qualitative features of these three regimes (fig. S1). The atomic packing den-

Departments of Chemistry and Biochemistry, Duke University, Durham, NC 27708, USA.

*To whom correspondence should be addressed. E-mail: david.beratan@duke.edu

sity method does not resolve the three regimes because there is little change in the overall packing density over the entire distance range. Although the XH electronic structure method is a qualitative one, we believe that the existence of the three coupling regimes is a robust characteristic of the solvated protein environment.

The structural origin of these three different electronic coupling regimes is explained by the interfacial water structure at difference distances, as shown in Fig. 1. At small distances, there are only a few water molecules at the interface, and they are positioned outside of the dominant ET coupling pathways. At intermediate distances, a small number of water molecules penetrate the space between the hemes, establishing strongly coupled tunneling pathways. Figure 2 shows the evolution of $\langle T_{DA}^2 \rangle$ in the coupling plateau region for time snapshots taken from an MD trajectory. In a number of conformations, ET is mediated by either a single water molecule (snapshot A) or by several water molecules that provide multiple ET pathways that interfere constructively (snapshot B). These constructively interfering geometries control the value of $\langle T_{DA}^2 \rangle$, and the relative abundance of these conformations (as compared to conformations with destructively interfering pathways, snapshot C) is characteristic of the plateau regime. This behavior arises from the confined space between proteins, combined with strong protein surface-water interactions (electrostatic and van der Waals interactions), in the plateau regime. At larger protein-protein distances, the water configurations that lead to strong T_{DA} values occur much less frequently than in the structured water regime. The electronic coupling between proteins in the shortest-distance regime, where the gap between proteins is too small for water to enter the dominant coupling pathways, is mediated by through-space tunneling. The through-space mechanism is known to decay rapidly with distance (*12*, *38*). These three ET regimes are essentially independent of protein orientation (figs. S1 and S2). We refer to the three regimes as the direct contact regime (short distances), the structured water–mediated regime (intermediate distances), and the bulk water–mediated regime (larger distances). Although the extended-Hückel method may introduce systematic errors, we expect it to capture the essential features of the bridge-mediated coupling and interference effects.

We have tested the consistency of a three-coupling regime model with ET self-exchange rates using a Brownian dynamics framework for computing the intermolecular ET rates (*28*, *29*, *35*). Table 1 shows that the computed ET rates are in good qualitative agreement with experimental self-exchange rates (*28*). Earlier simulation of Northrup and coworkers (*28*) based on single-exponent models with two adjustable parameters was also consistent with the data. The results of the present study lack adjustable T_{DA} parameters, although the quantitative accuracy of the

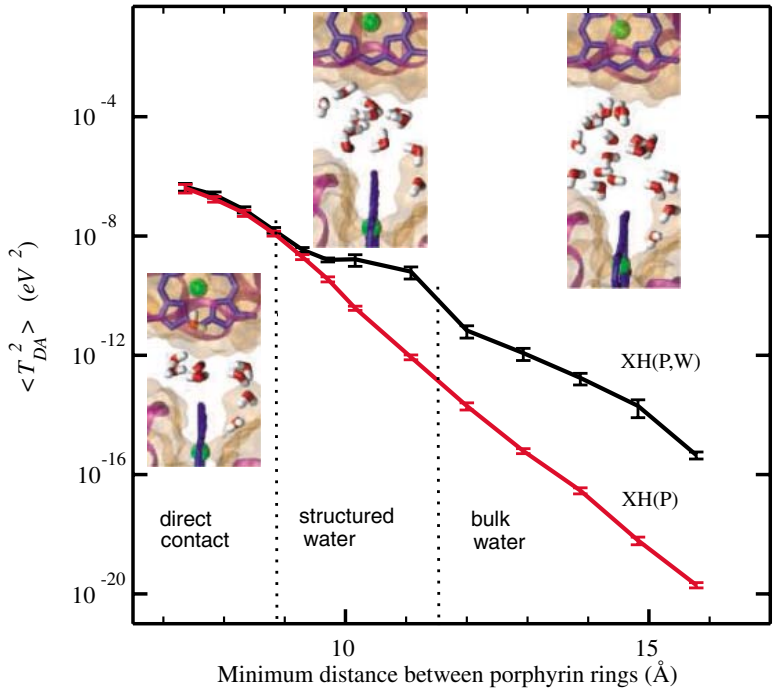

Fig. 1. The mean-square electronic coupling dependence on the distance between the two porphyrin rings (90° angle between porphyrin rings): XH(P,W), proteins and water included in the coupling calculation at the extended-Hückel level; XH(P), only protein mediation is included in the extended-Hückel coupling calculations. The three distance ranges correspond to the direct contact regime, structured water–mediated regime, and bulk water–mediated regime, respectively. The insets show configurations of the interfacial water molecules typical for each regime. The error bars show the sampling error estimated using a renormalization group-based method (*39*).

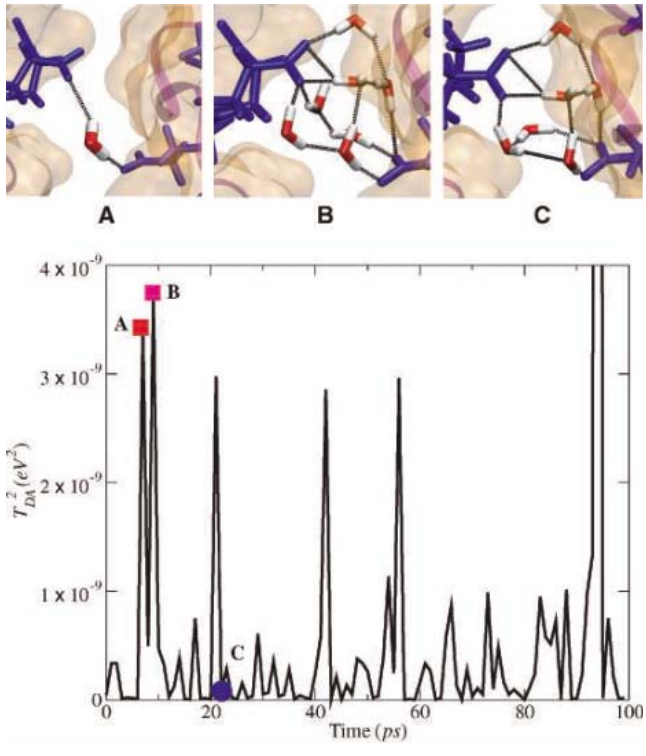

Fig. 2. A typical time series of computed T_{DA}^2 values in the structured water (plateau) regime. The relatively rare conformations that dominate the D-to-A coupling feature either a single dominant bridging water molecule (snapshot **A**), or several constructively interfering water-mediated pathways (snapshot **B**). In most of the time snapshots, the hydrogen-bonding network provides multiple ET pathways with mixed constructive and destructive interference, resulting in relatively small D-to-A coupling (snapshot **C**). The electrostatic and van der Waals interactions between the water and protein surfaces increase the probability of generating water-molecule configurations that provide large D-to-A coupling, leading to the smooth distance dependence of the ET rate in the plateau regime. The large peak at 94 ps arises from a constructively interfering coupling network established by three water molecules.

Table 1. Experimental (*28*) and theoretically estimated (Brownian dynamics) bimolecular rate constants k_2 (M^{-1} s^{-1}) for the cytochrome b_5 self-exchange ET as a function of ionic strength μ.

μ (M)	k_2 (M^{-1} s^{-1})	
	Experiment	Theory
0.1	2.6×10^3	1.0×10^3
0.3	4.6×10^3	2.4×10^4
0.6	1.6×10^4	7.6×10^4
1.0	2.8×10^4	1.1×10^5
1.5	4.5×10^4	1.7×10^5

extended-Hückel approach to electronic coupling calculation is certainly dependent on its parameterization.

The existence of multiple tunneling regimes also provides insight into several recent (and otherwise puzzling) experimental and theoretical observations in biological ET reaction kinetics. Winkler, Gray, and co-workers found that ET across protein-protein interfaces in protein crystals mediated by three water molecules is nearly as rapid as unimolecular ET is over the same distance (*7*). Canters and co-workers showed that water dimers between covalently cross-linked azurin complexes could substantially enhance the intermolecular ET kinetics (*15*). Similarly, Klinman and co-workers investigated the copper-to-copper ET over about 7 Å in the hydroxylating domain of peptidylglycine α-amidylating monooxygenase and found an unusually large electronic coupling mediated, apparently, by water rather than by the protein or substrate (*17*). Using Pathways-level analysis, Onuchic and co-workers found that water molecules mediate the dominant ET coupling routes between cytochrome c_2 and the photosynthetic reaction center (*18*). Cave and co-workers showed that water molecules between model D and A pairs substantially enhance intermolecular ET rates as well (*19*). All of these recent observations support our conclusion that a small number of structured water molecules interposed between the donor and the acceptor cofactors can substantially enhance ET rates.

The influence of aqueous tunneling pathways on interprotein ET kinetics has remained a key open issue in biological ET for some time. Single-exponential decay models fail to describe water-mediated ET reactions properly. The existence of multiple tunneling mediating regimes identified above is evinced by a body of recent experimental and theoretical observations. Most importantly, the structured water coupling regime may provide an important mechanism to facilitate ET reactions in the critical near-contact distance range relevant to biological ET kinetics. We hypothesize that water may be a particularly strong tunneling mediator when it occupies a sterically constrained space between redox cofactors with strong organizing forces that favor constructively interfering coupling pathways. It will be particularly interesting to use both theory and experiment to explore how the water-mediated coupling between proteins varies with protein-protein shape complementarity, surface charge and polarity, and dynamical fluctuations of the proteins and of the organized water at the interface.

References and Notes

1. J. M. Berg, L. Stryer, J. L. Tymoczko, *Biochemistry* (Freeman, New York, ed. 5, 2002).
2. H. B. Gray, J. R. Winkler, *Proc. Natl. Acad. Sci. U.S.A.* **102**, 3534 (2005).
3. Z. X. Liang *et al.*, *J. Am. Chem. Soc.* **126**, 2785 (2004).
4. A. Osyczka, C. C. Moser, F. Daldal, P. L. Dutton, *Nature* **427**, 607 (2004).
5. H. B. Gray, J. R. Winkler, *Q. Rev. Biophys.* **36**, 341 (2003).
6. R. E. Blankenship, *Nat. Struct. Biol.* **8**, 94 (2001).
7. F. A. Tezcan, B. R. Crane, J. R. Winkler, H. B. Gray, *Proc. Natl. Acad. Sci. U.S.A.* **98**, 5002 (2001).
8. G. McLendon, R. Hake, *Chem. Rev.* **92**, 481 (1992).
9. R. A. Marcus, N. Sutin, *Biochim. Biophys. Acta* **811**, 265 (1985).
10. S. S. Skourtis, I. A. Balabin, T. Kawatsu, D. N. Beratan, *Proc. Natl. Acad. Sci. U.S.A.* **102**, 3552 (2005).
11. I. A. Balabin, J. N. Onuchic, *Science* **290**, 114 (2000).
12. M. Jones, I. V. Kurnikov, D. N. Beratan, *J. Phys. Chem. A* **106**, 2002 (2002).
13. C. C. Page, C. C. Moser, X. X. Chen, P. L. Dutton, *Nature* **402**, 47 (1999).
14. M.-L. Tan, I. A. Balabin, J. N. Onuchic, *Biophys. J.* **86**, 1813 (2004).
15. I. M. C. van Amsterdam *et al.*, *Nat. Struct. Biol.* **9**, 48 (2002).
16. R. N. Barnett, C. L. Cleveland, U. Landman, G. B. Schuster, *Science* **294**, 567 (2001).
17. W. A. Francisco, G. Wille, A. J. Smith, D. J. Merkler, J. P. Klinman, *J. Am. Chem. Soc.* **126**, 13168 (2004).
18. O. Miyashita, M. Y. Okamura, J. N. Onuchic, *Proc. Natl. Acad. Sci. U.S.A.* **102**, 3558 (2005).
19. N. E. Miller, M. C. Wander, R. J. Cave, *J. Phys. Chem. A* **103**, 1084 (1999).
20. O. S. Wenger, B. S. Leigh, R. M. Villahermosa, H. B. Gray, J. R. Winkler, *Science* **307**, 99 (2005).
21. A. Ponce, H. B. Gray, J. R. Winkler, *J. Am. Chem. Soc.* **122**, 8187 (2000).
22. I. Benjamin, D. Evans, A. Nitzan, *J. Chem. Phys.* **106**, 6647 (1997).
23. M. D. Newton, *J. Electroanal. Chem.* **438**, 3 (1997).
24. S. Larsson, *J. Phys. Chem.* **88**, 1321 (1984).
25. J. R. R. Verlet, A. E. Bragg, A. Kammrath, O. Cheshnovsky, D. M. Neumark, *Science* **307**, 93 (2004).
26. K. Onda *et al.*, *Science* **308**, 1154 (2005).
27. R. C. E. Durley, F. S. Mathews, *Acta Crystallogr.* **D52**, 65 (1996).
28. S. M. Andrew, K. A. Thomasson, S. H. Northrup, *J. Am. Chem. Soc.* **115**, 5516 (1993).
29. S. H. Northrup, J. O. Boles, J. C. L. Reynolds, *Science* **241**, 67 (1988).
30. P. Strittmatter *et al.*, *Proc. Natl. Acad. Sci. U.S.A.* **71**, 4565 (1974).
31. E. Hegesh, J. Hegesh, A. N. Kaftory, *N. Engl. J. Med.* **314**, 757 (1986).
32. R. E. Utecht, D. M. Kurtz Jr., *Biochim. Biophys. Acta* **953**, 164 (1988).
33. D. W. Dixon, X. Hong, S. E. Woehler, A. G. Mauk, B. P. Sishta, *J. Am. Chem. Soc.* **112**, 1082 (1990).
34. W. L. Jorgensen, J. Chandrasekhar, J. D. Madura, R. W. Impey, M. L. Klein, *J. Chem. Phys.* **79**, 926 (1983).
35. Details of system setup, electronic structure, molecular dynamics, and Brownian dynamics simulations are available on *Science* Online.
36. T. Kawatsu, T. Kakitani, T. Yamato, *J. Phys. Chem. B* **106**, 5068 (2002).
37. P. Siddarth, R. A. Marcus, *J. Phys. Chem.* **97**, 1308 (1993).
38. D. N. Beratan, J. N. Betts, J. N. Onuchic, *Science* **252**, 1285 (1991).
39. H. Flyvbjerg, H. G. Petersen, *J. Chem. Phys.* **91**, 461 (1989).

40. This work was supported by the NIH (GM-048043). We are grateful to H. B. Gray and J. R. Winkler for stimulating discussions. We thank T. Kawatsu for providing code for the XH calculations, I. V. Kurnikov for providing code for the Pathways-based and atomic packing density-based calculations, and M. A. Pasquinelli for assistance with the Brownian dynamics calculations.

Supporting Online Material

www.sciencemag.org/cgi/content/full/310/5752/1311/DC1
SOM Text
Figs. S1 to S6
References

2 August 2005; accepted 20 October 2005
10.1126/science.1118316

Stable Carbon Cycle–Climate Relationship During the Late Pleistocene

Urs Siegenthaler,[1] Thomas F. Stocker,[1]* Eric Monnin,[1] Dieter Lüthi,[1] Jakob Schwander,[1] Bernhard Stauffer,[1] Dominique Raynaud,[2] Jean-Marc Barnola,[2] Hubertus Fischer,[3] Valérie Masson-Delmotte,[4] Jean Jouzel[4]

A record of atmospheric carbon dioxide (CO_2) concentrations measured on the EPICA (European Project for Ice Coring in Antarctica) Dome Concordia ice core extends the Vostok CO_2 record back to 650,000 years before the present (yr B.P.). Before 430,000 yr B.P., partial pressure of atmospheric CO_2 lies within the range of 260 and 180 parts per million by volume. This range is almost 30% smaller than that of the last four glacial cycles; however, the apparent sensitivity between deuterium and CO_2 remains stable throughout the six glacial cycles, suggesting that the relationship between CO_2 and Antarctic climate remained rather constant over this interval.

The European Project for Ice Coring in Antarctica (EPICA) recovered two deep ice cores from East Antarctica. One of the cores, located at Dome Concordia (Dome C) (75°06′S, 123°21′E, altitude of 3233 m above sea level, and mean annual accumulation rate of 25.0

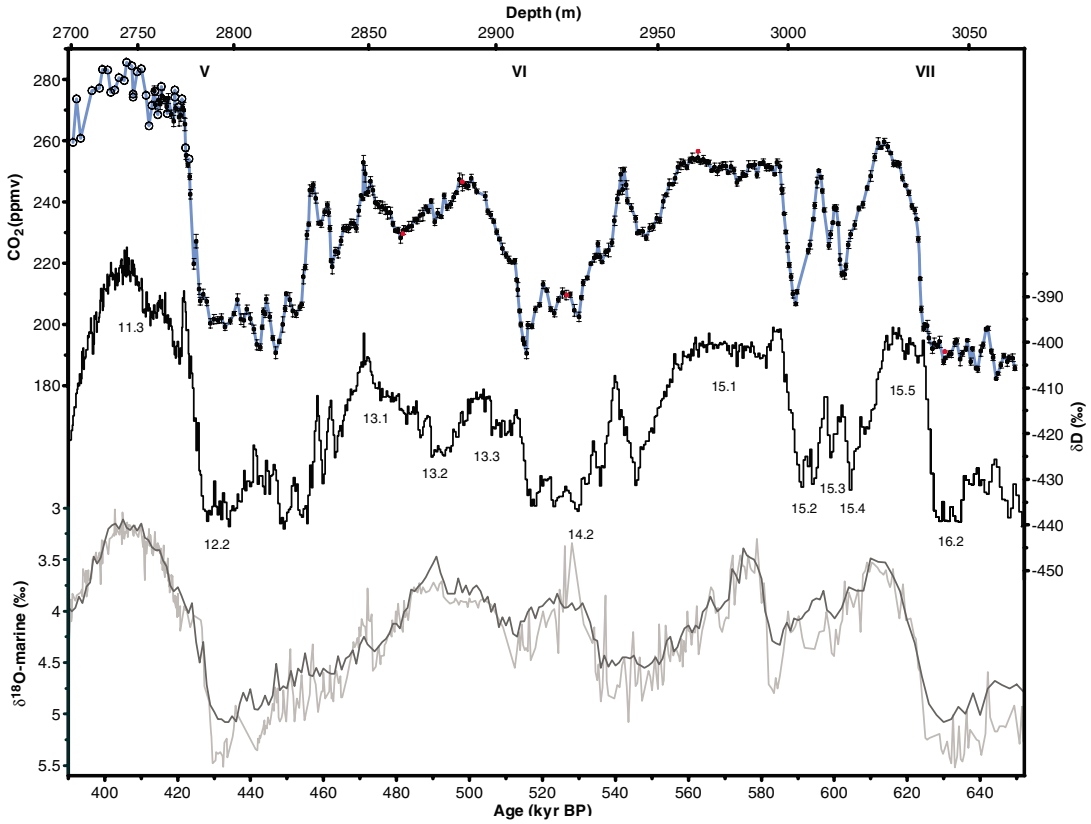

Fig. 1. Dome C CO_2 Bern data (black solid circles) are the mean of four to six samples, including the data from 31 depth intervals over termination V of (*1*); error bars denote 1σ of the mean. Red solid circles are test measurements with the use of the sublimation extraction technique. Dome C CO_2 Grenoble data are shown as black open circles. Dome C CO_2 measurements are connected with a blue line, and the high-resolution deuterium record is given as a black line (*18*). Benthic $\delta^{18}O$ stack and benthic $\delta^{18}O$ record from ODP site 980 are shown as a dark gray line (*19*) and a light gray line (*19*–*22*), respectively. The EDC2 time scale for Dome C is the same as in (*1*) (the depths at the top of the figure are only valid for the CO_2 record). Glacial terminations are given in roman numerals; marine isotope stages are given in arabic numerals according to (*17*).

kg m^{-2} $year^{-1}$), is the only ice core covering at least eight glacial cycles (*1*), four cycles longer than previously available from ice cores. This has allowed us to reconstruct the record of the concentration of atmospheric CO_2 much further back in time than was possible before. Here, we report results from the interval between 390 and 650 kyr B.P. (kyr B.P. is thousand years before the present, i.e., before A.D. 1950).

Analyzing the air extracted from ice cores is the only way to directly determine atmospheric greenhouse gas concentrations for times before routine atmospheric measurements were begun. Antarctic ice cores are very suitable for CO_2 measurements because of their low temperatures and low concentrations of impurities, which minimize the risk of artifacts. Data from different Antarctic ice cores (*2*–*13*) and drilled at sites with different temperatures, accumulation rates, and impurity concentrations [except cores with summer melting (*14*) and where elevated CO_2 values by up to 20 parts per million by volume (ppmv) are found] demonstrate that Antarctic ice cores are reliable recorders of atmospheric CO_2.

The concentrations of atmospheric CO_2 during the past four glacial cycles measured in the Vostok ice core vary between glacial and interglacial values of 180 ppmv and 280 to 300 ppmv, respectively (*7*). Including the data from Petit *et al.* (*7*), Fischer *et al.* (*5*) and Kawamura *et al.* (*10*), the lowest and highest values measured during a glacial cycle are on average 182 ± 4 ppmv (±1 standard deviation) and 296 ± 7 ppmv, respectively. This stable range of natural CO_2 variations on glacial-interglacial time scales led to the suggestion that feedbacks in the climate influence on the global carbon cycle maintain the rather narrow range observed (*15*).

The Dome C CO_2 record [mean sampling resolution of 731 years; details about the methods and the sampling are given in (*16*)] is plotted in Fig. 1, together with the δD record (Antarctic temperature proxy) of Dome C (*18*) [both records are shown on the EDC2 time scale (*1*)], a stack of benthic $\delta^{18}O$ records from globally distributed sites (*19*), and a high-resolution benthic $\delta^{18}O$ record from Ocean Drilling Project (ODP) site 980 (55°29′N, 14°42′W) (*19*–*22*). There is an excellent overall correlation between δD and benthic $\delta^{18}O$, a proxy of global ice volume (*19*).

First, we discuss the main features of the CO_2 record from Dome C from 650 to 390 kyr B.P. Our measurements begin at 650 kyr B.P., close to the lowest value for the entire record of 182 ppmv at 644 kyr B.P.. At marine isotope stage (MIS) 16, the CO_2 concentration is about 190 ppmv before the onset of termination VII. The entire transition between glacial and interglacial δD values occurred rapidly, within 3 kyear (ky) with the EDC2 dating. As expected from firnification processes, the corresponding CO_2 increase occurred deeper in the ice core, so there is no indication for an ice flow disturbance at this depth of about 3040 m, as has been observed at certain depths in the lowest 10% of some ice cores (*7*, *23*). After emerging slowly out of the baseline band, the CO_2 increase can be divided in two intervals. The first increase of 35 ppmv up to a CO_2 concentration of 235 ppmv takes less than 2 ky, whereas the second increase of another 20 ppmv takes about 5 ky. Although the CO_2 trend at the beginning of the interglacial MIS 15.5 does not show an early CO_2 peak as during the past four interglacials, this second CO_2 increase is very similar in magnitude (20 ppmv) and duration (5 ky) to the Holocene one, although evolving with generally lower CO_2 values by about 25 ppmv. Therefore, the Holocene increase during the last 8 kyear is not an anomalous trend in comparison to other interglacials as postulated recently (*24*); instead it is a likely response of the carbon cycle

[1]Climate and Environmental Physics, Physics Institute, University of Bern, Sidlerstrasse 5, CH-3012 Bern, Switzerland. [2]Laboratoire de Glaciologie et de Géophysique de l'Environnement (CNRS), 54 Rue Molières, 38402 St. Martin d'Hères Cedex, France. [3]Alfred Wegener Institute for Polar and Marine Research (AWI), Columbusstrasse, D-27568 Bremerhaven, Germany. [4]Institut Pierre Simon Laplace/ Laboratoire des Sciences du Climat et de l'Environnement, CEA-CNRS 1572, CE Saclay, Orme des Merisiers, 91191 Gif-sur-Yvette, France.

*To whom correspondence should be addressed. E-mail: stocker@climate.unibe.ch

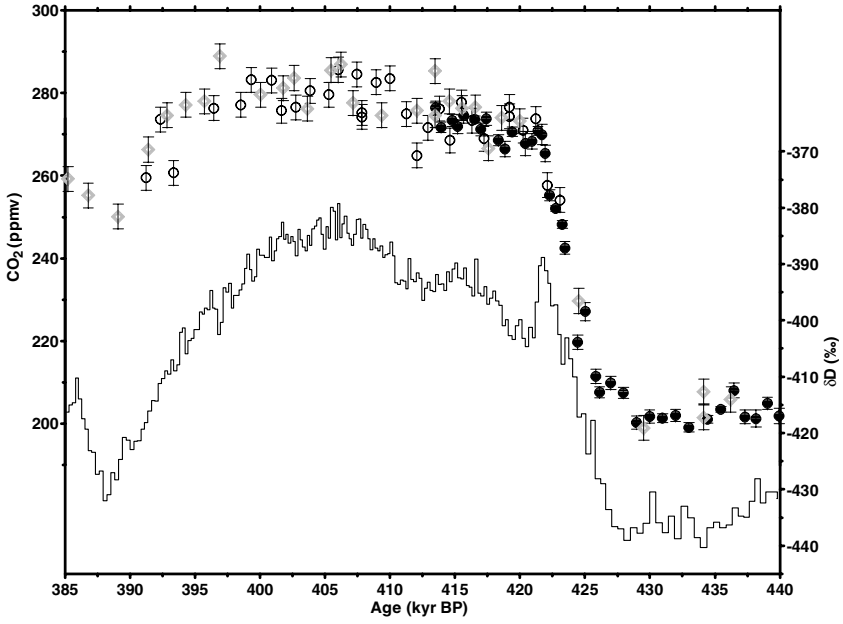

Fig. 2. CO_2 results of entire MIS 11, including end of MIS 12. Dome C CO_2 Bern data (solid circles) from EPICA community members (*1*) and this work; error bars, 1σ of the mean. Dome C CO_2 Grenoble data are indicated by open circles; error bars, accuracy of 2σ = 3 ppmv. High-resolution deuterium record is shown as a black line (*18*). Vostok CO_2 Grenoble data are indicated by gray open diamonds; error bars, accuracy of 2σ = 3 ppmv on the corrected time scale (*28*).

to large changes in biomass (*25*). At the end of MIS 15.5, CO_2 attains its local maximum of about 260 ppmv, which is the highest concentration in the record before MIS 11 but substantially lower than the interglacial concentrations measured during the last four glacial cycles. At MIS 15.4 and MIS 15.2, the deuterium record indicates near-glacial conditions, only interrupted by two peaks at MIS 15.3. During the time interval of MIS 15.4 to 15.2, CO_2 shows rather large variations, with values between 207 ppmv and 250 ppmv and with two peaks during MIS 15.3 that are very similar to the deuterium peaks. The lowest values are close to glacial CO_2 concentrations, which raise the question of whether MIS 15 was a single continuous interglacial or multiple ones.

The increases of CO_2 and δD into MIS 15.1 are very uniform and take 4 to 5 ky for each component. An unexpected feature is the very stable and long-lasting MIS 15.1. In contrast to the increasing global ice volume suggested by the benthic records of marine sediments (Fig. 1) (*19*), all indicators from Dome C exhibit almost constant values during MIS 15.1. This is observed in the records of deuterium (*1*), of CH_4 (*26*), and of aerosols (*27*) of the Dome C ice core but is most pronounced in our CO_2 results. We find a stable 251.5 ± 1.9 ppmv (±1 standard deviation) CO_2 concentration from 585 kyr B.P. to 557 kyr B.P. on the EDC2 time scale, which is unprecedented in any other time interval covered by previous CO_2 measurements on ice cores. This result suggests that the global carbon cycle operated in an exceptionally stable mode for many millennia. The current estimate for the duration of MIS 15.1, on the basis of the EDC2 time scale, is 28,000 years. Accordingly, this interval is a prime target for developing a better understanding of the influence of orbital geometry on climate and the global carbon cycle. However, we cannot, at this stage, exclude the possibility that at least part of the exceptionally long duration of stable conditions could be due to an exceptionally low thinning rate of the corresponding ice layer.

The decrease in δD from the end of MIS 15.1 to the start of MIS 14.2 is interrupted by a double peak, the older of which is most pronounced with a corresponding peak in the CO_2 record and with elevated values by more than 20 ppmv. The phase relationship between CO_2 and deuterium for this event is dicussed later in the text. The deuterium increase to the maximum value of MIS 13.3 ("termination" VI) evolves in two steps, with a rather stable concentration in between and a difference between glacial and interglacial values that is smaller in comparison to any other termination during the past 650 ky. The CO_2 increase can be divided again into two intervals, as for termination VII. The first increase of 30 ppmv takes 3 ky, whereas the duration for the second increase of 20 ppmv is more than 8 ky. During MIS 13, CO_2 values are in the range of about 230 to 250 ppmv, with a minimum at 481 kyr B.P. This minimum lags the deuterium minimum by about 10 ky. The decrease to MIS 12.2 is interrupted by another prominent set of deuterium and CO_2 double peaks. During MIS 12.2 (and also MIS 16.2) we find pronounced millennial CO_2 fluctuations of 10 to 20 ppmv. They are comparable in duration and amplitude to the distinct CO_2 peaks observed during the past four Antarctic warm events (A1 to A4) during the last glacial (*4*, *8*).

A detailed comparison with Vostok data (*28*) during MIS 11, an interglacial period that occurred some 400,000 years ago and lasted for about 30,000 years, is shown in Fig. 2 in order to examine the consistency of CO_2 values measured in this deep ice. Both records agree within the error limits and show interglacial CO_2 concentrations in MIS 11 similar to those found in the Holocene. Accordingly, we are confident that the Dome C data in the pre-Vostok era reflect true atmospheric CO_2 concentrations.

The coupling of CO_2 and δD is strong. The overall correlation between CO_2 data and Antarctic temperature during the time period of 390 to 650 kyr B.P. is $r^2 = 0.71$. Taking into account only the period 430 to 650 kyr B.P., where amplitudes of deuterium and CO_2 are smaller, the correlation is $r^2 = 0.57$. Corrections for changes in the temperature and δD of the water vapor source, which also affect δD of the ice, have not been made yet. The strong coupling of CO_2 to Antarctic temperature confirms earlier observations for the last glacial termination (*9*) and the past four glacial cycles (*7*) and supports the hypothesis that the Southern Ocean played an important role in causing CO_2 variations.

δD as a function of CO_2 from the Vostok (MIS 1 to MIS 11) and Dome C ice cores [MIS 12 to 16, Holocene (*11*), and termination I (*9*)] is shown in Fig. 3. The offset in the deuterium values of Dome C and Vostok is due to the different distances to the open ocean, elevations, and surface temperatures of the two sites (*29*). It is remarkable that the slope of the three records is essentially the same. This suggests that the coupling of Antarctic temperature and CO_2 did not change substantially during the last 650 ky.

Another important parameter elucidating the coupling of atmospheric CO_2 and Antarctic temperature is their relative phasing. Because of the enclosure process of air in ice, the phase relationship of CO_2 and δD is associated with uncertainties. Because the enclosed air is younger than the surrounding ice (*30*), CO_2 is plotted on a gas age chronology, whereas deuterium is plotted on an ice age chronology. For Dome C and the period under investigation, the gas age/ice age difference (Δ age) is in the range of 1.9 to 5.5 ky (fig. S1). The estimated uncertainty of Δ age in the upper 800 m of

the Dome C ice core is about 10% (*31*), neglecting uncertainties in the thinning rate. Deviations from the modeled thinning would introduce systematic errors in Δ age.

By shifting the time scales of the entire CO_2 and deuterium records between 390 and 650 kyr B.P. relative to each other, we obtained the best correlation for a lag of CO_2 of 1900 years. This lag is significant considering the uncertainties of Δ age. Over the glacial terminations V to VII, the highest correlation of CO_2 and deuterium, with use of a 20-ky window for each termination, yields a lag of CO_2 to deuterium of 800, 1600, and 2800 years, respectively. This value is consistent with estimates based on data from the past four glacial cycles. Fischer *et al.* (*5*) concluded that CO_2 concentrations lagged Antarctic warmings by 600 ± 400 years during the past three transitions. Monnin *et al.* (*9*) found a lag of 800 ± 600 years for termination I, and Caillon *et al.* (*32*), with use of the isotopic composition of argon in air bubbles instead of deuterium, calculated a value of 800 ± 200 years for termination III. Overall, the estimated lags over the entire Dome C record between 390 and 650 kyr B.P. and over the three terminations in this time period are small compared with glacial-interglacial time scales and do not cast doubt on the strong coupling of CO_2 and temperature or on the importance of CO_2 as a key amplification factor of the large observed temperature variations of glacial cycles.

An apparent exception of the lag of CO_2 to deuterium observed over most of the record occurs around 534 to 548 kyr B.P., where CO_2 seems to lead δD by about 2000 ± 500 year. We cannot conclude with certainty whether the observed lead of CO_2 at this time is real or an artefact in the EDC2 time scale. To make the CO_2 and the δD peaks simultaneous, we would need to increase the modeled depth offset of the gas record and the ice record (Δ depth) from 4.3 m to 7 m (fig. S2). This can be achieved by a reduced thinning rate, an increased accumulation rate, a decreased temperature, or a combination of them. However, because accumulation and temperature are strongly positively correlated at present (*33*), the required change in accumulation or temperature, or a change of both, is rather unlikely. An anomalously low thinning rate is therefore the more likely way to produce such an artefact in the EDC2 time scale.

A composite CO_2 record over six and a half ice age cycles back to 650,000 yr B.P. is shown in Fig. 4, created from a combination of records from the Dome C, Taylor Dome, and Vostok ice cores. This record shows the differences in amplitudes of CO_2 and deuterium before and after 430 kyr B.P. and demonstrates, within the resolution of our measurements, that the atmospheric concentration of CO_2 did not exceed 300 ppmv for the last 650,000 years before the preindustrial era.

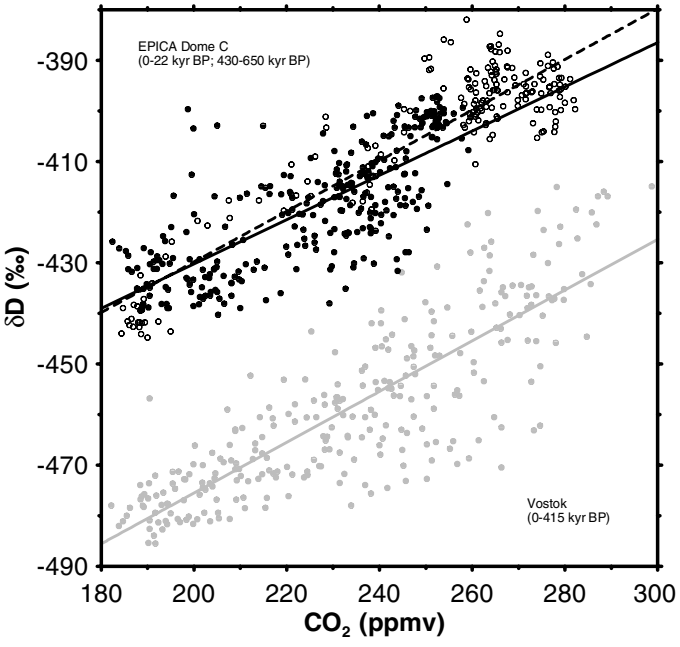

Fig. 3. Correlation between δD, a proxy for Antarctic temperature, and CO_2 for three data sets. The new data from Dome C cover the beginning of MIS 12 to MIS 16 (black solid circles; black line is the linear fit δD = 0.44‰ $ppmv^{-1}$ × CO_2 – 517.75‰, r^2 = 0.57), and the period from MIS 1 to MIS 11 is covered by data from the Vostok ice core [gray solid circles (*7*); gray line is linear fit, δD = 0.50‰ $ppmv^{-1}$ × CO_2 – 575.86‰, r^2 = 0.70] and Dome C Holocene and termination I [black open circles (*9*, *11*); black dashed line is the linear fit, δD = 0.50‰ $ppmv^{-1}$ × CO_2 – 529.87‰, r^2 = 0.84]. The offset in the δD values from these two cores is due to the different distances to the open ocean, elevations, and surface temperatures of the two sites (*29*).

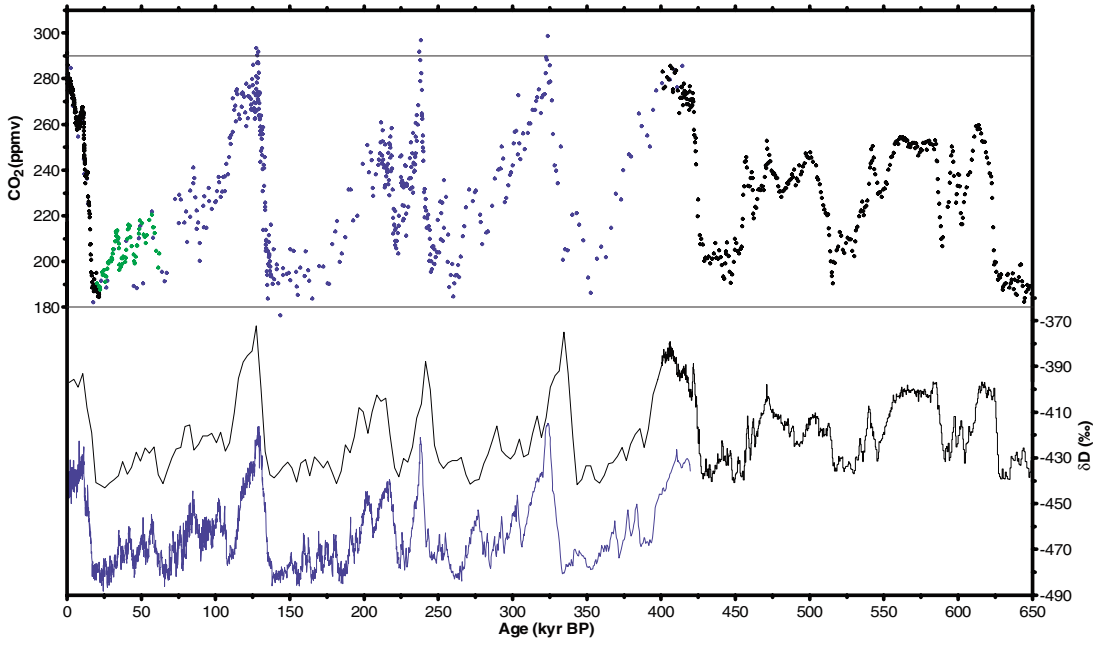

Fig. 4. A composite CO_2 record over six and a half ice age cycles, back to 650,000 years B.P. The record results from the combination of CO_2 data from three Antarctic ice cores: Dome C (black), 0 to 22 kyr B.P. (*9*, *11*) and 390 to 650 kyr B.P. [this work including data from 31 depth intervals over termination V of (*1*)]; Vostok (blue), 0 to 420 kyr B.P. (*5*, *7*), and Taylor Dome (light green), 20 to 62 yr B.P. (*8*). Black line indicates δD from Dome C, 0 to 400 kyr B.P. (*1*) and 400 to 650 kyr B.P. (*18*). Blue line indicates δD from Vostok, 0 to 420 kyr B.P. (*7*).

The CO_2 record from the EPICA Dome C ice core reveals that atmospheric CO_2 variations during glacial-interglacial cycles had a notably different character before and after 430 kyr B.P. Before MIS 11, the amplitude of temperature was lower, and the duration of the warm phases has been much longer since then. In spite of these differences, the significant covariation of δD and CO_2 is valid in both periods. Before MIS 11, CO_2 concentrations did not exceed 260 ppmv. This is substantially lower than the maxima of the last four glacial cycles. The lags of CO_2 with respect to the Antarctic temperature over glacial terminations V to VII are 800, 1600, and 2800 years, respectively, which are consistent with earlier observations during the last four glacial cycles.

Our measurements have revealed an unexpected stable climate phase (MIS 15.1) during which the atmospheric CO_2 concentration was 251.5 ± 1.9 ppmv for many millennia (28,000 years, based on the EDC2 time scale), although the duration of MIS 15.1 is uncertain because of possible inaccuracies in the Dome C EDC2 time scale between MIS 12 and 15. However, the roughly 30,000-year duration of MIS 11 (and possibly MIS 15.1) demonstrates that long interglacials with stable conditions are not exceptional. Short interglacials such as the past three therefore are not the rule and hence cannot serve as analogs of the Holocene, as postulated recently (*24*). Examining δD as a function of CO_2, we observe that the slope during the two new glacial cycles compared to the last four cycles is essentially the same. Therefore, the coupling of Antarctic temperature and CO_2 did not change significantly during the last 650 kyear, indicating rather stable coupling between climate and the carbon cycle during the late Pleistocene.

References and Notes

1. L. Augustin *et al.*, (EPICA community members), *Nature* **429**, 623 (2004).
2. J.-M. Barnola, D. Raynaud, Y. S. Korotkevich, C. Lorius, *Nature* **329**, 408 (1987).
3. D. M. Etheridge *et al.*, *J. Geophys. Res.* **101**, 4115 (1996).
4. B. Stauffer *et al.*, *Nature* **392**, 59 (1998).
5. H. Fischer, M. Wahlen, J. Smith, D. Mastroianni, B. Deck, *Science* **283**, 1712 (1999).
6. A. Indermühle *et al.*, *Nature* **398**, 121 (1999).
7. J. R. Petit *et al.*, *Nature* **399**, 429 (1999).
8. A. Indermühle, E. Monnin, B. Stauffer, T. F. Stocker, M. Wahlen, *Geophys. Res. Lett.* **27**, 735 (2000).
9. E. Monnin *et al.*, *Science* **291**, 112 (2001).
10. K. Kawamura *et al.*, *Tellus* **55B**, 126 (2003).
11. E. Monnin *et al.*, *Earth Planet. Sci. Lett.* **224**, 45 (2004).
12. U. Siegenthaler *et al.*, *Tellus* **57B**, 51 (2005).
13. J. Flückiger *et al.*, *Global Biogeochem. Cycles* **16**, 1010 (2002).
14. J. Ahn *et al.*, *J. Geophys. Res.* **109**, 10.1029/2003JD004415 (2004).
15. P. Falkowski *et al.*, *Science* **290**, 291 (2000).
16. Supplementary information concerning methods or assumptions is available on *Science* Online.
17. F. C. Bassinot *et al.*, *Earth Planet. Sci. Lett.* **126**, 91 (1994).
18. J. Jouzel *et al.*, in preparation.
19. L. E. Lisiecki, M. E. Raymo, *Paleoceanography* **20**, 10.1029/2004PA001071 (2005).
20. D. W. Oppo, J. F. McManus, J. L. Cullen, *Science* **279**, 1335 (1998).
21. J. F. McManus, D. W. Oppo, J. L. Cullen, *Science* **283**, 971 (1999).
22. B. P. Flower *et al.*, *Paleoceanography* **15**, 388 (2000).
23. A. Landais *et al.*, *J. Geophys. Res.* **109**, 10.1029/2003JD004193 (2004).
24. W. F. Ruddiman, *Clim. Change* **61**, 261 (2003).
25. F. Joos, S. Gerber, I. C. Prentice, B. L. Otto-Bliesner, P. J. Valdes, *Global Biogeochem. Cycles* **18**, 10.1029/2003GB002156 (2004).
26. R. Spahni *et al.*, *Science* **310**, 1317 (2005).
27. E. W. Wolff *et al*, in preparation.
28. D. Raynaud *et al.*, *Nature* **436**, 39 (2005).
29. V. Masson *et al.*, *Quaternary Res.* **54**, 348 (2000).
30. J. Schwander, B. Stauffer, *Nature* **311**, 45 (1984).
31. J. Schwander *et al.*, *Geophys. Res. Lett.* **28**, 4243 (2001).
32. N. Caillon *et al.*, *Science* **299**, 1728 (2003).
33. J. Jouzel *et al.*, *Nature* **329**, 403 (1987).

34. We thank K. Kawamura and G. Teste for assisting with the CO_2 measurements, L. Lisiecki and M. Raymo for access to the data of (*19*), and R. Spahni and F. Parrenin for fruitful discussions. This work is a contribution to the EPICA, a joint European Science Foundation/European Commission (EC) scientific program funded by the EC and by national contributions from Belgium, Denmark, France, Germany, Italy, Netherlands, Norway, Sweden, Switzerland, and United Kingdom. We acknowledge long-term financial support by the Swiss National Science Foundation, the University of Bern, the Swiss Federal Office of Energy, and EC Project EPICA-MIS. This is EPICA publication no. 133.

Supporting Online Material

www.sciencemag.org/cgi/content/full/310/5752/1313/DC1
Materials and Methods
Figs. S1 and S2
References

13 September 2005; accepted 1 November 2005
10.1126/science.1120130

Atmospheric Methane and Nitrous Oxide of the Late Pleistocene from Antarctic Ice Cores

Renato Spahni,[1] Jérôme Chappellaz,[2] Thomas F. Stocker,[1]* Laetitia Loulergue,[2] Gregor Hausammann,[1] Kenji Kawamura,[1]† Jacqueline Flückiger,[1]‡ Jakob Schwander,[1] Dominique Raynaud,[2] Valérie Masson-Delmotte,[3] Jean Jouzel[3]

The European Project for Ice Coring in Antarctica Dome C ice core enables us to extend existing records of atmospheric methane (CH_4) and nitrous oxide (N_2O) back to 650,000 years before the present. A combined record of CH_4 measured along the Dome C and the Vostok ice cores demonstrates, within the resolution of our measurements, that preindustrial concentrations over Antarctica have not exceeded 773 ± 15 ppbv (parts per billion by volume) during the past 650,000 years. Before 420,000 years ago, when interglacials were cooler, maximum CH_4 concentrations were only about 600 ppbv, similar to lower Holocene values. In contrast, the N_2O record shows maximum concentrations of 278 ± 7 ppbv, slightly higher than early Holocene values.

Earth's climate during the late Pleistocene was characterized by ice age cycles with relatively short warm periods (interglacials) and longer cold periods (glacials) (*1*). The Vostok ice core provided an archive of climate and atmospheric composition over the past four climatic cycles back to marine isotope stage (MIS) 11, about 420 thousand years before the present (420 kyr B.P.) (*2*). That record demonstrated the high correlation of temperature changes with greenhouse gas concentration changes in the atmosphere in the past. The European Project for Ice Coring in Antarctica (EPICA) Dome Concordia (Dome C) ice core (75°06′S, 123°21′E, 3233 m above sea level) provides an ice core archive much longer, spanning eight climatic cycles over the past 740 thousand years (ky) (*3*). It demonstrates that the oldest four interglacials were cooler but lasted longer than the younger interglacials. Such findings raise the question whether the greenhouse gases CH_4 and N_2O behaved differently before MIS 11. Here, we present CH_4 and N_2O records derived from the EPICA Dome C ice cores reaching back to 650 kyr B.P.

[1]Climate and Environmental Physics, Physics Institute, University of Bern, Sidlerstrasse 5, CH-3012 Bern, Switzerland. [2]Laboratoire de Glaciologie et Géophysique de l'Environnement (LGGE, CNRS-UJF), CNRS, 54 Rue Molières, 38402 St. Martin d'Hères, Grenoble, France. [3]Institut Pierre Simon Laplace/Laboratoire des Sciences du Climat et de l'Environnement, CEA-CNRS 1572, CE Saclay, Orme des Merisiers, 91191 Gif-sur-Yvette, France.

*To whom correspondence should be addressed: stocker@climate.unibe.ch
†Present address: Scripps Institution of Oceanography, University of California, San Diego, 9500 Gilman Drive, La Jolla, CA 92093–0244, USA.
‡Present address: Institute of Arctic and Alpine Research, University of Colorado at Boulder, 450 UCB Boulder, Colorado 80309–0450, USA.

Extracting air from bubbles trapped in polar ice enables us to reconstruct directly the past composition of the atmosphere. The records of CH_4 and N_2O over the past thousand years (*4*–*6*), the Holocene (*7*, *8*), the transition from the last glacial maximum (LGM) to the Holocene (*6*, *9*), parts of the last glacial period (*10*–*14*), and the last four glacial-interglacial cycles (*2*, *15*–*17*) have provided important information about environmental changes in response to regional and global climate variations. Variations in the concentration of globally well-mixed atmospheric CH_4 are attributed to variations in the extent and the productivity of natural wetlands, the main natural sources (*18*). Similarly, variations in the atmospheric N_2O burden are thought to be dominated by variations in the global source strength. About two-thirds of the total preanthropogenic N_2O sources are terrestrial soils, and one-third are nitrification and denitrification processes in the ocean (*13*).

We present high-resolution records of CH_4 and N_2O covering MISs 2 to 7 (Fig. 1), to compare with existing records, and MISs 11 to 16 (Fig. 2), to extend the records back to an age of 650 kyr B.P. Measurements were performed along the EPICA Dome C ice cores (EDC96 and EDC99) at 553 and 476 different depth levels for CH_4 and N_2O, respectively, at the University of Bern and at Laboratoire de Glaciologie et Géophysique de l'Environnement (LGGE) (*19*). The mean CH_4 time resolution is 770 years for MISs 2 to 7 and 840 years for MISs 11 to 16. All ages and their uncertainties are based on the EPICA EDC2 gas and ice age scales (*3*). N_2O analyses were performed only at Bern. Their resolution is similar for MISs 2 to 7 (760 years) but lower for MISs 12 to 16 (1110 years). To be consistent with existing Dome C data, offset corrections for both gases and both laboratories have been applied (*19*).

The Dome C N_2O record is disturbed by artifacts in certain depth intervals as in other ice cores (*6*, *13*, *17*, *20*). High scattering of N_2O values is observed in depth intervals with elevated dust concentrations (*19*) (figs. S1 and S2) during parts of the cold periods MISs 2, 4, 6, 12, 14, and 16 (fig. S3). The EPICA Dome C dust record (*19*) is used to define depth intervals where the dust concentration exceeds 300 ppbw (parts per billion by weight). N_2O measurements in these depths are considered to be disturbed by artifacts and excluded from the record (fig. S3). The good agreement of the remaining record with records measured along other ice cores (Fig. 1) with different characteristics in the concentration of chemical impurities (*6*, *13*, *14*, *17*) supports the assumption that this record shows atmospheric concentrations of the past. Although all samples might be contaminated at some level, no outliers are observed during the

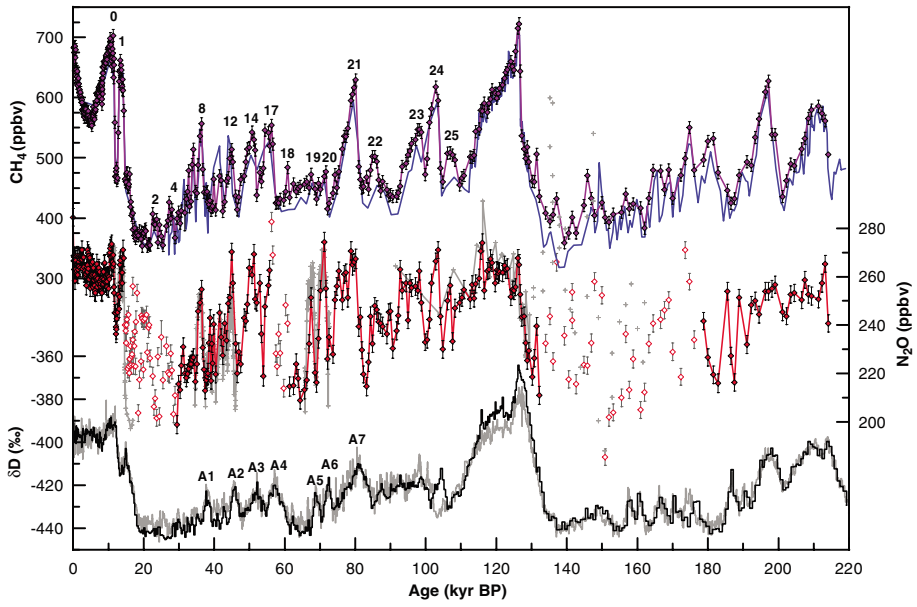

Fig. 1. Dome C CH_4 (purple line), N_2O (red line), and δD (black line) (*3*) records over the past 220 ky. Also shown are Vostok CH_4 data (blue line) (*2*, *15*) and δD data (gray line) (*2*). Vostok δD data were increased by 42‰ for better comparison. The Vostok CH_4 and δD records were individually synchronized to Dome C using wiggle matching (*35*). N_2O artifacts (open red diamonds) are separated from the N_2O record (red filled diamonds) with the aid of the dust record (figs. S1 to S3). Additionally, N_2O records published earlier (gray lines and crosses) (*6*, *13*, *17*), matched by CH_4 to Dome C, are shown for comparison. Error bars represent the 1 SD measurement uncertainty. Dome C CH_4 and N_2O data over the Holocene (*8*), the transition (*9*, *36*), and the LGM (*20*, *36*) are included in this data set. Dome C measurements covering the time period 0 to 40 kyr B.P. (depth interval 99.5 to 783.8 m) were performed along the EDC96 core, whereas older samples are from the EDC99 core. Numbers 0 to 25 above the CH_4 record denote D/O events (*23*), and A1 to A7 denote Antarctic warming events (*37*). Data are plotted on the EDC2 time scale (*3*).

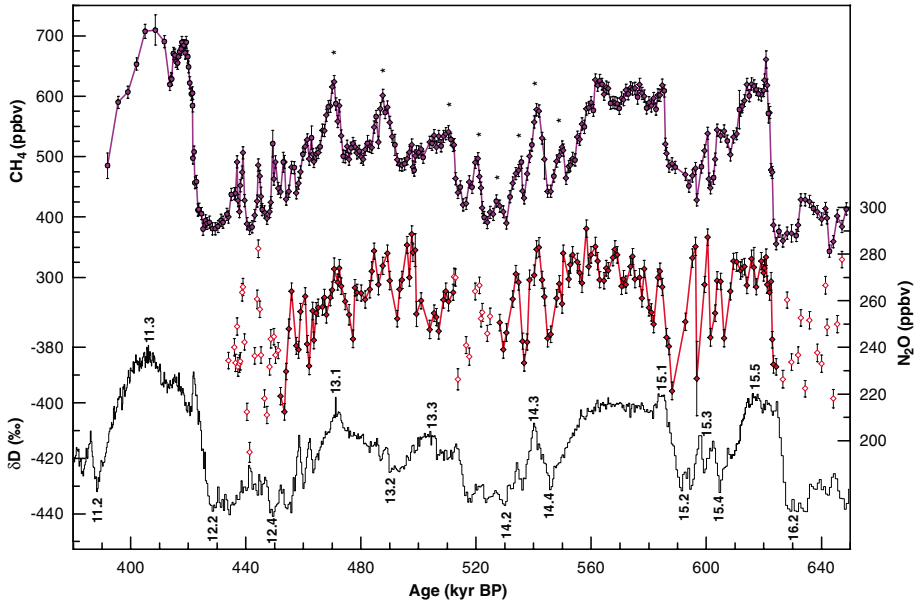

Fig. 2. Dome C CH_4 (purple line) and N_2O (red line) records over the period of MISs 11 to 16, together with high-resolution δD data from Dome C (*24*) (black line). CH_4 measurements performed at Bern are shown as purple diamonds, whereas LGGE measurements are shown as purple circles. N_2O artifacts (red open diamonds) are separated from the N_2O record (red filled diamonds) with the aid of the dust record (figs. S1 to S3). Error bars represent the 1 SD measurement uncertainty. Dome C CH_4 data over termination V (*3*) is included in this data set. Parts of the CH_4 record marked with a star (*) are regular events whose amplitude could be strongly influenced by the precession signal as seen in low-to mid-northern latitude summer insolation. MISs are labeled on the bottom (cold stages) and top (warm stages) of the δD record. Data are shown on the EDC2 time scale (*3*).

highly resolved Holocene. This supports our assumption that other interglacials are also likely free from artifacts.

The Dome C CH_4 data over the last two glacial cycles (Fig. 1) are in good agreement with the Vostok CH_4 record (*15*, *19*), as well as Greenland CH_4 records, when taking into account the interpolar difference (*7*, *21*) and the signal attenuation at low accumulation sites (*22*). The Dome C CH_4 data over the last glacial period confirm the close relation with the 25 Dansgaard/Oeschger (D/O) events as recorded in the North Greenland Ice-Core Project (NGRIP) temperature proxies (*23*). In addition, we find that N_2O also varied during the last glacial period in parallel with the most prominent D/O events (Fig. 1), in agreement with previous results (*6*, *13*, *14*, *16*). N_2O reaches Holocene concentrations of 253 to 272 ppbv (parts per billion by volume) (single values) (*8*) during the maximum of some of these events and during the last interglacial (*14*, *17*). The lowest values found, about 200 ppbv, are similar to those in records published earlier (*13*, *14*). Because the CH_4 and N_2O measurements were performed on the same extracted air samples, a direct comparison without relative time uncertainty is possible between the two gases. The start and end points of single D/O events in CH_4 and N_2O do not necessarily coincide (*13*); e.g., the N_2O concentrations at D/O event 21 start to rise more than 1000 years earlier than CH_4 concentrations. Furthermore, N_2O remains at interglacial values for this specific event, when CH_4 has already dropped to glacial values at the end of the event. The amplitude of some events differs substantially between the two gases as demonstrated by D/O events 19 and 20, also shown in the GRIP record (*13*) (Fig. 1).

The depth interval from 2700 to 3060 m in the EPICA Dome C core permits us to make reconstructions of climate and atmospheric composition for the interval 390 to 650 kyr B.P., most of which precedes the Vostok record (*2*). CH_4 and N_2O measurements performed over this depth interval are shown in Fig. 2, together with high-resolution δD measurements (*24*).

To better characterize warm and cold intervals during the past 650 ky, we refer to "interglacial" as a period during which δD exceeds –403‰ (per mil) (*3*). The use of this definition marks MISs 1, 5.5, 7.3, 7.5, 9.3, and 11.3 as interglacials, which is consistent with the marine records (*1*). In the following, we describe the individual counterparts of the marine stages (*25*) from MISs 16.2 to 11.2.

At 624 kyr B.P., at the end of MIS 16.2, CH_4 falls to a value of 368 ppbv (mean over 7 ky), comparable to the low CH_4 concentration during MIS 6 and MIS 2 in the Dome C record. The increase (termination VII) into MIS 15.5 by about 250 ppbv is smaller than at the younger terminations I, II, IV, and V (*15*). While CH_4 only reaches the mean Holocene (0.3 to 10 kyr B.P.) level of 608 ppbv during MIS 15.1 (600 ppbv, mean over 27 ky) and 15.5 (617 ppbv, mean over 7 ky), the corresponding mean N_2O concentrations of 272 ppbv and 274 ppbv are higher than the Holocene mean (262 ppbv) but similar to early Holocene values. Both records, CH_4 and N_2O, show the distinct separation of MISs 15.1 and 15.5 (Fig. 2) by lower concentrations and three shorter events each during the colder near-glacial periods of MISs 15.2 to 15.4. MIS 15.1 is a surprisingly stable climatic period (1 SD: ± 15 ppbv CH_4, ± 6 ppbv N_2O). Its duration is about 27 ky on the EDC2 age scale. A similar duration is seen in the records of δD (*24*) and CO_2 (*26*); related uncertainties are discussed in (*26*).

In Fig. 3A, δD is plotted together with CO_2 (*26*), CH_4, and N_2O, showing the transition from MISs 14 to 13. During MIS 14, the three gases are closely linked in terms of their timing: Relative maxima (dashed lines) occur at the same time within the data resolution. One of these maxima corresponds to MIS 14.3. CO_2, CH_4, and N_2O seem to lead the δD record and therefore, Antarctic temperature, by about 2000 ± 500 years. However, this could be due to an artifact in the EDC2 time scale, as discussed in Siegenthaler *et al.* (*26*). During MIS 13, the relative CO_2, CH_4, and N_2O maxima are slightly out of phase. In contrast to younger glacial terminations (*2*), the temperatures do not rise directly to a local maximum. Instead, the δD, CO_2, and CH_4 records reveal a transition to the warmest phase (MIS 13.1), which evolves in steps with relapses in between. Nevertheless, sequences of the CO_2 and CH_4 increases to

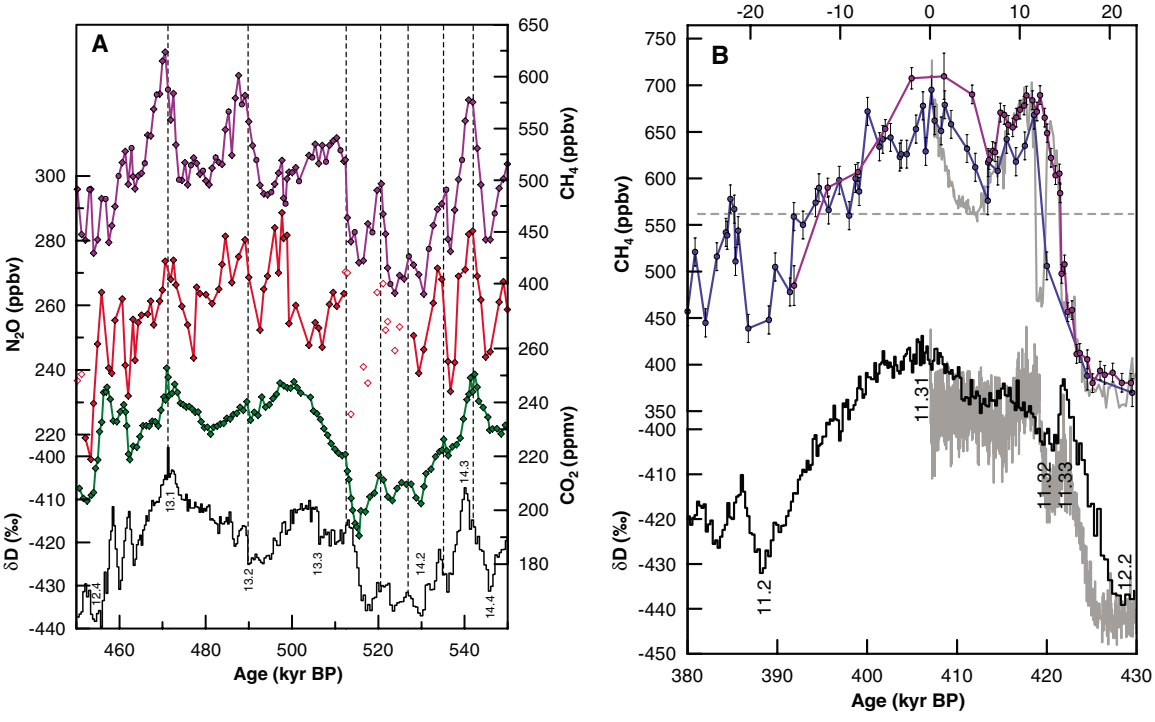

Fig. 3. (**A**) Dome C CO_2 (*26*) (green line), CH_4 (purple line), and N_2O (red line) records over the period of MISs 13 to 14 as shown in Fig. 2, together with high-resolution δD data from Dome C (*24*) (black line). Vertical dashed lines highlight the coincidence of local CO_2, CH_4, and N_2O maxima. Data are plotted on the EDC2 time scale (*3*). (**B**) CH_4 records from Dome C (purple line) and Vostok (*15*, *30*) (blue line), together with high-resolution δD data from Dome C (*24*) (black line) covering MIS 11 (labeled at the bottom). The data from MIS 1 are shown as gray lines (time axis on top) for comparison; the curves are aligned by synchronizing the two glacial-interglacial CH_4 increases. Error bars represent the 1 SD measurement uncertainty. Data are plotted on the EDC2 age scale (*3*).

MISs 13.3 and 13.1 look similar to those of the last deglaciation (*9*): CO_2 rises first, CH_4 is delayed, and CO_2 stops rising when CH_4 rises abruptly. In comparison to the last deglaciation, the CH_4 rise at 513 kyr B.P. is rather small. This may be explained by the colder interglacial temperatures that would have favored a relative increase in methanotrophy over methanogenesis, thereby contributing to lowered net CH_4 emissions in the northern extratropics and/or the subtropical and tropical regions. Additionally, the Northern Hemisphere ice sheets may not have retreated as far north during MIS 13. As a consequence, the uncovered areal extent of additional CH_4 source regions was smaller and therefore, the CH_4 overshoot, usually found at terminations, may not have occurred.

At this point, it is difficult to characterize MISs 13 and 15 as interglacials, because the δD values barely exceed –403‰. We therefore refer to these periods as intermediate warm periods (IWP) (*27*). This and their specific evolution of CH_4 suggests that they are similar to MISs 5.1 to 5.3 and MISs 7.1 to 7.3 (*2*) (Fig. 4). In all cases, regular events with CH_4 amplitudes of 50 to 140 ppbv occurred, similar to events marked by stars in Fig. 2. The average return time of the events during MIS 13 is approximately 20 ky, and they last for 5 to 10 ky. The origin of these fluctuations is probably related to the precession cycle (19 to 23 ky) of summer insolation in mid-low to low northern latitudes, as observed for the CH_4 amplitude during the last glacial period (*13*). The N_2O amplitude appears to be modulated by different mechanisms from those responsible for CH_4, as seen in MISs 13 and 15 (e.g., at 498 and 596 kyr B.P.), where N_2O peaks are quite large despite the small CH_4 peaks. Similar discrepancies are in fact found in the last glacial period, e.g., at D/O events 19 and 20 (*13*).

MIS 12 is believed to be a very cold period showing millennial time-scale variations similar to those observed in the last glacial period (*28*). The Dome C record shows CH_4 variations lasting about 1 to 3 ky, with amplitudes of 40 to 120 ppbv (Fig. 2). In addition, Antarctic warming events of 7 to 19‰ are present in the δD record. Their independent evolution on millennial time scales is an indication that the bipolar seesaw may have been operational also during MIS 12 (*29*), but the resolution of our measurements and the uncertainty in their timing prevent us from drawing final conclusions.

Our CH_4 measurements provide an undisturbed record for the entire MIS 11 (Fig. 3B) and support, except for a small offset (*19*), the recently reconstructed MIS 11 record of Vostok (*30*). This is important for two reasons. First, MIS 11 is the longest warm phase of the Antarctic temperature record over the past 740 ky (*24*), with a mean temperature comparable to the Holocene. CH_4 exceeded the minimum Holocene value of 560 ppbv for more than 28 ky. Second, CH_4 increased to 689 ppbv at termination V, followed by an early decrease for about 5000 years, which is very similar to the early Holocene CH_4 record (gray curves in Fig. 3B). It then rose to the high concentration of about 700 ppbv. Ruddiman (*31*) argued that such a behavior of the CH_4 during the early Holocene is due to early anthropogenic interference and that this would be unique. Our data provide a crucial counterexample to this postulated behavior: The early temporary reduction was clearly not an indication of an impending ice age, which started some 20,000 years later in MIS 11, and the increase after this reduction has been established without human influence.

The good agreement between the Dome C and the Vostok (*15*, *30*) record over MISs 1 to 7 and MIS 11 increases our confidence in the fidelity of a composite record of atmospheric CH_4 over the past 650 ky (Fig. 4). The composite record, established by wiggle matching (*32*), demonstrates, within the resolution of our measurements, that preindustrial atmospheric concentrations of CH_4 reconstructed from two Antarctic ice cores have not exceeded 773 ± 15 ppbv (single values at MIS 9.3) during the past 650 ky. The highest mean N_2O values (278 ppbv ± 7 ppbv) over at least a period of 7 ky covered by our records are found during MIS 15.1, slightly higher than early Holocene values. The differing response to climate change of CH_4 and N_2O during MISs 15.1 and 15.5 suggests that the main source regions and/or strengths may strongly differ during interglacials and IWP. High levels are sustained longer for N_2O than for CH_4 during MISs 5.5, 15.1, and 15.3 (Fig. 4), either due to the release of oceanic N_2O or because N_2O soil sources are also productive under semiarid conditions (*13*).

In general, CH_4 is well correlated with δD on glacial-interglacial time scales (>40 ky), including lower CH_4 concentrations during the IWP than during interglacials of the past 420 ky. At terminations, the amplitude of the CH_4 increase is highly correlated with the corresponding Antarctic temperature (r^2 = 0.80). CH_4 has mainly tropical and Northern Hemisphere sources, but only very small austral sources (mainly open-ocean contributions), which suggests that the generally smaller glacial-interglacial temperature change before 440 kyr B.P. revealed by Dome C δD was also of global importance at that time (*33*). The precessional insolation signal in low- to mid-northern latitudes has a strong influence on the amplitude of CH_4 variations for glacial periods and IWP, but the Northern wetlands, episodically covered by boreal ice sheets and exposed to different precipitation patterns, are likely to contribute to this D/O-like variability of the CH_4 concentration (*21*). Furthermore, sink feedbacks, through changes

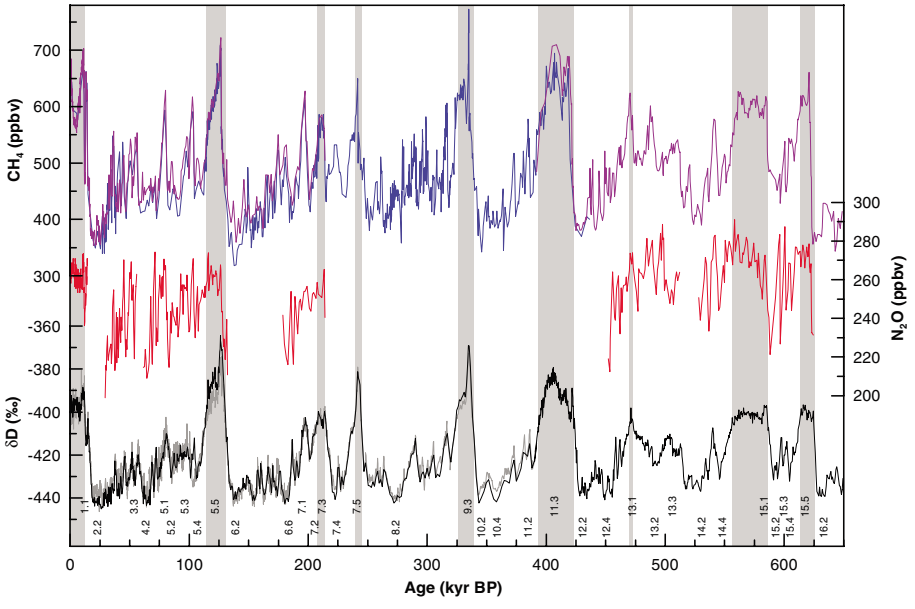

Fig. 4. CH_4 record over the past 650 ky, composed of Dome C CH_4 (purple line) [(*8*, *9*) and new data] and Vostok CH_4 (blue line) (*2*, *15*). Also shown are the N_2O data measured along the Dome C ice cores (red line) [(*8*, *20*, *36*) and new data] and δD records from Dome C (black line) (*24*) as well as those from Vostok +42‰ (gray line) (*2*). N_2O artifacts are not shown in this figure. Gray shaded areas highlight interglacial periods with a δD value >–403‰ as defined in (*3*). Numbers of MISs are given at the bottom of the figure (*25*). Data are shown on the EDC2 time scale (*3*).

of hydrocarbon emissions from the terrestrial biosphere, could have been considerable (*34*).

References and Notes

1. L. E. Lisiecki, M. E. Raymo, *Paleoceanography* **20**, PA1003 (2005).
2. J. R. Petit *et al.*, *Nature* **387**, 359 (1999).
3. EPICA Community Members, *Nature* **431**, 147 (2004).
4. T. Blunier *et al.*, *Geophys. Res. Lett.* **20**, 2219 (1993).
5. D. M. Etheridge, L. P. Steele, R. J. Francey, R. L. Langenfelds, *J. Geophys. Res.* **103**, 15979 (1998).
6. J. Flückiger *et al.*, *Science* **285**, 227 (1999).
7. J. Chappellaz *et al.*, *J. Geophys. Res.* **102**, 15987 (1997).
8. J. Flückiger *et al.*, *Global Biogeochem. Cycles* **16**, 1010 (2002).
9. E. Monnin *et al.*, *Science* **291**, 112 (2001).
10. T. Blunier *et al.*, *Nature* **394**, 739 (1998).
11. E. J. Brook, T. Sowers, J. Orchardo, *Science* **273**, 1087 (1996).
12. J. Chappellaz *et al.*, *Nature* **366**, 443 (1993).
13. J. Flückiger *et al.*, *Global Biogeochem. Cycles* **18**, GB1020 (2004).
14. T. Sowers, R. B. Alley, J. Jubenville, *Science* **301**, 945 (2003).
15. M. Delmotte *et al.*, *J. Geophys. Res.* **109**, D12104 (2004).
16. K. Kawamura, thesis, Tohoku University, Tohoku, Japan (2000).
17. T. Sowers, *J. Geophys. Res.* **106**, 31903 (2001).
18. J. Chappellaz, I. Y. Fung, A. M. Thompson, *Tellus* **45B**, 228 (1993).
19. Materials and methods are available as supporting material on *Science* Online.
20. B. Stauffer, J. Flückiger, E. Monnin, T. Nakazawa, S. Aoki, *Mem. Natl. Inst. Polar Res.* **57**, 139 (2003).
21. A. Dällenbach *et al.*, *Geophys. Res. Lett.* **27**, 1005 (2000).
22. R. Spahni *et al.*, *Geophys. Res. Lett.* **30**, 1571 (2003).
23. NorthGRIP Project Members, *Nature* **431**, 147 (2004).
24. J. Jouzel, in preparation.
25. M. Sarnthein, R. Tiedemann, *Paleoceanography* **5**, 1 (1990).
26. U. Siegenthaler *et al.*, *Science* **310**, 1313 (2005).
27. For MISs 13.1, 13.3, 15.1, and 15.5, δD barely exceeds –403‰, so we use the term intermediate warm period (IWP) for those periods with a lower δD that is still above –425‰ (minimum at MIS 13.2 in Fig. 2). This applies also to MISs 5.1, 5.3, 7.1, and 7.3.
28. D. W. Oppo, J. F. McManus, J. L. Cullen, *Science* **279**, 1335 (1998).
29. T. F. Stocker, S. J. Johnsen, *Paleoceanography* **18**, 1087 (2003).
30. D. Raynaud *et al.*, *Nature* **436**, 39 (2005).
31. W. F. Ruddiman, *Clim. Change* **61**, 261 (2003).
32. The synchronization of the Vostok to the longer Dome C record first has been wiggle matched (*35*) by δD. Then, Vostok gas ages are calculated using Vostok age A55 (*15*), refined by directly matching (*35*) CH_4 from Vostok to Dome C in overlapping periods.
33. V. Masson-Delmotte *et al.*, in preparation.
34. P. J. Valdes, D. J. Beerling, C. E. Johnson, *Geophys. Res. Lett.* **32**, L02704 (2005).
35. J. Schwander *et al.*, *J. Geophys. Res.* **102**, 19483 (1997).
36. B. Stauffer *et al.*, *Ann. Glaciol.* **35**, 202 (2002).
37. T. Blunier, E. J. Brook, *Science* **291**, 109 (2001).

38. We thank U. Siegenthaler, F. Lambert, T. Blunier, and B. Stauffer for discussions and two anonymous reviewers for their comments. This is EPICA publication no. 134. This work is a contribution to the European Project for Ice Coring in Antarctica (EPICA), a joint ESF (European Science Foundation)/European Commission (EC) scientific program, funded by the EC and by national contributions from Belgium, Denmark, France, Germany, Italy, the Netherlands, Norway, Sweden, Switzerland, and the United Kingdom. We acknowledge long-term financial support by the Swiss National Science Foundation and the Swiss Federal Office of Energy for both science and logistic contributions to EPICA and to the University of Bern. Support was also provided by the French program PNEDC (INSU-CNRS), and the EC project EPICA-MIS.

Supporting Online Material

www.sciencemag.org/cgi/content/full/310/5752/1317/DC1
Materials and Methods
Figs. S1 to S3
References

13 September 2005; accepted 2 November 2005
10.1126/science.1120132

Assistance of Microbial Glycolipid Antigen Processing by CD1e

Henri de la Salle,[1]* Sabrina Mariotti,[2]* Catherine Angenieux,[1]* Martine Gilleron,[3]* Luis-Fernando Garcia-Alles,[4] Dag Malm,[5] Thomas Berg,[6] Samantha Paoletti,[2] Blandine Maître,[1] Lionel Mourey,[4] Jean Salamero,[7] Jean Pierre Cazenave,[8] Daniel Hanau,[1] Lucia Mori,[2] Germain Puzo,[3]† Gennaro De Libero[2]†

Complexes between CD1 molecules and self or microbial glycolipids represent important immunogenic ligands for specific subsets of T cells. However, the function of one of the CD1 family members, CD1e, has yet to be determined. Here, we show that the mycobacterial antigens hexamannosylated phosphatidyl-*myo*-inositols (PIM_6) stimulate CD1b-restricted T cells only after partial digestion of the oligomannose moiety by lysosomal α-mannosidase and that soluble CD1e is required for this processing. Furthermore, recombinant CD1e was able to bind glycolipids and assist in the digestion of PIM_6. We propose that, through this form of glycolipid editing, CD1e helps expand the repertoire of glycolipidic T cell antigens to optimize antimicrobial immune responses.

Particular subsets of T cells recognize lipidic and glycolipidic antigens presented by CD1a, b, c, or d proteins, which are antigen-presenting molecules structurally similar to major histocompatibility complex (MHC) class I proteins (*1*). However, unlike classical MHC molecules, CD1 proteins are functionally nonpolymorphic and expressed in a restricted number of cell types, including myeloid dendritic cells (DCs) (*2*). Each CD1 isotype can be characterized by a distinct intracellular trafficking pathway, which allows the capture of lipid antigens either in late or early endosomal compartments (*2*). In particular, CD1b binds glycolipid antigens in MHC class II–enriched lysosomes (*3*) and returns to the plasma membrane to stimulate antigen-specific T cells.

CD1-presented lipid antigens can be of self (*4–7*) or microbial (*8–14*) origin and can include one or more acyl appendages that anchor into the hydrophobic pockets of CD1 protein, as well as a polar moiety directed out toward the T cell receptor (TCR). Exposed amino acids present in α helices of CD1 molecules, together with polar groups of the antigen, directly interact with the TCR and thus constrain the space between CD1 and TCR (*7*, *12*, *15*, *16*). Because such constraint is likely to prevent accommodation and recognition of antigens with large polar heads, it is generally accepted that antigenic glycolipids and lipoglycans with large oligosaccharide moieties are first processed so that T cell recognition can take place.

Relatively little is known about the molecular mechanisms of glycolipid processing. However, previous work has demonstrated that, to be recognized, the oligosaccharide moiety of Gal(α1→2)GalCer must first be cleaved by the lysosomal α-galactosidase (*17*) in the presence of lipid transfer proteins (LTPs) known as saposins, which are involved in the catabolism of endogenous glycolipids (*18*).

Some species express a particular CD1 isoform, CD1e, which has remained the only member of this protein family with undetermined function. CD1e molecules mainly localize within Golgi compartments of

[1]INSERM, U725, Etablissement Francais du Sang-Alsace, F-67065 Strasbourg, France. [2]Experimental Immunology, Department of Research, Basel University Hospital, CH-4031 Basel, Switzerland. [3]CNRS, UMR 5089, Immunochimie et Glycoconjugués Mycobacteriens, and [4]Biophysique Structurale, Département Mécanismes Moléculaires des Infections Mycobactériennes, Institut de Pharmacologie et de Biologie Structurale, F-31077 Toulouse Cedex, France. [5]Department of Medicine and [6]Department of Pathology, University Hospital of Northern Norway, N-9038 Tromsø, Norway. [7]CNRS, UMR 144, Institut Curie, F-75005 Paris, France. [8]INSERM, U311, Etablissement Francais du Sang-Alsace, F-67065 Strasbourg, France.

*These authors contributed equally to this work.
†To whom correspondence should be addressed. E-mail: gennaro.delibero@unibas.ch (G.D.L.); germain.puzo@ipbs.fr (G.P.)

immature DCs and exclusively in the lysosomes of mature DCs (*19*), in which they are cleaved into a stable soluble form (sCD1e). Unlike other CD1 proteins, CD1e does not transit via the cell surface of DCs, a characteristic that excludes a direct interaction with T cells. However, its accumulation in CD1b$^+$ lysosomes of mature DCs (*19*) suggests that it may have a role in processing and/or presentation of CD1b-restricted antigens.

In preliminary experiments, we had observed that certain CD1b-restricted T cell clones were efficiently activated by DCs but not by CD1b-transfected monocytic and lymphoblastoid cell lines incubated with purified glycolipids from *Mycobacterium tuberculosis* H37Rv. Because these antigen-presenting cells (APCs) differ in their expression of CD1e, we tested whether CD1e was required for the presentation of specific lipid antigens (*20*). Human promyelocytic THP-1 and melanoma M10 cells were transfected with *CD1B*, *CD1E*, or both genes and used as APCs to activate CD1b-restricted T cells. T cell activation, as quantified by cytokine release, was observed only after presentation of hexamannosylated phosphatidyl-*myo*-inositols (PIM_6) by CD1e-CD1b–coexpressing APCs (Fig. 1A). In contrast, two antigens that do not require intracellular processing, diacylsulfoglycolipid (Ac_2SGL) (*12*) (Fig. 1B) and GM1 ganglioside (*6*) (Fig. 1C), were efficiently presented by CD1b$^+$ APCs to specific T cells regardless of CD1e expression. These data suggested that CD1e was necessary for the CD1b-restricted presentation of specific glycolipids, possibly those that require processing.

CD1e is cleaved into a soluble form in lysosomes, suggesting that this cleavage may be required for its activity. To test this hypothesis, M10 cells were transfected with a *CD1E/CD1B* hybrid gene designed to express a CD1e chimera displaying the same late endosomes/lysosomes distribution as CD1b (*20*) but which remains largely membrane-associated (fig. S1). M10-CD1b cells expressing this hybrid CD1e molecule did not present PIM_6 (Fig. 1D) but retained the ability to efficiently present the CD1e-independent glycolipids Ac_2SGL (Fig. 1E) and GM1 (Fig. 1F). These results provide direct evidence that CD1e cleavage is necessary for its function.

To confirm the direct role of sCD1e, CD1b$^+$ M10 APCs were pulsed with recombinant sCD1e (rsCD1e) (*20*) to allow its uptake and subsequently washed before being incubated with PIM_6. Under these conditions, PIM_6 presentation was partially restored (Fig. 1G), whereas presentation of the CD1e-independent Ac_2SGL was unaffected (Fig. 1H). The addition of recombinant saposin C did not facilitate T cell

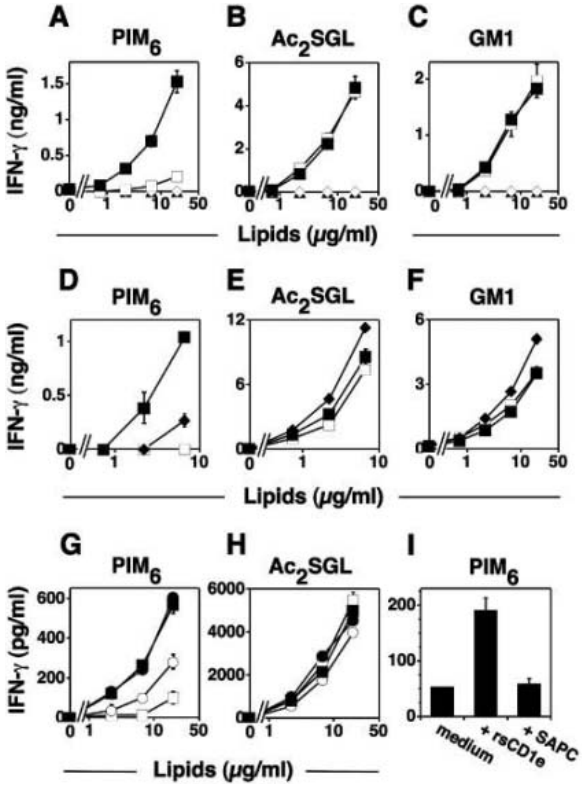

Fig. 1. CD1e is required for presentation of mycobacterial lipid antigens to CD1b-restricted T cells. Untransfected (filled triangles) and transfected M10 cells expressing CD1e (open diamonds), CD1b (open squares), or both CD1b and CD1e (filled squares) were used as APCs to present (**A**) PIM_6, (**B**) Ac_2SGL, or (**C**) GM1 ganglioside to specific T cell clones. (**D** to **F**) Presentation by CD1b$^+$ M10 cells expressing membrane-associated CD1e (filled diamonds) of (D) PIM_6, (E) Ac_2SGL, or (F) GM1. (**G** to **I**) Presentation of (G) PIM_6 or (H) Ac_2SGL by M10-CD1b-CD1e (filled squares), M10-CD1b (open squares), M10-CD1b-CD1e + rsCD1e (filled circles), or M10-CD1b + rsCD1e (open circles). (I) Presentation of PIM_6 by M10-CD1b + rsCD1e or recombinant saposin C (SAPC). Released interferon-γ (IFN-γ) is expressed as ng/ml or pg/ml ± SD. All experiments, including those shown in the other figures, were repeated at least three times.

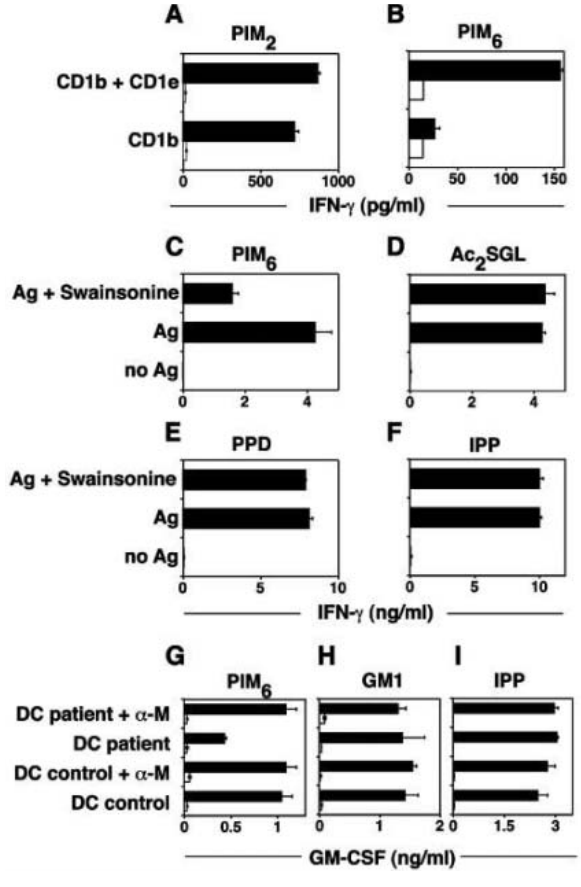

Fig. 2. CD1e is necessary to present PIM_6, which are digested by lysosomal α-mannosidase. (**A** and **B**) THP-1 cells expressing CD1b or both CD1b and CD1e were used to present (A) PIM_2 or (B) PIM_6 (black bars) to the T cell clone Z5B11. White bars indicate stimulation in the absence of antigens. (**C** to **F**) DCs incubated with relevant antigens and swainsonine were used to stimulate CD1b-restricted T cells specific for (C) PIM_6, (D) Ac_2SGL, (E) purified protein derivative (PPD)–specific MHC class II–restricted T cells, or (F) IPP-responsive TCR γδ T cells. (**G** to **I**) DCs from lysosomal α-mannosidase-deficient patient and control DCs were used to stimulate (G) PIM_6-specific T cells, (H) GM1-specific T cells, or (I) IPP-responsive TCR γδ cells. α-M, recombinant human lysosomal α-mannosidase. White bars indicate responses in the absence of the antigens. IFN-γ and granulocyte-macrophage colony-stimulating factor (GM-CSF) are expressed as ng/ml or pg/ml ± SD.

activation, suggesting that this LTP cannot functionally replace CD1e (Fig. 1I).

Exogenous rsCD1e failed to modify the T cell responsiveness to $CD1b^+$ $CD1e^+$ APCs (Fig. 1, G and H), indicating that CD1e does not facilitate PIM_6 uptake. We therefore tested the hypothesis that intracellular sCD1e was involved in processing glycolipids for antigen presentation to T cells. PIMs are characterized by a variable number of α-D-Man*p* units (*21*, *22*), and within this family the PIM_6 glycoforms are the largest, composed of a *myo*-inositol (*myo*-Ins) unit glycosylated in position 6 by the pentamannoside D-Man*p*(α1→2)-D-Man*p*(α1→2)-D-Man*p*(α1→6)-D-Man*p*(α1→6)-D-Man*p*(α1→6)-*myo*-Ins and in position 2 by one α-D-Man*p* (fig. S2). PIM_6 glycoforms represent a mixture of acyl forms, which differ by variable numbers and types of fatty acids that esterify four defined hydroxyl positions (*23*) (fig. S2). Because of the number of Man*p* units, it is likely that PIM_6 are processed before being presented to specific T cells. It is also noteworthy that PIM_2, which are metabolic precursors of PIM_6 in mycobacteria and contain only two α-D-Man*p* units (fig. S2), were presented equally well by APCs expressing either CD1b or both CD1b and CD1e (Fig. 2, A and B). This suggests that PIM_6 glycoforms are processed into PIM_2 in vivo in the presence of CD1e.

In mature DCs, CD1e is mainly localized as a soluble isoform in the lysosomes, which contain the enzymes responsible for glycolipid degradation (*19*). We therefore investigated whether lysosomal α-mannosidases are involved in the removal of four α-D-Man*p* units of PIM_6, thus generating PIM_2. Treatment of DCs with swainsonine, which is a selective inhibitor of α-mannosidases (*24*), decreased presentation of PIM_6 (Fig. 2C) but did not affect CD1b presentation of Ac_2SGL (Fig. 2D) or the responses of MHC class II-restricted TCR αβ cells (Fig. 2E) or of TCR γδ cells (Fig. 2F).

The involvement of α-mannosidase was confirmed by using DCs differentiated from the monocytes of a patient with a congenital deficiency of lysosomal α-mannosidase (*25*). These DCs presented PIM_6 less efficiently than DCs from a normal donor (Fig. 2G) but presented GM1 (Fig. 2H) and isopentenyl-pyrophosphate (IPP) (Fig. 2I) to specific T cells with a similar efficiency as control DCs. The finding that the patient DCs maintained a weak but detectable level of PIM_6 presentation might be explained by the endocytosis of mannosidase present in the serum. Consistent with this, the direct role of α-mannosidase could be confirmed by fully rescuing the presentation of PIM_6 by the DCs of the patient with recombinant human lysosomal α-mannosidase added in culture medium (Fig. 2G). This enzyme did not increase the presentation of PIM_6 by normal DCs to the same T cell clone (Fig. 2G) or the presentation of control antigens to T cells (Fig. 2, H and I). These last observations exclude that the preparation of α-mannosidase induced by itself the maturation of DCs, which would have resulted in the enhancement of T cell activation, whatever the lipid antigen structure.

To determine whether sCD1e directly facilitates PIM_6 digestion, purified PIM_6 glycoforms were digested in vitro using α-mannosidase in the presence or absence of rsCD1e, and the reaction subproducts were characterized by matrix-assisted laser desorption/ionization–time-of-flight (MALDI-TOF) mass spectrometry (*20*). The native PIM_6 fraction was

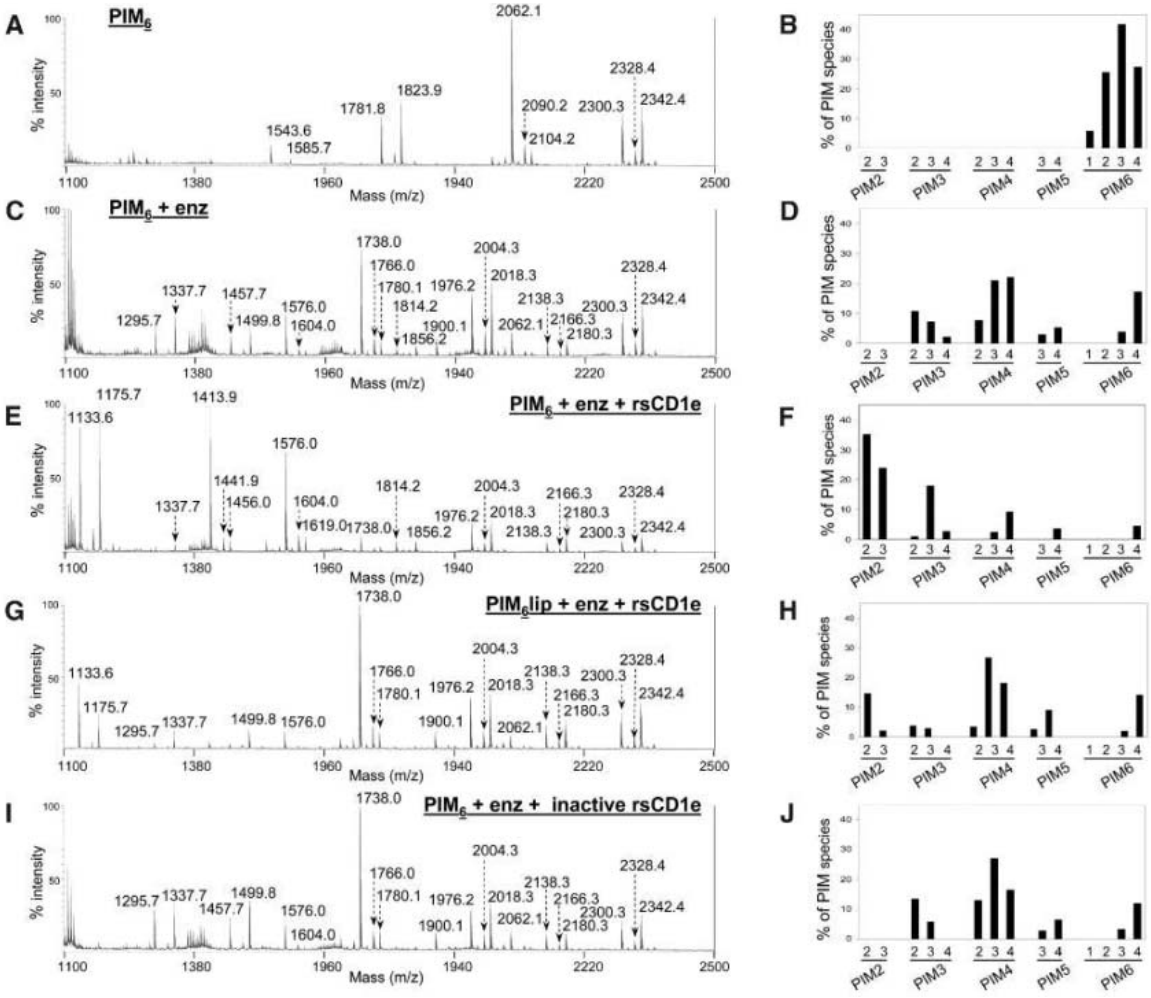

Fig. 3. CD1e facilitates digestion of PIM_6 by α-mannosidase. Negative MALDI-TOF spectra of (**A**) native PIM_6, (**C**) PIM_6 incubated with α-mannosidase (enz), (**E**) PIM_6 incubated with α-mannosidase and rsCD1e, (**G**) PIM_6-containing liposomes (PIM_6lip) with α-mannosidase and rsCD1e, and (**I**) PIM_6 incubated as in (E) but with α-mannosidase and inactivated rsCD1e (inactive rsCD1e). Mass attribution is given in table S1. (**B**, **D**, **F**, **H**, and **J**) Relative abundance of the different species for each PIM acyl and glycoforms. The numbers under the columns correspond to the PIM acylation states (1, monoacylated; 2, diacylated; 3, triacylated; 4, tetraacylated). All the spectra are from one representative experiment out of three recorded spectra.

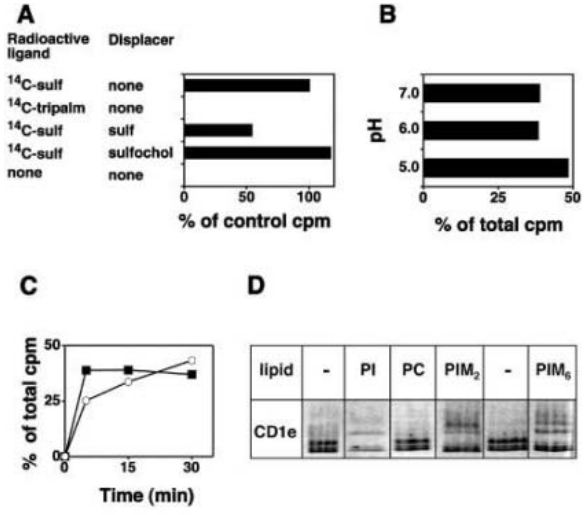

Fig. 4. CD1e binds glycolipids. (**A**) rsCD1e was incubated with ^{14}C-sulfatide or ^{14}C-tripalmitin, and separated by size exclusion chromatography (SEC) from micelles, and then the associated radioactivity was measured. In some experiments, cold sulfatide or cold cholesterol 3-sulfate were added to previously purified rsCD1e-^{14}C-sulfatide complexes, then purified by SEC, and then the remaining radioactivity was counted. Radioactivity of control rsCD1e-^{14}C-sulfatide complexes was always above 5×10^3 counts per minute (cpm). Each sample is expressed as percentage of control group. (**B** and **C**) Binding assays of ^{14}C-sulfatide to rsCD1e were performed (B) at various pH or (C) after incubation for 5, 15, or 30 min at pH 5.0 (filled squares) or 6.0 (open circles). Results are shown as percentage of the total radioactivity present in the sample. (**D**) Isoelectrofocusing of rsCD1e after incubation with indicated lipids. Migration of CD1e toward the cathode (top) evidences loading with negatively charged lipids. PI, phosphatidylinositol; PC, phosphatidylcholine.

composed of four acylated forms containing one to four fatty acyl appendages (Fig. 3, A and B). Digestion of PIM_6 by α-mannosidase yielded PIM species of lower molecular weight, which were assigned as different acylated forms of PIM_3, PIM_4, and PIM_5 (Fig. 3, C and D). The presence of CD1e induced the appearance of PIM_2 acylated forms at mass/charge ratio (*m/z*) 1133.6, 1175.7, and 1413.9 (Fig. 3, E and F) (see table S1 for peak assignments). In addition, PIM_2 were produced when POPC (2-oleyl-1-palmitoyl-*sn*-glycero-3-phosphocholine) liposomes containing PIM_6 were incubated with α-mannosidase and rsCD1e (Fig. 3, G and H), demonstrating that rsCD1e is also active when PIM_6 are inserted in lipid bilayers.

Addition of heat-denatured rsCD1e (Fig. 3, I and J), bovine serum albumin (fig. S3, A and B), or recombinant saposin C (fig. S3, C and D) failed to induce PIM_2 species, revealing the strict requirement of functional CD1e in the processing of PIM_6. Furthermore, low levels of CD1e could still facilitate PIM_6 digestion, indicating a high level of catalytic activity (fig. S3, E and F). In the absence of α-mannosidase, rsCD1e had no effects on PIM_6 (fig. S3, G and H), demonstrating that CD1e does not have any intrinsic enzymatic activity but activates the hydrolysis of PIM_6 by α-mannosidase.

How CD1e participates in processing of glycolipids was next tested using lipid-binding assays involving rsCD1e (*20*) and a ^{14}C-labeled glycolipid (^{14}C-sulfatide) capable of binding to all CD1 molecules (*7*). rsCD1e readily bound sulfatide but not ^{14}C-tripalmitin, a triacylglycerol chosen as negative control (Fig. 4A). In addition, ^{14}C-sulfatide could be displaced by cold sulfatide but not by a control sulfate-containing lipid (cholesterol 3-sulfate) (Fig. 4A), further supporting the specificity of interaction. Binding to rsCD1e occurred at pH 5.0, 6.0, or 7.0 (Fig. 4B) and was very efficient at lysosomal pH 5.0, as confirmed by kinetics analyses (Fig. 4C), which demonstrated that at this pH, binding was obtained faster than at pH 6.0. Furthermore, PIMs were also found to interact with CD1e. Thus, by using isoelectrofocusing, rsCD1e molecules that had been incubated with PIMs acquired a more acidic isoelectric point that demonstrates binding of CD1e to negatively charged PIMs (Fig. 4D).

These experiments indicate that sCD1e allows the processing of microbial antigens with a large carbohydrate component. We have recently isolated other CD1e-dependent T cell clones that recognize *M. tuberculosis* lipids differing from PIM_6 (fig. S4), which suggests that a variety of lipid antigens may require CD1e for presentation.

CD1e has acquired structural features that appear to be instrumental to its immunological role. For example, active CD1e is a soluble molecule that does not reach the cell surface, supporting the chaperone-like function we observe rather than that of an antigen-presenting molecule. Although CD1e shares an overall structure similar to that of other CD1 molecules, the almost complete absence of charged amino acids in the α1 helix (fig. S5) is likely to facilitate interaction with its ligands within membranes. Relevant differences between CD1e and other LTPs also exist. LTPs such as saposins are ubiquitous in their expression and dedicated to the degradation of glycosphingolipids (*18*). In contrast, CD1e is expressed specifically in immune cells, which is consistent with a dedicated role in lipid presentation rather than lipid catabolism. Our proposed model suggests a mode of CD1e glycolipid binding similar to that of other CD1 molecules and distinct from that of other LTPs (*18*). We also suggest that, through specific binding and assistance in carbohydrate degradation, CD1e is primarily involved in editing those microbial glycolipids and lipoglycans (and possibly endogenous glycolipids) that will be optimally immunogenic after processing. In conclusion, the characteristic functions of CD1e appear to have evolved to complement those of the other members of the CD1 family in ensuring effective protective immunity to microbial glycolipids (*26*).

References and Notes

1. S. A. Porcelli, *Adv. Immunol.* **59**, 1 (1995).
2. M. Brigl, M. B. Brenner, *Annu. Rev. Immunol.* **22**, 817 (2004).
3. M. Sugita *et al.*, *Immunity* **16**, 697 (2002).
4. A. Shamshiev *et al.*, *Eur. J. Immunol.* **29**, 1667 (1999).
5. J. E. Gumperz *et al.*, *Immunity* **12**, 211 (2000).
6. A. Shamshiev *et al.*, *Immunity* **13**, 255 (2000).
7. A. Shamshiev *et al.*, *J. Exp. Med.* **195**, 1013 (2002).
8. E. M. Beckman *et al.*, *Nature* **372**, 691 (1994).
9. P. A. Sieling *et al.*, *Science* **269**, 227 (1995).
10. D. B. Moody *et al.*, *Nature* **404**, 884 (2000).
11. D. B. Moody *et al.*, *Science* **303**, 527 (2004).
12. M. Gilleron *et al.*, *J. Exp. Med.* **199**, 649 (2004).
13. J. Mattner *et al.*, *Nature* **434**, 525 (2005).
14. Y. Kinjo *et al.*, *Nature* **434**, 520 (2005).
15. T. Sakai, O. V. Naidenko, H. Iijima, M. Kronenberg, Y. Koezuka, *J. Med. Chem.* **42**, 1836 (1999).
16. A. Melian *et al.*, *J. Immunol.* **165**, 4494 (2000).
17. T. I. Prigozy *et al.*, *Science* **291**, 664 (2001).
18. T. Kolter, K. Sandhoff, *Annu. Rev. Cell Dev. Biol.* **21**, 81 (2005).
19. C. Angenieux *et al.*, *Traffic* **6**, 286 (2005).
20. Materials and methods are available as supporting material on *Science* Online.
21. K. H. Khoo *et. al.*, *Glycobiology* **5**, 117, (1995).
22. M. Gilleron *et al.*, *J. Biol. Chem.* **276**, 34896 (2001).
23. M. Gilleron, V. F. Quesniaux, G. Puzo, *J. Biol. Chem.* **278**, 29880 (2003).
24. D. R. Tulsiani, O. Touster, *Arch. Biochem. Biophys.* **224**, 594 (1983).
25. D. Malm, O. K. Tollersrud, L. Tranebjaerg, J. E. Mansson, *Tidsskr. Nor. Laegeforen.* **115**, 594 (1995).

26. We thank J. Nigou for helpful discussions, P. Cullen for reading the manuscript, Z. Mazorra for participating in initial studies, S. Porcelli for providing the monoclonal antibody to CD1b, and L. Angman, D. Fricker, F. Proamer, and S. Sansano for technical assistance. This work was supported by Swiss National Foundation grant 31-66769.01, European Community FP6 TB-VAC and European Advanced Microscopy Network (EAMNET), the Conseil Scientifique (CS) of the Etablissement Français du Sang (EFS) (CS/2002/018), and Association de Recherche et de Développement en Médecine et Santé Publique (ARMESA). This work benefits also from the constant support of the Curie Institute, the CNRS (contract number ACI-DRAB 03/25), and the region Ile de France (SESAME program).

Supporting Online Material

www.sciencemag.org/cgi/content/full/310/5752/1321/DC1
Materials and Methods
Figs. S1 to S5
Table S1
References

25 May 2005; accepted 27 October 2005
10.1126/science.1115301

Vertebrate-Type Intron-Rich Genes in the Marine Annelid *Platynereis dumerilii*

Florian Raible,[1,2]* Kristin Tessmar-Raible,[1] Kazutoyo Osoegawa,[4] Patrick Wincker,[5] Claire Jubin,[5] Guillaume Balavoine,[6] David Ferrier,[7] Vladimir Benes,[3] Pieter de Jong,[4] Jean Weissenbach,[5] Peer Bork,[2] Detlev Arendt[1]*

Previous genome comparisons have suggested that one important trend in vertebrate evolution has been a sharp rise in intron abundance. By using genomic data and expressed sequence tags from the marine annelid *Platynereis dumerilii*, we provide direct evidence that about two-thirds of human introns predate the bilaterian radiation but were lost from insect and nematode genomes to a large extent. A comparison of coding exon sequences confirms the ancestral nature of *Platynereis* and human genes. Thus, the urbilaterian ancestor had complex, intron-rich genes that have been retained in *Platynereis* and human.

The vast majority of bilaterally symmetrical animals stem from the Urbilateria, the last common ancestors of humans and flies (*1*) (Fig. 1). Despite the sequencing of several bilaterian genomes, the complexity of the urbilaterian gene structure remains unknown. Complex genes enhance the potential of a genome to modify transcripts by intron-mediated editing and to encode alternative splice variants, two sources of proteome complexity that affect cellular diversity (*2*). Marked differences exist between orthologous genes of ecdysozoans (*3*) (such as *Drosophila* and *Caenorhabditis elegans*), which have fewer introns, and deuterostome vertebrates (such as mouse and human), which have many introns. This is explained either by intron gain in the evolutionary lineage leading to vertebrates (*4*) or by intron loss in ecdysozoans (*5*). To decide between these alternatives on the basis of new sequence data, we analyzed genomic loci and transcripts in the marine annelid *Platynereis dumerilii* (*6*). This species belongs to the Lophotrochozoa (*7*) (Fig. 1), for which no complete genome sequence is yet available. We also included data from the recently sequenced honeybee (*Apis mellifera*) genome (*8*) for a more general picture of insect genomic characteristics (*9*). From an initial comparison between 1000 randomly selected orthologs shared between insects, *Caenorhabditis elegans*, the ascidian *Ciona intestinalis*, and humans, we found that *Apis* shares 25% of human introns, exceeding the fraction conserved in other ecdysozoans (fig. S1). This ratio is reproduced in random 25-gene subsets of the data (fig. S1), implying that our limited *Platynereis* data set should yield a suitable estimate of intron conservation in this species relative to that in deuterostomes or in ecdysozoans (*10*).

From 2.3 megabases (Mb) of available bacterial artificial chromosome (BAC) sequence, we identified 30 *Platynereis* gene loci with orthologs in other Bilateria. Transcripts were validated by reverse transcription polymerase chain reaction and mapped onto these loci. From this, we inferred the position of introns in the resulting proteins (*8*). These *Platynereis* genes contain 233 introns, or 7.8 introns per gene, similar to their human orthologs (8.4 introns per gene) but exceeding the values for the ecdysozoans (2.4 to 5.4 introns per gene). Three-quarters of the *Platynereis* introns are found in one or more of the other tested Bilateria (Fig. 2A). Most of these are shared with humans or with the teleost fish *Fugu*, but far fewer with insects or *C. elegans*. Thus, in our data set *Platynereis* is more similar to vertebrates than to any ecdysozoan as far as shared introns are concerned. We then assessed how many of the human introns were shared with other species and found that the fraction of human introns conserved in *P. dumerilii* is more than twice as high as the fraction conserved in *Apis* and larger than the fraction of human introns shared with any of the four ecdysozoans (Fig. 2B). Given that introns shared between distant taxa are most likely due to common inheritance (*11*), we conclude that at least two-thirds of the compared human introns already existed in the urbilaterian ancestor at precisely the same amino acid position and phase. This indicates that urbilaterian genes were already rich in introns and that the apparent differences in intron abundance between insects and nematodes and vertebrates are in large part due to intron loss in the ecdysozoan lineages (Fig. 2C). This also correlates with elevated rates of other forms of genome evolution ascribed to the ecdysozoan model species, such as gene loss (*12*, *13*).

In our data set, the ascidian *C. intestinalis* also shares fewer introns with humans than does *Platynereis* (Fig. 2B). This is again counterintuitive, considering the phylogeny (Fig. 1). Although this may be partially due to the relatively fragmentary *Ciona* genome assembly (*14*), it more likely reflects rapid genome evolution in the tunicate lineage (*15*). Illustrative of this trend, *Platynereis* shares with humans an intron in the N-terminal region of the Pax6 Paired domain that is crucial for generating two functionally divergent Pax6 isoforms. This intron has been considered a vertebrate innovation (*16*), because it is absent in *Ciona* and in another ascidian, *Phallusia* (*17*). The apparent intron loss in *Ciona* is not simply due to genome compaction (~6% of the human genome size), because ancestral introns are largely retained in the small, intron-rich genome (*18*) of the teleost fish *Fugu* (~10% of human genome size) (Fig. 2).

Next, we tested whether the retention of ancestral gene features in *Platynereis* is also apparent from the evolution of exon sequences. Systematic comparisons already indicated that the human proteome has

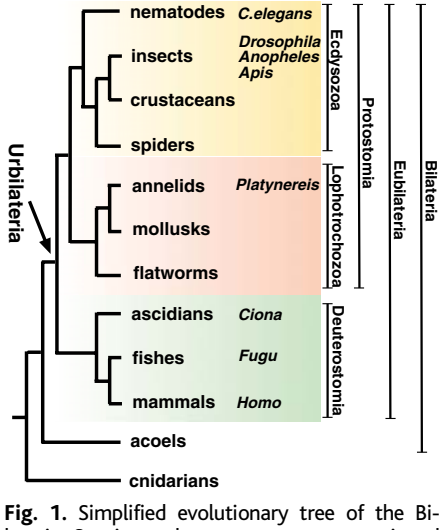

Fig. 1. Simplified evolutionary tree of the Bilateria. Species and group names as mentioned in the text.

[1]Developmental Unit, [2]Computational Unit, [3]Genomics Core Facility, European Molecular Biological Laboratory (EMBL), Meyerhofstraße 1, D-69117 Heidelberg, Germany. [4]Children's Hospital, Oakland Research Institute, 747 52nd Street, Oakland, CA 94609, USA. [5]Génoscope, Centre National de Séquençage and CNRS UMR 8030, 2 Rue Gaston Crémieux, CP 5706 91057 Evry Cedex, France. [6]Centre de Génétique Moléculaire du CNRS, Bâtiment 26, Avenue de la Terrasse, 91198 Gif-sur-Yvette, France. [7]Department of Zoology, University of Oxford, South Parks Road, Oxford OX1 3PS, UK.

*To whom correspondence should be addressed. E-mail: raible@embl.de (F.R.); arendt@embl.de (D.A.)

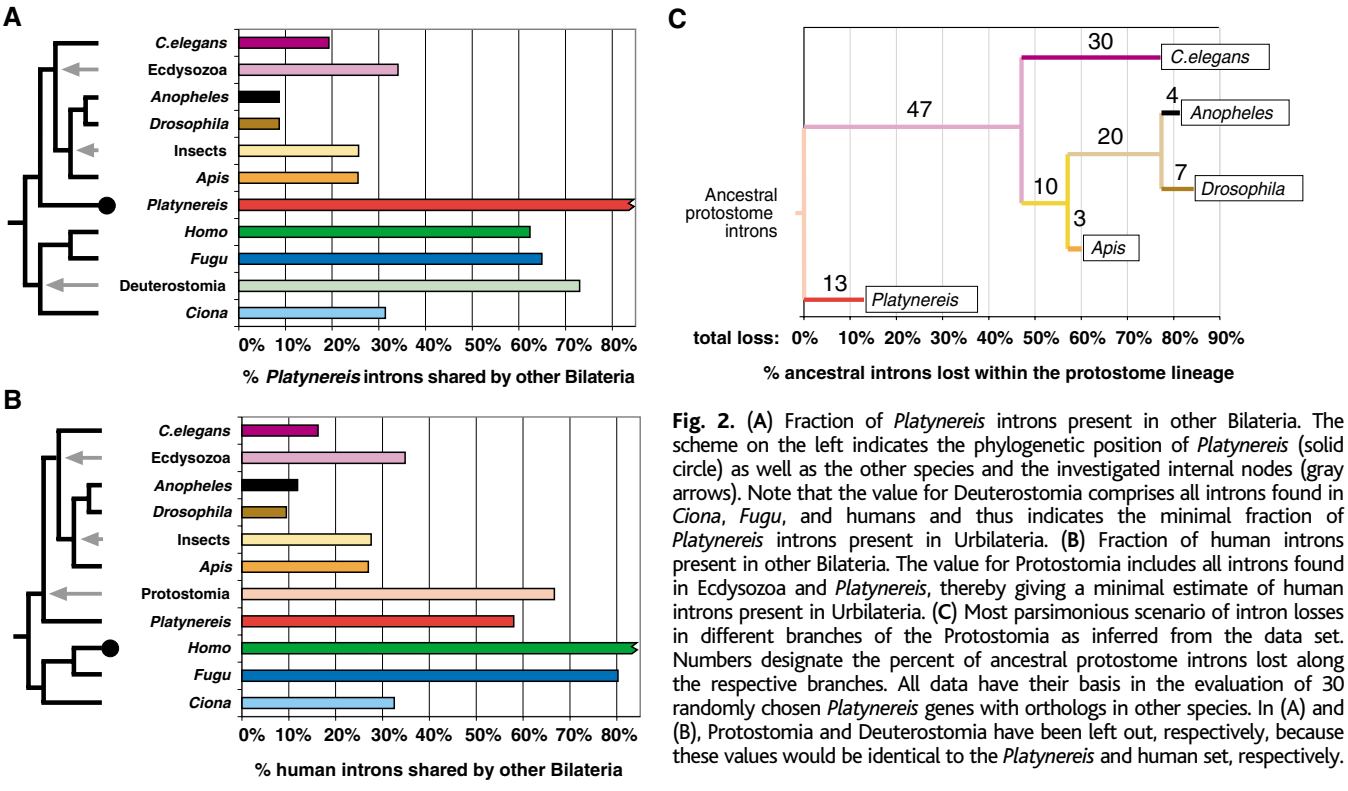

Fig. 2. (**A**) Fraction of *Platynereis* introns present in other Bilateria. The scheme on the left indicates the phylogenetic position of *Platynereis* (solid circle) as well as the other species and the investigated internal nodes (gray arrows). Note that the value for Deuterostomia comprises all introns found in *Ciona*, *Fugu*, and humans and thus indicates the minimal fraction of *Platynereis* introns present in Urbilateria. (**B**) Fraction of human introns present in other Bilateria. The value for Protostomia includes all introns found in Ecdysozoa and *Platynereis*, thereby giving a minimal estimate of human introns present in Urbilateria. (**C**) Most parsimonious scenario of intron losses in different branches of the Protostomia as inferred from the data set. Numbers designate the percent of ancestral protostome introns lost along the respective branches. All data have their basis in the evaluation of 30 randomly chosen *Platynereis* genes with orthologs in other species. In (A) and (B), Protostomia and Deuterostomia have been left out, respectively, because these values would be identical to the *Platynereis* and human set, respectively.

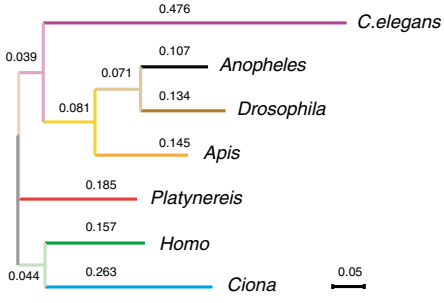

Fig. 3. Global distance tree based on concatenated alignments between conserved blocks of orthologous proteins found in *C. elegans*, *Anopheles*, *Drosophila*, *Apis*, *Platynereis*, humans, and *Ciona intestinalis*. Distances are indicated next to individual branches. The tree was calculated from 38,303 noninvariant amino acid positions according to the BLOSUM62 substitution model by using a maximum likelihood approach (*8*). All internal branches are fully supported.

departed less from the urbilaterian proteome than have the ones of *Drosophila* or *C. elegans* (*12*). To compare this to coding sequence evolution in polychaetes, we determined a set of 442 pan-bilaterian genes from 21,000 *Platynereis* expressed sequence tags. We then calculated distances to other bilaterians between aligned protein regions by using three different distance matrices (*8*). Both in single protein comparisons (fig. S2) and in a distance tree calculated from concatenated protein alignments (Fig. 3), *Platynereis* and human proteins were found to be more closely related to each other than to their ecdysozoan orthologs. Moreover, *Platynereis* proteins are closer to human than to *Ciona* orthologs, consistent with the trend observed for intron retention. We conclude that, at the intron and exon level, *Platynereis* and humans can be regarded as similarly slow-evolving representatives of protostomes and deuterostomes, respectively.

Our analyses consistently support the notion that Urbilateria possessed genes that, in both structure and sequence, were more similar to today's human or *Platynereis* genes than to those of dipterans, nematodes, or ascidians, where these initially complex genes have been secondarily simplified. Thus, in order to reconstruct the urbilaterian genome, comparisons of vertebrates with slow-evolving invertebrates will be of great benefit.

References and Notes

1. E. M. De Robertis, Y. Sasai, *Nature* **380**, 37 (1996).
2. B. R. Graveley, *Trends Genet.* **17**, 100 (2001).
3. A. M. Aguinaldo *et al.*, *Nature* **387**, 489 (1997).
4. I. B. Rogozin, Y. I. Wolf, A. V. Sorokin, B. G. Mirkin, E. V. Koonin, *Curr. Biol.* **13**, 1512 (2003).
5. S. W. Roy, W. Gilbert, *Proc. Natl. Acad. Sci. U.S.A.* **102**, 1986 (2005).
6. K. Tessmar-Raible, D. Arendt, *Curr. Opin. Genet. Dev.* **13**, 331 (2003).
7. K. M. Halanych *et al.*, *Science* **267**, 1641 (1995).
8. Materials and methods are available as supporting material on *Science* Online.
9. S. Kumar, *Nat. Rev. Genet.* **6**, 654 (2005).
10. To ensure accurate alignment of intron positions, we could only compare orthologous genes showing at least a moderate degree of coding sequence conservation. Less-conserved gene sets may show a lower degree of conservation in intron placement, but there is no a priori reason to expect that this should affect the ratio of intron conservation between species.
11. A. V. Sverdlov, I. B. Rogozin, V. N. Babenko, E. V. Koonin, *Nucleic Acids Res.* **33**, 1741 (2005).
12. R. D. Kortschak, G. Samuel, R. Saint, D. J. Miller, *Curr. Biol.* **13**, 2190 (2003).
13. A. Kusserow *et al.*, *Nature* **433**, 156 (2005).
14. P. Dehal *et al.*, *Science* **298**, 2157 (2002).
15. A. L. Hughes, R. Friedman, *Evol. Dev.* **7**, 196 (2005).
16. P. Callaerts, G. Halder, W. J. Gehring, *Annu. Rev. Neurosci.* **20**, 483 (1997).
17. S. Glardon, P. Callaerts, G. Halder, W. J. Gehring, *Development* **124**, 817 (1997).
18. S. Aparicio *et al.*, *Science* **297**, 1301 (2002); published online 25 July 2002 (10.1126/science.1072104).

19. We thank C. Burgtorf and H.-D. Pfannenstiel for providing *P. dumerilii* sperm DNA, H. Snyman, K. Willmann, and the GeneCore team for excellent help, and members of the Arendt and Bork groups for critical discussions. This work was supported by grants from the European Union (LSHG-CT-2003-503265, LSHG-CT-2003-503329, and QLRT-2001-02062 to P.B. and Marine Genomics Europe network to D.A.), the French Ministry of Research (to J.W. and G.B.), and the CNRS (to G.B.) and by a Boehringer Ingelheim Foundation Scholarship (to K.T.-R.). BAC library construction and characterization was supported by a subcontract (to K.O. and P.d.J.) from a grant (NSF IBN 0208138) awarded to L. Holland (Scripps Institution of Oceanography). The authors declare that they have no competing financial interests.

Supporting Online Material

www.sciencemag.org/cgi/content/full/310/5752/1325/DC1
Materials and Methods
Figs. S1 and S2
Tables S1 to S4

19 August 2005; accepted 25 October 2005
10.1126/science.1119089

SMEDWI-2 Is a PIWI-Like Protein That Regulates Planarian Stem Cells

Peter W. Reddien,* Néstor J. Oviedo,† Joya R. Jennings, James C. Jenkin, Alejandro Sánchez Alvarado‡

We have identified two genes, *smedwi-1* and *smedwi-2*, expressed in the dividing adult stem cells (neoblasts) of the planarian *Schmidtea mediterranea*. Both genes encode proteins that belong to the Argonaute/PIWI protein family and that share highest homology with those proteins defined by *Drosophila* PIWI. RNA interference (RNAi) of *smedwi-2* blocks regeneration, even though neoblasts are present, irradiation-sensitive, and capable of proliferating in response to wounding; *smedwi-2(RNAi)* neoblast progeny migrate to sites of cell turnover but, unlike normal cells, fail at replacing aged tissue. We suggest that SMEDWI-2 functions within dividing neoblasts to support the generation of cells that promote regeneration and homeostasis.

Members of the PIWI/Argonaute family of proteins fall into two main classes, one named after *Arabidopsis* Argonaute and the other after *Drosophila* PIWI (*1*). Members of this protein family contain PAZ and PIWI domains and mediate silencing via cleavage of mRNAs (*2*–*4*) or by inhibition of translation (*5*, *6*). These proteins are found in plants (*7*), yeast (*8*), and throughout the animal kingdom—including at least eight in humans. Some of the PIWI-class proteins have been implicated in the regulation of germ cells (*9*–*11*). Very little is known, however, about how PIWI proteins regulate germ cells and whether these proteins typically promote stem cell maintenance or differentiation. Furthermore, the types of stem cells and developmental events regulated by PIWI-class proteins remain unclear.

Here we report on the planarian *S. mediterranea* genes *smedwi-1* and *smedwi-2*. We studied *smedwi-1* and *-2* because they encode proteins similar to the PIWI class of PIWI/Argonaute proteins (fig. S1) and are thus candidates to regulate the adult somatic stem cells (neoblasts) of planarians (*12*, *13*). Furthermore, *smedwi-1* expression resembles the distribution of planarian neoblasts (*14*). Planarians present a promising venue for the study of PIWI-like genes because stem cells play prominent roles in homeostasis and regeneration and because the genetic study of planarian stem cells is now possible (*12*, *13*, *15*).

smedwi-1 and *smedwi-2* are expressed in small cells distributed like neoblasts—that is, posterior to photoreceptors and excluded from the pharynx (Fig. 1, A to C). *smedwi*-expressing cells, like neoblasts, reside in the parenchyma: mesenchymal tissue excluded from the nervous system, pharynx, and gastrovascular system (Fig. 1, D and E). Neoblasts are quickly and specifically eliminated after irradiation (*12*). Expression of *smedwi-1* and

Howard Hughes Medical Institute, Department of Neurobiology and Anatomy, University of Utah School of Medicine, Salt Lake City, UT 84132, USA.

*Present address: MIT Biology, Whitehead Institute, Cambridge, MA 02142, USA.
†Present address: Cytokine Biology Department, Forsyth Institute, Harvard Medical School, Boston, MA 02115, USA.
‡To whom correspondence should be addressed. E-mail: sanchez@neuro.utah.edu

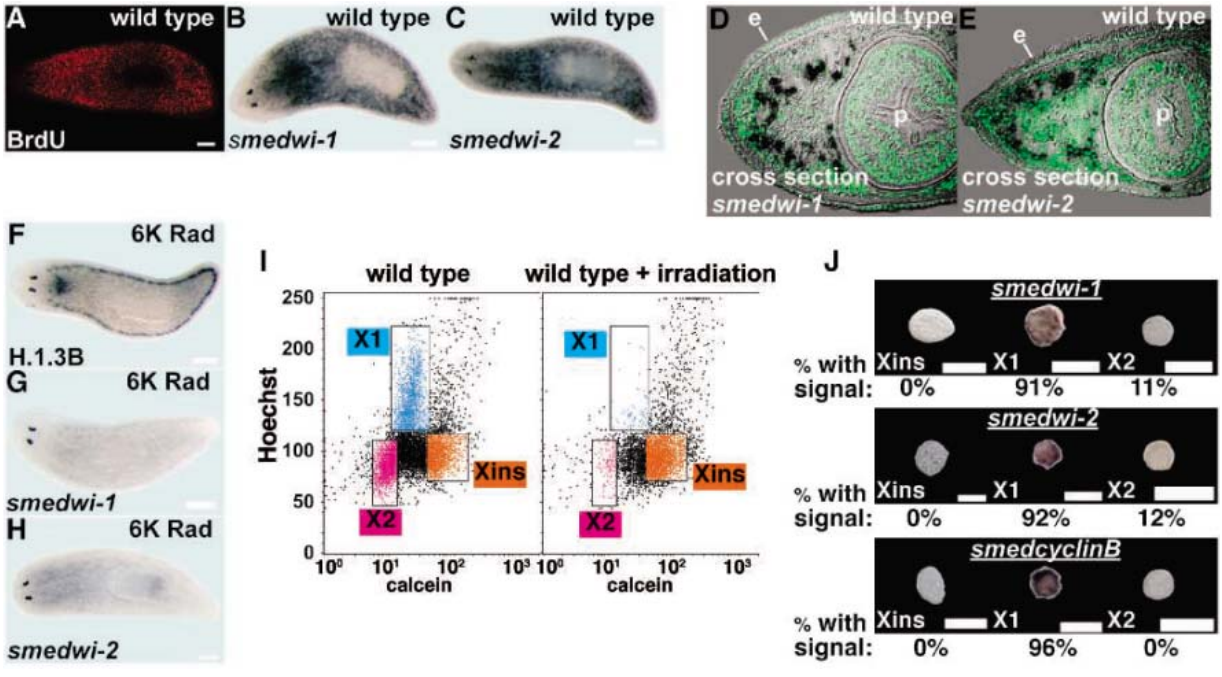

Fig. 1. Dividing neoblasts express *smedwi-1* and *smedwi-2*. (**A**) BrdU labeling demonstrates neoblast distribution; (**B** and **C**) *smedwi-1* and *-2* expression resembles neoblast distribution. Riboprobes are identified at lower left; anterior is to the left. (**D** and **E**) Tissue cross sections, dorsal up. Green, nuclei; black, *smedwi* expression; e, epidermis; p, pharynx. (**F** to **H**) Irradiation at 6000 rad. After irradiation, *smedwi-1* signals (4/4 at 48 hours, 5/5 at 72 hours) and *smedwi-2* signals (2/2 at 48 hours, 8/8 at 72 hours) were undetectable. H.1.3B is an irradiation-insensitive control. (**I**) FACS profile of *S. mediterranea* cells (≤20 μm), Hoechst- and calcein-labeled. X1 (blue) and X2 (pink) populations are irradiation-sensitive; Xins (orange) population is not. (**J**) *smedwi-1* (top), *smedwi-2* (middle), and *smedcyclinB* [clone NBE.6.09E (AY967658); bottom] in situ hybridizations on FACS-isolated cells. Representative results are shown. Expression was typically in X1 but not X2 or Xins cells. Percentages are signal-positive cells ($n > 210$ cells each). Scale bars, 0.2 mm [(A) to (C), (F) to (H)], 10 μm (J).

-2 was markedly reduced by irradiation, consistent with their possible expression in neoblasts (Fig. 1, F to H) (table S1).

Flow cytometry has been used to separate planarian cells and identify neoblasts (*16*, *17*). We used flow cytometry to isolate two populations of irradiation-sensitive cells with neoblast morphology, named X1 and X2, and examined *smedwi-2* expression (Fig. 1I). In situ hybridizations and quantitative reverse transcription polymerase chain reactions indicated that *smedwi* genes are predominantly expressed within X1 cells, at low percentages in X2 cells, and perhaps absent from control irradiation-insensitive Xins cells (Fig. 1J) (table S2). Because neoblasts proliferate, we asked whether cell cycle differences between X1 and X2 cells exist by examining expression of an *S. mediterranea* gene homologous to the cell division marker *cyclinB* (*smedcyclinB*). We observed *smedcyclinB* expression in 96% of X1 cells (n = 325) and 0% of X2 cells (n = 257) (Fig. 1J), which suggests that X1 cells are dividing. Together, our data indicate that *smedwi* genes are expressed directly and largely specifically within dividing neoblasts.

To investigate how SMEDWI proteins regulate neoblasts, we inhibited *smedwi-1* and *-2* with the use of RNA interference (RNAi). RNAi affected expression specifically (fig. S2A). RNAi of *smedwi-1* did not cause robust defects, but RNAi of *smedwi-2* resulted in 100% penetrant defects resembling those in irradiated animals lacking neoblasts. Irradiated and *smedwi-2(RNAi)* animals displayed regression of tissue anterior to the photoreceptors, were incapable of regeneration, and curled around their ventral surface (Fig. 2, A to C). Head regression likely occurred because tissue in front of the photoreceptors lacks dividing neoblasts and is constantly replaced by neoblast progeny (*12*). Because *smedwi-2(RNAi)* animals resemble irradiated animals, *smedwi-2* is likely needed for neoblast function.

smedwi-2(RNAi) defects progress through temporal stages, ending in lethality (fig. S2B). At ≥8 days after exposure to *smedwi-2* double-stranded RNA (dsRNA), animals were incapable of regeneration. Animals wounded earlier could regenerate small blastemas that regressed (fig. S2C). Homeostasis defects after *smedwi-2* silencing arose with kinetics similar to those in irradiated animals. For example, 9 days after irradiation, 15 of 30 animals displayed head regression, whereas 9 days after *smedwi-2* dsRNA feeding, 12 of 29 animals did so. Because irradiation prevents new cell production within 24 hours, homeostasis is likely disrupted within a day after *smedwi-2* inhibition (fig. S2B). SMEDWI-2 protein levels sufficient for neoblast function in tissue turnover likely do not perdure after RNAi. This hypothesis is supported by the observation that *smedwi-2* is expressed in dividing cells, which

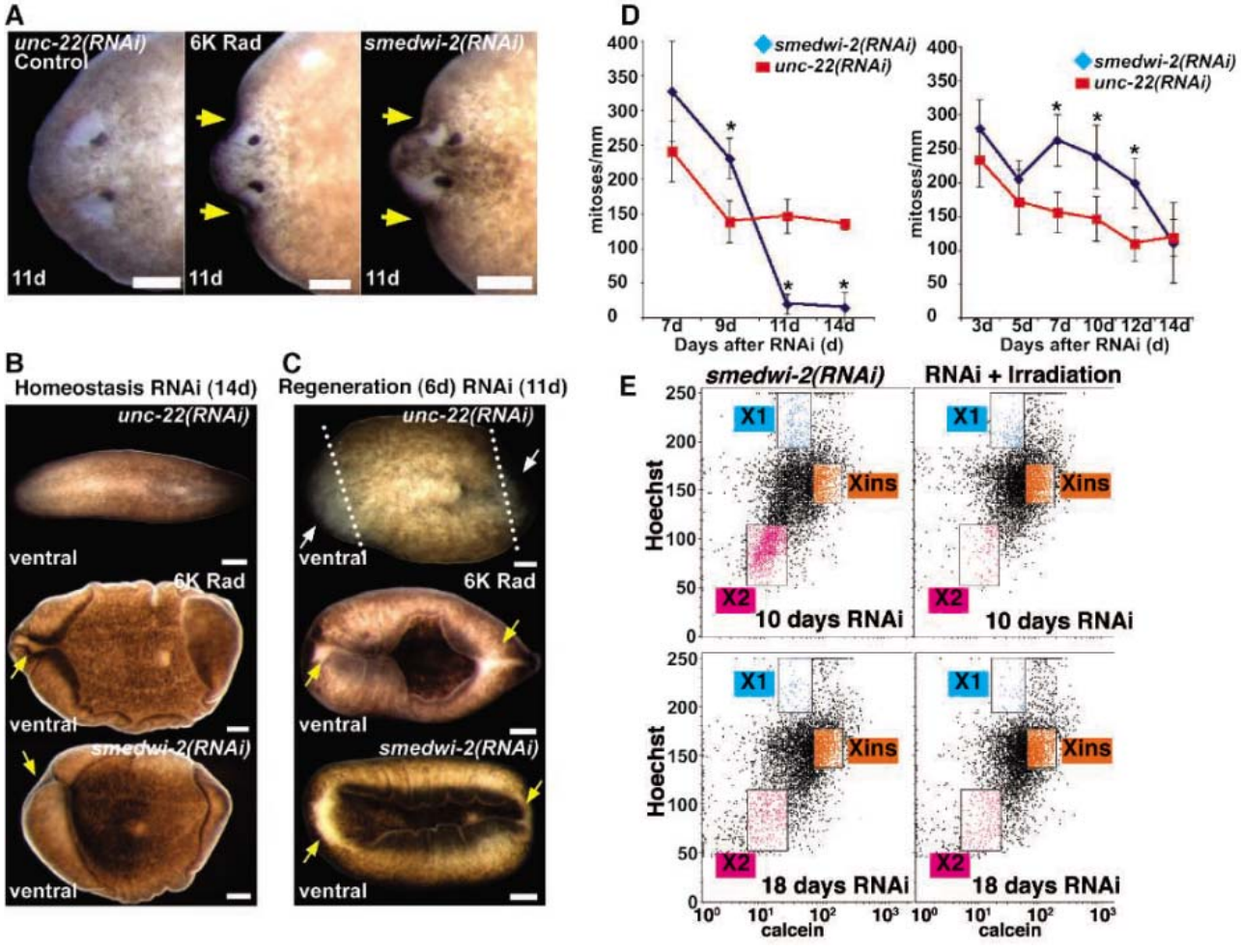

Fig. 2. *smedwi-2(RNAi)* animals display defects related to neoblast dysfunction. (**A** to **C**) Irradiation at 6000 rad. *C. elegans unc-22*, negative control. Anterior is to the left; scale bar, 0.2 mm. Yellow arrowheads show head regression. In (B) and (C); ventral is up; in (C), heads and tails are amputated [dotted line, blastema (unpigmented) boundary]. White arrows, blastemas; yellow arrows, healed wounds without blastema. (**D**) Mitotic numbers divided by animal length. Left panel: Two dsRNA feedings, ≥5 animals per time point. Times shown are days after first feeding. Right panel: One dsRNA feeding, ≥6 animals per time point. Control numbers decline with time because feedings boost mitotic numbers. *P < 0.001, t test. (**E**) Cell numbers were analyzed by FACS (see Fig. 1I for nomenclature). Control irradiations were done 5 days before analysis. *smedwi-2(RNAi)* X1 and X2 irradiation-sensitive populations were present 10 days after RNAi but were greatly reduced by 18 days.

indicates that new protein is produced with new cell production.

One simple explanation for the *smedwi-2(RNAi)* phenotype would be absence of neoblasts. Neoblasts are the only known mitotic cells in adult planarians (*12*). We observed that mitotic numbers in *smedwi-2(RNAi)* animals always eventually plummet (Fig. 2D). We quantified this defect in intact RNAi animals. As expected, at days 11 and 14, *smedwi-2(RNAi)* animals had far fewer mitotic cells than did controls ($P < 0.001$, *t* test). However, *smedwi-2(RNAi)* animals at day 9 were defective for regeneration but had greater mitotic numbers than did the control ($P < 0.001$). We designed a second time course to carefully observe this increase (Fig. 2D). Because feeding boosts mitotic numbers, a single feeding was used so that early time points could be more easily observed. A clear and significant increase in mitotic numbers above the control was observed at days 7, 10, and 12 in *smedwi-2(RNAi)* animals ($P < 0.001$). In situ hybridizations with the *smedwi-1* riboprobe indicated that X1 cells sharply decline in numbers rather than lose the capacity to divide at late time points after RNAi (fig. S2D). Fluorescence-activated cell sorting (FACS) analyses indicated that both X1 and X2 cells were present and irradiation-sensitive in *smedwi-2(RNAi)* animals incapable of regeneration 10 and 12 days after RNAi but were greatly diminished by days 14 through 18 (Fig. 2E) (fig. S3).

These experiments revealed several important aspects of the *smedwi-2* phenotype. First, and in contrast to irradiated animals, neoblasts were present and proliferating at times after RNAi when animals could not regenerate. This suggests that failed neoblast maintenance was not the primary cause of failed regeneration and tissue turnover. Second, at early time points after RNAi, a greater number of *smedwi-2(RNAi)* mitotic neoblasts were present than in controls, suggesting a feedback regulation from loss of tissue homeostasis. Because tissue turnover fails quickly after RNAi of *smedwi-2*, mitotic numbers may increase during this period as a consequence of failed homeostasis. Finally, in late phases of the *smedwi-2* phenotype, neoblasts are not maintained. Long-term neoblast maintenance abnormalities could be a secondary result of failed homeostasis.

We asked whether *smedwi-2(RNAi)* neoblasts were capable of responding to wounds in animals incapable of regeneration. Specifically, we quantified mitotic numbers in prepharyngeal animal fragments that were or were not proximal to a wound produced 14 hours earlier (Fig. 3A). We determined that *smedwi-2(RNAi)* animals were capable of mounting an apparently normal proliferative wounding response (Fig. 3A, $P < 0.001$). This finding indicates that the primary defect that blocked blastema formation in *smedwi-2(RNAi)* animals was not a gross dysfunction in the ability of neoblasts to detect wounds. We therefore propose that neoblast progeny function (e.g., differentiation, migration) is the primary abnormality underlying the *smedwi-2(RNAi)* phenotype.

To assess whether neoblast progeny can migrate, we labeled them with 5-bromo-2′-deoxyuridine (BrdU) and examined head tips, a region devoid of proliferating cells and into which labeled cells migrate (*18*). The progeny of *smedwi-2(RNAi)* neoblasts did not grossly fail to migrate in front of the photoreceptors of regressing heads (Fig. 3B); this result suggests that *smedwi-2(RNAi)*

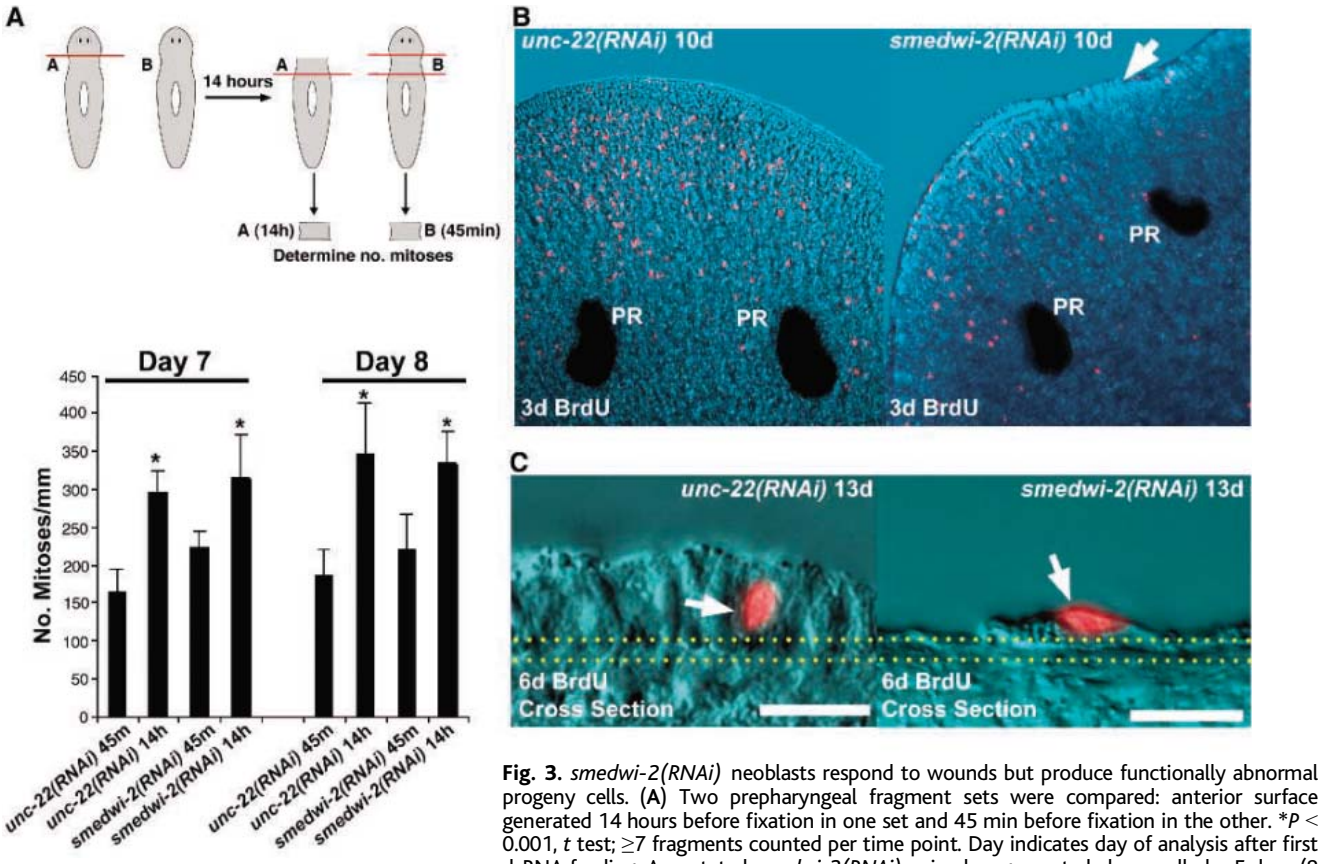

Fig. 3. *smedwi-2(RNAi)* neoblasts respond to wounds but produce functionally abnormal progeny cells. (**A**) Two prepharyngeal fragment sets were compared: anterior surface generated 14 hours before fixation in one set and 45 min before fixation in the other. *$P < 0.001$, *t* test; ≥7 fragments counted per time point. Day indicates day of analysis after first dsRNA feeding. Amputated *smedwi-2(RNAi)* animals regenerated abnormally by 5 days (8 of 22 animals amputated on day 7 had very small blastemas and 14 of 22 had no blastemas; 8 of 30 animals amputated on day 8 had very small blastemas and 22 of 30 had no blastemas). All controls were normal (day 7, $n = 26$; day 8, $n = 20$). (**B**) Cells in red are BrdU-positive 3 days after labeling. White arrowhead, tissue regression 10 days after dsRNA exposure; PR, photoreceptors. Proliferative neoblasts do not exist anterior to photoreceptors, which indicates that neoblast progeny migrated. Anterior is up; scale bar, 0.1 mm. (**C**) Postpharyngeal cross sections 13 days after RNAi and 6 days after BrdU labeling. White arrows, BrdU-positive cells in epidermis (outermost cells). Dotted lines are on both sides of the basement membrane of the single-cell epidermal layer. Ventral surface is up; scale bar, 10 μm.

neoblasts produced cells capable of reaching sites of tissue turnover.

Next, we asked whether neoblast progeny were capable of producing differentiated cells. Neoblast progeny normally begin to replace aged epidermal cells within a week after labeling (*18*). We sectioned BrdU-labeled *smedwi-2(RNAi)* animals after BrdU incorporation and determined that labeled cells entered the epidermis sooner than in the control and displayed a grossly abnormal morphology (Fig. 3C) (fig. S4 and table S3). Planarian epidermal cells reside in a single-cell layer and display classic columnar epithelial morphology. BrdU-labeled *smedwi-2(RNAi)* cells that reach the epidermis, however, fail to adopt a columnar morphology. For example, the average heights of BrdU-labeled epidermal cells were significantly different in *smedwi-2(RNAi)* animals and control *unc-22(RNAi)* animals: 3.5 ± 1.6 μm (n = 18) and 10.0 ± 1.9 μm (n = 10), respectively ($P < 0.0001$, t test). Regions posterior to the photoreceptors, where epidermis could be clearly visualized, were observed. In *smedwi-2(RNAi)* animals, heads regress and the cells that reach the epidermis in the body are morphologically abnormal; for this reason, we suggest that neoblast progeny cells migrate to sites of tissue turnover but fail to function normally. That the defect is within neoblast progeny is supported by the observations that *smedwi-2(RNAi)* animals resemble irradiated animals and that *smedwi-2* is expressed in the neoblasts.

How might a primary defect in *smedwi-2(RNAi)* neoblast progeny relate to the secondary defect in neoblast maintenance? Although it is unknown how an aging differentiated cell population affects neoblast division patterns, one possibility is that neoblasts are depleted because of their failure to quench an ever-increasing demand for differentiated cell replacement.

Our results provide mechanistic insight into how specific cellular events of planarian regeneration are controlled. PIWI-like proteins regulate molecular processes involving small RNAs; SMEDWI-2 may regulate some aspect of RNA metabolism within dividing neoblasts. Our data suggest that SMEDWI-2 is not needed primarily for neoblast maintenance, but rather for the production of neoblast progeny capable of replacing aged differentiated cells during homeostasis and missing tissues during regeneration. Consistent with this suggestion, the mouse PIWI-related proteins MIWI and MILI are needed for the completion of spermatogenesis but not for primordial germ cell formation (*10*, *11*). Because human *hiwi* is expressed in primitive hematopoietic cells, PIWI proteins may regulate multiple types of stem cells (*19*). We suggest that PIWI proteins may be universal regulators of the production of stem cell progeny competent for performing differentiated functions.

References and Notes

1. M. A. Carmell, Z. Xuan, M. Q. Zhang, G. J. Hannon, *Genes Dev.* **16**, 2733 (2002).
2. G. Meister *et al.*, *Mol. Cell* **15**, 185 (2004).
3. J. Liu *et al.*, *Science* **305**, 1437 (2004).
4. T. A. Rand, K. Ginalski, N. V. Grishin, X. Wang, *Proc. Natl. Acad. Sci. U.S.A.* **101**, 14385 (2004).
5. K. Okamura, A. Ishizuka, H. Siomi, M. C. Siomi, *Genes Dev.* **18**, 1655 (2004).
6. R. S. Pillai, C. G. Artus, W. Filipowicz, *RNA* **10**, 1518 (2004).
7. K. Bohmert *et al.*, *EMBO J.* **17**, 170 (1998).
8. A. Sigova, N. Rhind, P. D. Zamore, *Genes Dev.* **18**, 2359 (2004).
9. D. N. Cox *et al.*, *Genes Dev.* **12**, 3715 (1998).
10. S. Kuramochi-Miyagawa *et al.*, *Development* **131**, 839 (2004).
11. W. Deng, H. Lin, *Dev. Cell* **2**, 819 (2002).
12. P. W. Reddien, A. Sánchez Alvarado, *Annu. Rev. Cell Dev. Biol.* **20**, 725 (2004).
13. P. W. Reddien, A. L. Bermange, K. J. Murfitt, J. R. Jennings, A. Sánchez Alvarado, *Dev. Cell* **8**, 635 (2005).
14. A. Sánchez Alvarado, P. A. Newmark, S. M. Robb, R. Juste, *Development* **129**, 5659 (2002).
15. P. A. Newmark, A. Sánchez Alvarado, *Nat. Rev. Genet.* **3**, 210 (2002).
16. M. Asami *et al.*, *Zool. Sci.* **19**, 1257 (2002).
17. K. Ogawa *et al.*, *Dev. Growth Differ.* **44**, 191 (2002).
18. P. Newmark, A. Sánchez Alvarado, *Dev. Biol.* **220**, 142 (2000).
19. A. K. Sharma *et al.*, *Blood* **97**, 426 (2001).

20. We thank K. Agata for FACS protocols, N. H. Oh for FACS assistance, P. Newmark and F. Cebriá for discussions, B. Pearson for comments, and all Sánchez lab members for support. P.W.R. is a Helen Hay Whitney Foundation fellow. A.S.A. is a Howard Hughes Medical Institute Investigator. Supported by National Institute of General Medical Sciences grant RO-1 GM57260 (A.S.A.).

Supporting Online Material

www.sciencemag.org/cgi/content/full/310/5752/1327/DC1
Materials and Methods
Figs. S1 to S4
Tables S1 to S3
References

14 June 2005; accepted 26 October 2005
10.1126/science.1116110

LIN-12/Notch Activation Leads to MicroRNA-Mediated Down-Regulation of Vav in *C. elegans*

Andrew S. Yoo[1] and Iva Greenwald[2]*

Cell-cell interactions and cross-talk between signaling pathways specify *Caenorhabditis elegans* vulval precursor cells (VPCs) to adopt a spatial pattern: a central "1°" VPC, in which epidermal growth factor receptor (EGFR)–mitogen-activated protein kinase (MAPK) activity is high and LIN-12/Notch activity is low, flanked by two "2°" VPCs, in which LIN-12/Notch activity is high and EGFR-MAPK activity is low. Here, we identify a microRNA gene, *mir-61*, as a direct transcriptional target of LIN-12 and show that expression of *mir-61* promotes the 2° fate. We also identify *vav-1*, the ortholog of the Vav oncogene, as a target of *mir-61*, and show that down-regulation of VAV-1 promotes *lin-12* activity in specifying the 2° fate. Our results suggest that *lin-12*, *mir-61*, and *vav-1* form a feedback loop that helps maximize *lin-12* activity in the presumptive 2° VPCs.

Six multipotential VPCs, numbered P3.p to P8.p, adopt an invariant pattern of fates termed 3°-3°-2°-1°-2°-3° (Fig. 1A). Two signaling events specify this pattern: "inductive" signaling, mediated by an EGFR-Ras-MAPK pathway, and "lateral" signaling, mediated by LIN-12 (Fig. 1A) (*1*). The inductive signal from the gonad activates an EGFR-Ras-MAPK cascade in a graded fashion in the underlying VPCs, P5.p, P6.p, and P7.p. The centralmost VPC, P6.p, has the highest level of EGFR-Ras-MAPK activation and becomes the presumptive 1° VPC; it produces the lateral signal, which activates LIN-12 in P5.p and P7.p. When LIN-12 is activated, proteolysis releases its intracellular domain, which translocates to the nucleus and forms a transcriptional activation complex with the DNA binding protein LAG-1 (*2*). Transcriptional targets of LIN-12 in P5.p and P7.p can be identified by the presence of LAG-1 binding sites (LBSs) in their 5′ flanking regions and include genes that encode negative regulators of EGFR-Ras-MAPK activity in P5.p and P7.p, which inhibit the expression of 1° fate features in these cells (*3*).

Short regulatory microRNAs (miRNAs), first identified in *C. elegans* (*4*), mediate post-transcriptional down-regulation of target genes. The profound and pervasive roles that miRNAs play as critical regulators of developmental gene expression are only now becoming fully appreciated. We obtained an indication that a

[1]Integrated Program in Cellular, Molecular, and Biophysical Studies, [2]Department of Biochemistry and Molecular Biophysics, Howard Hughes Medical Institute, Columbia University College of Physicians and Surgeons, 701 West 168th Street, Room 720, New York, NY 10032, USA.

*To whom correspondence should be addressed. E-mail: greenwald@cancercenter.columbia.edu

miRNA may be involved in lateral signaling after observing a lateral signaling defect when a miRNA-processing gene was depleted (*5*). We then computationally identified *mir-61* as a potential miRNA that is transcribed when the lateral signal from P6.p activates LIN-12 in P5.p and P7.p (*5*). A *mir-61* transcriptional reporter is specifically expressed in P5.p and P7.p and their daughters (Fig. 1B) (*6*), consistent with a function for *mir-61* as a direct target of LIN-12 during lateral signaling. This inference was confirmed by mutating the LBSs in the *mir-61* promoter and finding that expression in P5.p and P7.p was lost (Fig. 1C) (*7*).

Ectopic expression has been a successful approach to elucidating the role of miRNAs for which null alleles are not available and obviates potential problems that may be posed by functional redundancy (*8*–*10*). Expression of *mir-61* ectopically in P6.p, the presumptive 1° VPC, causes expression of the canonical 2° fate marker *lin-11::gfp*, whereas expression of an unrelated miRNA does not (Fig. 2). These observations suggest that *mir-61* activity promotes the 2° fate.

miRNAs bind to sites in 3′ untranslated regions (UTRs) of target mRNAs and inhibit their translation (*8*). Thus, we hypothesized that *mir-61* is expressed in presumptive 2° VPCs in order to down-regulate potential target gene products that would interfere with specification of the 2° fate. We identified potential target genes of *mir-61* computationally (*5*), requiring that 3′ UTRs have at least seven bases of perfect complementarity to the 5′ end of *mir-61* and that the binding sites be conserved in *C. briggsae* orthologs. This analysis yielded three candidates, *vav-1*, *inx-1*, and *egl-46* (Fig. 3A) (*5*).

To assess candidate genes in vivo, we developed a simple heterologous assay to circumvent potential detection problems due to weak or transient *mir-61* expression in the VPCs. This assay may be used to test whether any miRNA can target the 3′ UTR of any candidate target gene. We expressed *mir-61* in coelomocytes, distinctive cells for which strong promoters are available (*11*, *12*). On a second transgene, we expressed two reporters in coelomocytes: one a yellow fluorescent protein (YFP) reporter with the 3′ UTR of the putative target gene and the other a cyan fluorescent protein (CFP) reporter with the *unc-54* 3′ UTR, which does not contain any *mir-61*–binding sites (*13*). If a candidate is a bona fide target, then we would expect to see coelomocytes displaying CFP expression and down-regulation of YFP expression. Using this assay, we obtained evidence that *mir-61* can regulate the expression of the three candidate genes identified by using the criteria described above (Fig. 3A) (*5*).

mir-61 is also expressed in cells other than the VPCs, and *lin-12* activity specifies many other cell fate decisions (*14*), so even bona fide targets of *mir-61* may not be relevant to lateral signaling. The desired target genes should be transcribed in the VPCs but post-transcriptionally down-regulated by way of their 3′ UTRs in P5.p and P7.p and their daughters. We fused the 5′ upstream sequence of *vav-1*, *inx-1*, or *egl-46* to *yfp::unc-54 3′UTR* and found that only *vav-1* is expressed in the VPCs and their daughters (Fig. 3B). When we replaced the *unc-54* 3′UTR with the *vav-1* 3′ UTR, creating a sensor construct, *vav-1* expression was lost in P5.p and P7.p in a significant proportion of hermaphrodites; this loss depends on an intact *mir-61* target site (Fig. 3B). These observations indicate that *vav-1* is posttranscriptionally regulated in P5.p and P7.p, consistent with regulation by endogenous *mir-61*, and suggest that VAV-1 may be down-regulated in presumptive 2° VPCs to promote *lin-12* activity.

VAV-1 is an ortholog of the Vav oncoprotein, which has guanine nucleotide exchange factor (GEF) activity and additional domains that mediate interactions with other proteins (*15*); thus, there are many different potential mechanisms by which Vav proteins may modulate the activity of signaling pathways in presumptive 2° VPCs. In mammalian cells, in some contexts, Vav appears to be a positive regulator of MAPK signaling, but in others, it has no effect (*15*). Loss of *vav-1* activity does not prevent vulval induction, which indicates that *vav-1* is not required for EGFR-MAPK signaling in the cellular context of VPCs (*16*) and that down-regulation of VAV-1 by *mir-61* may not specifically attenuate EGFR-MAPK signaling in presumptive 2° VPCs in response to the low level of inductive signal (*3*).

Alternatively, VAV-1 may be a negative regulator of LIN-12. If so, then down-regulation of VAV-1 by *mir-61* would increase *lin-12* activity in P5.p and P7.p, independent of any input from the inductive signaling pathway. We therefore looked at whether loss of *vav-1* activity enhances *lin-12* activity under con-

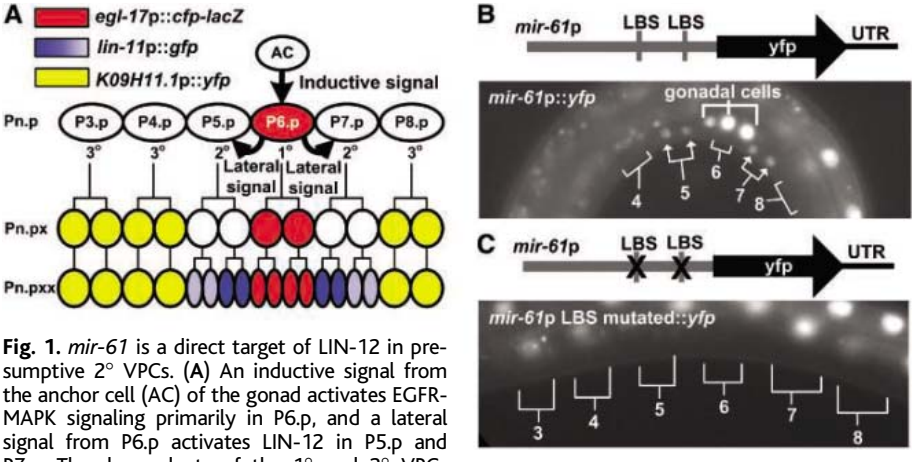

Fig. 1. *mir-61* is a direct target of LIN-12 in presumptive 2° VPCs. (**A**) An inductive signal from the anchor cell (AC) of the gonad activates EGFR-MAPK signaling primarily in P6.p, and a lateral signal from P6.p activates LIN-12 in P5.p and P7.p. The descendants of the 1° and 2° VPCs form the vulva, and the progeny of 3° VPCs fuse with the hypodermal syncytium. We used the 1° fate marker *arIs92[egl-17p::cfp-lacZ]* (*3*), the 2° fate marker *nIs106[lin-11p::gfp]* (*21*), and the 3° fate marker *arIs101[K09H11.1p::yfp]* (*22*). (**B**) *mir-61* is expressed in P5.p and P7.p. The *mir-61* promoter contains two LBSs that are conserved in the *C. briggsae* ortholog of *mir-61* (*5*). A reporter containing 1 kb upstream of *mir-61* fused to YFP is expressed in P5.p and P7.p (*22*) and their daughters (shown here). Prominent expression in cells of the gonad in which LIN-12 is active is also seen. (**C**) LBSs are required for *mir-61* expression in P5.p and P7.p. Two LBSs (YRTGRGAA) (*3*, *23*) that are conserved in *C. briggsae* were mutated to YRAGRGAA; a third nonconserved sequence, RTGGGAA, was also mutated to RAGGGAA. In three individual lines analyzed, expression of YFP in P5.p and P7.p disappeared. Expression in cells in which *lin-12* is not known to play a role in cell fate specification was normal, but gonadal expression was also abolished.

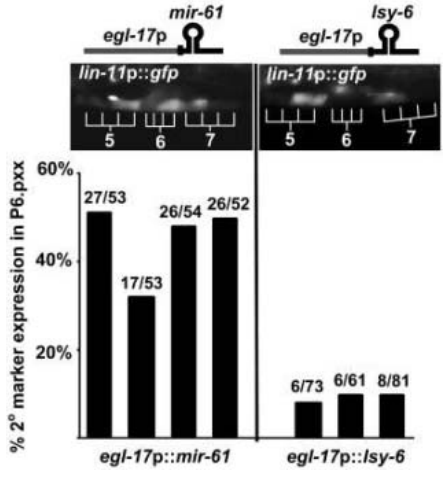

Fig. 2. Ectopic expression of *mir-61* in P6.p confers 2° fate characteristics. Expression of the 2° fate marker *nIs106[lin-11p::gfp]* (see Fig. 1A) was assessed when *egl-17p* (*3*, *24*) was used for ectopic expression of *mir-61* or the unrelated miRNA *lsy-6* (*25*) in P6.p and its descendants. Ectopic *lin-11p::gfp* expression in P6.p descendants was observed only when *mir-61* was expressed. Each bar represents an independent transgenic line. The number of individuals expressing the 2° marker out of the total is given above each bar.

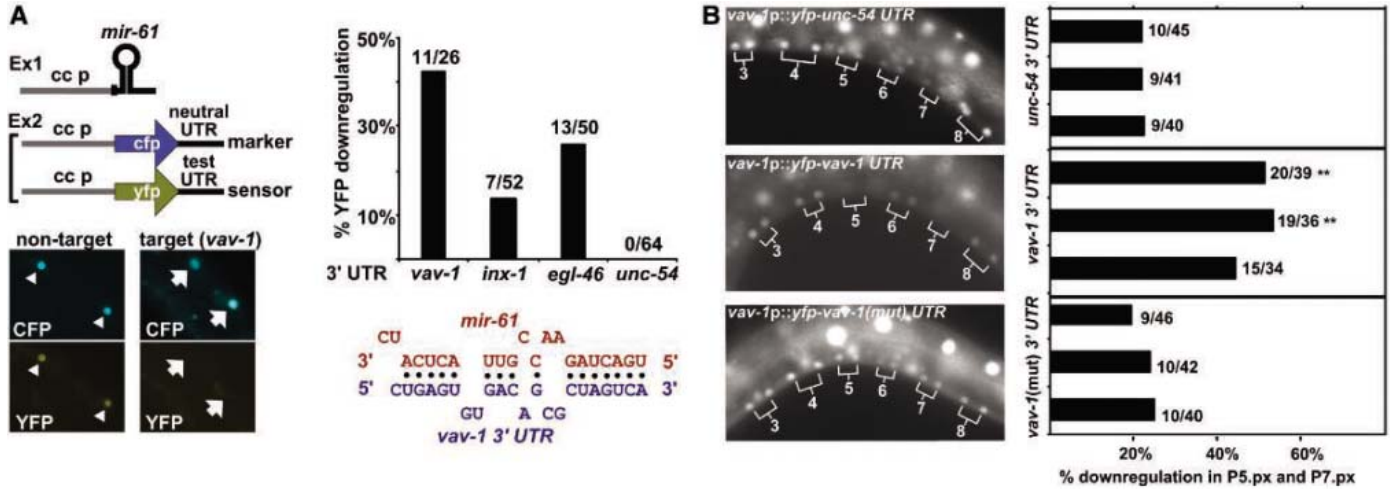

Fig. 3. *vav-1* is a target of *mir-61*. (**A**) Rapid assay to validate predicted miRNA targets. Components are expressed in coelomocytes to determine whether a miRNA causes down-regulation of YFP in a sensor construct containing a test UTR without affecting CFP in a marker construct with the neutral *unc-54* 3′ UTR (*26*). Here, an array carrying *unc-122*p::*mir-61* was combined with an array carrying the *unc-122*p::*cfp*::*unc-54 3′UTR* marker and *hlh-8*p::*yfp*::*vav-1 3′UTR* sensor (right) or an array carrying *hlh-8*p::*yfp*::*unc-54 3′UTR* in lieu of the sensor (left) (*6*). The presence of the *mir-61*–expressing array does not affect expression of YFP produced from a sensor construct that contains a nontarget UTR (in this case, the *unc-54* UTR) (triangles). In contrast, YFP expressed from a sensor construct that contains a target UTR (shown here, the *vav-1* UTR) is not seen, whereas the CFP marker shows that the array is present and expressed (arrows). The graphs indicate the percentage of worms that show the down-regulation of YFP signal. The alignment shows predicted configuration of *mir-61* (in red) binding to its target site in the 3′ UTR of *vav-1* (in blue). (**B**) VAV-1 is posttranscriptionally down-regulated in P5.p and P7.p. The 8.4-kb upstream region of *vav-1* drives expression of YFP in all VPCs and their daughters. When the *unc-54* 3′ UTR is replaced by *vav-1* 3′ UTR, down-regulation of YFP expression in P5.px and P7.px is evident. Mutation of the *mir-61*–complementary sequence in the *vav-1* 3′UTR from TAGTCA to GTCGAC causes persistent YFP expression. In the graph, each bar represents an individual line. $^{**}P < 0.01$ by Fisher's exact test. We minimized the potential lack of expression in P5.px or P7.px due to genetic mosaicism by including data only for animals in which expression could be seen in P3.px, P4.px, and P8.px.

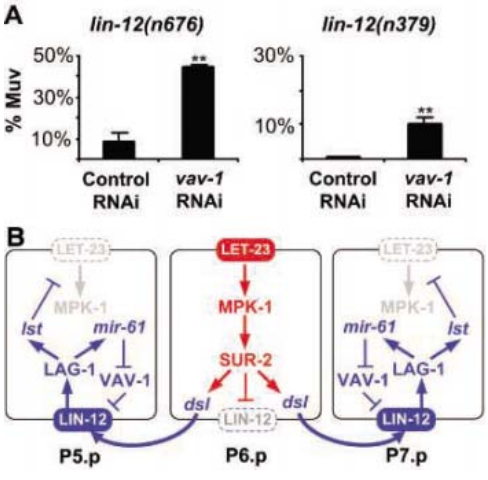

Fig. 4. vav-1 is a negative regulator of *lin-12* activity in the VPCs. (**A**) *vav-1(RNAi)* enhances *lin-12* activity in VPCs. The average percentage of worms with a Multivulva (Muv) phenotype (three or more pseudovulvae) on three independent plates is shown. For *lin-12(n676); vav-1(RNAi)*, the number of Muv hermaphrodites out of the total per plate was 50 out of 109, 49 out of 112, and 54 out of 125, with the control *lin-12(n676); gfp(RNAi)* values of 8 out of 157, 17 out of 168, and 18 out of 152. For *lin-12(n379); vav-1(RNAi)*, the numbers were 20 out of 187, 25 out of 208, and 13 out of 167, with *lin-12(n379); gfp(RNAi)* values of 1 out of 204, 1 out of 228, and 2 out of 225. Error bar indicates SD. $^{**}P < 0.01$ by Student's *t* test. (**B**) *mir-61*, *vav-1*, and the circuitry underlying specification of the 2° VPC fate. Activation of the EGFR-MAPK pathway in P6.p has two consequences for lateral signaling: transcription of the three Delta/Serrate/LAG-2 (DSL) ligands that constitute the lateral signal, which activates LIN-12/Notch in P5.p and P7.p (*27*), and internalization of LIN-12, which is necessary for lateral signal activity (*28*). Activation of LIN-12 in P5.p and P7.p activates a set of *lst* genes that counteract the EGFR-MAPK pathway (*3*), and *mir-61*, which posttranscriptionally down-regulates VAV-1 to promote *lin-12* activity.

ditions where inductive signaling does not occur. The alleles *lin-12(n379)* and *lin-12(n676)* result in mild constitutive activity: Hermaphrodites lack an anchor cell, and all VPCs generally adopt the 3° fate, as there is no inductive signal to specify a 1° fate and insufficient constitutive *lin-12* activity to promote anchor cell–independent 2° fates (*14*). In such backgrounds, loss of some negative regulators of LIN-12 increases LIN-12 stability or activity, which causes all six VPCs to adopt the 2° fate and to generate multiple pseudovulvae (*17*). Negative regulators that behave in this manner include SEL-10/Fbw7, which promotes ubiquitin-mediated turnover of LIN-12/Notch (*18*), and SEL-9, which functions in secretory protein quality control (*19*). We found that *vav-1(RNAi)* significantly enhances the constitutive activity of *lin-12(n379)* and *lin-12(n676)*, which increases the number of hermaphrodites with multiple pseudovulvae (Fig. 4A). These results suggest that *vav-1* is a negative regulator of *lin-12* activity.

We have shown that *mir-61* is a direct transcriptional target of the LIN-12/Notch pathway and that *vav-1* is a target of *mir-61* in the VPCs. We have also shown that ectopic *mir-61* promotes the 2° fate and that VAV-1 is a negative regulator of *lin-12* activity. We propose that activation of *mir-61* transcription by LIN-12 and the consequent down-regulation of VAV-1 constitute a positive-feedback loop that promotes LIN-12 activity in presumptive 2° VPCs (Fig. 4B).

Although there are many possible molecular mechanisms that may underlie this positive-feedback loop, it is notable that Vav has many domains that could couple it to receptors or to mediators of endocytosis (*15*). Indeed, Vav proteins have recently been shown to affect endocytosis of the activated Ephrin receptor (*20*). Perhaps down-regulation of VAV-1 in presumptive 2° VPCs decreases the rate of internalization, promotes endocytic recycling of LIN-12 or required proteases, or alters another aspect of trafficking that favors ectodomain shedding or transmembrane cleavage.

References and Notes

1. P. W. Sternberg, in *WormBook* (2005) (www.wormbook.org).
2. I. Greenwald, in *WormBook* (2005) (www.wormbook.org).
3. A. S. Yoo, C. Bais, I. Greenwald, *Science* **303**, 663 (2004).
4. R. C. Lee, R. L. Feinbaum, V. Ambros, *Cell* **75**, 843 (1993).

5. Supporting Online Material is available on *Science* Online.
6. All transcriptional reporters were made by polymerase chain reaction (PCR) fusion, from the predicted start to the next predicted upstream gene, and extrachromosomal arrays were marked with *pha-1(+)*. Expression of *mir-61* transcription was studied by using the *arIs107* integrant, which displayed the same pattern as extrachromosomal arrays.
7. *mir-61* is also expressed in cells of the somatic gonad in which LIN-12 is active, and this expression is also lost when the LBSs are mutated (Fig. 1, B and C). In contrast, expression in other tissues where we have no evidence that *lin-12* activity is functionally relevant, such as intestinal cells, is unaffected. These observations suggest that the loss of expression in P5.p and P7.p reflects lack of response to *lin-12* and not loss of a general enhancer.
8. V. Ambros, *Nature* **431**, 350 (2004).
9. C. Z. Chen, L. Li, H. F. Lodish, D. P. Bartel, *Science* **303**, 83 (2004).
10. S. Chang, R. J. Johnston Jr., C. Frokjaer-Jensen, S. Lockery, O. Hobert, *Nature* **430**, 785 (2004).
11. B. D. Harfe *et al.*, *Genes Dev.* **12**, 2623 (1998).
12. P. M. Loria, J. Hodgkin, O. Hobert, *J. Neurosci.* **24**, 2191 (2004).
13. We used two separate arrays because of possible promoter interference that we have experienced when using the same promoter to drive two different gene products in the same array. For the assessment of many targets, the assay could be improved by integrating the transgene expressing the miRNA.
14. I. S. Greenwald, P. W. Sternberg, H. R. Horvitz, *Cell* **34**, 435 (1983).
15. V. L. Tybulewicz, *Curr. Opin. Immunol.* **17**, 267 (2005).
16. K. R. Norman *et al.*, *Cell* **123**, 119 (2005).
17. M. Sundaram, I. Greenwald, *Genetics* **135**, 765 (1993).
18. E. J. Hubbard, G. Wu, J. Kitajewski, I. Greenwald, *Genes Dev.* **11**, 3182 (1997).
19. C. Wen, I. Greenwald, *J. Cell Biol.* **145**, 1165 (1999).
20. C. W. Cowan *et al.*, *Neuron* **46**, 205 (2005).
21. P. W. Reddien, S. Cameron, H. R. Horvitz, *Nature* **412**, 198 (2001).
22. A. S. Yoo, unpublished observations.
23. M. Rebeiz, N. L. Reeves, J. W. Posakony, *Proc. Natl. Acad. Sci. U.S.A.* **99**, 9888 (2002).
24. R. D. Burdine, C. S. Branda, M. J. Stern, *Development* **125**, 1083 (1998).
25. R. J. Johnston, O. Hobert, *Nature* **426**, 845 (2003).
26. From pPD95.67, gift of A. Fire (Stanford University).
27. N. Chen, I. Greenwald, *Dev. Cell* **6**, 183 (2004).
28. D. D. Shaye, I. Greenwald, *Development* **132**, 5081, (2005).
29. We are grateful to X. Zhou for performing microinjections; and to O. Hobert, R. Mann, and D. Shaye for discussion and insightful comments on the manuscript. This work was supported by NIH grant CA095389 (to I.G.). I.G. is an investigator with the Howard Hughes Medical Institute.

Supporting Online Material
www.sciencemag.org/cgi/content/full/1119481/DC1
Materials and Methods
SOM Text
Figs. S1 to S5
References and Notes

29 August 2005; accepted 13 October 2005
Published online 20 October 2005;
10.1126/science.1119481
Include this information when citing this paper.

Ecosystem Service Supply and Vulnerability to Global Change in Europe

Dagmar Schröter,[1,2*] Wolfgang Cramer,[1] Rik Leemans,[3] I. Colin Prentice,[4] Miguel B. Araújo,[5,6] Nigel W. Arnell,[7] Alberte Bondeau,[1] Harald Bugmann,[8] Timothy R. Carter,[9] Carlos A. Gracia,[10] Anne C. de la Vega-Leinert,[1] Markus Erhard,[11] Frank Ewert,[3] Margaret Glendining,[12] Joanna I. House,[4] Susanna Kankaanpää,[9] Richard J. T. Klein,[1] Sandra Lavorel,[13,14] Marcus Lindner,[15] Marc J. Metzger,[3] Jeannette Meyer,[15] Timothy D. Mitchell,[16] Isabelle Reginster,[17] Mark Rounsevell,[17] Santi Sabaté,[10] Stephen Sitch,[1] Ben Smith,[18] Jo Smith,[19] Pete Smith,[19] Martin T. Sykes,[18] Kirsten Thonicke,[4] Wilfried Thuiller,[20] Gill Tuck,[12] Sönke Zaehle,[1] Bärbel Zierl[8]

Global change will alter the supply of ecosystem services that are vital for human well-being. To investigate ecosystem service supply during the 21st century, we used a range of ecosystem models and scenarios of climate and land-use change to conduct a Europe-wide assessment. Large changes in climate and land use typically resulted in large changes in ecosystem service supply. Some of these trends may be positive (for example, increases in forest area and productivity) or offer opportunities (for example, "surplus land" for agricultural extensification and bioenergy production). However, many changes increase vulnerability as a result of a decreasing supply of ecosystem services (for example, declining soil fertility, declining water availability, increasing risk of forest fires), especially in the Mediterranean and mountain regions.

To sustain a future in which the Earth's life-support systems are maintained and human needs are met, human activities must first be recognized as an integral component of ecosystems (*1*, *2*). Scenarios of global change raise concern about alterations in ecosystem services such as food production and water supply, but the potential trajectories of change, especially at the regional scale, are poorly characterized (*3*). We investigated the changing supply of ecosystem services in a spatially explicit vulnerability assessment of Europe, using multiple global change scenarios and a set of ecosystem models. A dialogue with stakeholders from relevant sectors was conducted throughout the study (*4*).

Our assessment was based on multiple scenarios for major global change drivers (socioeconomic factors, atmospheric greenhouse gas concentrations, climate factors, and land use). The scenarios were quantified for Europe (15 pre-2004 European Union members, plus Norway and Switzerland, henceforth referred to as EU15+) during the 21st century at 10′-by-10′ latitude/longitude grid resolution, and for periods ending in 2020, 2050, and 2080, relative to baseline conditions in 1990 (*5*). Socioeconomic trends were developed from the global Intergovernmental Panel on Climate Change Special Report on Emission Scenarios (IPCC SRES) storylines B1, B2, A1FI, and A2 for EU15+ (*4*, *6*, *7*) (table S1). With this common starting point, socioeconomic changes relate directly to climatic changes through greenhouse gas concentrations and to land-use changes through climatic and socioeconomic drivers, such as demand for food. Four general circulation models (GCMs)—the Hadley Centre Coupled Model Version 3 (HadCM3), the National Center for Atmospheric Research–Parallel Climate Model (NCAR-PCM), the Second Generation

[1]Potsdam Institute for Climate Impact Research, 14473 Potsdam, Germany. [2]Center for International Development, Harvard University, Cambridge, MA 02138, USA. [3]Department of Environmental Sciences, Wageningen University, 6700 AA Wageningen, Netherlands. [4]Department of Earth Sciences, University of Bristol, BS8 1RJ Bristol, UK. [5]School of Geography and Environment, University of Oxford, OX1 3TB Oxford, UK. [6]Museo Nacional de Ciencas Naturales, 28006 Madrid, Spain. [7]Tyndall Centre for Climate Change Research, School of Geography, University of Southampton, Southampton SO17 1BJ, UK. [8]Department of Environmental Sciences, Eidgenössische Technische Hochschule, 8092 Zürich, Switzerland. [9]Finnish Environment Institute, 00251 Helsinki, Finland. [10]Center for Ecological Research and Forestry Applications, University of Barcelona, 08193 Barcelona, Spain. [11]Institute for Meteorology and Climate Research, Forschungszentrum Karlsruhe, 82467 Garmisch-Partenkirchen, Germany. [12]Agriculture and the Environment Division, Rothamsted Research, AL5 2JQ Harpenden, UK. [13]Laboratoire d'Ecologie Alpine, CNRS, Université Joseph Fourier, 38041 Grenoble, France. [14]Centre d'Ecologie Fonctionnelle et Evolutive, CNRS, Montpellier, France. [15]European Forest Institute, 80100 Joensuu, Finland. [16]Tyndall Centre for Climate Change Research, University of East Anglia, NR4 7TJ Norwich, UK. [17]Département de Géographie, Université Catholique de Louvain, 1348 Louvain-la-Neuve, Belgium. [18]Department of Physical Geography and Ecosystems Analysis, Lund University, 22362 Lund, Sweden. [19]School of Biological Sciences, University of Aberdeen, AB24 3UU Aberdeen, UK. [20]Kirstenbosch Research Center, South African National Biodiversity Institute, 7735 Cape Town, South Africa.

*To whom correspondence should be addressed. E-mail: dagmar.schroeter@gmail.com

Coupled Global Climate Model (CGCM2), and the Commonwealth Scientific and Industrial Research Organisation–Climate Model Version 2 (CSIRO2)—were used to simulate climatic changes (*4*). Out of 16 combinations of storylines and GCMs, we selected seven scenarios for interpretation: B1, B2, A1FI, A2 calculated with HadCM3 (variation across storylines, "socioeconomic options"), and A2 calculated additionally with three other GCMs (variation across climate models, "climatic uncertainty") (Table 1) (*4*).

Temperature-change scenarios in Europe vary regionally but show a clear trend toward warming. The average projected temperature increase in Europe ranged from 2.1° to 4.4°C (across storylines) and from 2.7° to 3.4°C for the A2 storyline (across GCMs) (Table 1), with the strongest warming consistently in the high latitudes (fig. S1). Seasonal and regional variation of changes in precipitation was considerable. Generally, all scenarios concurred on decreasing precipitation in the south of Europe, particularly in summer (Table 1), and increasing precipitation over much of northern Europe (fig. S2).

Land-use scenarios (*4*) showed little variation based solely upon different GCMs, indicating that socioeconomic assumptions had a greater effect on land use than did climatic drivers. The general trends were of reductions in agricultural areas for food production, partly compensated for by increases in bioenergy production and forests, as well as small increases in urban and protected areas (Table 2). In the A (economic) scenarios, the decline in agricultural land was especially pronounced (Fig. 1), mainly owing to assumptions about the role of technological development (*8*). The land that becomes "surplus" to the requirement of food production would allow balancing the production of other ecosystem services against food production, for example through extensification (*9*) or bioenergy production (*10*).

We next examined the changing supply of a number of ecosystem services owing to global change in Europe. The selected services reflect the availability of modeling tools adequate for pan-European assessment and the aim for a broad range of terrestrial services covering the four service categories identified by the Millennium Ecosystem Assessment (*1*).

The European Commission proposed a target of doubling the contribution of renewable energy sources to the EU's total primary energy needs to 12% by 2010 (*11*). Biomass energy will add to this goal. We assessed the potential distribution of 26 bioenergy crops under changing climatic conditions (*4*). The potential distribution of bioenergy crops increased in northern Europe as a result of increasing temperatures (Table 2). These potential gains are optimistic, given that restricting soil conditions are not taken into account. In contrast, the available choice of bioenergy crops decreased in southern Europe owing to increased drought, unless production systems are adapted (Table 2).

Table 1. Summary of the basic socioeconomic, atmospheric, and climatic drivers based on model outputs forced by SRES scenarios. Population and atmospheric CO_2 concentration estimates are for the year 2080. For the climatic indicators, 30-year averages 2051 to 2080 compared with 1961 to 1990 are shown. In this study, we focused on the HadCM3 climate model and the A2 storyline. The EU15+ population in 1990 was 376 million people. The GCMs were forced with these concentrations plus CO_2 equivalents accounting for the other greenhouse gases. The atmospheric CO_2 concentration in 1990 was 354 parts per million (ppm) by volume. Precipitation changes (%) on the Iberian Peninsula are given by season: JJA, summer (June, July, August); DJF, winter (December, January, February).

Scenarios by 2080	Climate model			
	HadCM3	NCAR-PCM	CGCM2	CSIRO2
	Storyline B1			
Population (10^6)	376	376	376	376
CO_2 concentration (ppm)	518	518	518	518
Δ Temperature (°C)	3.1	–	–	–
Δ Precipitation (%)				
Europe	4.8	–	–	–
Iberian Peninsula JJA	–17	–	–	–
Iberian Peninsula DJF	7	–	–	–
	Storyline B2			
Population (10^6)	346	346	346	346
CO_2 concentration (ppm)	567	567	567	567
Δ Temperature (°C)	2.1	–	–	–
Δ Precipitation (%)				
Europe	2.7	–	–	–
Iberian Peninsula JJA	–14	–	–	–
Iberian Peninsula DJF	7	–	–	–
	Storyline A1FI			
Population (10^6)	376	376	376	376
CO_2 concentration (ppm)	779	779	779	779
Δ Temperature (°C)	4.4	–	–	–
Δ Precipitation (%)				
Europe	–0.5	–	–	–
Iberian Peninsula JJA	–27	–	–	–
Iberian Peninsula DJF	2	–	–	–
	Storyline A2			
Population (10^6)	419	419	419	419
CO_2 concentration (ppm)	709	709	709	709
Δ Temperature (°C)	2.8	2.7	3.4	2.7
Δ Precipitation (%)				
Europe	0.5	2.3	0.0	–0.6
Iberian Peninsula JJA	–22	–18	–26	–19
Iberian Peninsula DJF	10	0	1	–3

Changes in the provision of water affect humans directly and indirectly through effects on other ecosystem services. At the global scale, increases in population and consumption alone will reduce water availability (*3*, *12*, *13*). We quantified the implications of population and climate change on water availability in EU15+ using a macroscale hydrological model (*4*). In 1995, approximately 193 million people out of a total EU15+ population of 383 million lived under water stress (water availability <1700 m^3 $capita^{-1}$ $year^{-1}$) (*14*). In the absence of climate change, these numbers decreased by 2080 where population decreased (scenario B2, Table 1). In contrast, population and climate change increased in the numbers of people living in water-stressed watersheds and exacerbated water deficiency for many already stressed areas (Table 2), particularly in southern Europe (Fig. 2). Under the A1FI, A2, and B1 scenarios, between 20 and 38% of the Mediterranean population would be living in watersheds with increased water stress (14% in B2). In this region, water scarcity would likely be aggravated by higher extractions per capita for irrigation and tourism (*15*).

Case studies for the Rhine, Rhône, and Danube basins, as well as for small Alpine catchments, indicated climate-induced changes in the timing of runoff (*4*). These result from impacts of rising temperatures on snow-cover dynamics, which enhanced winter runoff, reduced summer runoff (Table 2), and shifted monthly peak flows by up to two months earlier than at present (*16*). This reduced water supply at peak demand times and increased the risk of winter floods. Changes in snow-cover dynamics directly affect biodiversity at high elevations. Moreover, navigation and hydropower potential would be altered.

In addition to its importance for water supply and biodiversity conservation, snow cover is of course indispensable for winter tourism. The Alpine case studies indicated a rise in the elevation of reliable snow cover from about 1300 m today to 1500 to 1750 m at the end of

Table 2. Summary of land-use drivers and global change impacts for Europe, time period 2080 compared with baseline (1990), unless otherwise noted (*4*).

Storyline / GCM	B1 HadCM3	B2 HadCM3	A1FI HadCM3	A2 HadCM3	A2 NCAR-PCM	A2 CGCM2	A2 CSIRO2
Land-use model outputs forced by climate, CO_2, and interpretations of SRES storylines							
Land-use change (%)*							
Cropland (for food production)	−7.0	−6.4	−10.7	−10.4	−10.6	−10.7	−10.6
Grassland (for livestock)	−1.1	−6.7	−8.7	−10.0	−10.1	−10.2	−10.0
Forest	3.5	5.6	0.8	0.7	1.0	1.0	1.2
Urban	0.05	0.06	0.09	0.08	0.07	0.07	0.07
Bioenergy production	3.4	7.4	8.7	8.7	9.1	8.6	8.6
Protected	6.1	6.1	6.1	6.1	6.1	6.1	6.1
Surplus	1.1	0.0	9.8	10.9	10.5	11.2	10.8
Impacts as estimated by ecosystem models							
Δ Potential distribution of bioenergy crops (%)†							
Overall	3	4	1	3	6	7	5
Latitude 35 to 45	−7	−6	−13	−8	−1	−3	−2
Latitude 45 to 55	−1	0	−6	−2	4	8	−6
Latitude 55 to 65	12	13	12	13	11	14	15
Latitude 65 to 71	18	22	32	23	19	16	34
Additional people living under water stress (10^6)‡	44.3	25.8	44.3	15.7	7.5	11.7	5.8
People living under increased water stress (10^6)§	31.0	38.2	45.7	35.6	18.4	69.6	25.4
Δ Alpine summer runoff (%)‖	−24	-23	−46	−34	−12	−27	−20
Δ Elevation of reliable snow cover (m)‖	230	180	450	310	200	230	390
Species loss per grid cell (minimum to maximum %)¶	−7 to −58	−8 to −53	−8 to −59	−8 to −55			
Δ Area burnt, Iberian Peninsula (%)	112	57	80	55	−1	37	8
Δ Wood increment (%)	−10.0	9.7	3.8	4.4	2.9	2.9	6.2
Cumulative carbon balance (Pg C)#	2.2	2.4	1.8	3.0	4.9	4.1	3.7
Average carbon flux (% of emissions)**	2.5	2.7	2.1	3.5	5.5	4.7	4.2
Δ Soil organic carbon (Pg C)††							
Total	−0.1	−0.9	−4.1	−4.4	−4.3	−4.5	−4.8
Cropland	−4.3	−4.3	−5.9	−5.6	−5.4	−5.5	−5.8
Grassland	1.5	−1.2	−2.2	−2.7	−2.7	−2.7	−2.8
Forest	2.8	3.6	1.0	1.1	1.3	1.3	0.7

*Baseline areas (% of EU15+): Cropland, 23.0%; grassland, 17.2%; forest, 31.0%; urban, 1.5%; other (shrubland, barren land, wetland, inland waters, sea, permanent ice, and snow), 27.3%. For all scenarios, it is assumed that 20% of the area of Europe will become designated as "protected" by 2080. This was based on a judgment made from past and current increases in protected-areas coverage in Europe, the latter being due to member-state responses to the need for implementation of the NATURA 2000 network. Although this target was the same for all scenarios, it was assumed that it would be reached for different reasons: The economic scenarios require areas for recreation for a richer population, whereas the environmental scenarios require areas designated for conservation purposes (tables S1 and S2). "Surplus" is land that is left over when the demand for all land-use types is satisfied. †Change in potential distribution of 26 bioenergy crops (% land area) due to climate change. The estimates do not take soil conditions into account. ‡Additional people (millions) living in stressed watersheds due to climate change (compared with the hypothetical case of no climate change). Water-related resource problems are likely when water availability falls below the threshold of 1700 m^3 $capita^{-1}$ $year^{-1}$ (*14*). §People (millions) living in already water-stressed watersheds (less than 1700 m^3 $capita^{-1}$ $year^{-1}$), where climate change further reduces water availability by more than 10%. ‖Average of five Alpine case studies. ¶Year 2050 compared with the baseline (1990). The range of minimum (full instantaneous dispersal) to maximum (zero dispersal) loss is shown. Plants, mammals, reptiles, amphibians, and breeding birds were considered. This indicator records only losses from a specific grid cell and does not take potential gains into account. The indicator does not make a statement about potential losses of the species from Europe or about extinction. #Cumulative land-atmosphere carbon flux between 1990 and 2080. Positive values denote fluxes to land. **Average yearly land-atmosphere flux (1990 to 2080) relative to EU15+ CO_2 emissions in 1990. ††Change in cumulative soil organic carbon content in mineral soil down to a depth of 30 cm.

the 21st century (Table 2) (*16*). A 300-m rise of the snow line would reduce the proportion of Swiss ski areas with sufficient snow from currently about 85 to 63% (*17*).

Biodiversity is essential to ecosystem processes in ways that are not yet fully understood (*18*), and it is considered worth protecting in its own right (*3*). We used a statistical modeling framework to project the distribution of more than 2000 plant and animal species across Europe (*4*). These simulations do not incorporate effects of land-use change, because at the resolution of this study these were confounded with climate effects (*19*). We therefore present conservative estimates that neglect effects of habitat loss or landscape fragmentation (*20*). Projections of species loss per grid cell showed changes under all scenarios (Table 2). Mountains and Mediterranean species were disproportionately sensitive to climate change (fig. S3A) (*4*, *21*), in agreement with recent observations (*22*) and projections (*23*). Under the unrealistic assumption that all species can migrate instantaneously to newly suitable habitats, the relative potential gain of plant species in Mediterranean regions was relatively high because of habitat expansion (fig. S3B). However, unhindered expansion is unlikely because of the concurrent impacts of other drivers such as land use, nitrogen deposition, and biotic exchange, especially in the Mediterranean region (*20*). Flexible management of nature reserve areas may conserve species. However, stakeholders pointed out great difficulties in changing existing reserve boundaries under current policies and land-ownership restrictions.

To obtain more detailed results on tree species in the Mediterranean region, we used a process-based tree-growth model (*4*). The simulations corroborated negative effects on vegetation, especially over the long term, owing to increased drought. Furthermore, the area burnt by forest fires increased in this region under all but one scenario (*4*) (Table 2). The distribution of a number of typical tree species is likely to decrease in the Mediterranean region, such as cork oak (*Quercus suber*), holm oak (*Q. ilex*), aleppo pine (*Pinus halepensis*), and maritime pine (*P. pinaster*). These changes would have implications for the sense of place and cultural identity of the inhabitants, traditional forms of land use, and the tourism sector.

We assessed the potential impacts of management and global change on the overall wood production from European forest using an inventory-based model (*4*). In line with other industrialized areas, but opposed to global trends (*3*, *24*), the total European forest area was projected to increase (Table 2). Climate change resulted in increased forest growth (Table 2), especially in northern Europe. The impact of increased summer drought in southern Europe was partly mitigated by higher precipitation in spring and increased water-use efficiency in response to rising atmospheric CO_2 concentrations. Increasing forest area increased annual wood increment because of a high proportion of young stands. When low wood demand led to less intensive manage-

ment (B scenarios), forests grew old and less productive, and increment decreased by 10.0% in the B1 scenario (in B2, afforestation counteracted this effect; Table 2). In general, management had a greater influence on wood production in Europe than climate or land-use change. As corroborated by stakeholders, forest management is influenced more strongly by actions outside the forest sector, such as trade and policies, than from within.

The total amount of carbon stored in terrestrial biosphere is an important factor in climate regulation (*25*). The net carbon land-atmosphere flux is determined by net primary production and carbon losses due to soil heterotrophic respiration, fire, harvesting, and land-use change. The aggregate land-atmosphere flux over Europe was estimated using a dynamic global vegetation model (*4*). Our results confirm that Europe's terrestrial biosphere currently acts as a net carbon sink (*26*) (Table 2). Land-use change affected this sink positively through decreases in agricultural land and increased afforestation. Furthermore, CO_2 fertilization enhanced net primary production. However, soil carbon losses due to warming balanced these effects by 2050 and led to carbon releases by the end of this century. The temperature effect on soil carbon losses is confirmed by recent experimental and modeling studies (*27*–*29*) and by separate calculations using a soil carbon model (*4*). Although afforestation led to a net increase in soil organic carbon in forest soils despite the losses due to warming, the total amount of carbon in European soils decreased (Table 2).

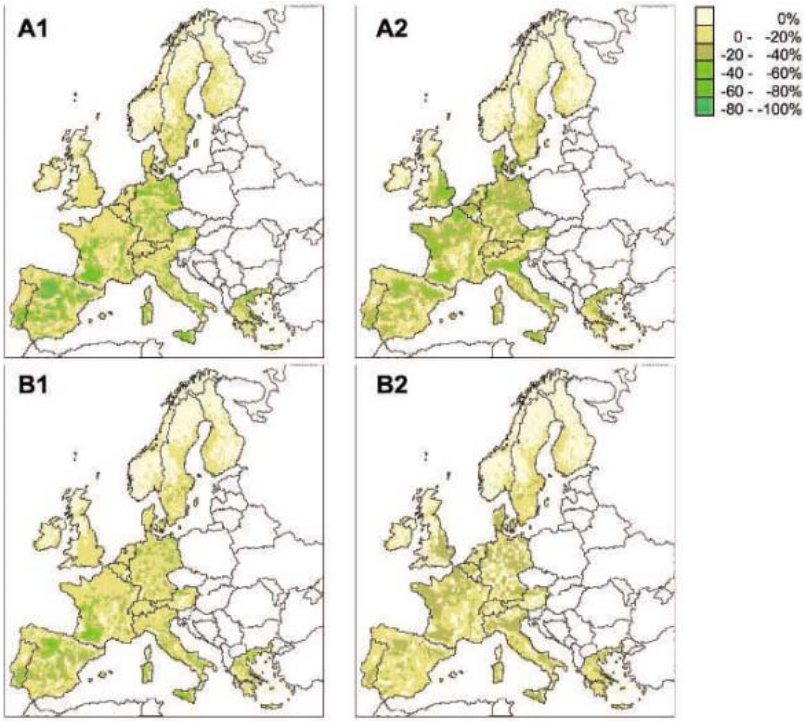

Fig. 1. Change in cropland area (for food production) by 2080 compared with the baseline (percentage of EU15+ area) for the four storylines [A1FI (A1), A2, B1, and B2] with climate calculated by HadCM3.

Stakeholders were primarily interested in the efficacy of land-use changes as a tool for mitigation. We found that the choice of land use is relevant concerning the average yearly carbon uptake and the emission reduction target of the European Union. However, carbon uptake remains small compared to fossil fuel emissions even under the land-use change scenario with maximum increase in forest area (Table 2).

Stakeholders from the agricultural sector were interested in soil organic matter content as a key factor in the carbon cycle and as an indicator of soil fertility. However, their greatest concern was the total amount of land available for farming. This may reflect that current agricultural subsidies disconnect farmers' success from actual ecosystem service supply, such as soil fertility and crop production. In some regions it is therefore questionable whether land that is "surplus" to food demands would readily be open for other uses.

The trends in European change drivers differ from global trends (*3*, *24*) in several ways:

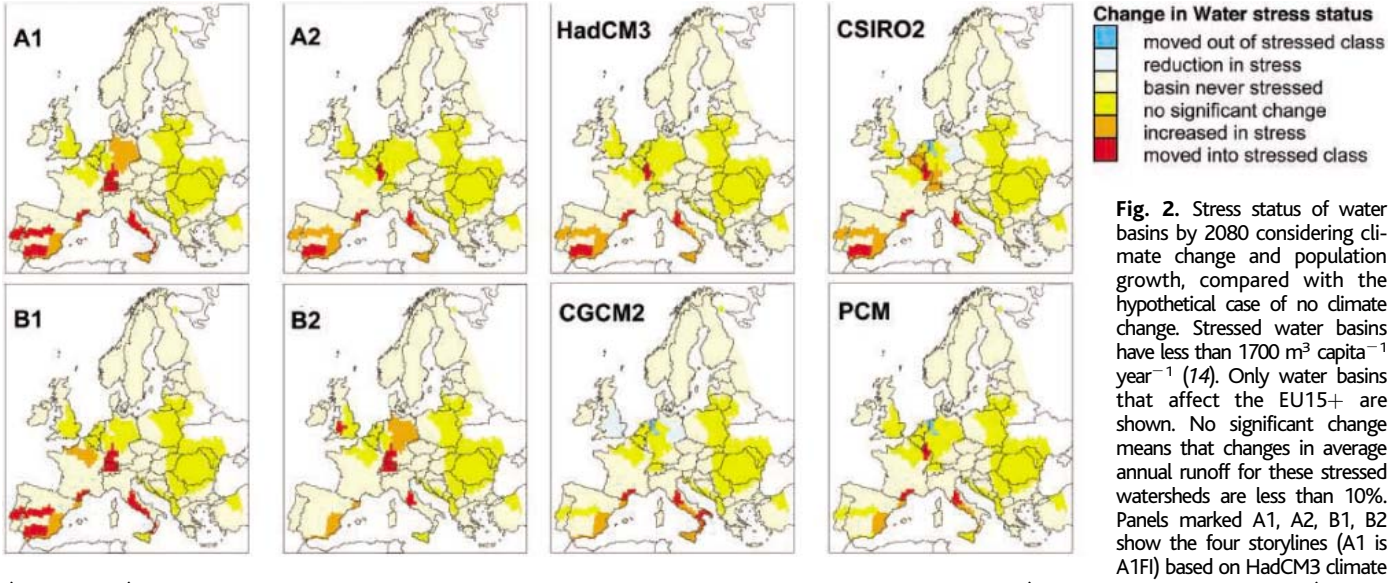

Fig. 2. Stress status of water basins by 2080 considering climate change and population growth, compared with the hypothetical case of no climate change. Stressed water basins have less than 1700 m^3 $capita^{-1}$ $year^{-1}$ (*14*). Only water basins that affect the EU15+ are shown. No significant change means that changes in average annual runoff for these stressed watersheds are less than 10%. Panels marked A1, A2, B1, B2 show the four storylines (A1 is A1FI) based on HadCM3 climate (2051 to 2080) and respective population sizes. Panels marked HadCM3, CSIRO2, CGCM2, and PCM show the four GCMs (2051 to 2080; PCM is NCAR-PCM) and A2 population size.

Population increases moderately if at all, the extent of urbanization is relatively small, forest area increases, and demand for agricultural land decreases. This allows changes in land management that could decrease vulnerability. Problematic trends in the EU15+ are mostly climate related.

The range of potential impacts in Europe covers socioeconomic options (storylines) and variation among GCMs. For most ecosystem services the A1FI scenario produced the biggest negative impacts, and the B scenarios seemed preferable. However, a division into either "economic" (A scenarios) or "equitable and environmental" (B scenarios) does not reflect all societal choices, given that sustainability does not forbid economic prosperity (*3*). The four storylines help explore but do not contain our optimal future pathway.

Among all European regions, the Mediterranean appeared most vulnerable to global change. Multiple potential impacts were projected, related primarily to increased temperatures and reduced precipitation. The impacts included water shortages, increased risk of forest fires, northward shifts in the distribution of typical tree species, and losses of agricultural potential. Mountain regions also seemed vulnerable because of a rise in the elevation of snow cover and altered river runoff regimes.

The sustained active participation of stakeholders indicated that global change is an issue of concern to them, albeit among many other concerns. The development of adaptation strategies, such as for reduced water use and long-term soil preservation, can build on our study but requires further understanding of the interplay between stakeholders and their environment in the context of local, national, and EU-wide constraints and regulations.

References and Notes

1. Millennium Ecosystem Assessment, *Ecosystems and Human Well-Being: A Framework for Assessment* (Island Press, Washington, DC, 2003).
2. M. Palmer *et al.*, *Science* **304**, 1251 (2004).
3. W. V. Reid *et al.*, *Millennium Ecosystem Assessment Synthesis Report* (Island Press, Washington, 2005).
4. Materials and methods are available as supporting material on *Science* Online.
5. The periods represent 30-year averages: baseline 1990 (mean over 1961 to 1990), 2020 (mean over 1991 to 2020), 2050 (mean over 2021 to 2050), and 2080 (mean over 2051 to 2080).
6. The economic A scenarios represent a world focused on material consumption, whereas the environmental B scenarios focus on sustainability, equity, and environment. The second dimension distinguishes globalization (dimension 1) from regionalization (dimension 2).
7. N. Nakicenovic, R. Swart, Eds., *Intergovernmental Panel on Climate Change Special Report on Emissions Scenarios* (Cambridge Univ. Press, Cambridge, 2000).
8. F. Ewert, M. D. A. Rounsevell, I. Reginster, M. J. Metzger, R. Leemans, *Agric. Ecosyst. Environ.* **107**, 101 (2005).
9. We refer to extensification as the transition of a land-use type with high intensity of use to a lower intensity (e.g., improved grassland to seminatural cover).
10. M. D. A. Rounsevell, F. Ewert, I. Reginster, R. Leemans, T. R. Carter, *Agric. Ecosyst. Environ.* **107**, 117 (2005).
11. "Energy for the future: Renewable sources of energy—White paper for a community strategy and action plan" *European Communities Tech. Report No. 599* (1997).
12. United Nations Environment Programme, "GEO-3: Global environmental outlook report 3" (UNEP, United Nations Environment Programme, Earthscan, London, 2002).
13. N. W. Arnell, *Glob. Environ. Change* **14**, 31 (2004).
14. M. Falkenmark, J. Lundquist, C. Widstrand, *Nat. Resour. Forum* **13**, 258 (1989).
15. In addition to increasing the number of people served with water in a region, tourists' water consumption has been shown to be far in excess of that of local residents (*30*).
16. B. Zierl, H. Bugmann, *Water Resour. Res.* **41**, WO2028 (2005).
17. H. Elsässer, P. Messerli, *Mt. Res. Dev.* **21**, 335 (2001).
18. D. U. Hooper *et al.*, *Ecol. Monogr.* **75**, 3 (2005).
19. W. Thuiller, *Glob. Change Biol.* **10**, 2020 (2004).
20. O. E. Sala *et al.*, *Science* **287**, 1770 (2000).
21. W. Thuiller, S. Lavorel, M. B. Araújo, M. T. Sykes, I. C. Prentice, *Proc. Natl. Acad. Sci. U.S.A.* **102**, 8245 (2005).
22. G.-R. Walther *et al.*, *Nature* **416**, 389 (2002).
23. M. Gottfried, H. Pauli, K. Reiter, G. Grabherr, *Diversity Distrib.* **5**, 241 (1995).
24. J. A. Foley *et al.*, *Science* **309**, 570 (2005).
25. A. D. McGuire *et al.*, *Global Biogeochem. Cycles* **15**, 183 (2001).
26. G. J. Nabuurs *et al.*, *Glob. Change Biol.* **9**, 152 (2003).
27. C. Fang, P. Smith, J. B. Moncrieff, J. U. Smith, *Nature* **433**, 57 (2005).
28. W. Knorr, I. C. Prentice, J. I. House, E. A. Holland, *Nature* **433**, 298 (2005).
29. E.-D. Schulze, A. Freibauer, *Nature* **437**, 205 (2005).
30. World Tourism Organization, First International Conference on Climate Change and Tourism, Djerba, Tunisia, 9 to 11 April 2003.

31. This work was funded by the EU-project ATEAM (Advanced Terrestrial Ecosystem Assessment and Modelling, EVK2-2000-00075). We gratefully acknowledge the support of our EU scientific officer D. Peter, and our external observers P. Leadley, D. Ojima, and R. Muetzelfeldt. We thank M. Welp for advice on stakeholder dialogue and our stakeholders for their voluntary collaboration (a full list is available in the supporting online material). Part of this work was carried out while D.S. was hosted by the *Science, Environment, and Development Group* at the Center for International Development, Harvard University.

Supporting Online Material

www.sciencemag.org/cgi/contents/full/1115233/DC1
Materials and Methods
Figs. S1 to S3
Tables S1 and S2
References and Notes

24 May 2005; accepted 18 October 2005
Published online 27 October 2005;
10.1126/science.1115233
Include this information when citing this paper.

Representation of Action-Specific Reward Values in the Striatum

Kazuyuki Samejima,[1]*† Yasumasa Ueda,[2] Kenji Doya,[1,3] Minoru Kimura[2]*

The estimation of the reward an action will yield is critical in decision-making. To elucidate the role of the basal ganglia in this process, we recorded striatal neurons of monkeys who chose between left and right handle turns, based on the estimated reward probabilities of the actions. During a delay period before the choices, the activity of more than one-third of striatal projection neurons was selective to the values of one of the two actions. Fewer neurons were tuned to relative values or action choice. These results suggest representation of action values in the striatum, which can guide action selection in the basal ganglia circuit.

Animals and humans flexibly choose actions in pursuit of their specific goals in the environment on a trial-and-error basis (*1*, *2*). Theories of reinforcement learning (*3*) describe reward-based decision-making and adaptive choice of actions by the following three steps: (i) The organism estimates the action value, defined as how much reward value (probability times volume) an action will yield. (ii) It selects an action by comparing the action values of multiple alternatives. (iii) It updates the action values by the errors of estimated action values. Reinforcement learning models of the basal ganglia have been put forward (*4*–*6*). The midbrain dopamine neurons encode errors of reward expectation (*7*–*9*) and motivation (*9*), and they regulate the plasticity of the corticostriatal synapses (*10*, *11*). Neuronal discharge rates in the cerebral cortex (*12*–*15*) and striatum (*16*–*18*) are modulated by rewards that are estimated by sensory cues and behavioral responses. These observations are consistent with action selection through the reinforcement learning rule (*3*) and with the notion of stimulus-response learning (*19*, *20*). However, two critical questions remain unanswered: Do the striatal neurons acquire action values in their activity through learning? How is the striatal neuron activity involved in reward-based action selection? Here we show by using a reward-based, free-choice paradigm that the striatal neurons learn to encode the action values through trial-and-error learning and

[1]Department of Computational Neurobiology, ATR Computational Neuroscience Laboratories, 619-0288 Kyoto, Japan. [2]Department of Physiology, Kyoto Prefectural University of Medicine, 602-8566 Kyoto, Japan. [3]Initial Research Project, Okinawa Institute of Science and Technology, 904-2234 Okinawa, Japan.

*To whom correspondence should be addressed. E-mail: samejima@lab.tamagawa.ac.jp (K.S.); mkimura@koto.kpu-m.ac.jp (M.K.)
†Present address: Brain Science Research Center, Tamagawa University Research Institute, 194-8610 Tokyo, Japan.

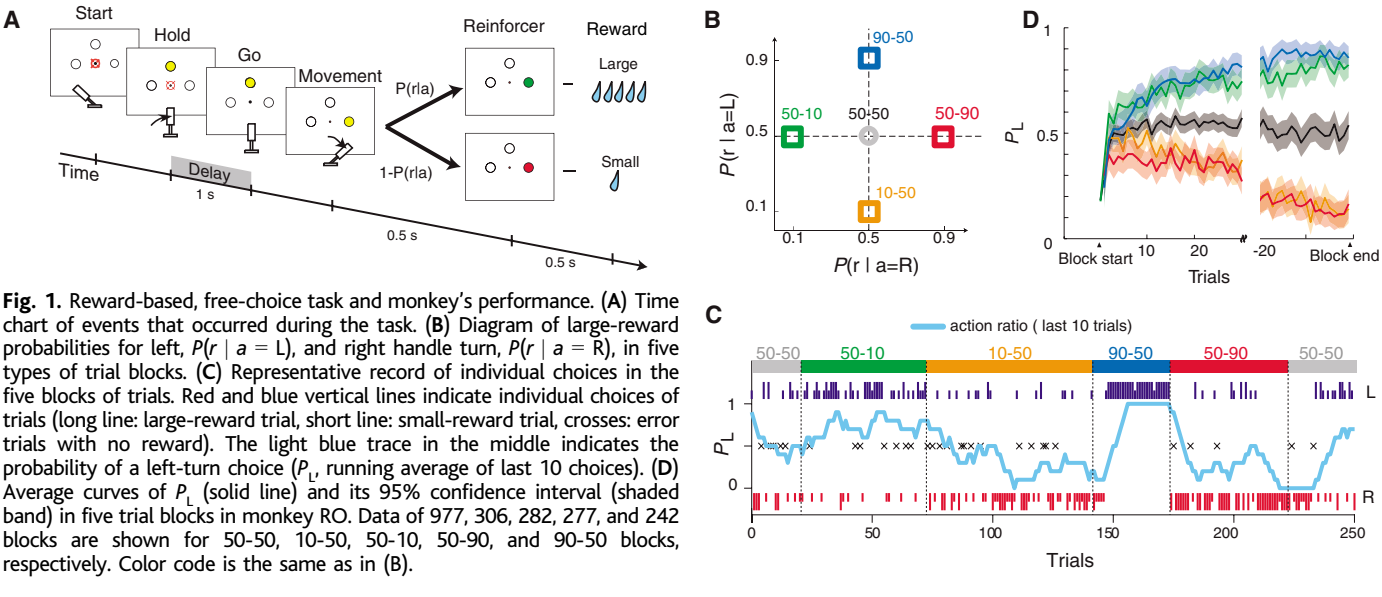

Fig. 1. Reward-based, free-choice task and monkey's performance. (**A**) Time chart of events that occurred during the task. (**B**) Diagram of large-reward probabilities for left, $P(r \mid a = L)$, and right handle turn, $P(r \mid a = R)$, in five types of trial blocks. (**C**) Representative record of individual choices in the five blocks of trials. Red and blue vertical lines indicate individual choices of trials (long line: large-reward trial, short line: small-reward trial, crosses: error trials with no reward). The light blue trace in the middle indicates the probability of a left-turn choice (P_L, running average of last 10 choices). (**D**) Average curves of P_L (solid line) and its 95% confidence interval (shaded band) in five trial blocks in monkey RO. Data of 977, 306, 282, 277, and 242 blocks are shown for 50-50, 10-50, 50-10, 50-90, and 90-50 blocks, respectively. Color code is the same as in (B).

predict choice probability of action options under a reinforcement learning algorithm.

Two macaque monkeys performed a reward-based, free-choice task of turning a handle to the left or right (Fig. 1A). The monkeys held a handle in the center position for 1 s (delay period) with their left hand. Then, they turned the handle in either the left (a = L) or right (a = R) direction. A light-emitting diode (LED) on the turned side was illuminated stochastically in either green or red. The green and red LEDs instructed monkeys that either a large reward (0.2 ml of water) or a small reward (0.07 ml), respectively, would follow. The probabilities of a large reward after left and right turns were fixed during a block of 30 to 150 trials and varied between five types of trial blocks. In the "90-50" block, for example, the probability of a large reward for the left turn was 90%, and for the right turn, 50%. In this case, by taking the small reward as the baseline (r = 0) and the large reward as unity (r = 1), the left action value Q_L was 0.9 and the right action value Q_R was 0.5. We used four asymmetrically rewarded blocks, "90-50," "50-90," "50-10," and "10-50," and one symmetrically rewarded block, "50-50" (Fig. 1B). An important feature of this block design was that the neuronal activity related to the action value could be dissociated from that related to action choice. Although the monkeys should prefer the left turn in both 90-50 and 50-10 blocks, the action value Q_L for the left turn changes from 0.9 to 0.5. Conversely, in the 90-50 and 10-50 blocks, although the monkey's choice behavior should be the opposite, the action value Q_R remains at 0.5.

Figure 1C shows a representative time course of choices on individual trials and the left-turn choice probability, P_L. Figure 1D shows the average curves of P_L during 2084 blocks of trials by monkey RO. The P_L started at around 0.5 (average of first 10 trials: 0.48 for monkey RO and 0.39 for monkey AR) and stayed around 0.5 in a symmetrically rewarded block in both monkeys. In asymmetrically rewarded blocks, the choice probability gradually shifted toward the action with higher reward values (binomial test, $P < 0.01$ for 50-50 versus four asymmetrically rewarded blocks). Although the time courses of the P_L shifts were variable among individual blocks, such as those in Fig. 1C, the average P_L at the same number of trials after the block start were not significantly different between 90-50 and 50-10 blocks, and between 50-90 and 10-50 blocks (Fig. 1D, $P > 0.05$).

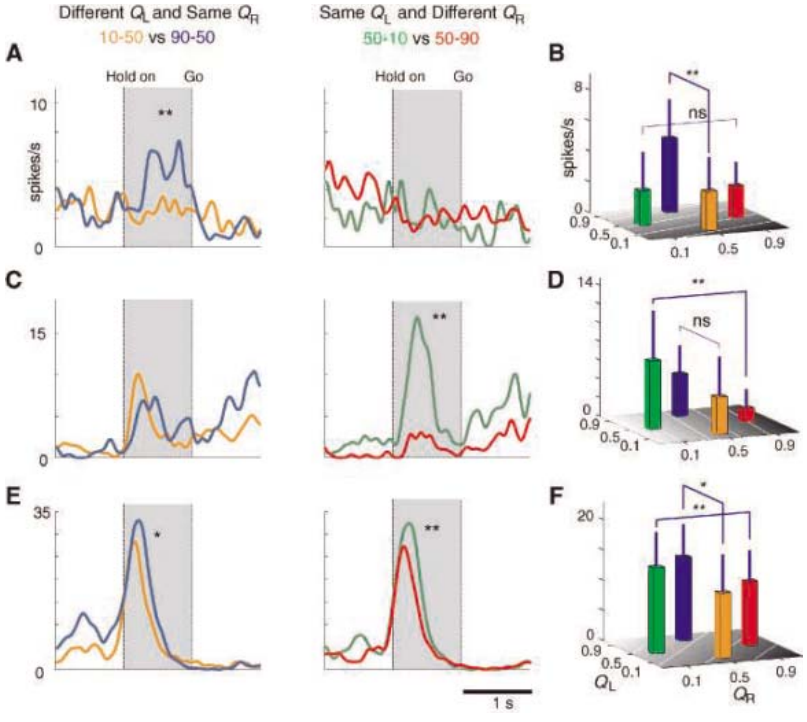

Fig. 2. Three representative reward-value coding neurons in the striatum. (**A**) A left–action value (Q_L-type) neuron in the anterior striatum. Average discharge rates during 10-50 and 90-50 blocks (left panel) and during 50-10 and 50-90 blocks (right panel) are shown. (**B**) Three-dimensional bar graph of average magnitudes and standard deviation of activity during delay period [shaded period in (A)]. Floor gradient shows the regression surface of neuronal activity by large-reward probability after left and right turns. (**C** and **D**) A right–action value (Q_R-type) neuron in anterior putamen. (**E** and **F**) A differential–action value (ΔQ and m-type) neuron with correlation also to action choice. The average activity curves in (A), (C), and (E) are smoothed with a Gaussian kernel (σ = 50 ms). Double and single asterisks indicate significant difference at $P < 0.001$ and $P < 0.01$ in Mann-Whitney U test, respectively.

We recorded 504 striatal projection neurons in the right putamen and caudate nucleus of two monkeys. The present study focused on the 142 (61 in monkey RO, 81 in monkey AR) neurons that displayed increased discharges during at least one task event and those that had discharge rates higher than 1 spike/s during the delay period. We compared the average discharge rates during the delay period from two asymmetrically rewarded blocks. The comparison was based on the trials after the monkey's choices had reached a "stationary phase," when the choice probability was biased toward the action with higher reward probability in more than 70% of trials. In half of the neurons (72/142 in two monkeys), activity was modulated by either Q_L or Q_R. Figure 2, A and B, shows a representative neuron in which the delay-period discharge rate was significantly higher in the 90-50 block (blue) than in the 10-50 block (orange) (P = 0.003, two-tailed Mann-Whitney U test). Delay period discharges were not significantly different (P = 0.70) between the 50-10 and 50-90 blocks (Fig. 2B), for which preferred actions were the opposite. Thus, the neuron encodes the left action value, Q_L, but not the action itself. Another neuron in Fig. 2, C and D, showed a significantly higher discharge rate in the 50-10 block than in the 50-90 block (P < 0.001), but there was no significant difference between the 10-50 and 90-50 blocks (P = 0.67). This neuron may code a negative right action value, $-Q_R$. We also found neurons (Fig. 2, E and F) that discharged more in the 90-50 block than in the 10-50 block (P = 0.028), but less in the 50-90 block than in the 50-10 block (P = 0.003). This neuron may encode the difference of action values, $Q_L - Q_R$, and choice of left turn.

To study the representation of action values in the population of striatal neurons, we made a multiple regression analysis of neuronal discharge rates with Q_L and Q_R as regressors (*21*). Figure 3A shows a scatter plot of t-values of the regression coefficients. We found 24 (17%) "Q_L-type" neurons, which had significant regression coefficients to Q_L (t-test, P < 0.05) but not to Q_R, and 31 (22%) "Q_R-type" neurons correlated to Q_R but not to Q_L. There were 16 (11%) "differential action value (ΔQ-type)" neurons correlated with the difference between Q_L and Q_R. One neuron was classified as "value (V)-type" (<1%), which was positively correlated with reward values independent of actions. In 41 neurons, there were significant regression coefficients to the behavioral measures including chosen action, reaction time, and movement time (Fig. 3A, open symbols). There were 18 "motor related (m)-type" neurons that had significant t-values only for behavioral measures. The discharge rates of most action value neurons (19/24 in Q_L-type, 24/31 in Q_R-type) were not correlated significantly with the behavioral measures. We concluded that, during a delay period before action choices, more than one-third of striate projection neurons examined (43/142) encoded action values, and that 60% (43/72) of all the reward value–sensitive neurons were action-value neurons.

We next examined whether the neuronal activity encoding action values predict monkey's action choices (*21*). The action values $Q_L(i)$ and $Q_R(i)$ at the ith trial of a single block of trials were estimated based on a standard reinforcement learning model and the past

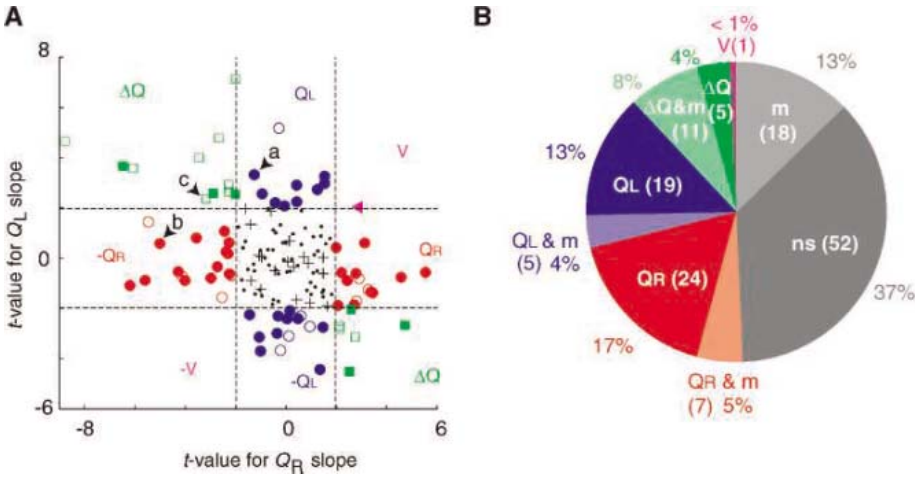

Fig. 3. Multiple regression analysis of neuronal activity with regressor of action value. (**A**) A scatter plot of partial regression coefficients of action values for left turn (Q_L) and right turn (Q_R). Blue circles, Q_L-type; red circles, Q_R-type; green squares, ΔQ-type; magenta triangles, V-type; crosses, m-type. Dark dots indicate neurons with no significant t-values for either regressor. Interrupted lines indicate levels of significant Q_L and Q_R slopes at P = 0.05 (t = ±1.97, 140 degrees of freedom). Open symbols indicate the neurons that also have significant regression coefficient of animals' choice, reaction time, or movement time. Letters a, b, and c indicate the example neurons in Fig. 2; A and B, C and D, and E and F, respectively. (**B**) Pie chart of neurons categorized into the four main types (Q_L, Q_R, ΔQ, and m) and three subtypes (ΔQ and m, Q_L and m, and Q_R and m).

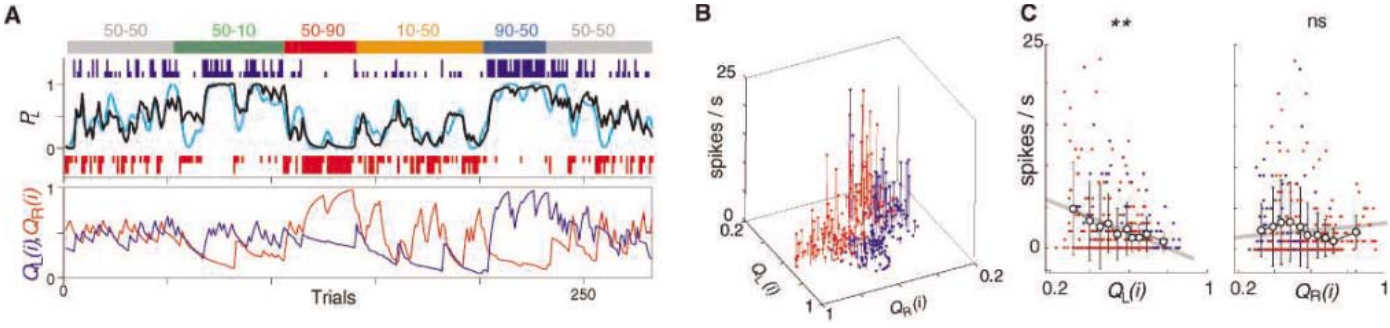

Fig. 4. Prediction of action choices and multiple regression analysis of neuronal activity by action values based on a reinforcement learning model. (**A**) An example of the time course of action values and predicted actions. From the data of actions and rewards (top panel: long vertical blue and red lines, large-reward trial; short lines, small-reward), the action values were estimated (bottom panel: $Q_L(i)$, blue line; $Q_R(i)$, red line) by a reinforcement learning model (*21*). Black and cyan curves indicate the action probability P_L given by the action values and the actual action choice ratio given by the weighted averages with a Gaussian kernel (σ = 2.5). (**B**) An example of the activity of a caudate neuron plotted on the space of estimated action values $Q_L(i)$ and $Q_R(i)$. It had significant regression coefficients with $Q_L(i)$ (slope k_{QL} = –9.7, P < 0.001, t-test), but not with $Q_R(i)$ (k_{QR} = 2.3, P = 0.29). Heights and colors of stem plots indicate the discharge rates of the neuron and individual choices of actions (blue, left; red, right), respectively. (**C**) The discharge rates of the neuron in (B) are projected on the $Q_L(i)$ and $Q_R(i)$ axes. The color code is the same as in (B). Gray lines are derived from the regression model. Circles and error bars indicate average and SD of neural discharge rates for each of 10 equally populated action value bins. The double asterisk indicates that the discharge rates were significantly correlated with $Q_L(i)$. This neuron was not selective to action itself (Mann-Whitney U test, P = 0.33). ns, not significant.

action $a(j)$ and reward $r(j)$ ($j = 1,\ldots, i-1$) (*3*, *22*). The estimated action values successfully predicted the probability of subsequent action choices, $a(i)$, (Fig. 4A and fig. S2). Figure 4, B and C, shows a Q_L-type neuron whose discharge rate during the delay period followed the time course of $Q_L(i)$ but not of $Q_R(i)$ (double asterisk regression slope for $Q_L(i) = -9.7$, $P < 0.001$, slope for $Q_R(i) = 2.3$, $P = 0.29$) (Fig. 4, B and C). These results suggest that a large subset of striatal neurons encode the action values that are updated by the history of actions and rewards and determine the probability of selecting a particular action.

Action-value coding in the striatum may be a core feature of information processing in the basal ganglia. The striatum is the primary target of dopaminergic signals, which regulate the plasticity of cortico-striatal synaptic transmission (*10*, *11*), conveying signals of actions and cognition. Thus, the striatum may be the locus where reward value is first encoded in the brain. This idea was supported by theoretical prediction (*23*) and by neural recordings from the striatum and the prefrontal cortex during association learning (*24*). Our finding of the successful prediction of individual action choices by estimated action values suggests the involvement of striatal action-value neurons in the process of selection of an action under a reinforcement learning algorithm. Whereas a large population of striatal neurons encoded action values, a much smaller population of neurons encoded forthcoming action during a premovement delay period. This favors action value–based models (*4*, *25*) for the striatal functions over stimulus-response learning and actor-critic models (*5*, *6*). However, further studies on the neuronal activity before and after action choices, not only in the striatum but also downstream from it, are necessary to clarify whether action selection is realized within the striatum through lateral inhibition (*5*, *26*) or in the globus pallidus (*4*, *27*). Deficits in action-value coding may lead to an inappropriate selection of competing actions or an inability to select any action, which might underlie some of the core symptoms of Parkinson's disease.

References and Notes

1. E. L. Thorndike, *Psychol. Rev. Monogr. Suppl.* **2**, 1 (1898).
2. R. A. Rescorla, R. L. Solomon, *Psychol. Rev.* **74**, 151 (1967).
3. R. S. Sutton, A. G. Barto, *Reinforcement Learning* [The Massachusetts Institute of Technology (MIT) Press, Cambridge, MA, 1998].
4. K. Doya, *Curr. Opin. Neurobiol.* **10**, 732 (2000).
5. J. C. Houk, J. L. Adams, A. G. Barto, *Models of Information Processing in the Basal Ganglia*, J. C. Houk, J. L. Davis, D. G. Beiser, Eds. (The MIT Press, Cambridge, MA, 1995).
6. J. O'Doherty *et al.*, *Science* **304**, 452 (2004).
7. W. Schultz, P. Dayan, P. R. Montague, *Science* **275**, 1593 (1997).
8. G. Morris, D. Arkadir, A. Nevet, E. Vaadia, H. Bergman, *Neuron* **43**, 133 (2004).
9. T. Satoh, S. Nakai, T. Sato, M. Kimura, *J. Neurosci.* **23**, 9913 (2003).
10. P. Calabresi, A. Pisani, N. B. Mercuri, G. Bernardi, *Trends Neurosci.* **19**, 19 (1996).
11. J. N. Reynolds, B. I. Hyland, J. R. Wickens, *Nature* **413**, 67 (2001).
12. B. Coe, K. Tomihara, M. Matsuzawa, O. Hikosaka, *J. Neurosci.* **22**, 5081 (2002).
13. K. Shima, J. Tanji, *Science* **282**, 1335 (1998).
14. D. J. Barraclough, M. L. Conroy, D. Lee, *Nat. Neurosci.* **7**, 404 (2004).
15. M. Watanabe, *Nature* **382**, 629 (1996).
16. R. Kawagoe, Y. Takikawa, O. Hikosaka, *Nat. Neurosci.* **1**, 411 (1998).
17. M. Shidara, T. G. Aigner, B. J. Richmond, *J. Neurosci.* **18**, 2613 (1998).
18. H. C. Cromwell, W. Schultz, *J. Neurophysiol.* **89**, 2823 (2003).
19. R. Hirsh, *Behav. Biol.* **12**, 421 (1974).
20. M. S. Jog, Y. Kubota, C. I. Connolly, V. Hillegaart, A. M. Graybiel, *Science* **286**, 1745 (1999).
21. Materials and methods are available as supporting material on *Science* Online.
22. K. Samejima, K. Doya, Y. Ueda, M. Kimura, *Advances in Neural Information Processing Systems 16*, S. Thrun, L. K. Saul, B. Sholkopf, Eds. (The MIT Press, Cambridge, MA, 2004).
23. J. C. Houk, S. P. Wise, *Cereb. Cortex* **5**, 95 (1995).
24. A. Pasupathy, E. K. Miller, *Nature* **433**, 873 (2005).
25. B. Lau, P. W. Glimcher, *Soc. Neurosci. Abstr.* **29**, 518.16 (2003).
26. J. R. Wickens, J. N. Reynolds, B. I. Hyland, *Curr. Opin. Neurobiol.* **13**, 685 (2003).
27. D. Arkadir, G. Morris, E. Vaadia, H. Bergman, *J. Neurosci.* **24**, 10047 (2004).

28. We thank M. Campos, T. Minamimoto, H. Yamada, S. C. Tanaka, K. Toyama and M. Kawato for discussion and R. Sakane for technical assistance. This research was supported by Grant-in-Aid for Scientific Research on Priority Areas, Ministry of Education, Culture, Sports, Science, and Technology of Japan (M.K., K.D., and K.S.), and by Creating the Brain, Core Research for Evolutional Science and Technology, Japan Science and Technology Agency (K.D.). Conducted as a part of Research on Human Communication, with funding from the National Institute of Information and Communications Technology of Japan.

Supporting Online Material

www.sciencemag.org/cgi/content/full/310/5752/1337/DC1
Materials and Methods
SOM Text
Figs. S1 to S4
Table S1
References

25 May 2005; accepted 28 October 2005
10.1126/science.1115270

Nucleus Accumbens Long-Term Depression and the Expression of Behavioral Sensitization

Karen Brebner,[1,3]* Tak Pan Wong,[1,2]* Lidong Liu,[1,2] Yitao Liu,[1,2] Paul Campsall,[1,2] Sarah Gray,[1,3] Lindsay Phelps,[1,3] Anthony G. Phillips,[1,3]† Yu Tian Wang[1,2]†

Drug-dependent neural plasticity related to drug addiction and schizophrenia can be modeled in animals as behavioral sensitization, which is induced by repeated noncontingent or self-administration of many drugs of abuse. Molecular mechanisms that are critical for behavioral sensitization have yet to be specified. Long-term depression (LTD) of α-amino-3-hydroxy-5-methyl-isoxazole-4-propionic acid receptor (AMPAR)–mediated synaptic transmission in the brain has been proposed as a cellular substrate for learning and memory. The expression of LTD in the nucleus accumbens (NAc) required clathrin-dependent endocytosis of postsynaptic AMPARs. NAc LTD was blocked by a dynamin-derived peptide that inhibited clathrin-mediated endocytosis or by a GluR2-derived peptide that blocked regulated AMPAR endocytosis. Systemic or intra-NAc infusion of the membrane-permeable GluR2 peptide prevented the expression of amphetamine-induced behavioral sensitization in the rat.

Behavioral sensitization of motor activity induced by repeated noncontingent or self-administration of drugs of abuse such as amphetamine, cocaine, heroin, and nicotine is an animal model of enduring drug-induced neuroplasticity (*1*–*4*). Behavioral sensitization involves neural adaptations in mesocorticolimbic regions, including the NAc, that receive dopaminergic (DA) projections from the ventral tegmental area (VTA) and excitatory glutamatergic inputs from the prefrontal cortex (PFC) (*5*, *6*). Initial work on behavioral sensitization focused on pre- and postsynaptic changes in DA systems, but recent evidence implicates synaptic plasticity in glutamatergic transmission in both the VTA and NAc (*6*–*9*). Whereas experience-dependent alterations in synaptic strength in the VTA are linked to the induction of behavioral sensitization, synaptic plasticity in the NAc appears to mediate its long-term maintenance and expression (*7*, *10*, *11*). Recent experiments indicate a role for LTD, a proposed cellular substrate for learning and memory, in behavioral sensitization. Sensitized mice show an enhanced depression

[1]Brain Research Centre, [2]Department of Medicine, and [3]Department of Psychiatry, University of British Columbia, Vancouver, British Columbia V6T 2B5, Canada.

*These authors contributed equally to this work.
†To whom correspondence should be addressed. E-mail: aphillips@psych.ubc.ca (A.G.P.); ytwang@interchange.ubc.ca (Y.T.W.)

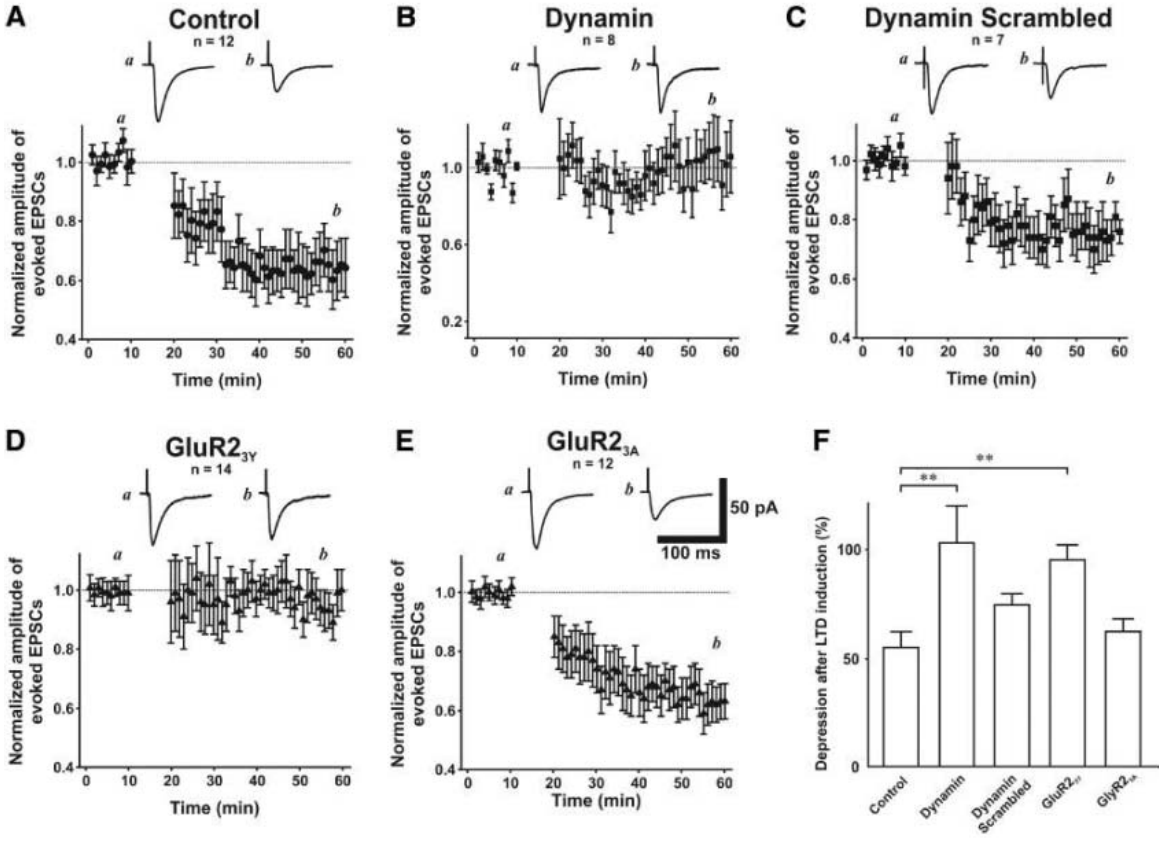

Fig. 1. Expression of LTD in NAc is mediated by clathrin- and GluR2-dependent AMPAR endocytosis. EPSCs evoked by electrical stimulation of glutamatergic cortical inputs were recorded from medium spiny neurons in NAc under whole-cell voltage-clamp mode at a holding potential of –70 mV before and after LTD induction. In all graphs, the amplitude of individual EPSCs was normalized to the mean value of amplitudes of all EPSCs during the 10-min baseline recordings before the induction of LTD. (**A**) LTD was induced by pairing presynaptic stimulation (1 Hz, 480 pulses) with postsynaptic depolarization by holding membrane potential at –50 mV. (**B** and **C**) NAc LTD required facilitated clathrin-dependent endocytosis in the postsynaptic neuron. Inclusion in the patch pipette of a dynamin peptide (Dyn, 100 μg/ml, $n = 8$) prevented LTD (B), whereas the inclusion of a scrambled form of the dynamin peptide (scrambled Dyn, 100 μg/ml, $n = 7$) had little effect on LTD (C). (**D** and **E**) GluR2-dependent endocytosis of postsynaptic AMPARs is required for expression of NAc LTD. The application of GluR2$_{3Y}$ (GluR2$_{3Y}$, 100 μg/ml, $n = 14$) (D), but not the control GluR2$_{3A}$ (GluR2$_{3A}$, 100 μg/ml, $n = 12$) (E) peptide via recording pipettes abolished LTD expression. (**F**) Bar graphs summarize data shown in (A) to (E). The double asterisks indicate $P < 0.01$ versus control (Tukey-Kramer test). Error bars indicate SEM.

of excitatory glutamatergic transmission in the NAc after repeated cocaine applications (*12*), providing the first correlation between acquired LTD and experience-dependent neural plasticity mediated by addictive drugs. The molecular mechanisms underlying NAc LTD remain to be specified, and no specific inhibitor for LTD is available to test its causative role in the expression of behavioral sensitization.

Experiments with hippocampal brain slices have linked LTD to a specific reduction in synaptic transmission mediated by facilitated endocytosis of postsynaptic α-amino-3-hydroxy-5-methyl-isoxazole-4-propionic acid receptors (AMPARs) (*13*–*15*). To determine whether a similar mechanism underlies NAc LTD, we performed whole-cell recordings of excitatory postsynaptic currents (EPSCs) in medium spiny neurons in the shell region of the NAc that were evoked by electrical stimulation of prelimbic cortical synaptic inputs. LTD was induced by using a pairing protocol (*16*). Clear and persistent depression of EPSC amplitude was obtained in 8 of 12 recorded neurons. Pooling all data revealed a 58 ± 8% ($n = 12$ neurons) reduction in the amplitude of EPSC relative to control values 40 min after LTD induction (Fig. 1A).

We then examined whether facilitated clathrin-dependent endocytosis at the postsynaptic neuron is required for the expression of this LTD using a dynamin-derived synthetic peptide (QVPSRPNRAP; Dyn) (*17*). This peptide inhibits clathrin-mediated endocytosis by blocking the recruitment of dynamin to clathrin-coated pits (*18*) and, when applied into postsynaptic cells, prevents the expression of certain forms of LTD (*14*, *19*). The presence of peptide (100 μg per ml of intracellular recording solution) in the recording pipette had little effect on basal synaptic transmission but prevented LTD expression (103 ± 15%, $P < 0.001$ versus control, $n = 8$) (Fig. 1, B and F). In contrast, the control scrambled dynamin peptide (QPPASNPRVR; scrambled Dyn) failed to block LTD expression (76 ± 4%, $P > 0.05$ versus control, $n = 7$) (Fig. 1, C and F).

We next investigated whether, similar to LTD characterized in other brain regions (*13*, *15*, *19*, *20*), the required clathrin-dependent endocytosis process in NAc LTD also involves GluR2-dependent endocytosis of postsynaptic AMPARs. We used a synthetic peptide derived from rat GluR2 carboxyl tail (GluR2$_{3Y}$; ^{869}YKEGYNVYG^{877}), which specifically blocks regulated, but not constitutive, AMPAR endocytosis and the expression of CA1 homosynaptic LTD, but not long-term potentiation (LTP), in hippocampal slices (*21*–*23*). The inclusion of the GluR2$_{3Y}$ peptide (100 μg/ml) completely abolished the expression of NAc LTD (96 ± 7%, $P < 0.001$ versus control, $n = 14$) (Fig. 1, D and F). Specific action of the GluR2$_{3Y}$ peptide, involving the blockade of GluR2-dependent AMPAR endocytosis, was confirmed. The control peptide GluR2$_{3A}$ (AKEGANVAG) failed to alter LTD expression (62 ± 6%, $n = 12$) (Fig. 1, E and F). No GluR2-derived peptides affected basal synaptic transmission (fig. S1). These results are in agreement with the specific role of GluR2$_{3Y}$ peptide in blocking regulated AMPAR endocytosis and hence the expression of LTD, without affecting constitutive AMPAR endocytosis and hence, the steady-state level of cell-surface expression of AMPARs, which mediates basal synaptic transmission (*21*).

The GluR2$_{3Y}$ peptide was used to test the hypothesis that LTD plays a critical role in the expression of behavioral sensitization. To

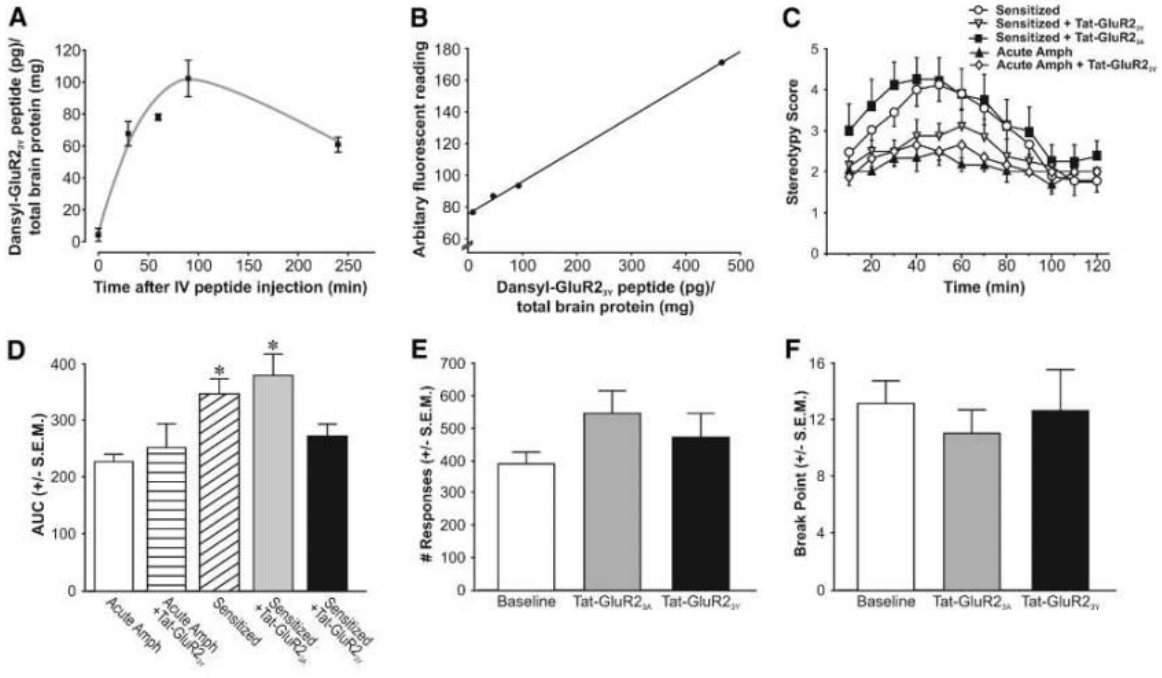

Fig. 2. Intravenous administration of the interference Tat-GluR2$_{3Y}$ peptide blocks D-amphetamine–induced behavioral sensitization of stereotypy. (**A** and **B**) Transduction of Tat-GluR2$_{3Y}$ peptide in rat brain. After iv injection of dansyl-Tat-GluR2$_{3Y}$ peptide (1.5 nmol/g), animals were perfused with saline at indicated time points to remove residual peptide in the blood stream. The concentrations of peptide at different time points (A) were then determined with reference to a standard curve constructed with different known amounts of dansyl-Tat-GluR2$_{3Y}$ peptide added into brain extract from control animals (B). (**C** and **D**) Systemic pretreatment of Tat-GluR2$_{3Y}$, but not Tat-GluR2$_{3A}$, prevented the sensitized behavioral response to a challenge dose of D-amphetamine in sensitized rats. Sensitized rats (n = 6 to 8 per group) were pretreated with Tat-GluR2$_{3Y}$, Tat-GluR2$_{3A}$, or saline by iv injection (1.5 nmol/g) 90 min before a challenge dose of D-amphetamine (2 mg/kg, ip). In (C), stereotypy scores were assessed at 10-min intervals. Points represent mean stereotypy scores (mean ± SEM) for each group of rats tested over the 2-hour session. Chronic saline-treated rats served as controls. (D) shows a summary of changes in stereotypy scores across the 2-hour test session converted to the area under the curve for individual groups depicted in (C). (**E**) Neither Tat-GluR2$_{3A}$ nor Tat-GluR2$_{3Y}$ affected lever-presses for food pellets on a fixed-ratio 2 schedule during 2-hour test sessions (n = 11). (**F**) Neither peptide had an effect on self-administration of D-amphetamine (0.2 mg/kg/infusion) delivered on a progressive ratio schedule. No significant differences in the break point measures for drug reward were observed after Tat-GluR2$_{3Y}$ or Tat-GluR2$_{3A}$ administered 90 min before the test session (n = 6). Error bars indicate SEM.

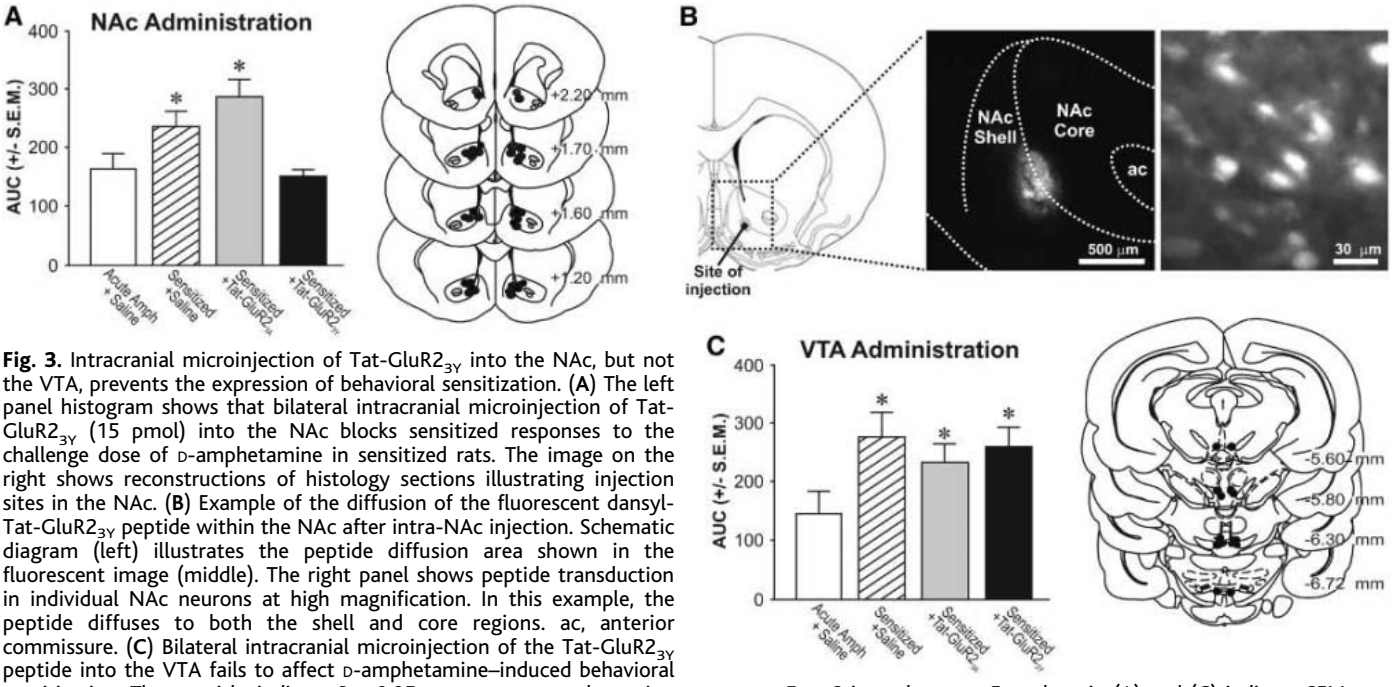

Fig. 3. Intracranial microinjection of Tat-GluR2$_{3Y}$ into the NAc, but not the VTA, prevents the expression of behavioral sensitization. (**A**) The left panel histogram shows that bilateral intracranial microinjection of Tat-GluR2$_{3Y}$ (15 pmol) into the NAc blocks sensitized responses to the challenge dose of D-amphetamine in sensitized rats. The image on the right shows reconstructions of histology sections illustrating injection sites in the NAc. (**B**) Example of the diffusion of the fluorescent dansyl-Tat-GluR2$_{3Y}$ peptide within the NAc after intra-NAc injection. Schematic diagram (left) illustrates the peptide diffusion area shown in the fluorescent image (middle). The right panel shows peptide transduction in individual NAc neurons at high magnification. In this example, the peptide diffuses to both the shell and core regions. ac, anterior commissure. (**C**) Bilateral intracranial microinjection of the Tat-GluR2$_{3Y}$ peptide into the VTA fails to affect D-amphetamine–induced behavioral sensitization. The asterisks indicate $P < 0.05$ versus acute amphetamine group. n = 5 to 8 in each group. Error bars in (A) and (C) indicate SEM.

facilitate the intracellular delivery of the peptide, both the wild-type GluR2$_{3Y}$ peptide and inactive control GluR2$_{3A}$ peptide were fused to the cell membrane transduction domain of the HIV-1 Tat protein [YGRKKRRQRRR (*24*)] to generate Tat-GluR2$_{3Y}$ and Tat-GluR2$_{3A}$ using previously published methods (*25*). Tat-GluR2$_{3Y}$ was transduced into neurons and blocked N-methyl-D-aspartate (NMDA)–induced AMPAR endocytosis in a neuronal cultured model of LTD (fig. S2) (*26*).

We next examined the potential role of NAc LTD in mediating the expression of behavioral sensitization to psychostimulant drugs after intravenous (iv) injection of Tat-GluR2$_{3Y}$ or Tat-GluR2$_{3A}$ peptides. Using fluorescently tagged peptides, we detected the presence of the peptides in the brain after a single iv injection of 1.5 nmol of peptide per g of body weight (nmol/g). Brain concentrations of the peptide increased in a time-dependent manner, with a peak concentration reached 90 min after injection (Fig. 2, A and B). Behavioral sensitization was induced by 10 intraperitoneal (ip) injections of D-amphetamine [2.0 mg drug per kg body weight (mg/kg)] on alternate days. The expression of behavioral sensitization was evoked by a challenge dose of D-amphetamine (2.0 mg/kg, ip) 21 days later. Pretreatment of sensitized rats with iv Tat-GluR2$_{3Y}$ (1.5 nmol/g) 90 min before the challenge dose of D-amphetamine prevented the expression of behavioral sensitization. Pretreatment with control Tat-GluR2$_{3A}$ or with saline had no effect (Fig. 2, C and D). Coadministration of Tat-GluR2$_{3Y}$ with an acute injection of D-amphetamine did not significantly change ($P > 0.05$) stereotypy responses (Fig. 2, C and D) or locomotor scores (636.5 ± 153.3, $n = 6$) relative to acute D-amphetamine alone (563.8 ± 94.7, $n = 4$). No noticeable behavioral side effects were associated with peptide pretreatment.

The effects of Tat-GluR2$_{3Y}$ do not appear to represent a general disruption of learned motor behavior, because systemic treatment with Tat-GluR2$_{3Y}$ failed to disrupt operant responding for food pellets delivered on a fixed ratio–2 schedule of reinforcement (Fig. 2E). Similar treatment with Tat-GluR2$_{3Y}$ or Tat-GluR2$_{3A}$ did not affect motivation to respond for iv D-amphetamine in a more demanding progressive ratio schedule of reinforcement (Fig. 2F), in which successive deliveries of drug reward require progressively more operant responses (*27*). To determine whether systemically applied Tat-GluR2$_{3Y}$ peptide disrupted the expression of behavioral sensitization by its action in the NAc but not the VTA, we performed intracranial microinfusion of Tat-GluR2$_{3Y}$ (15 pmol, 60 min before D-amphetamine challenge) into the NAc or VTA, with Tat-GluR2$_{3A}$ or saline serving as controls. Consistent with our hypothesis, microinfusion of Tat-GluR2$_{3Y}$ directly into the NAc (Fig. 3, A and B), but not the VTA (Fig. 3C), prevented the expression of behavioral sensitization. Pretreatment with either Tat-GluR2$_{3A}$ or saline failed to influence D-amphetamine–induced behavioral sensitization of stereotyped behavior.

Synaptic plasticity at excitatory synapses has been proposed as the cellular substrate of information processing and memory formation in the brain under both physiological (*28*, *29*) and pathological conditions, including addiction (*7*). Experiments characterizing the nature of synaptic plasticity in sensitized animals have observed both LTP (*30*) and LTD (*16*) in the NAc. Furthermore, increased excitatory drive in the NAc is observed during drug-seeking behavior (*31*). Within a given nucleus such as the NAc, it is suggested that the relative balance between LTP and LTD at different afferent inputs determines the expression of specific patterns of behavior (*32*). In sensitized animals, the abnormal induction of LTD at PFC inputs to the NAc may disrupt the influence of this pathway on neural activity involved in goal-directed behavior (*32*). However, as in any other area of the brain, exact roles of either NAc LTP or LTD in behavioral sensitization have not previously been defined because of the lack of specific inhibitors that block the expression of LTP or LTD without affecting any upstream signaling.

Here we identified clathrin-mediated and GluR2-dependent endocytosis of postsynaptic AMPARs as the final step in the expression of NAc LTD. We also demonstrated that the GluR2$_{3Y}$ peptide, which specifically blocks the endocytosis of postsynaptic AMPARs, prevented the expression of NAc LTD without affecting basal synaptic transmission and other upstream signaling processes involved in LTD. Using the membrane-permeant form of GluR2$_{3Y}$ peptide, we were able to probe the role of LTD in freely moving rats with great specificity and thereby provide evidence for the involvement of NAc LTD in the expression of behavioral sensitization. Because the GluR2$_{3Y}$ peptide used here has no effect on hippocampal CA1 LTP (*23*), a form of LTP involving regulated AMPAR insertion (*15*), the peptide appears not to affect the pool of AMPARs available for regulated insertion and hence does not affect the NAc LTP. Thus, determination of the exact role of NAc LTP in behavioral sensitization awaits the availability of an LTP-specific inhibitor.

Our work provides strong evidence for an essential role of NAc LTD in behavioral sensitization and thereby demonstrates the utility of peptides that disrupt the final step in the expression of synaptic plasticity as tools to examine the critical role of LTD and/or LTP in specific aspects of learning and memory in conscious animals. Given the links between behavioral sensitization and neuroplasticity induced by a potent psychostimulant drug of abuse, these data raise the possibility that treatment with new compounds, such as the GluR2$_{3Y}$ peptide used here, that disrupt psychostimulant-induced synaptic and behavioral plasticity may form the basis for a rational drug-development strategy for treating maladaptive neuroadaptations related to drug addiction.

References and Notes

1. T. E. Robinson, K. C. Berridge, *Brain Res. Brain Res. Rev.* **18**, 247 (1993).
2. A. G. Phillips, P. Di Ciano, *Psychopharmacology (Berl.)* **124**, 279 (1996).
3. P. Vezina, *Neurosci. Biobehav. Rev.* **27**, 827 (2004).
4. C. R. Ferrario *et al.*, *Biol. Psychiatry*, doi:10.1016/j.biopsych.2005.04.046, (2005).
5. R. C. Pierce, P. W. Kalivas, *Brain Res. Brain Res. Rev.* **25**, 192 (1997).
6. J. L. Cornish, P. W. Kalivas, *J. Addict. Dis.* **20**, 43 (2001).
7. S. E. Hyman, R. C. Malenka, *Nat. Rev. Neurosci.* **2**, 695 (2001).
8. M. E. Wolf, *Prog. Neurobiol.* **54**, 679 (1998).
9. P. W. Kalivas, N. Volkow, J. Seamans, *Neuron* **45**, 647 (2005).
10. P. Vezina, J. Stewart, *Brain Res.* **516**, 99 (1990).
11. M. Perugini, P. Vezina, *J. Pharmacol. Exp. Ther.* **270**, 690 (1994).
12. M. J. Thomas, C. Beurrier, A. Bonci, R. C. Malenka, *Nat. Neurosci.* **4**, 1217 (2001).
13. H. Y. Man, W. Ju, G. Ahmadian, Y. T. Wang, *Cell. Mol. Life Sci.* **57**, 1526 (2000).
14. C. Luscher *et al.*, *Neuron* **24**, 649 (1999).
15. D. S. Bredt, R. A. Nicoll, *Neuron* **40**, 361 (2003).
16. M. J. Thomas, R. C. Malenka, A. Bonci, *J. Neurosci.* **20**, 5581 (2000).
17. Single-letter abbreviations for the amino acid residues are as follows: A, Ala; C, Cys; D, Asp; E, Glu; F, Phe; G, Gly; H, His; I, Ile; K, Lys; L, Leu; M, Met; N, Asn; P, Pro; Q, Gln; R, Arg; S, Ser; T, Thr; V, Val; W, Trp; and Y, Tyr.
18. B. Marks, H. T. McMahon, *Curr. Biol.* **8**, 740 (1998).
19. Y. T. Wang, D. J. Linden, *Neuron* **25**, 635 (2000).
20. A. Luthi *et al.*, *Neuron* **24**, 389 (1999).
21. G. Ahmadian *et al.*, *EMBO J.* **23**, 1040 (2004).
22. Y. Wang *et al.*, *J. Biol. Chem.* **279**, 41267 (2004).
23. Hippocampal CA1 LTP was induced in rat slice preparations by pairing Schaffer collateral stimulation (200 pulses stimulation at 2 Hz) with postsynaptic depolarization of the cell to –5 mV from a holding membrane potential of –60 mV. LTP was reliably induced in cells recorded with pipette solutions supplemented with or without GluR2$_{3Y}$ peptide [normalized EPSC amplitude: 164 ± 22% for GluR2$_{3Y}$ (100 μg/ml, $n = 7$) versus 168 ± 18% for control ($n = 7$, $P > 0.5$)]. Thus, the GluR2$_{3Y}$ peptide appears not to affect LTP expression.
24. S. R. Schwarze, A. Ho, A. Vocero-Akbani, S. F. Dowdy, *Science* **285**, 1569 (1999).
25. M. Aarts *et al.*, *Science* **298**, 846 (2002).
26. E. C. Beattie *et al.*, *Nat. Neurosci.* **3**, 1291 (2000).
27. N. R. Richardson, D. C. Roberts, *J. Neurosci. Methods* **66**, 1 (1996).
28. M. F. Bear, R. C. Malenka, *Curr. Opin. Neurobiol.* **4**, 389 (1994).
29. T. V. P. Bliss, G. L. Collingridge, *Nature* **361**, 31 (1993).
30. W. D. Yao *et al.*, *Neuron* **41**, 625 (2004).
31. J. A. Hollander, R. M. Carelli, *Neuropsychopharmacology* **30**, 1464 (2005).
32. Y. Goto, A. A. Grace, *Neuron* **47**, 255 (2005).

33. This work was supported by the Brain Repair Program of Neuroscience Canada (A.G.P and Y.T.W.) and the Canadian Institutes of Health Research (CIHR). Y.T.W. is an international research scholar of the Howard Hughes Medical Institute and T.P.W. is a Research Fellow of CIHR. We gratefully acknowledge useful initial discussions with Y. Dong and advice from N. Gorelova for NAc slice preparation and from M. Thomas and A. Bonci on recording of NAc LTD in slices.

Supporting Online Material

www.sciencemag.org/cgi/content/full/310/5752/1340/DC1
Materials and Methods
Figs. S1 and S2
References

5 July 2005; accepted 21 October 2005
10.1126/science.1116894

Wingless Signaling at Synapses Is Through Cleavage and Nuclear Import of Receptor DFrizzled2

Dennis Mathew,[1] Bulent Ataman,[1] Jinyun Chen,[2] Yali Zhang,[2] Susan Cumberledge,[2] Vivian Budnik[1]*

Wingless secretion provides pivotal signals during development by activating transcription of target genes. At *Drosophila* synapses, Wingless is secreted from presynaptic terminals and is required for synaptic growth and differentiation. Wingless binds the seven-pass transmembrane DFrizzled2 receptor, but the ensuing events at synapses are not known. We show that DFrizzled2 is endocytosed from the postsynaptic membrane and transported to the nucleus. The C terminus of DFrizzled2 is cleaved and translocated into the nucleus; the N-terminal region remains just outside the nucleus. Translocation of DFrizzled2-C into the nucleus, but not its cleavage and transport, depends on Wingless signaling. We conclude that, at synapses, Wingless signal transduction occurs through the nuclear localization of DFrizzled2-C for potential transcriptional regulation of synapse development.

Members of the WNT signaling family function in synapse formation and maturation (*1*–*4*). In *Drosophila*, the WNT homolog Wingless (Wg) is secreted from presynaptic cells at glutamatergic larval neuromuscular junctions (NMJs) (*1*). The Wg receptor DFrizzled2 (DFz2) is present in both pre- and postsynaptic cells and is required for synaptic Wg function (*1*). Wg secretion from the presynaptic cell is crucial for both the formation of active zones (regions where synaptic vesicles accumulate adjacent to the presynaptic membrane) and postsynaptic specializations that are assembled during proliferation of synaptic boutons in larval development (*1*). How these Wg-dependent signaling events coordinate synapse differentiation remains unknown. To investigate the effect of Wg signaling on the distribution of its receptor and subsequent signal transduction, we used antibodies to the extracellular amino acids 1 to 114 (DFz2-N), and to the intracellular amino acids 600 to 694 (DFz2-C) (fig. S1). Staining of body wall muscles from third instar larvae showed that DFz2-C antibodies labeled the same NMJs as DFz2-N (Fig. 1, A and B) (*1*).

Antibodies against DFz2-C also labeled spotlike structures within each of the multiple nuclei in each muscle cell (Fig. 1, C to F; fig. S1). Quantification of the number of DFz2-C spots in each nucleus revealed that spots were more numerous in nuclei close to the NMJ than in those more distal (fig. S1). DFz2-N immunoreactive puncta were observed near the nucleus, but unlike those seen from DFz2-C immunoreactivity, these puncta were much smaller, were localized outside the nuclear boundary, and were never observed inside the nucleus (Fig. 1, G to J). Smaller DFz2-C immunoreactive puncta were also observed at the perinuclear area, but their abundance was low (arrowheads in Fig. 1C).

Intranuclear localization of DFz2-C was confirmed by double-labeling with propidium iodide (PI) and antibodies against the chromatin remodeling protein OSA (*5*, *6*), which associates with chromosomal DNA (Fig. 2, A and B). We also labeled preparations with antibody against HP-1, which labels heterochromatin (*7*). Regions of the nuclei containing HP-1 had either no DFz2-C spots (Fig. 2C) or only marginal coincidence (Fig. 2, D and E), which suggests that DFz2-C spots are mostly excluded from regions of transcriptionally inactive DNA. Nuclear localization of DFz2-C appeared to be cell-type–specific. Although DFz2-C spots were always observed in the nuclei of larval muscles, DFz2-C was not observed in epithelial cells (fig. S1E) or neurons.

To test whether DFz2 might be cleaved, as are some other membrane receptors such as Notch and β-amyloid precursor protein (APP) (*8*), we transfected *Drosophila* Schneider-2 (S2) cells with full-length DFz2 or with DFz2 fragments containing the N-terminal region (amino acids 1 to 605) or C-terminal region (amino acids 606 to 694). On Western blots of lysate from S2 cells transfected with DFz2, two protein bands were detected, an 83-kD band (full-length DFz2) and an 8-kD band (Fig. 2F). The 83-kD band was recognized by both the DFz2-N and the DFz2-C antibodies, but only the DFz2-C antibody recognized the 8-kD band, which suggested that full-length DFz2 may be cleaved to produce a C-terminal fragment. In extracts of wild-type body wall muscle, full-length DFz2 was detected at very low levels by Western blots, but the 8-kD band was not detected. However, if full-length DFz2 was overexpressed in muscle cells, an 8-kD fragment was detected (Fig. 2G).

We compared the putative amino acid sequence of DFz2 with those of its most related Frizzled counterparts from different species (*9*), because regions of functional significance are highly conserved across phylogenies. A sequence in the cytoplasmic domain proximal to the transmembrane do-

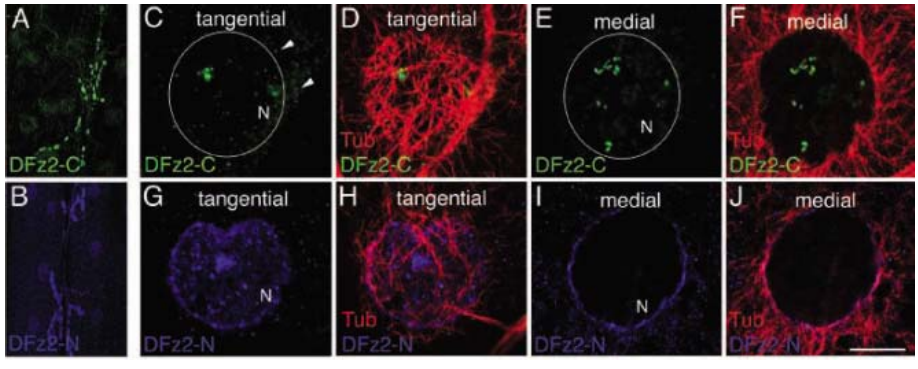

Fig. 1. Localization of DFz2-C and DFz2-N to the same NMJs, but to different subcellular compartments, inside the nucleus (DFz2-C) and at the perinuclear region (DFz2-N). (**A** and **B**) Wild-type third instar NMJs from muscles 6 and 7 (A3) stained with antibodies against (A) DFz2-C and (B) DFz2-N. (**C** through **J**) Representative muscle nuclei at muscle 6 (A3) in preparations double-stained with antibodies against (C through F) DFz2-C (green) and tubulin (red) and (G through J) DFz-N (blue) and tubulin (Tub) (red). Note that (C to F) and (G to J) were obtained from different preparations. (C, D, G, H) show a confocal slice at a focal plane through the nuclear-cytoplasmic boundary (defined by the microtubular array; tangential), and (E, F, I, J) a confocal slice at a focal plane midway through the nucleus (medial). N, nucleus, arrowheads in C point to cytoplasmic DFz2-C. Scale bar, 9 μm in (A and B), and 8 μm in (C to J).

[1]Department of Neurobiology, University of Massachusetts Medical School, Worcester, MA 01605, USA. [2]Department of Biochemistry and Molecular Biology, University of Massachusetts, Amherst, MA 01003, USA.

*To whom correspondence should be addressed. E-mail: vivian.budnik@umassmed.edu

main (VWIWSGKTLESW) (*10*) is virtually identical in all species, from flies to humans, and contains a glutamyl-endopeptidase cleavage site (fig. S2). In eukaryotes, glutamyl-endopeptidase activity is observed in peptidases of the ADAM (a disintegrin and metalloprotease) family (*11*), and ADAM members have also been implicated in APP (*12*) and Notch (*13*) receptor cleavage. Although, in the case of APP and Notch, ADAM proteases cleave the extracellular domain of the proteins, ADAM proteases are also observed intracellularly (*14*).

We used site-directed mutagenesis to construct three mutants: two deleting the coding sequences for KTLES, which contains the glutamyl endopeptidase cleavage site (ΔKTLES and ΔSGKTLESW), and another mutating the adjacent upstream sequence VWIWSG (DFz2-ΔVWIWSG). The amount of cleavage product was reduced in DFz2-ΔKTLES–expressing S2 cells, and no cleavage product was detected in DFz2-ΔSGKTLESW cells, but DFz2-ΔVWIWSG cells had normal amounts (Fig. 2H). Thus, KTLES is apparently contained in the cleavage site or required for cleavage.

Localization of DFz2-C and DFz2-N fragments into different compartments within and around the nucleus may occur immediately after DFz2 biosynthesis, or DFz2 fragments may translocate to the nucleus through a retrograde pathway after integration into the plasma membrane (fig. S3). To distinguish between these possibilities, we tested whether cell surface DFz2 was internalized and transported to the nucleus. Larvae were dissected, and body wall muscles were incubated in situ in physiological saline containing antibody against DFz2-N. Under these conditions, the antibody was expected to label only surface DFz2 (*15*). Then, unbound antibody was washed away, the preparations were fixed, and a secondary antibody conjugated to a blue fluorescent marker (Alexa-647) was added under nonpermeabilizing conditions to detect surface DFz2. To determine whether any cell surface DFz2 had been internalized during the initial incubation, the preparation was permeabilized and then incubated with secondary antibody conjugated to a green fluorescent marker (FITC) (*15*). A prerequisite for such an experiment is that the antibody should label the extracellular region of DFz2 in situ, and indeed, we found that anti-DFz2-N could label NMJs in situ (Fig. 3A). A fraction of surface-labeled DFz2 was internalized into the muscle and appeared as puncta at the NMJ (Fig. 3, B and C).

To determine whether nuclear DFz2 was derived from receptors that were internalized at the postsynaptic membrane, we conducted an antibody pulse-chase experiment in living preparations. The primary antibody-binding step was done at 4°C to inhibit internalization during antibody incubation. Unbound antibody was washed away, and samples were shifted to room temperature for various time intervals before fixation (Fig. 3; fig. S3). In samples that were fixed after a 5-min shift at room temperature, most of the internalized DFz2 was observed close to the NMJ (Fig. 3, B and C), but after 60 min, little internalized DFz2 was observed at the NMJ (Fig. 3, D to F). There was a comparatively small decrease in surface DFz2 over time at the NMJ, suggesting that only a fraction of labeled DFz2 was internalized (Fig. 3, A and D). Parallel with the changes in DFz2 internalization at the NMJ, at 5 min, minimal internalized DFz2 was observed at the periphery of nuclei (Fig. 3G), whereas at 60 min, the amount of internalized DFz2 at the nuclear periphery was increased (Fig. 3H). Thus, cell surface DFz2 appears to be transported from the plasma membrane to the nucleus.

If cell surface DFz2 is endocytosed and transported to the nucleus, then blocking endocytosis or retrograde vesicle transport should block the nuclear localization of DFz2. Therefore, in a subset of muscle cells, we expressed dominant-negative transgenes that block endocytosis [dominant-negative form of the *Drosophila* Dynamin, Shibire (Shi-DN) (*16*)] or retrograde transport [dominant-negative form of Glued, a component of the dynein-dynactin complex (*17*)]. In both cases, the number of DFz2-C spots per nucleus was reduced (Fig. 4A; fig. S4). These results, together with the in vivo internalization assays, indicate that DFz2 is internalized from the plasma membrane and is carried by retrograde transport to the nucleus.

We also tested whether Wg signaling was required for DFz2 transport to the nucleus. To decrease Wg signaling, we used a temperature-sensitive wg^{ts} mutant, as well as two conditions that disrupt Wg-dependent DFz2 signaling: overexpression of full-length DFz2 in muscles (*1*, *18*) and expressing a DFz2 dominant-negative DFz2 construct (DFz2-DN) (*19*). We also overexpressed Wg in the presynaptic cells, which caused those cells to increase Wg secretion (*1*, *16*, *18*). Disrupting Wg signaling caused a decrease in the number of DFz2-C spots inside muscle nuclei (Fig. 4A). In contrast, when presynaptic secretion of Wg was increased, there was an increase in the number of nuclear spots (Fig. 4A; fig. S4).

We also expressed transgenic DFz2 variants in muscles, full-length DFz2, DFz2ΔSGKTLESW,

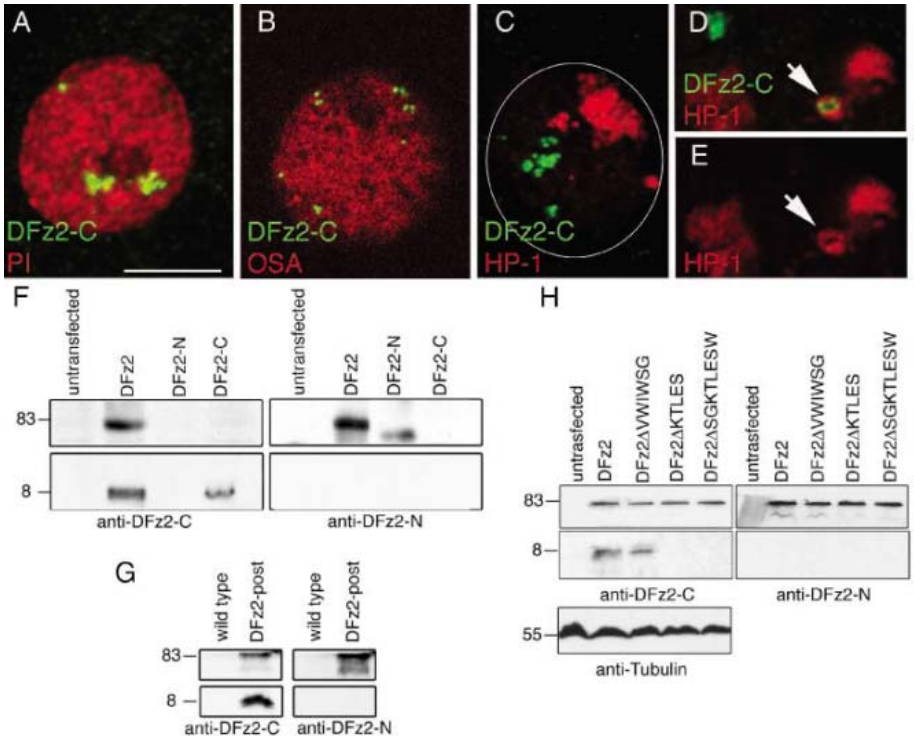

Fig. 2. Localization of DFz2-C to euchromatin and evidence for cleavage of DFz2. (**A** and **B**) Colocalization of (A) DFz2-C (green) and PI (red) and (B) DFz2-C and OSA. In (**C** to **E**), muscle nuclei were double-labeled with antibodies against the heterochromatin-specific protein HP-1 (red) and DFz2-C (green). Arrows point to regions of adjacent DFz2-C and HP-1 immunoreactivity. Scale bar, 9 μm in (A to C), and 6 μm in (D and E). (**F**) Western blot of S2 cells transfected with full-length DFz2, DFz2-N, and DFz2-C. (**G**) Western blots of body wall muscle extracts from wild-type larvae and larvae overexpressing full-length DFz2. (**H**) Western blot of S2 cells and S2 cells transfected with DFz2 constructs. Blots were sequentially probed with antibodies to DFz2-C, DFz2-N, and tubulin.

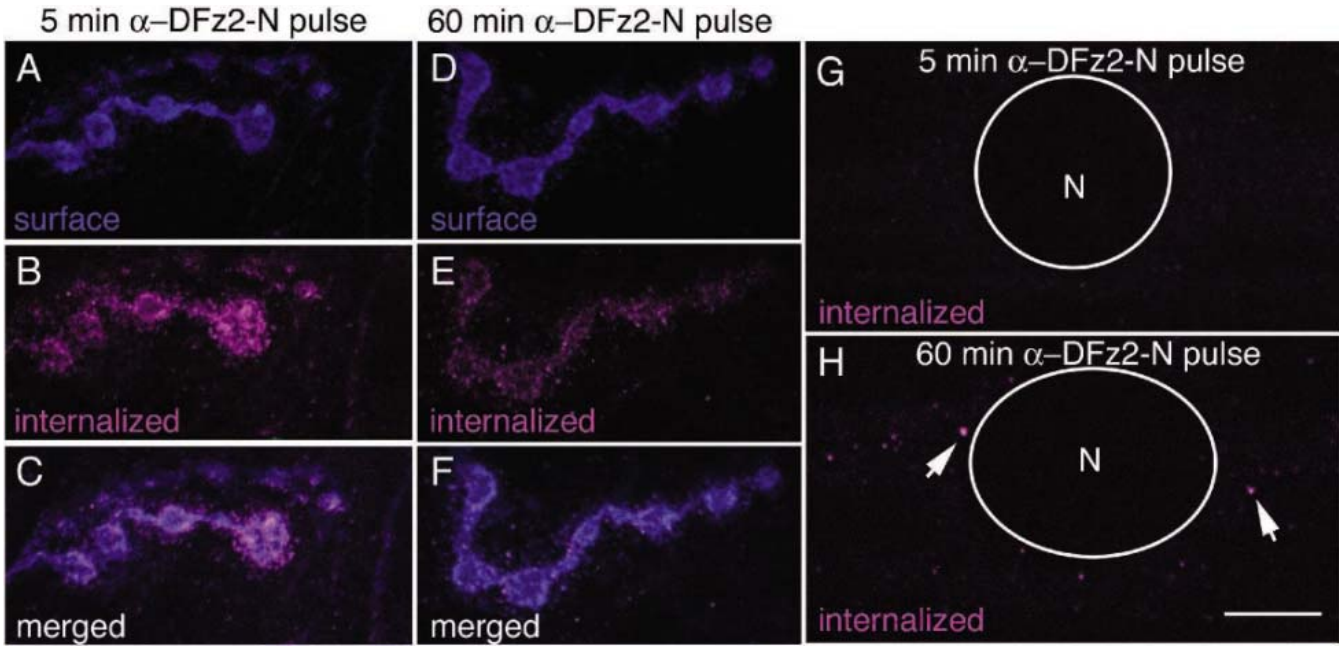

Fig. 3. In vivo transport of DFz2 from the cell surface to the nucleus. (**A** to **F**) show anti-DFz2-N immunoreactivity at NMJs during the in vivo DFz2 internalization assay. (A and D) Surface DFz2 (blue) and (B and E) internalized DFz2 (magenta) are shown at 5 and 60 min after pulse-labeling. (C and F) show the merged blue and magenta channels. (**G** and **H**) DFz2-N immunoreactivity around a muscle nucleus at 5 and 60 min after pulse-labeling. Scale bar, 9 μm in (A to F), and 6 μm in (G and H).

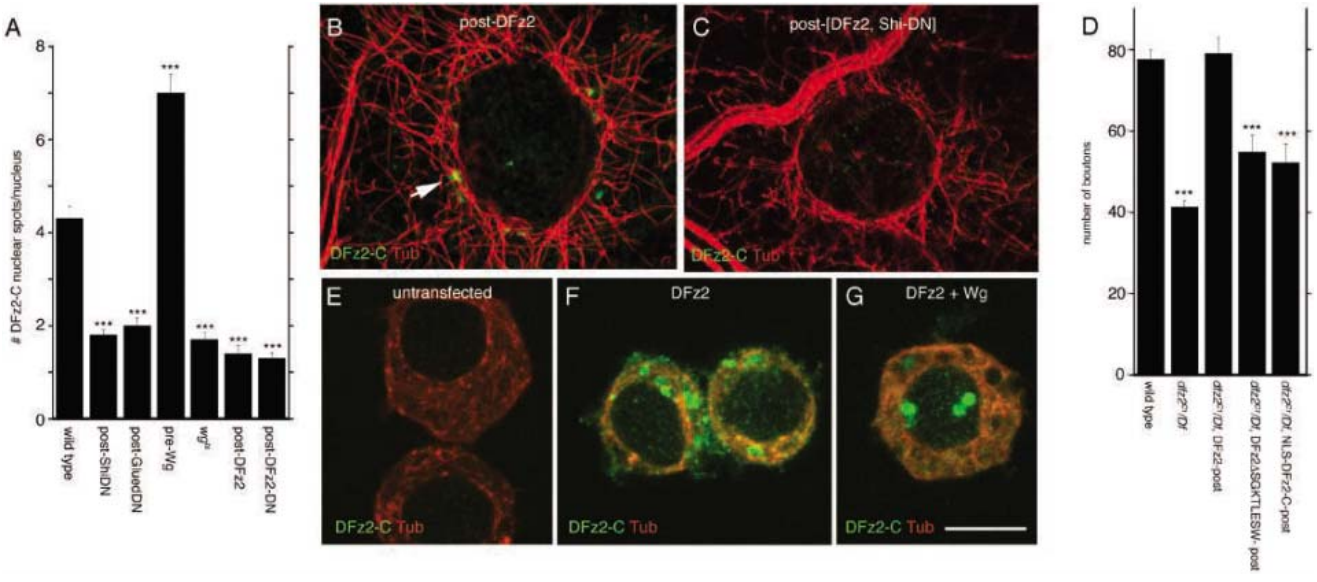

Fig. 4. Role of endocytosis, retrograde transport, and Wg signaling in DFz2-C nuclear import. (**A**) Mean number of nuclear spots per nucleus in different genotypes. (**B** and **C**) Muscle nuclei in larva expressing (B) DFz2 and (C) DFz2 and Shi-DN in the muscles. Tissues were double-labeled with antibodies against tubulin and DFz2-C. Arrow in (B) points to DFz2-C spots that accumulate just outside of the nuclear perimeter. (**D**) Number of synaptic boutons in wild type and *dfz2^{C1}/Dfdfz2* mutants expressing various DFz2 transgenes in muscle as indicated. ***$P < 0.0001$ compared with wild type [ANOVA (*20*)]. (**E** to **G**) DFz2-C and tubulin immunoreactivity in (E) S2 cells, and [(F and G)] S2 transfected with DFz2, and treated with and without Wg-conditioned medium. Scale bar, 9 μm in (B) and (C), and 7 μm in (E) to (G).

and Myc-NLS-DFz2-C [consisting of a Myc-tagged DFz2-C fragment alone (*20*) or fused to a nuclear localization sequence]. When DFz2 was overexpressed in muscle, bright DFz2-C immunoreactivity accumulated just outside the nucleus (Fig. 4B; fig. S4), which suggests that overexpression of DFz2 does not disrupt retrograde transport of DFz2, but rather, the nuclear import of DFz2-C. To further test the model that the DFz2 pool transported to the nucleus is derived by endocytosis from the plasma membrane, and not from an internal pool, we simultaneously expressed DFz2 and the Shi-DN in muscle cells. In the presence of Shi-DN, no accumulation of DFz2-C at the perinuclear area was observed (Fig. 4C; fig. S4). Mutations in the DFz2 cleavage site did not alter the endocytosis of DFz2, because expression of transgenic DFz2ΔSGKTLESW in muscles did not suppress the accumulation of perinuclear DFz2-C spots (although it did not enter the nucleus), and the perinuclear spots had a distribution that was indistinguishable from that of cells expressing transgenic wild-type

DFz2. Muscle cells expressing the DFz2-C transgenes showed diffuse Myc immunoreactivity in the cytoplasm and nuclei.

We also tested whether expressing DFz2, DFz2ΔSGKTLESW, or DFz2-C could rescue the synaptic phenotypes of a mutant of the *dfz2* gene (*dfz2^{C1}/Dfdfz2*) (*1*). Interfering with DFz2 function prevents the proliferation of synaptic boutons and the formation of pre- and postsynaptic specializations in many boutons (*1*). Like *wg^{ts}* mutants, *dfz2^{C1}/Dfdfz2* NMJs had irregular and tightly spaced boutons and a reduced number of boutons (Fig. 4D; fig. S5).

Expression of DFz2 in a *dfz2^{c1}/Dfdfz2* mutant background completely rescued the decrease in bouton number and partially restored the abnormal morphology of the boutons (Fig. 4D; fig. S5). It also restored the presence of nuclear spots in the mutant larvae. In contrast, only a slight rescue was observed when DFz2ΔSGKTLESW was expressed, and no rescue was detected when Myc-NLS-DFz2-C was expressed (Fig. 4D; fig. S5). Thus, cleavage of DFz2 appears to be needed for DFz2 signaling at the NMJ, and DFz2-C is necessary but not sufficient for DFz2 function. The slight rescuing activity observed in *dfz2^{c1}/Dfdfz2* mutants expressing DFz2ΔSGKTLESW may indicate that not all of DFz2's function at the NMJ is accomplished through DFz2 cleavage and nuclear import (*21*).

To test whether Wg is required for nuclear import of DFz2, we treated DFz2-transfected S2 cells with conditioned medium containing soluble Wg (*20*, *22*). In the presence of Wg, prominent immunoreactive spots were detected inside the nucleus of DFz2-transfected cells, but not in DFz2-ΔSGKTLESW–transfected cells or in transfected cells not exposed to Wg-conditioned medium (Fig. 4, E to G; fig. S4).

Our results indicate that, at the *Drosophila* NMJ, Wg secretion initiates a signaling mechanism, whereby DFz2 receptors at the postsynaptic muscle membrane are endocytosed and undergo retrograde transport to the nucleus. The C-terminal fragment is cleaved during this process and is ultimately transported into the nucleus. We propose that Wg binding to DFz2 may initiate an event that marks the DFz2 C-terminal region. Endocytosed vesicles containing the entire DFz2 receptor travel toward the nucleus. Once at the periphery of muscle nuclei, the C terminus is cleaved, and only marked C-terminal fragments are imported into the muscle nuclei, where they may regulate gene transcription. Our studies help unravel a mechanism by which pre- and postsynaptic cells communicate during the coordinated growth and maturation of synaptic specializations.

References and Notes

1. M. Packard *et al.*, *Cell* **111**, 319 (2002).
2. A. C. Hall, F. R. Lucas, P. C. Salinas, *Cell* **100**, 525 (2000).
3. O. Krylova *et al.*, *Neuron* **35**, 1043 (2002).
4. M. Packard, D. Mathew, V. Budnik, *Nat. Rev. Neurosci.* **4**, 113 (2003).
5. R. T. Collins, T. Furukawa, N. Tanese, J. E. Treisman, *EMBO J.* **18**, 7029 (1999).
6. J. E. Treisman, A. Luk, G. M. Rubin, U. Heberlein, *Genes Dev.* **11**, 1949 (1997).
7. T. C. James *et al.*, *Eur. J. Cell Biol.* **50**, 170 (1989).
8. M. E. Fortini, *Nat. Rev. Mol. Cell Biol.* **3**, 673 (2002).
9. F. Corpet, *Nucleic Acids Res.* **16**, 10881 (1988).
10. Single-letter abbreviations for the amino acid residues are as follows: A, Ala; C, Cys; D, Asp; E, Glu; F, Phe; G, Gly; H, His; I, Ile; K, Lys; L, Leu; M, Met; N, Asn; P, Pro; Q, Gln; R, Arg; S, Ser; T, Thr; V, Val; W, Trp; and Y, Tyr.
11. M. D. Tortorella *et al.*, *Science* **284**, 1664 (1999).
12. S. Lammich *et al.*, *Proc. Natl. Acad. Sci. U.S.A.* **96**, 3922 (1999).
13. D. Pan, G. M. Rubin, *Cell* **90**, 271 (1997).
14. D. F. Seals, S. A. Courtneidge, *Genes Dev.* **17**, 7 (2003).
15. D. Mathew, A. Popescu, V. Budnik, *J. Neurosci.* **23**, 10710 (2003).
16. M. M. Moline, C. Southern, A. Bejsovec, *Development* **126**, 4375 (1999).
17. M. J. Allen *et al.*, *J. Neurosci.* **19**, 9374 (1999).
18. K. M. Cadigan, M. P. Fish, E. J. Rulifson, R. Nusse, *Cell* **93**, 767 (1998).
19. J. Zhang, R. W. Carthew, *Development* **125**, 3075 (1998).
20. Materials and methods are available as supporting material on *Science* Online.
21. F. R. Lucas, R. G. Goold, P. R. Gordon-Weeks, P. C. Salinas, *J. Cell Sci.* **111**, 1351 (1998).
22. F. Reichsman, L. Smith, S. Cumberledge, *J. Cell Biol.* **135**, 819 (1996).

23. We thank M. Gorczyca, S. Waddell, S. Reppert, S. Marfatia, and. J. Ashley for critical reading of the manuscript, members of the Budnik lab for discussions, T. Schwarz for the UAS-Glued-DN flies, A. Spradling for antibodies against OSA and HP-1, and S. Baker for statistical help. Supported by NIH grants R01 MH70000 to V.B. and GM R01 HD36000 to S.C.

Supporting Online Material

www.sciencemag.org/cgi/content/full/310/5752/1344/DC1
Materials and Methods
Figs. S1 to S5
References and Notes

6 July 2005; accepted 25 October 2005
10.1126/science.1117051

Gordon Research Conferences

Session II Meetings (June - October, 2006)

VISIT THE *frontiers of science* GO TO A GORDON CONFERENCE

Phone: **401-783-4011** Fax: **401-783-7644** E-mail: **grc@grc.org**

Visit the GRC web site for more program & meeting details: **www.grc.org**

INTERNATIONAL (June - October)

Conference Title	Chair(s)	Dates	Location
Angiotensin	Martin Paul	Sep 10-15	Aussois, France
Basement Membranes	Reinhard Faessler	Jun 18-23	Il Ciocco, Italy
Bioelectrochemistry	Justin Teissie	Sep 3-8	Aussois, France
Biointerface Science	Ashutosh Chilkoti & Jeffrey Hubbell	Oct 22-27	Les Diablerets, Switzerland
Biology of 14-3-3 Proteins	Alastair Aitken	Aug 27-Sep 1	The Queen's College
Bioorganic Chemistry	Peter Tonge & Leslie Sloan	Jul 30-Aug 4	Magdalen College, Oxford
Brain Energy Metabolism & Blood Flow	Martin Lauritzen	Aug 20-25	Magdalen College, Oxford
Chemotactic Cytokines	Sergio Lira	Sep 17-22	Aussois, France
Combinatorial Chemistry	R. Kip Guy	Aug 20-25	The Queen's College, Oxford
Computational Aspects - Biomolecular NMR	Martin Blackledge	Sep 24-29	Aussois, France
Computational Chemistry	Wilfred Van Gunsteren	Oct 8-13	Les Diablerets, Switzerland
Electronic Spectroscopy & Dynamics	Frederic Merkt	Sep 10-15	Les Diablerets, Switzerland
Environmental Endocrine Disruptors	Paolo Mocarelli & Rex Hess	Jun 4-9	Il Ciocco, Italy
Granular & Granular-Fluid Flow	Christine Hrenya	Jul 23-28	The Queen's College, Oxford
Green Chemistry	Gary Sheldrake & Romas Kazlauskas	Aug 27-Sep 1	Magdalen College, Oxford
Industrial Ecology	Valerie Thomas	Aug 6-11	The Queen's College, Oxford
Ligand Recognition & Molecular Gating	Benjamin Kaupp	Jun 11-16	Il Ciocco, Italy
Magnetic Nanostructures	Jagadeesh Moodera	Sep 3-8	The Queen's College, Oxford
Metals In Medicine	Peter Caravan & Peter Sadler	Jul 9-14	The Queen's College, Oxford
Mitochondria & Chloroplasts	Michael Yaffe	Aug 13-18	Magdalen College, Oxford
Molecular & Cellular Neurobiology	Li-Huei Tsai	Jun 11-16	Hong Kong, China
Molecular Basis of Microbial One-Carbon Metabolism	Cornelius Friedrich	Aug 6-11	Magdalen College, Oxford
Molecular Mechanisms in Lymphatic Function & Disease	Kari Alitalo	Sep 3-8	Les Diablerets, Switzerland
Molecular Therapeutics of Cancer	Alan Eastman	Jul 16-21	The Queen's College, Oxford
NOX Family NADPH Oxidases	Karl-Heinz Krause	Oct 15-20	Les Diablerets, Switzerland
Oscillations & Dynamic Instabilities in Chemical Systems	Patrick Dekepper	Jul 30-Aug 4	The Queen's College, Oxford
Periodontal Diseases	Michael Curtis	Jun 4-9	Il Ciocco, Italy
Post-Transcriptional Gene Regulation, The Biology of	Jane Wu	Aug 13-18	The Queen's College, Oxford
Salt & Water Stress In Plants	Dorotea Bartels	Sep 3-8	Magdalen College, Oxford
Three Dimensional Electron Microscopy	Helen Saibil	Jun 25-30	Il Ciocco, Italy

NEW ENGLAND (June - August)

Conference Title	Chair(s)	Dates	Location
Adhesion, Science of	William Unertl	Aug 6-11	Tilton School
Atomic & Molecular Interactions	David Yarkony	Jul 9-14	Colby-Sawyer College
Bacterial Cell Surfaces	Arnold Driessen & Ryland Young	Jun 25-30	Colby-Sawyer College
Barriers of the CNS	Jane Preston	Jun 25-30	Tilton School
Biocatalysis	Bernhard Hauer & Donald Hilvert	Jul 9-14	Bryant University
Biomineralization	Joanna Aizenberg	Jul 30-Aug 4	Colby-Sawyer College
Biopolymers	Sarah Woodson & David Lynn	Jun 11-16	Salve Regina University
Cancer Models & Mechanisms	Rene Bernards	Jul 30-Aug 4	Bryant University
Cardiac Regulatory Mechanisms	Kenneth Philipson	Jul 16-21	Colby-Sawyer College
Catalysis	Robert Davis	Jun 25-30	Colby-Sawyer College
Cell Biology of the Neuron	Yukiko Goda & Craig Garner	Jun 18-23	Colby-Sawyer College
Cellular & Molecular Fungal Biology	Aaron Mitchell & Anne Osbourn	Jun 18-23	Holderness School
Ceramics, Solid State Studies in	John Blendell	Aug 13-18	Proctor Academy
Correlated Electron Systems	Steven Girvin & J.C. Seamus Davis	Jun 18-23	Mount Holyoke College
Corrosion - Aqueous	Philippe Marcus	Jul 16-21	Colby-Sawyer College
Cyclic Nucleotide Phosphodiesterases	Rick Cote & Marie-Joseph Leroy	Jun 4-9	University of New England
Defects in Semiconductors	Wladek Walukiewicz	Jul 2-7	Colby-Sawyer College
Diffraction Methods in Structural Biology	Paul Adams	Jul 16-21	Bates College
Drinking Water Disinfection By-Products	Susan Richardson & Mark Nieuwenhuijsen	Aug 13-18	Mount Holyoke College
Drug Metabolism	Leslie Benet	Jul 9-14	Holderness School
Electrodeposition	Jay Switzer	Jul 30-Aug 4	Colby-Sawyer College
Electron Donor Acceptor Interactions	Clifford Kubiak & Matthew Zimmt	Aug 13-18	Salve Regina University
Electronic Processes in Organic Materials	Paul Barbara	Jul 30-Aug 4	Mount Holyoke College
Endothelial Cell Phenotypes in Health & Disease	Joe Garcia	Aug 6-11	University of New England
Energetic Materials	Charles Wight	Jun 18-23	Tilton School
Environmental Bioinorganic Chemistry	Alison Butler & Bradley Tebo	Jun 18-23	Proctor Academy
Environmental Sciences: Water	Eric Weber	Jun 25-30	Holderness School
Enzymes, Coenzymes & Metabolic Pathways	Susan Miller & John Richard	Jul 16-21	University of New England
Flow & Transport In Permeable Media	Martin Blunt	Jul 30-Aug 4	Proctor Academy
Fuel Cells	Brian Benicewicz & Jeremy Meyers	Jul 23-28	Bryant University
Graduate Research Seminar: Origin Of Life	Janet Siefert, Nicolle Zellner & Heather Bean	Jul 21-23	Bates College
Growth Factor Signalling	Deborah Morrison	Jul 16-21	Connecticut College
Hemostasis	Jose Lopez	Jul 9-14	Colby College
Heterocyclic Compounds	John Macor	Jul 2-7	Salve Regina University

Celebrating our 75th Anniversary on the Frontiers of Science (1931-2006)

NEW ENGLAND (continued) (June - August)

Conference Title	Chair(s)	Dates	Location
High Pressure, Research at	Reinhard Boehler	Jun 25-30	University of New England
High Temperature Materials, Processes & Diagnostics	Brian Sheldon	Jul 16-21	Colby College
Host-Parasite Interactions, Biology of	Michael A. Ferguson	Jun 25-30	Salve Regina University
In Vivo Magnetic Resonance	Richard Buxton	Jul 23-28	Mount Holyoke College
Inorganic Chemistry	Bahram Moasser	Jul 16-21	Salve Regina University
Interfaces, Chemistry at	Nicholas Spencer	Jul 9-14	University of New England
Intermediate Filaments	M. Bishr Omary	Jul 30-Aug 4	Salve Regina University
Ion Channels	Steve Goldstein	Jul 9-14	Tilton School
Iron-Sulfur Enzymes	John Peters	Jun 11-16	Colby-Sawyer College
Laser Interactions with Materials	Dave Blank	Aug 6-11	Proctor Academy
Lasers in Medicine & Biology	Ralf Brinkmann & Charles Lin	Jul 2-7	Holderness School
Lipoprotein Metabolism	Mary Sorci-Thomas	Jul 2-7	Mount Holyoke College
Lysosomes & Endocytosis	Gregory Payne	Jun 25-30	Proctor Academy
Macromolecular Organization & Cell Function	Ronald Lynch & Stephen Oliver	Aug 6-11	Mount Holyoke College
Mammalian Gametogenesis & Embryogenesis	Marisa Bartolomei	Jun 18-23	Connecticut College
Marine Microbes	Alexandra Worden & David Caron	Jul 23-28	University of New England
Mechanisms of Epilepsy & Neuronal Synchronization	Kevin Staley & Ivan Soltesz	Aug 6-11	Colby College
Mechanisms of Toxicity	Charlene Mcqueen	Jul 23-28	Colby College
Medicinal Chemistry	George Hartman & John Lowe	Aug 6-11	Colby-Sawyer College
Meiosis	Miriam Zolan	Jun 11-16	Colby-Sawyer College
Membrane Transport Proteins	Jonathan Javitch	Aug 13-18	University of New England
Membranes: Materials & Processes	Matthias Wessling & Glenn Lipscomb	Aug 6-11	Colby-Sawyer College
MEMS Technology & Biomedical Applications	Rafael Kleiman	Jun 25-30	Connecticut College
Metabolic Basis of Ecology	Val Smith & Pablo Marquet	Jul 9-14	Bates College
Microbial Stress Response	Patricia Kiley	Jul 9-14	Mount Holyoke College
Microbial Toxins & Pathogenicity	Drusilla Burns	Jul 16-21	Proctor Academy
Molecular & Cellular Bioenergetics	Stanley Dunn	Jun 11-16	Proctor Academy
Molecular Cell Biology	Erin O'Shea	Jul 2-7	Tilton School
Multiphoton Processes	Robert Jones	Jun 11-16	Tilton School
Muscle: Excitation / Contraction Coupling	Susan Hamilton	Jun 4-9	Colby-Sawyer College
Musculoskeletal Biology & Bioengineering	Cyril Frank	Jul 23-28	Proctor Academy
Mutagenesis	Sue Jinks-robertson	Aug 6-11	Salve Regina University
Nanostructure Fabrication	Theresa Mayer	Jul 16-21	Tilton School
Natural Products	Frederick Luzzio	Jul 23-28	Tilton School
Neural Development	Hollis Cline	Aug 20-25	Salve Regina University
Nuclear Chemistry	Roy Lacey	Jun 4-9	Colby-Sawyer College
Nucleic Acids	Stephen Kowalczykowski & Scott Strobel	Jun 4-9	Salve Regina University
Organic Geochemistry	Steve Larter	Aug 6-11	Holderness School
Organic Reactions & Processes	Matt McIntosh	Jul 16-21	Bryant University
Organometallic Chemistry	Gerard Parkin	Jul 9-14	Salve Regina University
Origin of Life	Janet Siefert	Jul 23-28	Bates College
Permeable Sediments	Timothy Shaw & Carolyn Oldham	Jun 25-30	Colby College
Phosphorylation & G-Protein Mediated Signaling Networks	Natalie Ahn & Beverly Errede	Jun 11-16	University of New England
Photonuclear Reactions	Adam Sarty	Jul 30-Aug 4	Tilton School
Photosynthesis	R. David Britt	Jul 2-7	Bryant University
Physical Metallurgy	Alex King, Douglas Medlin & Eugen Rabkin	Jul 23-28	Holderness School
Physics Research and Education	Kerry Browne & Stamatis Vokos	Jun 11-16	Mount Holyoke College
Plant & Fungal Cytoskeleton	Anthony Bretscher	Aug 20-25	Proctor Academy
Plant Cell Walls	Nicholas Carpita	Jul 30-Aug 4	University of New England
Plant Molecular Biology	Sheila Mccormick	Jul 16-21	Holderness School
Plasma Processing Science	Alexander Fridman	Jul 16-21	Mount Holyoke College
Plasmonics	Albert Polman	Jul 23-28	Keene State College
Polymer Physics	Frank Bates	Jul 23-28	Connecticut College
Postharvest Physiology	Christopher Watkins	Jul 9-14	Connecticut College
Proprotein Processing, Trafficking & Secretion	Nabil Seidah	Jul 9-14	Colby-Sawyer College
Proteoglycans	Alan Rapraeger	Jul 9-14	Proctor Academy
Proteolytic Enzymes & their Inhibitors	Roy Black	Jul 2-7	Colby-Sawyer College
Radiation Chemistry	John Miller	Jul 2-7	Colby College
Reproductive Tract Biology	James Cross & Jeffrey Pollard	Jun 18-23	Connecticut College
Signal Transduction by Engineered Extracellular Matrices	Michael Sheetz	Jul 2-7	Connecticut College
Signaling by Adhesion Receptors	Joan Brugge	Jun 25-30	Mount Holyoke College
Single Molecule Approaches to Biology	Lori Goldner & Xiaoliang Xie	Jun 18-23	Colby-Sawyer College
Solid State Chemistry I	Terrell Vanderah	Jul 23-28	Colby-Sawyer College
Stereochemistry	Erick Carreira	Jun 18-23	Salve Regina University
Synaptic Transmission	Julie Kauer	Jul 23-28	Colby-Sawyer College
Tetrapyrroles, Chemistry & Biology of	Ann Smith	Jul 23-28	Salve Regina University
Theoretical Biology & Biomathematics	Paul Bressloff & Stephen Coombes	Jun 4-9	Tilton School
Thin Film & Small Scale Mechanical Behavior	Zhigang Suo	Jul 30-Aug 4	Colby College
Thiol-Based Redox Regulation & Signaling	Vadim Gladyshev	Jun 18-23	University of New England
Tribology	Tom Dickinson	Jun 18-23	Colby College
Vibrational Spectroscopy	F. Fleming Crim	Jul 2-7	University of New England
Water & Aqueous Solutions	Branka Ladanyi	Jul 30-Aug 4	Holderness School

MONTANA (August - September)

Conference Title	Chair(s)	Dates	Location
Cell Death	J. Marie Hardwick	Sep 10-15	Big Sky Resort
Drug Carriers in Medicine & Biology	Thomas Kissel & Alexander Kabanov	Aug 20-25	Big Sky Resort
Rock Deformation	Mark Jessell	Sep 3-8	Big Sky Resort
Science & Technology Policy	Fred Grinnell & Skip Stiles	Aug 13-18	Big Sky Resort
Sensory Coding and the Natural Environment	Jack Gallant & Michael Lewicki	Aug 27-Sep 1	Big Sky Resort

Leap into *Science*

Put your face on the cover of *Science* in a free, online game on EurekAlert!'s *Science* for Kids site.

To play, visit:
www.EurekAlert.org/beonthecover

Science for Kids
AAAS

Science Online

http://www.sciencenow.org

Q

What's the best way to get science news in your inbox on a daily basis?

A

Sign up for *Science*NOW e-mail alerts

*Science*NOW is a daily collection of news items from every corner of the world of science. Covering a wide spectrum of fields, *Science*NOW offers a variety of articles to keep you informed of what's happening. Our newest member benefit is *Science*NOW e-mail alerts – science articles sent directly to your inbox on a daily or weekly basis.

Sign up today and start receiving the latest scientific news stories automatically!
http://sciencenow.sciencemag.org/cgi/alerts/etoc

Science
AAAS

New Products

http://science.labvelocity.com

Cancer Protein Microarray

The Panorama Human Cancer Version 1 Protein Functional Microarray contains 130 correctly folded proteins selected from a recent seminal scientific publication that reviewed and compiled all proteins that are implicated in mediating cancer. The microarray features a proprietary immobilization technology that allows proteins to be correctly folded, uniformly oriented, and stearically unencumbered, so the analysis of protein function and interactions involved in the cancer process that have physiological relevance can be confidently identified.

Sigma-Aldrich For information 314-286-7431 www.sigma-aldrich.com

RNA Amplification

TargetAmp aRNA Amplification Kits can produce microgram quantities of antisense RNA from either 10 pg or 25 ng of total RNA. Data on the high reproducibility, quality, and concordance with established Affymetrix protocols is provided at the manufacturer's website.

Epicentre Biotechnologies For information 800-284-8474 www.EpiBio.com

Red Fluorescent Stain

Rubeo is a new fluorescent protein stain suitable for high-sensitivity one-dimensional and two-dimensional staining that features red emission at 605 nm. It can detect nanogram levels of protein and allows quantitative comparisons of proteins. It is compatible with subsequent analysis, including mass spectroscopy, microsequencing, and immunostaining. It can be used with native, denaturing, and isoelectric focusing gels.

G Biosciences/Genotech. For information 314-991-6034 www.genotech.com

Bulk Powder Enclosures

New XPert Bulk Powder Enclosures provide user protection from hazardous airborne particulates and fumes generated during powder transfer operations. Exclusive features include an ergonomic air foil with aerodynamic Clean-Sweep airflow openings that create a constant, protective barrier from contaminants; upper dilution air supply with bypass air that bathes the back of the sash with clean air; upper containment sash foil that lowers concentrations near the user's breathing zone; and a zoned perforated rear baffle that directs inflow air in non-turbulent laminar streams. The enclosures include a base stand and transfer caddy. A push button operates an electric hydraulic lift mechanism that raises the container to the proper ergonomic height. An electronic beam senses the location of the container and triggers the lift mechanism to automatically stop at the proper access height. The stainless steel work surface has a spill trough and offers a right-side, center, or left-side mounted access opening for the source container.

Labconco For information 800-821-5525 www.labconco.com

Modeling Software

Comsol has released version 3.2 of Multiphysics, a scientific modeling package with new features to boost productivity through the modeling and simulation process. The software now reads geometry files created with all major computer-assisted design packages. Comsol Script is a standalone product featuring command-line modeling. The graphical user interface encourages the use of a consistent system of engineering units, and a moving-mesh feature allows a model to simulate moving parts and parametric geometries. Improved solvers handle models with millions of degrees of freedom and calculate the answers faster than ever before.

Comsol For information 781-273-3322 www.comsol.com

Image Analyzer

The G:BOX is an image analyzer approach that allows scientists to choose their image analyzer's components. The G:BOX consists of an ergonomically designed darkroom with an easy access chamber and camera/lens mounting pod that allows users to add their choice of Syngene camera, lens, and lighting options. This darkroom design has the advantage of permitting easy component exchange, making the G:BOX cost-effective because the system can be upgraded to fit in with any future imaging applications. Scientists can choose a standard camera for gel and blot imaging, an advanced cooled camera for chemiluminescence applications, or a super camera for imaging two-dimensional (2-D) gels. Because the G:BOX is fully computer-controlled, users can add a motor-driven zoom lens (with feedback), a fixed lens, or a manually controlled zoom lens. Scientists can also specify different filters (either a computer-controlled filter wheel or manual filter selector) and lighting choices that allow users to tailor the system to match fluorescence and chemiluminescence imaging needs.

Syngene. For information 800-686-4407 www.syngene.com

Protein Stabilizing Cocktail

The Protein Stabilizing Cocktail is a versatile stabilizing solution that increases the shelf life of purified or partially purified proteins during routine storage. The proprietary formulation of low molecular weight, naturally occurring molecules helps protect proteins from environmental stresses that can otherwise lead to enzyme inactivation, aggregation, and freeze/thaw damage. Although the degree of stabilization is protein-specific, the cocktail significantly stabilizes most proteins compared with conventional buffer alone.

Pierce For information 815-968-0747 www.piercenet.com

Protein Membrane Stain

The ProAct Membrane Stain is for the detection of proteins on nitrocellulose or poly(vinylidine fluoride) membranes. This ready-to-use protein membrane stain confirms transfer prior to protein immunoblotting. It contains no harmful solvents and is completely reversible. ProAct stains proteins instantly and provides results suitable for photography.

Amresco For information 800-448-4442 www.amresco-inc.com

For more information visit GetInfo, *Science*'s new online product index at *http://science.labvelocity.com*

From the pages of GetInfo, you can:
- Quickly find and request free information on products and services found in the pages of *Science*.
- Ask vendors to contact you with more information.
- Link directly to vendors' Web sites.

Newly offered instrumentation, apparatus, and laboratory materials of interest to researchers in all disciplines in academic, industrial, and government organizations are featured in this space. Emphasis is given to purpose, chief characteristics, and availability of products and materials. Endorsement by *Science* or AAAS of any products or materials mentioned is not implied. Additional information may be obtained from the manufacturer or supplier by visiting www.science.labvelocity.com on the Web, where you can request that the information be sent to you by e-mail, fax, mail, or telephone.

ScienceCareers.org

Classified Advertising

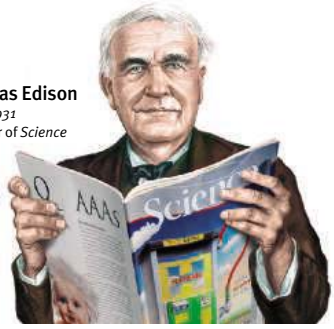

Thomas Edison
1847–1931
Founder of *Science*

For full advertising details, go to **www.sciencecareers.org** and click on **How to Advertise,** or call one of our representatives.

United States & Canada

E-mail: advertise@sciencecareers.org
Fax: 202-289-6742

JILL DOWNING
(CT, DE, DC, FL, GA, MD, ME, MA, NH, NJ, NY, NC, PA, RI, SC, VT, VA)
Phone: 631-580-2445

KRISTINE VON ZEDLITZ
(AK, AZ, CA, CO, HI, ID, IA, KS, MT, NE, NV, NM, ND, OR, SD, TX, UT, WA, WY)
Phone: 415-956-2531

KATHLEEN CLARK
Employment: AR, IL, LA, MN, MO, OK, WI, Canada; Graduate Programs; Meetings & Announcements (U.S., Canada, Caribbean, Central and South America)
Phone: 510-271-8349

EMNET TESFAYE
(Display Ads: AL, IN, KY, MI, MS, OH, TN, WV; Line Ads)
Phone: 202-326-6740

GABRIELLE BOGUSLAWSKI
(U.S. Recruitment Advertising Sales Director)
Phone: 718-491-1607

Europe & International

E-mail: ads@science-int.co.uk
Fax: +44 (0) 1223-326-532

TRACY HOLMES
Phone: +44 (0) 1223-326-525

HELEN MORONEY
Phone: +44 (0) 1223-326-528

CHRISTINA HARRISON
Phone: +44 (0) 1223-326-510

SVITLANA BARNES
Phone: +44 (0) 1223-326-527

JASON HANNAFORD
Phone: +81 (0) 52-789-1860

To subscribe to *Science*:
In U.S./Canada call 202-326-6417 or 1-800-731-4939
In the rest of the world call +44 (0) 1223-326-515

Science makes every effort to screen its ads for offensive and/or discriminatory language in accordance with U.S. and non-U.S. law. Since we are an international journal, you may see ads from non-U.S. countries that request applications from specific demographic groups. Since U.S. law does not apply to other countries we try to accommodate recruiting practices of other countries. However, we encourage our readers to alert us to any ads that they feel are discriminatory or offensive.

ScienceCareers.org
We know science AAAS

POSITIONS OPEN

ASSISTANT PROFESSOR: MAMMALIAN DEVELOPMENTAL GENETICS. The Biochemistry and Cellular and Molecular Biology (BCMB) Department at the University of Tennessee seeks to fill a tenure-track faculty position at the Assistant Professor level to begin in August 2006. We will particularly welcome applications from individuals who apply genomic or proteomic methods and/or use mouse genetic models to address problems in developmental biology, and from individuals with interests in developmental neurobiology, but outstanding applications from individuals in all areas of developmental genetics will be considered. The successful candidate for this position will benefit from interactions with strong research groups within the BCMB Department and in other units on campus and at the nearby Oak Ridge National Laboratory in neurobiology, chromatin and chromosome dynamics, biology of cancer and aging, cell division and cell cycle, structural biology, enzyme mechanisms, mouse genetics/genomics, proteomics, and computational biology. The successful applicant will be expected to develop an independent, externally funded research program in mammalian developmental genetics, to provide state-of-the-art training for graduate students and postdoctoral researchers, and to contribute to the teaching mission of the BCMB Department at both the undergraduate and graduate levels. Required qualifications include a Ph.D. and postdoctoral experience in relevant areas of biology, evidence of significant scientific productivity, and a commitment to an integrated program of teaching and research. The University welcomes and honors people of all races, creeds, cultures, and sexual orientations, and values intellectual curiosity, pursuit of knowledge, and academic freedom and integrity.

Interested candidates should send a cover letter, a resume, a description of research experience and of the proposed research program, and the names of three individuals who can provide letters of reference to: **Ranjan Ganguly, Chair, Faculty Search Committee, Biochemistry and Cellular and Molecular Biology Department, M407 WLS, University of Tennessee, Knoxville, TN 37996-0840.** Review of applications will begin on December 1, 2005, and continue until the position is filled.

The University of Tennessee is an Equal Employment Opportunity/Affirmative Action/Title VI/Title IX/Section 504/ADA/ADEA Institution in the provision of its education and employment programs and services.

ASSISTANT PROFESSOR: Physics, Biochemistry, and Chemistry Department at Niagara University (NU) seeks tenure-track Assistant Professor committed to undergraduate teaching in support of the biology, chemistry, biochemistry, and pre-engineering programs (fall 2006) Ph.D. in physics required, preferably successful postdoctoral experience(s), strong potential to develop an externally funded research program, demonstrated commitment to teaching at undergraduate level, and strong oral and written communication skills. Responsibilities: provision of high quality teaching and scholarship, mentoring students, supervising practicums, and serving on departmental and college committees.

Niagara University is a Catholic, comprehensive Masters' university located on the Niagara Gorge, minutes from the famous Falls and an easy drive from Buffalo and Rochester, New York and Toronto, Canada, with an enrollment of over 2,800 undergraduate and 800 graduate students.

The Department is at an exciting spot as NU celebrates its 150th year. With many new state-of-the-art facilities, including a shared GRID network with other colleges and computational and analytic equipment, the successful candidate will have the opportunity to develop a strong research platform.

Application letter, curriculum vitae, three recommendation letters, teaching philosophy and research plan to: **Dr. Mary McCourt, Chairperson, Biochemistry, Chemistry, and Physics Department, Niagara University, NY 14109-2044.**

Applications reviewed until position filled. *Affirmative Action/Equal Opportunity Employer.*

POSITIONS OPEN

DEPARTMENT OF BIOLOGY
Loyola University Chicago

The Biology Department at Loyola University Chicago seeks applications for two tenure-track positions at the **ASSISTANT PROFESSOR** level beginning August 2006. We seek applicants in the research areas of molecular cell biology and of genomics and evolution, and particularly encourage candidates with expertise in malaria biology, or in cellular/developmental neurobiology or systems neurobiology. Applicants will be expected to establish an externally funded research program involving undergraduates and M.S. students. Teaching responsibilities for one position may include undergraduate courses in cell biology or biochemistry and an upper level course in the candidate's area of specialization, while for the second position may include undergraduate courses in neurobiology, including participation in the interdisciplinary neuroscience minor, or general biology and an upper level course in the candidate's area of specialization. Applicants must have a Ph.D. and postdoctoral experience, and teaching experience is preferred.

Candidates should send letter of application, statements of research interests and teaching philosophy, curriculum vitae, and three letters of recommendation by December 30, 2005, to: **Chair, Search Committee, Department of Biology, Loyola University Chicago, 6525 N. Sheridan Road, Chicago, IL 60626.** Please visit our **website: http://www.luc.edu/depts/biology/** for additional information about the Department. *Loyola University Chicago is an Equal Opportunity/Affirmative Action Employer. Loyola University Chicago strives for diversity in its faculty, students and staff, and underrepresented minorities are particularly encouraged to apply.*

FACULTY POSITIONS IN PHARMACOLOGY
East Tennessee State University

The Department of Pharmacology at the James H. Quillen College of Medicine invites applications for two Faculty Positions. Candidates with an established research program in the area of central nervous system pharmacology and/or central control of cardiovascular function are sought. Outstanding applicants in closely related research areas will also be considered. Applicants must have a Ph.D. and/or M.D. with over three years of postdoctoral training, and will preferably have a nationally funded research program. Additional responsibilities will include teaching medical and graduate students. Appointments will be tenure or research track commensurate with qualifications and experience. Successful applicants will be provided competitive salaries and startup packages. East Tennessee State University **(website: http://www.etsu.edu)** is located in one of the nation's most beautiful regions, just north of the Great Smokey Mountain National Park. Applicants should submit curriculum vitae, a brief statement of current and future research goals, and names and addresses of three references to: **Gregory A. Ordway, Ph.D., Department of Pharmacology, James H. Quillen College of Medicine, East Tennessee State University, P.O. Box 70577, Johnson City, TN 37614-1708.** *Equal Opportunity / Affirmative Action Employer.*

FACULTY POSITION
School of Natural Sciences
Institute for Advanced Study
Princeton, New Jersey

The Institute for Advanced Study intends to make a new professional appointment in the School of Natural Sciences. It will be in astrophysics. Only candidates with distinguished scholarly accomplishments will be considered.

Applications and nominations, including bibliography and curriculum vitae, should be sent by February 15, 2006, to: **Administrative Officer, School of Natural Sciences, Institute for Advanced Study, Einstein Drive, Princeton, New Jersey 08540.** All communications will be held in strict confidence. *The Institute is an Equal Opportunity Employer.*

PENNSTATE
University Park

Director
Dorothy Foehr Huck and J. Lloyd Huck Institutes of the Life Sciences

The Search Committee for the Director of the Huck Institutes of the Life Sciences seeks nominations and applications for an innovative Director of the Huck Institutes of the Life Sciences. The Huck Institutes is a novel university-wide organization whose mission is to strengthen research and education in the life/health sciences at Penn State through inter- and cross disciplinary approaches. Penn State is committed to building academic and research excellence in the life sciences. The new Director has the opportunity to build upon the exciting advances in the life sciences at Penn State over the past decade and play a prominent role in the strategic directions of this endeavor.

The Huck Institutes – including the Institute for Genomics, Proteomics, and Bioinformatics, the Biotechnology Institute, and the Neuroscience Institute – comprise a virtual organization within seven of Penn State's colleges, including the College of Medicine at Hershey. The purpose of the Huck Institutes is to enhance Penn State's ability to prepare students for tomorrow's challenges and to support the integration of research and teaching across disciplines in the life sciences at Penn State. Core funding for the Huck Institutes is provided by the University.

As part of the Huck Institutes initiative, the University has committed the funds to recruit new faculty into key disciplines. Also supported are twelve state-of-the-art shared technology facilities, including the recently established MRI for laboratory animals, proteomics and mass spectrometry and macromolecular X-ray crystallography facilities (http://www.huck.psu.edu/stf/home.html). Further support comes from the State's Tobacco Settlement Funds, which offer a unique opportunity to initiate creative life sciences programs. Cohesion and growth of these interdisciplinary initiatives is enabled, in part, by the facilities in the 145,000-square-foot Life Sciences Building (completed in the fall of 2004), by recent renovations to the adjacent Wartik Building to house the Institute for Genomics, Proteomics and Bioinformatics, and another contiguous life science building to be completed in 2008. The Huck Institutes often engage other interdisciplinary institutes at Penn State, including the Penn State Institutes of the Environment, Materials Research Institute, and the Social Sciences Research Institute. Another exciting initiative is a planned new building for the Materials Research Institute that will physically couple with Penn State's planned new Life Sciences Building; nanobiotechnology, biomaterials, and biosensor activities are envisioned in this enriched setting.

The Director of the Huck Institutes reports directly to the Vice President for Research, who oversees a research activity exceeding $635 million annually. The responsibilities of the Director include: (1) supporting research and education at the interface between the life sciences, technology, and business; (2) proactively fostering collaboration among the core colleges and developing policies and incentives for active faculty participation, which build an atmosphere of inclusion of diverse perspectives; (3) chairing the faculty steering committee which oversees all activities and is responsible for developing policies and programs for the Huck Institutes; (4) chairing the Dean's Advisory Committee, which gives advice to the Director on operational, financial, and space matters; (5) identifying exciting new funding opportunities and coordinating interdisciplinary research programs; (6) enhancing graduate and undergraduate education in the life sciences including supporting graduate students through fellowships, assistantships, joint recruiting, and counseling; (7) supporting a variety of enhancements including seminars, workshops, and symposia; and (8) serving as liaison between the University's life sciences programs and state, national, and international life sciences organizations.

The successful candidate will be an international leader in the life sciences, recognized for scientific accomplishment and vision and the skills necessary to develop new initiatives and advance ongoing programs in research, teaching, and outreach in the life sciences within the academic environment of this land grant university. Candidates must have qualifications suitable for a tenured faculty appointment in one of the University's academic colleges. Review of applications will begin on December 14, 2005, and will continue until the position is filled. Nominations may be sent via e-mail to vxi2@psu.edu. Applicants should send a letter with a detailed visionary statement, a resume or curriculum vitae, and the names, addresses, telephone numbers, and e-mail addresses of four references via an e-mail to:

William Easterling, Chair
Search Committee for Director of the Huck Institutes
The Pennsylvania State University
304 Old Main
University Park, PA 16802
E-mail: vxi2@psu.edu

Interested individuals are invited to visit the following web site for more information: www.huck.psu.edu

Penn State is committed to affirmative action, equal opportunity and the diversity of its workforce.

PENN STATE ***Making Life Better***

Health Research in a Changing World

Fighting Diseases and Improving Lives

Department of Health and Human Services
National Institutes of Health
National Institute of Allergy and Infectious Diseases

Tenure Track Position in Immunology

The Laboratory of Immunology, Division of Intramural Research, National Institute of Allergy and Infectious Diseases, National Institutes of Health invites applications for a tenure track position in immunology. While applicants in any area of immunological science will be considered, those interested in the immunology of infectious diseases, in B-cell biology or in innate immunity are particularly encouraged to apply. Applicants should have a Ph.D., M.D. or equivalent degree and a strong record of post-doctoral scientific accomplishment. The successful candidate will be expected to establish an independent research program. Support for salary, technical personnel, post-doctoral fellows, equipment and research supplies will be provided. Current PIs in the Laboratory of Immunology are: Ronald Germain, Michael Lenardo, Rose Mage, David Margulies, William Paul, and Ethan Shevach. Active areas of research include lymphocyte development and dynamics; B-cell development, selection and diversification processes; MHC molecule, NK cell receptor and T cell receptor structure and function; dendritic cells and antigen processing; T cell and cytokine receptor signal transduction; cell death in normal immune responses and in HIV infection; regulation of cytokine expression and activity of cytokines; regulatory T cells and control of autoimmune responses; advanced imaging of immune cell interactions; and mathematical modeling of signal transduction in immune cells.

Applicants should send a CV and bibliography, outline of a proposed research program (no more than two pages), and three letters of recommendation to Dr. Jonathan Ashwell, Chair, NIAID Search Committee, C/O Mrs. Lynn Novelli, Committee Manager, 10 Center Drive MSC 1356, Building 10, Room 4A26, Bethesda, Maryland 20892-1356. Applications must be received by **December 15, 2005**.

A full package of benefits (including retirement, health, life and long term care insurance, Thrift Savings Plan participation, etc.) is available.

We invite to you explore our Institute and other opportunities at http://healthresearch.niaid.nih.gov/science.

Please reference "Science" on your resume

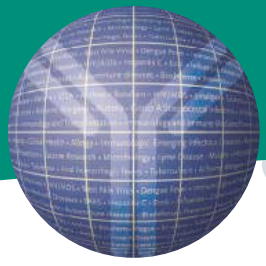

Health Research in a Changing World

Fighting Diseases and Improving Lives

Tenure Track Position in Bacterial Pathogenesis
Laboratory of Clinical Infectious Diseases
National Institute of Allergy and Infectious Diseases
National Institutes of Health
Department of Health & Human Services

The National Institute of Allergy & Infectious Diseases (NIAID), Division of Intramural Research (DIR), Laboratory of Clinical Infectious Diseases (LCID) is seeking an outstanding investigator to develop a clinical and basic program in bacterial pathogenesis.

The LCID studies the pathogenesis, pathophysiology, treatment and prevention of infectious diseases, including emerging infections and pathogens that are of concern in biodefense, as well as microorganisms that cause persistent, recurrent, or fatal disease. Current areas of clinical and basic expertise in the LCID include viral, fungal, and mycobacterial pathogenesis and pathophysiology and the pathophysiology of defects in cellular apoptosis.

The successful candidate will establish an independent research program in bacterial pathogenesis with both laboratory and clinical components. The incumbent will develop clinical protocols, which may include natural history, pathophysiology, mechanism of action, treatment, or all of the above. Board eligibility/board certification or the equivalent in Internal Medicine or Pediatrics and Infectious Diseases or Allergy and Immunology are desirable, but Ph.D.'s with active clinical programs are also encouraged to apply. Sufficient independent resources including space, support personnel and an annual budget for services, supplies and salaries have been committed to the position to ensure success.

The appointment is a Tenure Track appointment and will be at the appropriate level under Title 42, which is equivalent to a University Assistant Professor rank. Salary is dependent on experience and qualifications.

Interested candidates may contact Dr. Steven Holland, Chief, LCID, DIR, and NIAID at 301/402-7684 or email (smh@nih.gov) for additional information about the position.

To apply for the position, candidates must submit a curriculum vitae, bibliography, three letters of reference, a detailed statement of research interests, and reprints of up to three selected publications by January 31, 2006 to Patrick Murray, Ph.D., Chair, NIAID Search Committee, c/o Mrs. Lynn Novelli, Committee Manager, 10 Center Drive, MSC 1356, Building 10, Room 4A26, Bethesda, Maryland 20892-1356. Further information on this position and guidance on submitting your application is available on our website at: http://healthresearch.niaid.nih.gov/science

Please reference "Science" on your resume.

WWW.NIH.GOV

National Institute of General Medical Sciences
National Institutes of Health

The National Institute of General Medical Sciences (NIGMS) in Bethesda, MD is seeking applications from outstanding candidates for a Health Scientist Administrator (HSA) position in the Pharmacological and Physiological Sciences Branch within the Pharmacology, Physiology, and Biological Chemistry Division. The recruiting branch currently supports research and training into understanding the basis of traumatic and burn injury and the perioperative period, the molecular basis of action of anesthetics, the mechanisms of and genetics underlying the actions of therapeutic drugs, and the development of predictive preclinical toxicology approaches.

The individual hired will be responsible for applying his/her clinical and research expertise to manage and develop research and training grants in NIGMS' broad areas of basic studies in pharmacological and physiological sciences, and to foster the translation of results from fundamental research areas into clinical studies. The person should have experience gained in a medical research institution and understand how research is conducted with human subjects or patients in a clinical setting. A background in at least one of the following areas is preferred: trauma, injury and recovery, or clinical pharmacology, or immune system biology, or alternatively in a cross-cutting area such as studies of the role of inflammation in the disease process or of molecular/cellular signaling in these systems. Experience in modern methods of genome or proteome analysis would also be desirable.

Applicants must possess an MD and/or PhD plus scientific knowledge in the fields of pharmacology, physiology, immunology, systems biology, medicine, or related fields. Applicants must be familiar with both clinical and laboratory approaches in his/her own field(s) of expertise. Experience in the NIH peer review and grant award process would be beneficial. Salary will be commensurate with qualifications, may include a physician's comparability allowance, and will have a full package of benefits. Detailed vacancy announcements **NIGMS-05-100271** and **NIGMS-05-100881** with the qualifications and application procedures are available at the NIGMS web page at **http://www.nigms.nih.gov/about/job_vacancies.html**. Questions about application procedures may be directed to **Erin Bandak at 301-594-2324**. Applications must be received by **January 4, 2006**.

Health Scientist Administrator
National Institute of General Medical Sciences

The National Institute of General Medical Sciences (NIGMS) in Bethesda, Maryland is seeking applications from outstanding candidates for one Health Scientist Administrator position in the Division of Pharmacology, Physiology and Biological Chemistry, which supports primarily basic, non-disease-oriented research and training, including a substantial portfolio of bio-related chemical research.

The incumbent for this position will be responsible for developing and managing a portfolio of research grants that support studies that utilize organic chemistry to understand and/or control biological systems. The ideal candidate will have a substantial background in the design, synthesis and evaluation of small organic molecules as well as a thorough grounding in such areas as biochemistry, pharmacology or molecular biology. Prior research experience in bio-related organic chemistry is desirable.

Applicants must possess a Ph.D. or M.D. plus scientific knowledge and demonstrated expertise in at least one of the following areas: organic chemistry, biochemistry, pharmacology, or related areas, and knowledge of the NIH peer review and grants process. Salary is commensurate with qualifications, and includes a full package of benefits. A detailed vacancy announcement **(NIGMS-05-100284)** with the mandatory qualifications and application procedures can be obtained via the NIGMS web page at **http://www.nigms.nih.gov/about/job_vacancies.html** and NIH Home page at **http://www.jobs.nih.gov**. Questions on application procedures may be addressed to **Erin Bandak at (301) 594-2324**. Applications must be received by close of business **January 6, 2006**.

Scientific Director
Division of Intramural Research
National Institute of Neurological Disorders and Stroke

The National Institute of Neurological Disorders and Stroke (NINDS) seeks a new Scientific Director to lead its intramural neuroscience programs. The successful candidate will oversee a diverse group of 65 independent principal investigators conducting research in basic, translational and clinical neuroscience (see http://intra.ninds.nih.gov/) and help chart the future of a vibrant, growing neuroscience research community across the NIH (see www.neuroscience.nih.gov). The Scientific Director allocates a $140M research budget to intramural NINDS laboratories and clinical programs in coordination with rigorous, quadrennial reviews by the Board of Scientific Counselors, a panel comprising prominent extramural researchers. The Scientific Director will recruit new faculty and oversee the expansion of the intramural program into several new, state-of-the-art research facilities on NIH's Bethesda and Rockville campuses.

The successful candidate will have a Ph.D. and/or M.D. and an established record of outstanding research accomplishments, scientific leadership and service within the basic or clinical neuroscience community. The Scientific Director also will supervise their own research laboratory, supported by resources commensurate with the size and scope of their program. Applicants should send a cover letter, curriculum vitae and bibliography to: **James F. Battey, Jr., M.D., Ph.D., Chair, Search Committee, c/o Ms. Peggy Rollins, OSD, NINDS, Building 35, Room GA908, 35 Convent Drive, Bethesda, MD 20892-3167**. Applications will be considered upon receipt.

US Department of Energy
Office of Science
Office of Basic Energy Sciences

Program Manager for Chemical Physics

Chemical Sciences, Geosciences and Biosciences Division
Announcement Number PN-05-SC22-006

The U.S. Department of Energy, Office of Science, Office of Basic Energy Sciences (BES), Chemical Sciences, Geosciences and Biosciences Division is seeking applicants for a Chemist, GS-1320-15, with a CY2005 salary range of $103,947 to $135,136 per annum. The incumbent will serve as a program manager within the Chemical Physics program. The incumbent conceives, justifies, plans, initiates, manages, and coordinates aspects of this program consisting of a broad range of theoretical and experimental research aimed at a molecular level understanding of physical and chemical processes in the condensed phase and at interfaces (gas-liquid, gas-solid and liquid-solid). This research includes, but is not limited to, fundamental studies of the structure and dynamics of water and aqueous solutions, chemical reaction dynamics on surfaces and at interfaces relevant to heterogeneous catalysis and the transport of environmental wastes, and the physical and chemical properties of nano-structured materials, including clusters. The incumbent will act as a recognized expert in condensed phase and interfacial molecular sciences and will assist with new program planning and current program conduct in other core research areas within the Division related to chemical physics, including atomic, molecular and optical science, photophysics, biophysics and radiation sciences. The incumbent will also develop connections between the projects supported within the chemical physics program and the other research programs in the Division and throughout BES, including new opportunities and challenges in complex physical systems, nanoscale materials, chemical imaging, and heterogeneous catalysis. Potential applicants can learn more about the Chemical Physics program and related programs in Photochemistry and Radiation Research and Atomic, Molecular and Optical Sciences by visiting **http://www.sc.doe.gov/bes/chm/chmhome.html**.

For further information about this position and the instructions on how to apply and submit an application, please go the following website: **https://jobsonline.doe.gov/**. To be considered for this position you must apply online. Faxed or email applications will NOT be accepted. It is imperative that you follow the instructions as stated on the announcement (**PN-05-SC22-006**) located at the website indicated above for DOE JOBS.

The Department of Energy is an Equal Opportunity Employer. All qualified applicants will be considered without regard to race, religion, color, sex, age, national origin, lawful political affiliation, marital status, union membership, or other non-qualifying physical or mental handicaps.

WESTERN CONNECTICUT STATE UNIVERSITY

Asst. Professor of Biology Anatomy and Physiology Fall 2006

The Department of Biological and Environmental Sciences seeks candidates for a tenure track position at the level of Assistant Professor. The Biology Department is housed in a new Science building with extensive modern facilities and equipment. Primary teaching duties will include shared responsibility for lecture and laboratory sections of a large, year-long, freshman level Anatomy and Physiology course taken primarily by Nursing students. The successful candidate will also teach one or more upper level or graduate courses in his or her area of specialty, as well as engage in an active research program involving undergraduate and M.A. students. Preferred specialties include neurobiology, evolutionary developmental biology, or regenerative biology.

Qualifications: Applicants must have a Ph.D. or equivalent terminal degree and documented teaching excellence at the undergraduate level.

Salary & Benefits: WCSU offers competitive salaries commensurate with candidate's experience and a comprehensive benefit package.

Application Material: Interested candidates should submit a cover letter, a current vita, graduate transcripts, a statement of teaching philosophy and research interests, and contact information (name, title, address, and telephone number) of three professional references to: **Dr. Richard Halliburton, Chair of Department of Biology, Western Connecticut State University, 181 White St., Danbury, CT 06810**. Review of qualified applications will begin Friday, January 13, 2006 and will continue until the position is filled.

Western is an AA/EEO Educator/Employer.

SCOTT & WHITE

College of Medicine
The Texas A&M University System Health Science Center

Pediatric Hematology-Oncologist

The Section of Pediatric Hematology/Oncology at **Scott and White Clinic** and the **Texas A&M University System Health Science Center College of Medicine** (TAMUS HSC-COM) are seeking a clinician scientist with current research grants for a faculty position in a rapidly growing program. The candidate should be BE/BC in pediatric oncology and committed to an academic career. The successful candidates will join and enhance ongoing efforts in basic and translational research, with an institutional commitment to building a world-class experimental therapeutics program. An outstanding start-up package includes high quality laboratory space, excellent benefits and competitive salaries commensurate with academic qualifications. The position guarantees 75% protected time for research activities.

Scott & White Clinic is a 500+ physician directed multi-specialty group practice that is the leading provider of cancer care in Central Texas. Scott and White Clinic and the 486 bed tertiary Scott & White Memorial Hospital is the main clinical teaching facility for TAMUS HSC-COM. Outstanding clinical practice and laboratory facilities on campus that perform state of the art molecular and cellular biology research, flow cytometry, genomics and biostatistics are in place to support the research effort.

Please contact: **Don Wilson, M.D. Professor and Chairman, Department of Pediatrics, Scott & White, 2401 S. 31st, Temple, TX 76508. (800)725-3627 dwilson@swmail.sw.org Fax (254) 724-4974.**

For more information about Scott & White, please visit www.sw.org For Texas A&M www.tamhsc.edu. Scott & White is an equal opportunity employer.

UNIVERSITÄT BAYREUTH

As part of the newly established *elite study program* in *Macromolecular Science* within the **Elite Network of Bavaria**, the University Bayreuth is seeking candidates for an

Associate Professor (W2) for the Physics / Physical Chemistry of Polymers

Applicants must have an outstanding research record in polymer physics or in the physical chemistry of polymers. With their research they should further strengthen the interdisciplinary research priority on Polymer and Colloid Science at the University Bayreuth. They are expected to contribute to teaching both within the *elite study program* in *Macromolecular Science* and in physical chemistry at the undergraduate and graduate level.

The temporary position is limited to 5 years. A permanent position at the W2 level may be possible depending on the candidate's achievements and on the availability of the position. The deadline for application is **December 31, 2005**. Applications, supplied with a curriculum vitae, list of publications, statement of research plans and teaching prospectus, together with full contact information (address, phone, fax, and e-mail) and three references should be sent to: **Faculty of Biology, Chemistry and Geological Sciences, Prof. Dr. Carl Beierkuhnlein, Dean, D-95440 Bayreuth, Germany**.

For further information, please contact Prof. Dr. Georg Krausch at *+49-921-552751* or at *georg.krausch@uni-bayreuth.de.*

Lectureships in Plant Molecular Sciences (2)

School of Biological Sciences

Vacancy Number A713-05

The School of Biological Sciences invites applications for two tenured positions as Lecturer in Plant Molecular Sciences. Applicants for these positions should have a strong background and interest in plant biology and a track record of research in one or more of the following areas: plant development, physiology, cellular and molecular biology, biochemistry and metabolomics. Preferred candidates will have expertise in molecular genetics, use model plants and will be familiar with current trends in plant genomics, proteomics and/or metabolomics. The appointee is expected to collaborate with other researchers as well as to establish her/his own research portfolio which attracts funding and graduate students. The successful candidate is further expected to teach in the School's academic programme at both undergraduate and graduate levels.

The School of Biological Sciences currently employs 180 staff and supervises 120 PhD students. Facilities include greenhouses and chambers for plant growth in controlled environments, as well as state-of-the-art equipment centres for genomics, proteomics, mass spectrometry and molecular structure determination (see SBS web site: http://www.sbs.auckland.ac.nz/). The University is situated in the heart of Auckland, a modern lively city with a beautiful harbour and beaches, a warm climate and easy access to many outdoor activities.

For further information and to apply online please visit www.vacancies.auckland.ac.nz or alternatively call +64-9-373 7599 ext 83000. Please quote the vacancy number.

Applications close 15 January 2006.

The University has an equal opportunities policy and welcomes applications from all qualified ersons.

EEO Employers Group

THE UNIVERSITY OF AUCKLAND

NEW ZEALAND

Te Whare Wānanga o Tāmaki Makaurau

Featured Employers

Search a comprehensive list of job postings from these employers on **ScienceCareers.org.** Listings updated three times a week.

Pfizer, Inc.
www.pfizer.com

Scios
www.sciosinc.com

If you would like to be a featured employer, call 202-326-6534.

ScienceCareers.org
We know science AAAS

Dream. Challenge. Succeed.

BIOCHEMISTRY FACULTY POSITION

The Department of Molecular and Cellular Biochemistry invites applications for a tenure track faculty position at the Associate, or Full Professor level. Successful candidates must possess a Ph.D., M.D. or equivalent degree and an active, independent research program. We are seeking individuals to complement existing departmental programs including, but not limited to the areas of diabetes, cardiovascular disease, neuroscience, and cancer research, but we welcome all qualified applicants. Preference will be given to candidates with a proven track record of independent research and sustained extramural funding.

The successful candidate will benefit from a stimulating and collaborative environment within the department and a strong graduate program. Competitive start-up funds, salaries, state-of-the-art facilities and appropriate space will be offered in a new 185,000 ft² research building.

Evaluation of applicants will begin February 2006. Interested individuals should send their curriculum vitae, a brief statement of research plans and three references to:

MCB Faculty Search Committee
B278 Biomed. Biol. Sc. Res. Bldg.
741 South Limestone St.
Lexington, KY 40536-0509

UK UNIVERSITY OF KENTUCKY

For further information about the Department, visit: **www.mc.uky.edu/biochemistry**

The University of Kentucky is an equal opportunity employer and encourages applications from minorities and women.

ETH

Eidgenössische Technische Hochschule Zürich
Swiss Federal Institute of Technology Zurich

Professor of Physical Chemistry

Research activities should focus on physical chemistry oriented towards relevant biological questions, whereby emphasis on methodological and experimental aspects is expected. Participation in interdisciplinary research (medicine, biology) is desirable. The new professor will be expected to participate in the undergraduate and graduate physical chemistry teaching. Courses at Master level may be taught in English.

Applications with a curriculum vitae and a list of publications should be sent **to the President of ETH Zurich, ETH Zentrum, CH-8092 Zurich, Switzerland, no later than January 31, 2006**. ETH Zurich specifically encourages female candidates to apply with a view towards increasing the proportion of female professors.

Lecturer Introductory Biology

Located in Ithaca, N.Y., Cornell University is a bold, innovative, inclusive and dynamic teaching and research university where staff, faculty, and students alike are challenged to make an enduring contribution to the betterment of humanity.

The office of Undergraduate Biology invites applications for the position of Lecturer to offer a two-semester, auto-tutorial sequence in INTRODUCTORY BIOLOGY, beginning July 1, 2006. This position is a full-time 12-month position. This self-paced sequence is designed for biology majors, pre-grad, pre-med, and pre-vet students seeking a challenging, broad introduction to biology. The auto-tutorial format is offered at Cornell in parallel with the more traditional lecture/lab introductory biology courses. The auto-tutorial sequence attracts between 150 and 200 students who are guided through reading, laboratory, and discussion modules by the lecturer and a staff of about twenty teaching assistants. The successful candidate must have strong interpersonal relationship skills and is expected to incorporate developments in present-day biology into a vibrant curriculum. Located in Ithaca, N.Y.

Qualifications: PhD or equivalent in Biology or related field strongly preferred. College-level teaching experience in related area preferred. Salary will be commensurate with background and experience. An attractive benefits package is available. For further information, please contact **Dr. Robert Turgeon (607) 255-8395** or **ert2@cornell.edu**

Applicants should send a curriculum vitae, a narrative describing teaching interests, and contact information for at least three references to: **Ms. Christie Sayre, Introductory Biology Search Committee, 20 Plant Science Building, Cornell University, Ithaca, NY 14853.**

The deadline for receipt of applications is Jan. 10, 2006.

Cornell University

Cornell University is an Affirmative Action/ Equal Opportunity, Employer and Educator

http://chronicle.com/jobs/profiles/2377.htm

10YR ANNIVERSARY

جامعة كارنيجي ميلون قطر
Carnegie Mellon QATAR CAMPUS
مؤسسة قطر
Qatar Foundation

Human-Computer Interaction Visiting Faculty Position in the School of Computer Science

Carnegie Mellon University established a branch campus in Qatar in the fall of 2004. We are offering a BS degree in Computer Science to an international student body. The university invites applications for a visiting faculty position to begin as early as January 2006.

We are seeking a faculty member in the area of Learning Science and Technology with research experience ideally in designing, implementing, deploying, and evaluating educational technology in school or college settings. An ability to teach courses in human-computer interaction, artificial intelligence, cognitive psychology, or related areas is also desired. The position will involve research in collaboration with the Pittsburgh Science of Learning Center and faculty at the Human-Computer Interaction Institute at Carnegie Mellon in Pittsburgh. The position offers competitive salaries, overseas assignments, travel and housing allowances and other benefits packages, as well as attractive research support.

Interested candidates should send their resume, statement of teaching interest and research, and names of three references to: **Faculty Hiring Committee, c/o Ruth Gaus, Qatar Office SMC 1070, 5032 Forbes Avenue, Pittsburgh, PA 15289; Ruth.Gaus@cs.cmu.edu; Fax 412-253-0924.**

- For more information on the Pittsburgh Science of Learning Center, see **http://learnlab.org**.
- For more information on the Human-Computer Interaction Institute, see **http://www.hcii.cs.cmu.edu**.
- For more information on the BS in CS program, see **http://www.csd.cs.cmu.edu/education/bscs/index.html**.
- For more information on the Carnegie Mellon Qatar Campus, see **http://www.qatar.cmu.edu/.**
- Information on Qatar is available at: **http://www.experienceqatar.com/** .

EXECUTIVE DIRECTOR / CEO
CHILD HEALTH RESEARCH INSTITUTE INC
SOUTH AUSTRALIA www.chri.com.au

Due to the retirement of the current Executive Director, Professor Heddy Zola, the Child Health Research Institute (CHRI) is seeking a new Executive Director. CHRI is well positioned for a new growth phase and thus provides exciting possibilities for the right applicant. The Institute has an excellent track record in attracting funding from national and international funding agencies and Industry and is equipped with state of the art facilities.

CHRI is an independent medical research institute committed to improving the health and development of children. Established in 1989, CHRI has around 60 staff and students located in seven research groups: Basic Nutrition, Applied Nutrition, Epithelial Biology, Skin Biology, Leukaemia, Leucocyte Biology and Stem Cell Biology. The research groups are located in 3 hospitals in the Adelaide metropolitan area in keeping with our commitment to clinically relevant research. Our scientists are highly collaborative, both within and outside the Institute.

The Executive Director will bring to this role excellent leadership, communication, negotiation, planning and interpersonal skills, as well as an outstanding international track record of basic and/or clinical research relevant to CHRI's vision. The successful candidate will be expected to enhance CHRI's profile both in the international research community and with Government and the local community. The Executive Director will also be expected to attract peer reviewed research funds to continue internationally recognised research.

Terms, conditions and salary will be competitive and commensurate with the qualities sought in a successful applicant.

More information is available from the Chair of the Search Committee, Professor Grant Sutherland **<grant.sutherland@adelaide.edu.au>** or current staff http://www.chri.com.au

Resumes including covering letter and the names of two referees to: The Business Manager, Child Health Research Institute, 72 King William Rd, North Adelaide, South Australia, 5006
Or may be submitted electronically to: kathy.kingston@adelaide.edu.au

Closing Date: 21 January 2006

ARGONNE NATIONAL LABORATORY

Scientific Positions at the Center for Nanoscale Materials

The Center for Nanoscale Materials is seeking outstanding scientists to provide World Leadership in nanoscience; to Create, explore and understand nanoscale materials; and to collaborate with and support users of our unique and state-of-the-art facility. The outstanding scientists will fill approximately 20 positions in six scientific groups starting in late FY06:

- **BioNanocomposites**
- **Electronic and Magnetic Materials & Devices**
- **Nanophotonics**
- **Theory**
- **Nanopatterning**
- **X-Ray Imaging/Nanoprobe**

Successful candidates will lead the mission of the CNM by providing the expertise and creating the tools for the design, synthesis, characterization, and theory of materials at the nanoscale.

Highly accomplished scientists with demonstrated leadership abilities will be considered for 'Group Leader' or 'Lead Scientist' positions, with responsibilities for day-to-day operations, supervisory and long-term vision for one of the six scientific groups.

Interested candidates should send a detailed CV, along with a list of publications, and the names and addresses of three reference through the Argonne website at: http://www.anl.gov/jobs under job search for requisition number CNMJOBS CNM.

Argonne is managed by The University of Chicago for the US Department of Energy.

Argonne is an equal opportunity employer, and we value diversity in our workforce.

THE UNIVERSITY OF CHICAGO

Office of Science
U.S. DEPARTMENT OF ENERGY

Focus Area Lead, Geological and Environmental Sciences
U.S. Department of Energy
National Energy Technology Laboratory

The National Energy Technology Laboratory (NETL) is a science, technology, and energy laboratory owned and operated by the U.S. Department of Energy. NETL's mission is to implement national research, development, and demonstration programs to help resolve environmental, supply, and reliability issues and constraints associated with the production and use of fossil energy resources. These programs are implemented by R&D funding arrangements with scientific and engineering organizations located within all 50 States, and within NETL by its Office of Science and Engineering Research (OSER) located in Pittsburgh, PA and Morgantown, WV.

NETL is currently recruiting for a scientist or engineer with an international reputation for scientific excellence and leadership. This senior-level position within OSER will lead the Focus Area for Geological and Environmental Sciences (GES). The incumbent will lead scientific and applied research in geological, chemical, microbiological, and engineering processes important to the extraction, production, and utilization of fossil energy resources. R&D performed by the GES Focus Area includes work on the improved exploration and production (E&P) of natural gas and oil from unconventional domestic resources including, for example, natural gas from tight gas and methane hydrate formations, oil shale and oil/tar sands, and geological sequestration of carbon dioxide and other greenhouse gases.

As a National Laboratory, NETL strives to maintain an environment that encourages creativity, values diversity, and brings out the best in people. We value teamwork while appreciating individuality. And we offer qualified individuals the opportunity to apply new ideas and approaches to fossil energy resources that will establish new paradigms for their economic, clean, and efficient production and use.

The salary range for this position is $107,550 to $140,300, with excellent benefits and flexible work schedules. Pay will be set within this range based on experience. The position may be located in either Morgantown, WV or Pittsburgh, PA. Both locations offer affordable living, excellent schools, cultural attractions, and the natural beauty and abundant outdoor activities of the Allegheny Mountains.

For information about qualification requirements and procedures for applying, contact **Scott Sigley** at **(304) 285-4470**, or visit the career opportunities page on the NETL website at **www.netl.doe.gov**. U.S. citizenship is required for all Federal positions.

The Department of Energy is an Equal Opportunity Employer.

Brown University
Center for Computational Molecular Biology
Faculty Positions

As part of a major new initiative, Brown University seeks highly qualified candidates for two open rank, tenure-track or tenured faculty positions with a preference for assistant professors in the Center for Computational Molecular Biology (CCMB). The Center's activities focus in three areas and candidates in these three areas are strongly encouraged to apply: (1) regulatory genomics and networks; (2) comparative genomics and evolutionary biology; (3) structural and functional proteomics.

Successful applicants will be expected to have a demonstrated record of excellence in research, maintain an externally funded research program, and have good communication and teaching skills. They also will participate in the continuing development and improvement of Brown's established undergraduate curriculum and a new graduate curriculum that is being built on the foundation of Brown's widely recognized record in teaching innovation and academic excellence. Appointees will have the opportunity to participate in several NIH or NSF funded interdisciplinary programs, such as the new initiative in Genetics, Genomics and Proteomics as well as a number of other multi-disciplinary collaborations with Brown and hospital based faculty and students. The appointments will be in the following top rank departments: Division of Applied Mathematics, Department of Computer Science or a participating department in the Division of Biology and Medicine. The Center has recently hired two senior faculty members, **Sorin Istrail** in Computer Science and **Chip Lawrence** in Applied Mathematics, whose expertise are focused in genomics, sequence analysis and regulatory genomics, systems and networks.

Applicants should submit curriculum vitae, representative preprints or reprints, and a concise description of research interests and goals with emphasis in their interdisciplinary expertise. Additionally, candidates for Assistant Professorship should arrange to have at least three letters of recommendation sent directly to the contact address. Candidates for Associate or Full Professor should provide names and contact information for at least five references, and these will be contacted for letters of recommendation by the search committee at an appropriate time. All applications will be treated confidentially. Application review will commence on **December 14, 2005** and continue until available positions are filled.

Applications should be submitted electronically in PDF form to: **ccmbsearch@dam.brown.edu**. Letters of recommendation to be sent to the following contact address: **ATTN: CCMB Search, c/o Ms. Louise Patterson, Division of Applied Mathematics, Brown University, Box F, Providence, RI 02912.**

For further information, visit our Website at: **http://www.brown.edu/Research/CCMB/**

Brown University is an Affirmative Action/Equal Opportunity Employer.
Women and minorities are encouraged to apply.

Stanford University
Broad Search in Multi-Physics Modeling in Mechanical Engineering

The Department of Mechanical Engineering recognizes the need to model complex mechanical, physical and/or biological systems with functionalities dependent on interactions among chemical, mechanical and/or electronic phenomena. These systems are often characterized by wide ranges in time and length scales which requires the development of technologies to describe and model, using numerical and mathematical techniques, the coupling between those scales with the goal of designing and/or optimizing new engineering devices.

Accordingly, the Department of Mechanical Engineering at Stanford University invites applications for a tenure-track faculty position at the junior level (Assistant or untenured Associate Professor). We are seeking applicants in the broad area of theoretical and computational multi-physics modeling, with an emphasis on multi-disciplinary research. The candidate is expected to perform research and teaching in the areas of analytical and computational modeling with a focus on multi-physics phenomena in fluid and/or solid mechanics. Ideally, the candidate would combine novel modeling approaches with experimental investigations. Candidates should have a substantial breadth of expertise, combined with a strong background in applied mathematics and quantum, statistical and/or continuum mechanics. Higher priority will be given to the overall originality and promise of the candidate's work rather than the candidate's sub-area of specialization within Mechanical Engineering.

Application areas include, but are not limited to: biomechanics, bio-transport phenomena, microfluidics, turbulence modeling, atomic or Brownian dynamic simulations, energy technology, nanoscale phenomena and devices, biopolymers and polymer-based materials, and structures and composites.

Applicants must hold a doctorate in an appropriate field and be able to demonstrate an ability to carry out outstanding research and have a strong record of, or promise for, exceptional teaching. The appointment will be at a rank commensurate with the applicant's experience.

Applicants are requested to send a curriculum vitae, a brief statement of interests including their vision for their research area and teaching (~ 5 pages), copies of one or two publications, and complete contact information for at least five references, to the following address:

Professor Peter M. Pinsky
Chair, Multi-Physics Modeling Search Committee
Department of Mechanical Engineering
261 Durand Building – 496 Lomita Mall
Stanford University
Stanford, CA 94305-4040

Applications will be reviewed starting **January 1, 2006**, and applicants are strongly encouraged to submit their applications by that date; however, applications will continue to be accepted until **May 1, 2006**.

Stanford University is an Equal Opportunity, Affirmative Action Employer.

DIRECTOR
Institute of Physics, Academia Sinica, Taipei

Academia Sinica, Taiwan, R.O.C. invites applications and nominations for the position of Director of the Institute of Physics (IOP). The initial appointment is for a period of three years (renewable for a second term). The appointee will also carry the title of Distinguished Research Fellow with competitive remuneration. Academia Sinica is the most pre-eminent research institution in Taiwan. It is devoted to basic and applied research in mathematics and physical sciences, life sciences, and humanities and social sciences. The Institute was founded in Shanghai in 1928 and was reestablished in Taiwan in 1962. Under the strong leadership of the succeeding Directors, IOP has prospered and earned recognition worldwide in many areas of research, particularly, in the newly launched Nanoscience. IOP is fully cognizant of the challenge of elevating this great Institute to a new height with distinction and international stature. Academia Sinica is determined to work with the new Director to realize the aspiration of members of the IOP. We are looking for a strong and visionary leader to continue the excellent tradition of quality research at the IOP. The area of research is less important than intellectual and leadership qualities. However, with the present makeup and the intellectual thrusts of the Institute, preference will be given to a scientist with interest in one or more of the three general areas: Nanoscience, Complexity, Medium and High Energy Physics, and particularly particle physics and cosmology, experimental high-energy physics, nuclear physics, condensed-matter and surface physics, statistical and computational physics, biophysics, as well as fluid and nonlinear physics.

The new Director is expected to have a distinguished research reputation in at least one of the intellectual thrust areas noted above, and to continue to pursue a vigorous research program in one of these or related fields. Resources will be available to establish the research program of the incoming Director at IOP. Additionally, he or she will be responsible for directing and coordinating the diverse research activities of the Institute to ensure maximum integration and synergy without compromising individual creativity. In addition to superb managerial and administrative skills, the applicant should also exhibit strong leadership qualities and experience to motivate young scientists in pursuit of excellence in scientific research. IOP encourages both applications and nominations, which should include a full curriculum vitae, together with a publication list, and three letters of recommendation, to be submitted to **Chair, Director Search Committee, Institute of Physics, 128 Academy Road Section 2, Nankang, Taipei, 115 Taiwan**; **e-mail: ithuang@phys.sinica.edu.tw; phone: 886-2-27896718.** Screening of applications/nominations will begin immediately, and will continue until the position is filled.

UNIVERSITY OF FLORIDA COLLEGE OF MEDICINE

Assistant/Associate/Professor Clinical Assistant/Clinical Associate/Professor

Department of Pediatrics is recruiting an Assistant/Associate/Professor, tenure accruing track or Clinical Assistant/Clinical Associate/ Professor, non-tenure track faculty member to the Division of Critical Care Medicine. The division's research focuses on lung injury and repair, the immunologic response to lung injury and bacterial and viral infections in the lung. In addition, there are significant research opportunities at the University of Florida for collaboration with the McKnight Brain Institute, the Davis Cancer Center, the Powell Gene Therapy Center and the Genetics Institute here at the University of Florida, College of Medicine. This position is for a Ph.D, M.D./Ph.D or an M.D. Researcher. Salary and rank for this position will be commensurate with experience and training. Application deadline is **March 1, 2006** with and anticipated hiring date of June 2, 2006.

Interested applicants should send a letter of interest, a current C.V., and names of three references to:

Ann Marie LeVine, M.D., Associate Professor
Division of Critical Care Medicine
Department of Pediatrics
University of Florida
College of Medicine
PO Box 100296
Gainesville, FL 32610-0296

AN EQUAL OPPORTUNITY INSTITUTION

Scripps Institution of Oceanography

DIRECTOR

Scripps Institution of Oceanography (SIO) at the University of California, San Diego invites nominations and applications for the position of Director, who will also be the Vice Chancellor of Marine Sciences and Dean of the Graduate School of Marine Sciences. The incumbent will lead the Institution in articulating a clear scientific vision, provide direction for its academic programs, expand revenue sources, and optimize the administrative organization. The SIO Director represents and provides leadership nationally and internationally in scientific matters related to the on-going research efforts of SIO scientists and in relations with Federal, State and local governmental entities and private organizations and individuals.

We are seeking a distinguished scientist in oceanography, the earth sciences, or a closely related field who will promote Scripps' scientific and educational mission. He or she should be an innovative leader with a demonstrated successful record in strategic planning, administration and fundraising. Effective communication and interpersonal skills are essential, together with an understanding of, and commitment to, academic shared governance.

Scripps Institution was founded in 1903, and today occupies 230 acres mostly along the Pacific coastline. One hundred faculty and more than 200 research scientists conduct basic and applied research covering all facets of the ocean, earth and atmospheric sciences, including biological sciences, through five research divisions, and eight special purpose laboratories and multidisciplinary centers. The graduate program in Marine Sciences is carried out in eight curricular groups with a current enrollment of 241 students. Scripps' offerings of undergraduate classes at UCSD are expanding in all areas of its expertise. The Birch Aquarium-Museum at Scripps is a self-supporting educational resource for the region and receives more than 340,000 visitors annually. SIO receives 70% of its funding from Federal sources with future emphasis on developing support from the private sector and individuals.

The Search Committee will accept nominations and applications through February 2006 with resume review beginning early December 2005. Please submit resumes and/or nominations In Confidence to: **Nicholas Brill, Brill Neumann Associates, Inc., 312 Stuart Street, Boston, MA 02116** or email to: **scrippssearch@brillneumann.com**

SIO/UCSD is an equal opportunity/affirmative action employer and welcomes the interest of qualified women and minorities.

POSITIONS OPEN

DIRECTOR
Environmental Research Center

The Academy of Natural Sciences has an immediate opening for Director of its Patrick Center for Environmental Research (PCER). The Center has an international reputation for its ecosystem approach to understanding and managing the influences of human activities and has a special focus on team research. The Center has over 35 staff (including ten Ph.D.s) researching aquatic ecosystems throughout the United States, primarily rivers and their watersheds. Director is responsible for all aspects of the Center's operation, including scientific, financial, and general management. Requires Ph.D. in aquatic ecology or closely related field, strong record of research achievement, leadership and management skills, and an understanding of and commitment to basic and applied ecological research. The Director must be effective in developing new projects and programs, and in fundraising and marketing. Must also participate in externally-funded research programs. Send letter of interest and curriculum vitae to: **Patrick Center for Environmental Research Director Search Committee, The Academy of Natural Sciences, 1900 Benjamin Franklin Parkway, Philadelphia, PA 19103-1195.** Applications may be sent to **e-mail: pcerdirectorsearch@acnatsci.org;** contact same for more information about the position. Also see **website: (http://www.acnatsci.org/learn/employment.html).** Review process will begin December 15, 2005, and continue until position is filled. Full benefits package. *Affirmative Action/Equal Opportunity Employer.*

VASCULAR SURGERY RESEARCH POSITION

The Department of Surgery, Indiana University School of Medicine is seeking applicants for an Assistant/Associate Professor research position in Vascular Surgery. Candidates must have either a Ph.D. in basic science or a M.D. Degree. Academic teaching experience at the university/college level required. A minimum of five years of laboratory research experience or two years postdoctoral research experience/study, preferably vascular-related, is also required. This is a tenure-track position. Good communication and manuscript writing skills are also preferred. In addition to responsibilities in vascular surgery research, successful candidate will assist in laboratory training of graduate students and surgery residents. Please send acurrent curriculum vitae to:

Zorina Galis, Ph.D., Professor
Department of Surgery
1801 N. Senate Avenue, D3500
Indianapolis, Indiana 46202
Telephone: 317-962-0282 Fax: 317- 962-0289
E-mail: zgalis@iupui.edu

Indiana University is an Affirmative Action/Equal Opportunity Employer, Minorities/Females/Persons with Disabilities are encouraged to apply.

BIOCHEMISTRY, HENDRIX COLLEGE
TENURE TRACK ASSISTANT PROFESSOR

in biochemistry, beginning August 2006. Ph.D. required, postdoctoral experience preferred. Candidates must be committed to excellence in teaching and research. Competitive startup funding and research time assignment provided in new facilities. Details regarding this position are available at **website: http://www.hendrix.edu/chemsearch.** Hendrix College is a selective liberal arts college with particular strength in the sciences. Send letter, curriculum vitae, undergraduate and graduate transcripts, teaching philosophy, detailed research plans, and arrange for three letters of reference to be sent to: **Dr. Randall Kopper, Department of Chemistry, Hendrix College, 1600 Washington Avenue, Conway, AR 72032.** Consideration of applications will begin on January 17, 2006. *Hendrix is an Equal Opportunity Employer. Women and members of minority groups are especially encouraged to apply.*

CLINICIAN SCIENTIST POSITION
Inflammation Research
Departments of Medicine and Microbiology and Immunology
Schulich School of Medicine and Dentistry
The University of Western Ontario

The Departments of Medicine and Microbiology and Immunology are seeking a Clinician Scientist for a faculty position in the general area of inflammation at the rank of Assistant Professor, although outstanding candidates will be considered at a higher rank. The successful candidate will join and enhance the ongoing efforts in basic and translation research with an institutional commitment to building a world-class experimental therapeutics program. The candidate is expected to establish an independent, externally funded research program and collaborate with others at the University, J.P. Robarts Research Institute, and Lawson Health Research Institute. Priority will be given to candidates with research interests and expertise in the areas of infectious diseases, autoimmunity, transplantation, allergy and viral immunology which will complement existing areas of research strength in both departments. The successful candidate will hold a clinical academic position in the Department of Medicine and will require participation in clinical and teaching activities in the Departments of Medicine and Microbiology and Immunology at both undergraduate and graduate levels.

Candidates must have an M.D. or equivalent and must be eligible for licensure in the Province of Ontario.

For a look at the full advertisement please see the ad on Science Careers **website: http://sciencecareers.org** or the Department of Microbiology and Immunology **website: http://www.uwo.ca/mni.**

ASSISTANT PROFESSOR
FOREST WATERSHED SCIENCE

The University of Missouri (MU) is seeking a tenure-track (12 month) Faculty Member for a teaching and research position. She/he will teach undergraduate courses in watershed management and summer field studies and a graduate course in her/his specialty. Development of a nationally recognized, extramurally funded research program in a relevant area is expected. Ph.D. required, with one degree in forestry or a comparable area; postdoctoral experience preferred. Send letter of application, resume, transcripts, description of research interests, teaching philosophy and contact information for three references by February 1, 2006, to: **Dr. S. G. Pallardy, Department Forestry, 203 ABNR Bldg., University of Missouri, Columbia, MO 65211. Telephone: 573-882-3548. E-mail: PallardyS@missouri.edu.** Additional information at **website: http://www.snr.missouri.edu/jobs/watershed.html.** *MU is an Equal Opportunity, Affirmative Action Employer.*

NEUROSCIENCE AND LABORATORY RESEARCH AND TEACHING POSITIONS
Tenure Track
Department of Psychiatry

The Department of Psychiatry and the Center for the Study of Traumatic Stress at the Uniformed Services University of the Health Sciences (USUHS) seeks to fill tenure-track neuroscience laboratory research and teaching positions (**ASSISTANT/ASSOCIATE PROFESSOR**). The Department, twenty full-time faculty, seeks to expand ongoing neuroscience research, animal and human, in: stress, anxiety (particularly acute stress responses, PTSD and dissociation), depression, behavior, and drug use. Individuals who hold Ph.D. or M.D. degrees and have active fundable research are invited to apply. Send curriculum vitae, description of current and anticipated research, and three references to: **Robert Ursano, M.D., Chairman, Department of Psychiatry, USUHS, 4301 Jones Bridge Road, Bethesda, MD 20814-4799. E-mail: rursano@usuhs.mil.** Applications should be received before December 1, 2005. *The University is an Affirmative Action/Equal Opportunity Employer.*

ASSISTANT PROFESSOR
Vertebrate Biology
Pacific Lutheran University

The Department of Biology at Pacific Lutheran University (PLU) invites applications from organismal-level Vertebrate Biologists for a tenure-track Assistant Professor position to begin 1 September 2006. Ph.D. required. Teaching responsibilities will include participation in introductory biology courses for majors/non-majors, an upper-division majors' course focusing on vertebrates, and other courses related to the candidate's area of specialty. Research involving undergraduates is expected and supported. Please submit your curriculum vitae, copies of undergraduate and graduate transcripts, a statement of teaching philosophy, and a summary of current research interests; also arrange to have three letters of recommendation sent on your behalf. Send all materials to: **Dr. Dana Garrigan, Chair of Vertebrate Biology Search Committee, Department of Biology, Pacific Lutheran University, Tacoma, WA 98447.** Review of applications will begin on 10 January 2006. Tacoma is located on Puget Sound in Washington, a uniquely scenic and biologically diverse region. Seattle and Mount Rainier are about 40 miles from our suburban campus. Pacific Lutheran University enrolls 3,700 students and is committed to finding connections between the liberal arts and professional schools and to promoting international education and undergraduate research. PLU enjoys a healthy and progressive relationship with the Evangelical Lutheran Church in America and values its tradition of academic freedom. The majority of our faculty has lived abroad or speaks a second language. The Department of Biology has 13 faculty members. For more information, please visit **website: http://www.nsci.plu.edu/biol/jobs.htm.** *In addition to having a diverse faculty, PLU serves a diverse clientele and is an Affirmative Action/Equal Opportunity Employer.*

BIOINFORMATICS FACULTY POSITIONS

Colorado State University (CSU) is recruiting three special appointment non-tenure-track faculty in bioinformatics at the Assistant Professor level to establish the CSU Center for Bioinformatics. Candidates must possess a Ph.D. degree or equivalent. Successful applicants will have demonstrated expertise in one or more of the following areas: comparative and functional genomics and proteomics, mining of biological data, predictive modeling, design and implementation of bioinformatics tools/databases, computer hardware and software management, statistical methods for bioinformatics analysis, systems biology and/or algorithm development. Salary and startup packages will be competitive and commensurate with qualifications. Applications will be accepted until positions are filled, but evaluation will begin January 9, 2005. Applications should be submitted online at **website: http://www.natsci.colostate.edu/searches/bioinformatics/.** Applicants should provide referee contact information online as early as possible.

Colorado State University is an Affirmative Action/Equal Opportunity Employer and values diversity.

VERTEBRATE ZOOLOGY

Ripon College seeks a tenure-track **ASSISTANT PROFESSOR** to teach general and upper division courses starting August 2006. The candidate must have a Ph. D. and be able to lead undergraduate research. Send letter of application, curriculum vitae, statements of instructional philosophy and research interests, and arrange to have official undergraduate and graduate transcripts, and three letters of reference sent to: **Dr. George H. Wittler, Chair, Department of Biology, Ripon College, P.O. Box 248, Ripon, WI 54971.** Applicant review begins December 15, 2005, until position is filled. See **website: http://www.ripon.edu/news/employment.** *Affirmative Action/Equal Opportunity Employer.*

AAAS

ADVANCING SCIENCE, SERVING SOCIETY

CHIEF INTERNATIONAL OFFICER

The American Association for the Advancement of Science (AAAS) is the world's largest general scientific society, and publisher of the journal, *Science*. AAAS was founded in 1848, and serves some 262 affiliated societies and academies of science, reaching 10 million individuals. The non-profit AAAS (**www.aaas.org**) is open to all and fulfills its mission to "advance science and serve society" through initiatives in science policy, international programs, science education, and more. AAAS has a combined staff of over 300 in the Washington, DC headquarters and in Cambridge, UK.

AAAS has retained Dinte Resources, Inc. to conduct the search for a **Chief International Officer**.

The Chief International Officer reports to the CEO and is a member of the AAAS senior leadership staff. He/she will be responsible for participating fully in developing and implementing overall Association strategies to accomplish the goals and objectives set by the AAAS Board of Directors. This individual will work collaboratively with other members of the senior leadership team to develop and implement AAAS' strategic initiatives.

- Develops a comprehensive and coherent AAAS strategy for international programmatic work; conducts long-range planning and establishes program priorities and methods of program evaluation. Responsible for proposal development and fundraising.
- Directs the programs and activities of the International Office, which coordinates international activities across AAAS to further enhance the image of the organization internationally.
- Sets broad, strategic international goals and objectives and builds relationships both internally and externally to help fulfill AAAS' international goals.

The Chief International Officer will represent AAAS and the International Office at meetings, conferences, congressional hearings, and community forums to share information, foster cooperation, and develop and implement mutual programmatic interests.

The position requires mastery of a professional field typically acquired through the completion of a doctoral degree and recognized achievement within the field as evidenced by publications, academic or other appoints, or other relevant professional recognition. Ideally, he/she will have 15 or more years experience in progressively responsible positions in program development and management of international programs. Experience may be obtained through managing large-scale projects in academia, government, or business and should also include fundraising responsibilities. For more information about this opportunity please contact:

DAVID S. MARTIN, Vice President
Dinte Resources, Inc.
dmartin@dinte.com

EOE

Assistant Professor
Neuroscience and Psychology

Pending budgetary approval, **THE UNIVERSITY OF CALIFORNIA AT BERKELEY** invites applications for a 100% tenure-track position at the ASSISTANT PROFESSOR level. The proposed start date is July 1, 2006. This position is a joint appointment (50%/50%) with the **Department of Psychology** and the **Helen Wills Neuroscience Institute**.

Applicants should hold a doctoral degree in Psychology, Neuroscience, Cognitive Neuroscience or a related field. We are particularly interested in candidates employing neuroimaging techniques to study the human life span (e.g., child development, developmental psychopathology, or aging processes). **Applications must be postmarked by February 1, 2006** and should include a resume, selected publications, and a brief statement of research interests and future plans sent to:

Neuroscience Search Committee
Helen Wills Neuroscience Institute
132 Barker Hall, MC 3190
University of California
Berkeley, CA 94720-3190

Candidates should also arrange to have at least three letters of recommendation sent to the same address and to request that referees read the University's statement on confidentiality (**http://apo.chance.berkeley.edu/evalltr.html**) prior to submitting their letters. **Applications postmarked after February 1, 2006 cannot be considered.**

Review of completed applications will begin **January 15, 2006**.

The University of California is an Equal Opportunity/Affirmative Action Employer. All qualified applicants including minorities and women are encouraged to apply.

McGill University
Tenure Track Position in Cell Biology

The Department of Biology at McGill University invites applications for a Cell Biologist utilizing a genetically well-characterized plant, fungal or non-mammalian animal system. Candidates focusing on subcellular structures using advanced imaging and microscopy techniques or nano scale manipulations are particularly encouraged to apply. The successful candidate would be joining the Developmental Biology Research Initiative (DBRI), a dynamic, interactive group of researchers working on a range of subjects in yeast, C. elegans, Drosophila, Xenopus, Arabidopsis and other model organisms (**http://www.biology.mcgill.ca/DBRI/dbri_home.htm**). The DBRI is presently engaged in a $19.8M infrastructure renovation and renewal project, and is an integral part of the McGill University Life Sciences Research Complex.

We anticipate that this position will be filled at the Assistant Professor (tenure-track) level, but applications from more established candidates may be considered for recruitment at the Associate or Full Professor rank. Competitive start-up packages and the opportunity to apply for equipment funding through the Canadian Foundation for Innovation will be available. The successful candidate is expected to significantly contribute to undergraduate and graduate teaching in the department and to maintain an externally funded research program.

Applicants should forward a curriculum vitae, a statement of research interests, a statement of teaching interests, copies of major publications and arrange to have three letters of reference submitted directly to: **Cell Biology Search, c/o Ms. Louise Sabaz, Department of Biology, McGill University, 1205 Docteur Penfield Ave., Montreal, Quebec, H3A 1B1, Canada**. The application deadline is **January 15, 2006**.

In accordance with Canadian immigration regulations, this advertisement is directed in the first instance to Canadian citizens and landed immigrants, however, all qualified candidates are encouraged to apply.

POSITIONS OPEN

BIOLOGICAL SCIENCE EDUCATOR

The Department of Biological Sciences at California State University (CSU), Chico invites applications for a full-time, academic year, tenure-track faculty position as an Assistant Professor or Associate Professor as a Biological Science Educator to begin fall 2006. A Ph.D. in any area of biological sciences by no later than the fall 2006 appointment date is preferred. A doctoral degree in science education will be considered based on experience in the discipline of biology. Postdoctoral experience is desired. Teaching responsibilities include an introductory biology course for future elementary teachers and an upper-division course for prospective secondary teachers, as well as a graduate course in biology for the Master's in science teaching. Candidates must have a record of research in biological science education and will be expected to establish an active research program and seek extramural funding in biological science education. Master's and undergraduate student participation in the research program is expected. Submit a letter of application, statement of teaching philosophy and instructional methodologies employed, curriculum vitae, complete academic transcripts (student copy acceptable), representative reprints, and three current letters of reference to: **Dr. Patricia Edelmann, Chair, Department of Biological Sciences, Attn: Biological Science Educator Search, California State University, Chico, CA 95929-0515.** Review will begin January 16, 2006. Applications completed after that date may be considered. For full announcement and description of science education opportunities at CSU, Chico, please see **website: http://www.csuchico.edu/.** *For disability-related accommodations, call 530-898-6192 or TDD 530-898-4666. I-9/Equal Opportunity Employer/Affirmative Action/ADA.*

ASSISTANT, ASSOCIATE, OR FULL PROFESSOR OF VETERINARY NUTRITION: 11 month, tenure-track. Salary dependent on qualifications and experience. Required: Ph.D. in nutrition or related field, strong research program/advanced training in large animal nutrition, documented research record/high potential to develop an independent research program in animal nutrition, demonstrated ability in acquisition of extramural funding, demonstrated experience/aptitude in teaching in nutrition, possess excellent interpersonal and communication skills and a demonstrated ability to work with others in a collegial team atmosphere. Preferred (not required): D.V.M., Ph.D., or equivalent, competence in herbivore nutrition/experience in clinical equine nutrition. Apply by February 6, 2006; position open until filled. Submit letter outlining special interest in the position, overall related qualifications, experience and career goals; curriculum vitae; three publications; and names and addresses of three professional references to: **Dr. Robert Hansen, Chair, Department of Molecular Biosciences, School of Veterinary Medicine, University of California, Davis, CA 95616-8741. E-mail: rjhansen@ucdavis.edu.** *University of California, Davis is an Affirmative Action/Equal Opportunity Employer.*

POSTDOCTORAL POSITIONS

Projects include: (1) functional characterization of the Par-1 protein kinases in polarized cells and mice; (2) regulation of cell cycle using high throughput short interfering RNA screens; (3) applications of molecular imaging and mouse modeling to cancer biology. Applicants must have a Ph.D. and/or M.D. Ideal candidates would have experience with mouse modeling, cell culture, protein biochemistry, and/or cellular or molecular imaging. Please submit curriculum vitae and contact information for three references via e-mail to: **Helen Piwnica-Worms, Ph.D., Howard Hughes Medical Institute and Department of Cell Biology, Washington University School of Medicine, 660 S. Euclid Avenue, St. Louis, MO 63110. E-mail: hpiwnica@cellbio.wustl.edu.**

POSITIONS OPEN

POSITION ANNOUNCEMENT
DEPARTMENT OF ENVIRONMENTAL HEALTH SCIENCES
Arnold School of Public Health
University of South Carolina

ASSISTANT/ASSOCIATE PROFESSOR, Environmental Health Sciences, tenure track. The University of South Carolina seeks applications from scholars committed to teaching and research excellence in human environmental health sciences. Preferred research areas related to human health include occupational hygiene, exposure and/or risk assessment, toxicology, biological monitoring, biohazards, infection control, environmental microbiology, and indoor air quality, but others will be considered. The Department offers Ph.D. and Master's degrees with specializations in occupational hygiene, environmental quality, and hazardous materials management. The successful applicant will have postdoctoral experience, a record of excellence in funded research and scholarship (or strong evidence of talents to develop a funded research program) and be expected to contribute to the National Institute for Occupational Safety and Health-supported occupational hygiene program. Application reviews begin January 5, 2006 (open until filled). Applicants should apply online at **website: http:// uscjobs.sc.edu,** Requisition 041325, and also forward curriculum vitae, statement of professional goals in research and teaching, and names of three references (with mailing address, e-mail, and telephone number) to: **Dr. Alan Decho, Search Chair** at **e-mail: awdecho@gwm.sc.edu.** *The University of South Carolina is an Affirmative Action, Equal Opportunity Employer. Women and Minorities are encouraged to apply.*

NEUROBEHAVIORAL BIOLOGY

The University of Mississippi Medical Center Department of Psychiatry is seeking a faculty applicant at the rank of **ASSISTANT** or **ASSOCIATE PROFESSOR** (tenure-track). The successful applicant will join a group engaged in neuroscience research. Candidates must have the ability to attract extramural funding and research experience that complements ongoing research, such as molecular and behavioral mechanisms of psychotherapeutic drugs, behavioral pharmacology of substance abuse and neuropathobiology of mental illnesses. Expertise with in vitro, cellular and/or molecular biological techniques and their relationship to central nervous system function in the study of the behavioral neurobiology of drug and/or alcohol abuse will be preferred. Candidates should have a Ph.D. and/or M.D. and postdoctoral experience. Salary will be commensurate with experience. Modern laboratory space and a competitive start-up package are available. Mail or fax curriculum vitae, a statement of current and future research goals, and three references to:

Search Committee
Department of Psychiatry
Division of Neurobiology and Behavior Research
University of Mississippi Medical Center
2500 North State Street
Jackson, MS 39216-4505
Fax: 601-984-5899

Equal Opportunity Employer, Minorities/Females/Persons with Disabilities/Veterans.

Postdoctoral Position for DEVELOPMENTAL BIOLOGIST to Study Melanocyte Biology: Position available immediately to study the contribution made by cell cycle regulators to melanocyte biology. Applicants must have a Ph.D. and/or M.D. Ideal candidate would have experience in mouse developmental biology. Please submit curriculum vitae and contact information for three references via e-mail to: **Helen Piwnica-Worms, Ph.D., Howard Hughes Medical Institute and Department of Cell Biology, Washington University School of Medicine, 660 S. Euclid Avenue, St. Louis, MO 63110. E-mail: hpiwnica@cellbio.wustl.**

POSITIONS OPEN

FACULTY POSITION
MEDICINAL CHEMISTRY
University of Washington

The Department of Medicinal Chemistry at the University of Washington invites applications for one or more tenure-track positions from individuals with interests in areas that complement current research efforts of the Department. These include chemical genomics, metabolomics, proteomics, drug metabolism and toxicity, pharmacogenetics and protein misfolding diseases. These positions may be filled at the assistant, associate, or full professor levels. Applicants must have a Ph.D. degree. The Department has excellent core resources including a large mass spectrometry facility, nuclear magnetic resonance, and protein expression facilities. In addition, ample opportunities for collaborative research exist in the Department, School and University. (See **website: http://depts.washington.edu/medchem/** for further details.) Responsibilities of these positions include graduate and undergraduate teaching, mentoring of graduate students and the development of an independent extramurally-funded research program. These positions will remain open until filled. Applicants should forward a cover letter, curriculum vitae, a statement that describes current and future research interests, and arrange for three letters of reference to be forwarded to: **Dr. Kent L. Kunze, Search Committee Chair, Medicinal Chemistry, University of Washington, Box 357610, Seattle, WA 98195-7610. E-mail: medchem@u.washington.edu.**

The University of Washington is building a culturally diverse faculty and strongly encourages applications from female and minority candidates. The University of Washington is an Affirmative Action/Equal Opportunity Employer.

The University of Nevada, Las Vegas (UNLV), Department of Chemistry is seeking candidates for a full-time, nine-month tenure-track, **ASSISTANT PROFESSOR** position in biochemistry, commencing fall 2006. Applications are encouraged from individuals with interests in enzymatic biosensing or related fields. The Department (**website: http://sciences.unlv.edu/Chemistry**) has experienced significant growth resulting in a doctoral program initiated in 2005. The successful candidate will be expected to excel in teaching biochemistry at both undergraduate and graduate levels; develop rigorous extramurally funded research programs; and provide service to the Department, College, University and the profession. A Ph.D. in chemistry or biochemistry from an accredited college or university is required and postdoctoral experience is preferred. Salary competitive; contingent on labor market. Position contingent upon funding. Application materials must include a cover letter, curriculum vitae, proposed research plans (five page limit), statement of teaching philosophy and interests, and three letters of recommendation. Materials should be addressed to: **Dr. David Hatchett, Search Committee Chair,** and are to be submitted via online application at **website: https://hrsearch.unlv.edu.** Review of applications will begin immediately. To assure consideration completed applications are due by November 30, 2005.

UNLV is an Affirmative Action/Equal Opportunity Educator and Employer committed to excellence through diversity.

ASSISTANT PROFESSOR, BIOLOGY
COORDINATOR OF BIOLOGY
SECONDARY EDUCATION

The Biology Department at Framingham State College seeks applicants for a tenure-track position starting in September 2006. The successful applicant will be a broadly trained Biologist with experience in biology secondary education and/or teacher preparation (see **website: http://www.framingham.edu/biology/**). Send curriculum vitae, transcripts, statement of research and teaching interests, and the names of three references by January 16, 2006, to: **Gene Muller, Ph.D., Chair, Department of Biology, Framingham State College, P.O. Box 9101, Framingham, MA 01701. E-mail: gmuller@frc.mass.edu.** *An Equal Opportunity /Affirmative Action Employer.*

THE HONG KONG UNIVERSITY OF SCIENCE AND TECHNOLOGY

Director of the Institute for the Environment

The **Institute for the Environment** is a newly established institute under The Hong Kong University of Science and Technology which is a research university offering degree programs up to the level of PhD. The Institute, comprising faculty representatives from various disciplines of the University from the Schools of Science, Engineering, Business & Management, and Humanities & Social Science, aims at addressing high priority environmental research issues which are of local relevance and international significance. It will coordinate environmental teaching and out-reach programs. As air and water quality problems extend to regions beyond Hong Kong, the Institute will work closely with researchers, industry and governments in the Pearl River Delta and southern China to help develop environmental strategies and policies in Hong Kong and the Region. An Environmental Central Facility has been established under the Institute to support the teaching and research activities of the Institute.

Applications are invited for a tenured faculty position at the rank of professor to serve as the **Director of the Institute**. Candidates should have a doctoral degree in environmental engineering/science or related disciplines; outstanding research records in core research areas of the Institute, such as air, water, solids/land and marine; and substantial experience in managing major research programs and human resources in an academic or large research setting. Candidates should also have strong leadership skills, be able to promote the Institute and help attract major external funds for large interdisciplinary research projects. Development of collaborative programs with the Mainland, in particular with the Pearl River Delta region, is expected. Previous experience in managing major multi-disciplinary research programs/institutes is preferred.

Salary is highly competitive and will be commensurate with experience. Fringe benefits include medical/dental and annual leave. Housing will also be provided where applicable.

Applications together with a curriculum vitae and names and addresses of three referees should be sent to the Chair of the Search Committee for Director of the Institute for the Environment at email: **DIENV@ust.hk,** or c/o Personnel Office, HKUST, Clear Water Bay, Kowloon, Hong Kong [fax no: (852) 2358 0700]. Review of applications will start in **January 2006**. The search will continue until an appointment is made. More information about the University and the Institute can be found on the websites **<http://www.ust.hk>** and **<http://ienv.ust.hk>** respectively.

(Information provided by applicants will be used for recruitment and other employment-related purposes.)

Translational Research Architect

IS and Biomedical Informatics Faculty Appointment

The Ohio State University Medical Center is currently seeking a **Translational Research Informatics Architect** to join our growing team. This new position offers the opportunity to dramatically impact research efforts at OSU Medical Center.

As the Translational Research Architect, the candidate will:

- Lead efforts in designing an enterprise information architecture that dynamically facilitates translational research through integration across all sectors of the medical center: clinical care, operations, education, and research.
- Serve as a tenure- or research-track faculty member, publish, and participate in and develop informatics-related proposals.
- Serve as a member of both the Information Warehouse and Biomedical Informatics teams and coordinate the application of each department's resources to best meet the needs of specific research projects.
- Develop and implement new informatics technologies in areas such as grid computing, image analysis and mining, high throughput genomics data analysis and natural language processing.

M.D./Ph.D. or Ph.D. in a biomedical field and at least one year of research experience is required. Experience with bioinformatics software development, data warehousing and data mining, modern application analysis and design, object-oriented programming, and statistical analysis is desired. Familiarity with HIPAA regulation and privacy protection requirements is also desired.

OSU is one of the country's top health systems and offers a comprehensive compensation package and excellent benefits. Qualified candidates should have their application materials, including CVs and 3 letters of reference, sent to **TRAposition@lists.bmi.ohio-state.edu**. Electronic submissions are preferred, however hard copy submissions may be sent to: **Biomedical Informatics, The Ohio State University, 3190 Graves Hall, 333 W. 10th Ave., Columbus, Ohio 43210**.

EEO/AA Employer.

Penn Engineering

Department of Electrical and Systems Engineering

The University of Pennsylvania seeks outstanding individuals for tenure-track or tenured faculty positions in the Department of Electrical and Systems Engineering to start July 1, 2006. Applicants must have a Ph.D. in Engineering or equivalent. Suitable candidates in all EE and Systems research fields will be considered, with particular interest in (i) the general areas of Nanostructures and Devices, Molecular Electronics, and other novel computational devices and systems and (ii) the areas of communication systems and networks, with special interest in wireless systems and signal processing, sensor networks and distributed computation, and network architectures. Candidates should be prepared to collaborate with faculty in appropriate related areas such as bio-engineering, computer science, materials science, or mechanical engineering. The University seeks indviduals with exceptional promise for, or proven record of, research achievement who will excel in teaching undergraduate and graduate courses and take a position of international leadership in defining their field of study.

Interested persons should submit an application by completing the form located on the Faculty Recruitment Web site at https://www.seas.upenn.edu/ese/fsrch/apply.html including curriculum vitae, and the names of at least three references.

The University of Pennsylvania is an affirmative action/equal opportunity employer and is strongly committed to diversity. Minorities/Females/Individuals with Disabilities/Veterans are encouraged to apply.

POSITIONS OPEN

POSTDOCTORAL FELLOW/RESEARCH ASSOCIATE POSITION is available to study in vivo validation of new drugs for muscular dystrophies. Ideal candidate will hold a Ph.D. in physiology/pharmacology with hands-on experience in muscle physiology preferably on isolated muscle fibers. The position will remain open until filled but preference will be given to candidates who have submitted their applications prior to November 15, 2005. Interested candidates should forward curriculum vitae along with three reference letters to: **Dr. Kanneboyina Nagaraju, D.V.M., Ph.D., Research Center for Genetic Medicine, Children's National Medical Center, 111 Michigan Ave N.W., Washington, DC 20010. Fax: 202-884-6014. E.mail: knagaraju@cnmcresearch.org.**

DEVELOPMENTAL BIOLOGIST

The Biology Department of Carthage College invites applications for a tenure-track position in developmental biology to teach introductory biology, cell and molecular biology, and courses in the candidate's area of interest. Candidates must hold the Ph.D. degree in biology or a related field at time of appointment. We are seeking an individual with a strong commitment to teaching and involving undergraduates in research. In addition to formal scholarly credentials, candidates must have enthusiasm for teaching and undergraduate research in a small college atmosphere. Carthage faculty members also teach general education courses regularly, including Heritage seminars, the College's core curriculum.

Salary and benefits are fully competitive. Rank of appointment is dependent on qualifications.

Situated on the shore of Lake Michigan, midway between Milwaukee and Chicago, Carthage (**website: http://www.carthage.edu**) offers quick urban access from the relaxed environment of a small city. Founded in 1847, Carthage is affiliated with the Evangelical Lutheran Church in America.

Applications including a current curriculum vitae, a statement of teaching philosophy, and three letters of recommendation, should be sent to: **Dr. Kevin Crosby, Chair, Division of Natural Sciences, Carthage College, 2001 Alford Park Drive, Kenosha, WI 53140-1994.** Review of applications will begin immediately and continue until the position is filled. *Women and minorities are encouraged to apply.*

POSTDOCTORAL AND/OR RESEARCH TECHNICIAN POSITIONS
University of Georgia
Complex Carbohydrate Research Center

Two positions are open at either the postdoctoral or research technician level work on a major initiative to generate and characterize monoclonal antibodies against plant cell wall carbohydrate structures:

(1) fragmentation, chemical modification, protein coupling (Postdoctoral position).

(2) Immunoassays (enzyme-linked immunosorbentassay, dot blots) and immunolocalizations (fluorescence and immunogold) (Research Technician position).

Preference will be given to candidates having prior experience with these techniques. All interested applicants should forward curriculum vitae and list of three references to: **Michael Hahn, University of Georgia/Complex Carbohydrate Research Center, 315 Riverbend Road, Athens, GA 30602-4712. E-mail: hahn@ccrc.uga.edu. Fax: 706-542-4412.** Review of applications is ongoing and will continue until positions are filled. *Equal Employment Opportunity/Affirmative Action employer.*

ASSISTANT PROFESSOR
Department of Biochemistry and Molecular Biology

The Department of Biochemistry and Molecular Biology (**website: http://www.msstate.edu/dept/Biochemistry/**) at Mississippi State University invites applications for a nine-month tenure-track teaching and research position at the Assistant Professor rank to be filled by late spring 2006. Mississippi State University is a land-grant institution located adjacent to Starkville, Mississippi and has an enrollment of about 13,500 undergraduate and 2,500 graduate students. The Department has an undergraduate degree program in biochemistry with about 90 students. There are about 15 students in the Ph.D. program. Department faculty are currently funded by National Institutes of Health, National Science Foundation, Department of Energy, United States Department of Agriculture, and National Oceanic and Atmospheric Administration. Startup funds will be available for initial support; however, the successful applicant will be expected to generate external funding. The ideal candidate is a Molecular Biologist with expertise in proteomics or functional genomics and should have experience (or at least interest) in working with corn or other crops. The Scientist should be willing to work as part of a multidisciplinary research team with a goal of reducing aflatoxin contamination of corn. The Scientist will be expected to participate in our undergraduate and graduate teaching programs and establish an active research program. Satisfactory progress towards tenure and promotion will be measured by publication in refereed journals, teaching evaluations, and extent of external funding. Requirements include a Ph.D. in biochemistry or molecular biology with postdoctoral experience. Applicants must have demonstrated involvement in quality research as evidenced by publications in peer-reviewed journals. Send curriculum vitae, summaries of research and teaching interests, and names of three references to: **Dr. John Boyle, Department of Biochemistry and Molecular Biology, P.O. Box 9650, Mississippi State, MS 39762.** Applications will be accepted until February 15, 2006. *Mississippi State University is an Affirmative Action/Equal Opportunity Employer.*

EVOLUTIONARY DEVELOPMENTAL PLANT BIOLOGIST

The Department of Environmental and Plant Biology at Ohio University invites applicants at the Assistant Professor level for a full-time, tenure-track, nine-month appointment beginning in September 2006. Candidates must be committed to teaching and to developing an externally funded research program that involves undergraduate, M.S. and Ph.D. students. Experience and ongoing research in plant development from an organismal and evolutionary perspective is essential; we seek an organismal Biologist using molecular biology, microscopy and/or other tools to investigate plant development within a broader context. Postdoctoral experience is required. Teaching responsibilities will include an introductory biology course together with coordination of its labs, and teaching upper level/graduate courses in plant anatomy, development and/or microscopy.

Submit a cover letter, curriculum vitae, statements of teaching philosophy and research interests, reprints of up to five publications, graduate transcripts, and three letters of recommendation to: **Chair of the Search Committee, Department of Environmental and Plant Biology, Porter Hall 315, Ohio University, Athens, OH 45701-2979.** Review of applications begins December 20, 2005, and continues until the position is filled. Direct inquiries to: **Gar W. Rothwell, Chair (e-mail: pollard@ohio.edu** or **fax: 740-593-1130).**

Further information about the Department, College, and University is available at **websites: http://www.plantbio.ohiou.edu** and **http://www.cas.ohiou.edu/.**

Ohio University is an Equal Opportunity/Affirmative Action Employer. The University places a high priority on the creation of an environment supportive of the promotion of women, minorities, veterans, and persons with disabilities.

POSTDOCTORAL, RESEARCH, AND CLINICAL FELLOWSHIPS
at the
National Institutes of Health
U.S. Department of Health and Human Services

Website: http://www.training.nih.gov

NIH is dedicated to building a diverse community in its training and employment programs.

ASSISTANT PROFESSOR OF AQUATIC TOXICOLOGY

The Department of Biological Sciences invites applications for a tenure-track Assistant Professor position in the area of mechanistic or biochemical toxicology, to serve in the Environmental Sciences division (**website: http://www.ias.unt.edu**). The successful candidate will conduct research, perform service, and teach at the undergraduate and graduate levels in aquatic toxicology, emphasizing the mechanistic (biochemical, molecular, physiological, pathological) basis of chemical action in aquatic biota. The individual should have demonstrated background in evaluating mechanisms of toxic action of agents and applying that knowledge to areas such as selective toxicity, chemical protection, toxicity reduction/enhancement, risk assessment or other relevant topics. The successful applicant will have demonstrated ability or potential to teach, mentor students, seek out competitive research grants, and build a research program in cooperation with interdisciplinary scientists both within and outside the Department. Funding for this position is anticipated in 2006. Send a current resume, detailed cover letter describing research interests, and the names, addresses, and telephone numbers of three references. Review of materials will begin January 1, 2006, and continue until the position is filled. Questions and materials should be addressed to: **Dr. Thomas W. La Point, Aquatic Toxicologist Search Committee Chair, University of Northern Texas, P.O. Box 310559, Denton, TX 76203-0559. Telephone: 940-369-7776. E-mail: lapoint@unt.edu.** *The University of Northern Texas is an Affirmative Action/ADA/Equal Opportunity Employer Institution that encourages applications from members of minority groups and women and is committed to diversity.*

BIOLOGICAL SCIENCE EDUCATOR

The Department of Biological Sciences at the University of North Texas (UNT) (**website: http://biol.unt.edu/**) invites applications for a Biological Science Educator at the Assistant Professor level beginning August 2005, whose research program includes activity and publication in science education/pedagogy. The successful candidate will have exceptional teaching skills and experience with introductory biology courses. This individual will be expected to develop an extramurally funded research program that impacts the Department's undergraduate and graduate programs and K-12 regional science teachers. K-12 teaching experience will be viewed positively. Applicants must have a Ph.D. or Ed.D. in biology, (science) education or related area. Preference will be given to applicants whose primary interest overlaps departmental research areas. Application materials must include a detailed cover letter describing qualifications and experience, current resume, and names, addresses, and telephone numbers of three professional references. Review of materials will begin January 15, 2006, and continue until the position is filled. Questions and materials should be addressed to: **Dr. James Kennedy, e-mail: kennedy@unt.edu, Search Committee Chair, University of North Texas, P.O. Box 310559, Denton, TX 76203.** *UNT is an Affirmative Action/ADA/Equal Opportunity Employer Institution that encourages applications from members of minority groups and women and is committed to diversity.*

FELLOWSHIPS

UNCF • MERCK SCIENCE INITIATIVE

"A mind is a terrible thing to waste"

MERCK

UNDERGRADUATE SCIENCE RESEARCH SCHOLARSHIP AWARDS

- 15 Awards Annually
- Scholarships up to $25,000
- Two Summer Internships at a Merck Research Facility

An applicant must:

- Be a full-time student at any four-year college or university
- Have junior year academic status
- Major in a life or physical science (first professional degrees excluded)
- Have a minimum cumulative GPA of 3.3 (4.0 point scale)

GRADUATE SCIENCE RESEARCH DISSERTATION FELLOWSHIPS

- 12 Fellowships Annually
- Fellowship Stipends up to $42,000
- Department Grants of $10,000
- Support for 12-24 months

An applicant must:

- Be enrolled full-time in a Ph.D. or equivalent doctoral program in a biomedical life or physical science
- Be engaged in and within 1-3 years of completing dissertation research

POSTDOCTORAL SCIENCE RESEARCH FELLOWSHIPS

- 10 Fellowships Annually
- Fellowship Stipends up to $70,000
- Department Grants of $15,000
- Support for 12-24 months

An applicant must:

- Hold a Ph.D. or equivalent degree in a biomedical life or physical science
- Be appointed as a new or continuing postdoctoral fellow by the end of 2006 at an academic or non-academic research institution (private industrial laboratories are excluded)

Applicants must be African American (Black), U.S. citizens or permanent residents, and attending an institution in the U.S.A. Applications must be postmarked by December 15, 2005

For application forms and more information, please contact your department chairperson or Jerry L. Bryant, Ph.D., at the **United Negro College Fund**, 8260 Willow Oaks Corporate Drive, P.O. Box 10444, Fairfax, VA 22031-4511, by fax (703) 205-3574, by e-mail at ***uncfmerck@uncf.org***. Apply online or download from our website at ***www.uncf.org/merck/***

POSITIONS OPEN

INDIANA UNIVERSITY SCHOOL OF MEDICINE

Asthma and Allergic Disease Program Assistant/Associate Professor

The Department of Pediatrics, Section of Pulmonology, Critical Care and Allergy and the HB Wells Center for Pediatric Research (www.wellscenter.iupui.edu) is recruiting two faculty positions at the Assistant/Associate Professor level. While we are interested in all candidates in this area, we are particularly interested in mast cell, eosinophil and airway epithelial cell biology, and genetics of allergic disorders to complement existing strengths in T cell biology. Candidates will have a PhD, MD or MD/PhD and must have a strong research background and either current, or potential for, independent funding. New faculty will be provided with generous start-up packages and join an active multi-disciplinary Immunology and airway disease research community with a strong collaborative atmosphere.

Interested candidates are encouraged to submit a curriculum vitae and a short description of research interests to:

Mark H. Kaplan, PhD
Director of Pediatric Pulmonary Basic Research
Wells Center for Pediatric Research
Department of Pediatrics
Indiana University School of Medicine
702 Barnhill Drive, Room 2600
Indianapolis, IN 46202
airway@iupui.edu

Indiana University is an EEO/AA Employer, (M/F/D).

POSITIONS OPEN

Physician Scientists

Center for Infectious Diseases and Microbiology Translational Research

University of Minnesota

The University of Minnesota Medical School and Departments of Microbiology, Medicine, and Pediatrics are seeking 4 tenure-track physician scientists for a new interdisciplinary program in the Center for Infectious Diseases and Microbiology Translational Research (CIDMTR). We seek individuals with an MD/PhD or MD degree who wish to pursue careers in infectious disease-oriented research. These physician scientists will hold a primary appointment at the Assistant Professor level and will have 80% protected time for research. The academic appointment will be 50% in Microbiology, and 50% in either Medicine or Pediatrics. Successful candidates will be given a generous start-up package, including laboratory space in the CIDMTR which encompasses 20,000 square feet in the new McGuire Translational Research Facility. Successful candidates will be expected to develop independent extramurally funded research programs and to mentor graduate students, post-doctoral students, and fellows.

Minimum qualifications: MD/PhD or MD degree, plus postdoctoral research experience. Positions will remain open until suitable candidates are found. Early applications are encouraged and will be considered promptly.

To apply, submit a curriculum vitae, letter outlining research interests and plans, and the names and contact information for three references to:

CIDMTR Physician Scientist Search
c/o Department of Microbiology
MMC 196
420 Delaware Street S.E.
Minneapolis, MN 55455

Applications may also be submitted via email to:
microbiology@umn.edu

The University of Minnesota is an Equal Opportunity Educator and Employer.

Point. Click. Silence.

Guaranteed Silencing with *Silencer*® Pre-designed and Validated siRNAs

The most extensively verified design algorithm—tested on >1100 siRNAs.

Designed for maximum potency and specificity.

Silencer® Pre-designed siRNAs

- Guaranteed—
  at least two siRNAs guaranteed to reduce target mRNA levels by 70% or more when three purchased
- Available for >34,000 human, mouse, and rat genes

Silencer® Validated siRNAs

- Functionally tested in cells
- Every one guaranteed to reduce target mRNA levels 70% or more
- Available to hundreds of human targets

Find effective siRNAs for >34,000 human, mouse, and rat genes in seconds at

www.ambion.com/prod/siRNA

Ambion®
THE RNA COMPANY®

Ambion, Inc.
U.S. 800-888-8804 • Canada 800-445-1161
fax +1-512-651-0201

Ambion (Europe) Ltd
tel +44 (0)1480-373-020
fax +44 (0)1480-373-010

Ambion K.K. (Japan)
tel +81 (0)3-5638-2181
fax +81 (0)3-5638-2182

For a list of Ambion direct free phone numbers and distributors in your country, go to www.ambion.com/contact